

**AN EXAMINATION OF THE FORMS AND PROCESSES
ASSOCIATED WITH BED WAVES IN GRAVEL-BED RIVERS WITH
SPECIAL REFERENCE TO THE BRAIDED RIVER TYPE**

A thesis submitted in fulfilment of the
requirements for the degree of
Doctor of Philosophy
in the University of Canterbury by
Trevor Bernard Hoey

Department of Geography,
University of Canterbury

July 1989

ERRATA

<u>Page</u>	<u>Para.</u>	<u>Line</u>	
21	1	17	1953 <i>should read</i> 1951
40	3	7	Channel pattern.. <i>should read</i> <u>However</u> , channel pattern..
44	3	11	..argue that a <u>change</u> in.. <i>should read</i> ..argue that <u>an increase</u> in..
45	3	8	.. <u>and</u> macro- and mega-scales.. <i>should read</i> ..macro- and mega-scales..
82	3	17-8	..Froude scaling over the gravel-sand size range is unable to replicate channel morphologies,.. <i>should read</i> ..Froude scaling with shallow flows is at variance with theoretically predicted channel morphologies,..
115	2	6	Under <u>field</u> conditions.. <i>should read</i> Under conditions..
117	1	2	..bedload transport <u>capacity</u> further. <i>should read</i> .. bedload transport <u>rate</u> further.
153			Caption to Figure 5.16 line 3. ..adjacent to the right bank. <i>should read</i> ..adjacent to the <u>true</u> right bank.
159			Caption to Figure 5.21 Add 'The dashed line separates d_{50} data from d_{10x} data.'
212	1	6,7	..together as ' <u>regularly</u> mobilised' and adds two or more less <u>regularly</u> mobilised subdivisions.. <i>should read</i> ..together as ' <u>frequently</u> mobilised' and adds two or more less <u>frequently</u> mobilised subdivisions..
236	3	2	..channel geometry.. <i>should read</i> .. <u>characteristic</u> channel geometry..

ABSTRACT

A review of the literature leads to a classification of bed waves and bedload pulses in gravel-bed rivers, on the basis of their spatial and temporal scales. Mesoscale waves and pulses are associated with distinctly different processes from macro- and mega-scale features. Whether the sources of sediment for the wave / pulse are endogenous or exogenous to the river channel is used as a basis for sub-classification.

Froude number scale modelling of gravel-bed streams was performed in order to elucidate the mechanisms responsible for the production of bed waves. Three experimental runs were conducted, in which sediment transport rates and channel morphology were monitored. This was augmented by investigation of two reaches of the Kowai River, New Zealand, involving surveys of sediment storage and channel morphology, and palaeohydrological reconstruction of the flows responsible for production of the recorded morphology.

Measured fluctuations in the sediment output rates from the model streams were related to cycles of aggradation and degradation in the channels. The aggradational phases were associated with decreasing bed relief, and transfer of sediment from inactive to semi-active and active storages within the channel bed. Degradational phases were associated with inverse patterns. The switch between aggrading and degrading states was weakly dependent on stream power per unit bed area. The sediment transport rate was only close to that predicted by the Bagnold (1980) equation at times of channel stability, which occurred in about 40 % of locations. The equation overpredicted actual transport during aggradation and underpredicted during degradation.

Even with constant water and sediment inputs to the channel, waves and pulses of different spatial and temporal scales were produced. The relationships developed between aggradation and degradation, channel morphology, and sediment transport rates were supplemented by observations of the evolution of bed waves in the modelling experiments. Field data supported these results and added information on the textural properties of deposits within a bed wave. There were no significant differences between bed waves produced by endogenous sediment and exogenous material delivered to the river reach from upstream. Descriptive models of bed morphology changes as a bed wave passes through a cross-section were developed for the laboratory and field situations.

Introduction of dyed tracer sediment to one of the experimental runs showed that the input sediment was rapidly dispersed, but this wasn't indicative of bed wave attenuation. A stochastic model of sediment transfers between in-channel storage reservoirs illustrated the differences between aggrading, stable and degrading channel conditions. The times taken for sediment from different reservoirs to reach the downstream end of the experimental channel were equal under given conditions, implying the existence of a form of equilibrium.

The results enable the classification of wave types to be refined with waves of exogenous material that behave similarly to endogenous ones being separated from other exogenously supplied forms. The latter group have distinctive modes of behaviour. Equilibrium conditions were infrequently encountered at the mesoscale, but can be identified when the data are aggregated in both space and time. Bed waves of endogenous types can thus be regarded as equilibrium forms which lie within the geomorphological regime of gravel-bed river systems.

TABLE OF CONTENTS

CHAPTER	PAGE NUMBER
ABSTRACT	i
TABLE OF CONTENTS	iii
LIST OF TABLES	vi
LIST OF FIGURES	viii
LIST OF SYMBOLS	xi
ACKNOWLEDGEMENTS	xiv
1. INTRODUCTION	1
2. VARIATIONS IN SEDIMENT TRANSPORT RATES, AND THEIR RELATIONSHIPS WITH CHANNEL PATTERN IN GRAVEL-BED RIVERS	4
2.1 Rationale for separate consideration of gravel-bed rivers	4
2.2 Evidence for bed waves and bedload pulses in gravel-bed rivers	6
2.2.1 Spatial and temporal scales considered	6
2.2.2 Sources of evidence for bed waves and bedload pulses	9
2.2.3 Types and scales of bedload pulse and bed wave reported in the literature	11
2.2.4 Suggested mechanisms of wave and pulse development	21
2.2.5 Sediment supply- transport capacity relationships in bed waves	32
2.3 Interlinkages between channel patterns, and sediment storage and transport	34
2.3.1 Hydraulic controls of channel pattern and their implications for sediment transport	34
2.3.2 Sediment supply effects on channel pattern	41
2.3.3 The sediment storage implications of downstream variations in channel pattern	44
2.4 Conclusions	45
3. METHODS USED IN THE PRESENT STUDY	49
3.1 Physical modelling of gravel-bed rivers	49
3.1.1 The use of physical models in fluvial geomorphology	49
3.1.2 Application of scale modelling to gravel-bed rivers	51
3.1.3 The experimental equipment	54
3.1.4 Standard experimental procedures	59
3.1.5 The experiments	66

3.1.6 Tests of similarity and scaling	73
3.2 The prototype river study	78
3.2.1 The field site	78
3.2.2 Methods used in the present study	80
3.3 Synopsis	82
4. TEMPORAL VARIATIONS IN SEDIMENT TRANSPORT RATES	85
4.1 Sediment transport in the sand tray experiments	85
4.2 Channel form and sediment transport	94
4.2.1 Channel geometry at the downstream end of the sand tray	94
4.2.2 Comparisons of measured and predicted sediment transport rates	100
4.3 Possible controls of bedload pulse generation	108
4.4 Discussion and conclusions	113
5. THE FORM OF BED WAVES IN THE SAND TRAY AND FIELD	119
5.1 Bed wave characteristics derived from reach scale patterns of sediment storage and channel morphology in the sand tray	119
5.2 Morphology of an endogenous bed wave / bedload pulse in the sand tray	128
5.2.1 Sediment storage and transport during the bed wave cycle	128
5.2.2 Bar and channel morphologies during the bed wave cycle	133
5.2.3 A model of endogenous bed waves derived from the sand tray results	137
5.3 An exogenous bed wave in the sand tray	140
5.4 Exogenous bed waves in the Kowai River	143
5.4.1 Development of Porters and Bridge Reaches prior to 1987	143
5.4.2 Morphology of a bed wave in Porters Reach	152
5.4.3 Bed waves in Porters Reach: conclusions and a model	164
5.5 Discussion and conclusions	168
6. PATTERNS OF SEDIMENT REDISTRIBUTION ASSOCIATED WITH BED WAVES	172
6.1 Sediment dispersion processes and channel morphology	172
6.1.1 Sand tracing techniques	172
6.1.2 Output of dyed sand from the tray	173
6.1.3 Redistribution of dyed sand within the tray	176
6.1.4 Implications of the dyed sand redistribution patterns	184
6.2 Stochastic modelling of sediment redistribution	185
6.2.1 Description of the model	186

6.2.2	Model testing and application	197
6.2.3	Uses and limitations of the modelling procedure	209
6.3	Discussion and conclusions	212
7.	DISCUSSION	218
7.1	Spatial and temporal scales of bed waves and bedload pulses	218
7.2	Sediment supply- transport capacity relationships in bed waves	221
7.3	The use of channel pattern information for the identification of bed waves	227
7.3.1	Correlations between channel form and sediment transport rates	227
7.3.2	Processes associated with aggradation and degradation	228
7.3.3	An example of inference of sediment storage volumes from channel morphology: the Kowai River	233
7.4	The implications of bed waves for the assessment of channel equilibrium	236
7.5	The potential for small scale modelling in fluvial geomorphology	239
8.	CONCLUSIONS	242
8.1	Prognosis	245
	REFERENCES	247
	APPENDICES	260
1.	Bedload pulse and bed wave data from published studies	260
2.	Dimensioned and dimensionless hydraulic geometry data for the experimental runs	263
3.	Flow parameters for the experimental runs	265
4.	Sources of aerial photographs, Kowai River	267
5.	Sediment output rates and particle sizes for the experimental runs	267
6.	Stream power per unit bed area and channel condition data, Runs 1 and 3	273
7.	Cross-sectional morphology sediment storage and data, Runs 1 and 3	275
8.	Volumes of stored sediment, Kowai River, 1975, 1979, 1987	281
9.	Particle size data, Kowai River	281
10.	Output of dyed sand from experimental Run 3	282
11.	Distributions of dyed sand within the model channel, Run 3	283
12.	Exchanges of sediment between storage reservoirs (by area), Run 3	285
13.	Stochastically modelled sediment storage volumes, Run 3	286

LIST OF TABLES

TABLE	PAGE NUMBER	
2.1	Hierarchical bedform classification for prototype gravel-bed rivers (adapted from Jackson (1975) and Church and Jones (1982))	8
2.2	Types and scales of bedload pulse and bed wave in prototype rivers	9
2.3	Classification of the spatial scale and origin of bedload pulses and bed waves reported in the literature	12
2.4	Summary of the site characteristics, methods, and pulse / wave scales reported in the literature	13-16
3.1	Boundary conditions for the experimental runs	68
3.2	Dimensioned hydraulic geometry relationships for the experimental runs	70
3.3	Summary of data used to test dynamic similarity in the laboratory channels	74
3.4	Dimensionless hydraulic geometry relationships for the experimental runs	78
4.1	Frequencies of oscillations in the three-point moving mean series of sediment output	88
4.2	Parameters of the log-transformed sediment output series	90
4.3	Parameters of the appropriate autoregressive models for the experimental runs	93
4.4	General relationships between channel condition, cross-section morphology and sediment storage derived from the experimental runs	100
4.5	Measured and predicted bedload transport rates, using the Bagnold (1980) equation	103- 4
4.6	Observed channel stability at the times of bedload transport rate calculation	106
4.7	Ranked values of stream power per unit bed area, ω , ($\text{kg m}^{-1}\text{s}^{-1}$), associated with different channel conditions	109
4.8	Summary of stream power per unit bed area data for Runs 1 and 3	109
4.9	Results of t-tests to assess the significance of differences between stream power per unit bed area values in Table 4.8	110
5.1	Frequency of occurrence of synchronous peaks or troughs in mean bed elevation, bed relief index, and volume stored in the semi-active reservoir over different reach lengths, for Runs 1 and 3	124
5.2	Frequency of time intervals between successive troughs in the mean bed elevation, bed relief index and volume stored in the semi-active reservoir data series, for Runs 1 and 3	127
5.3	Mean width changes in Porters and Bridge Reaches, 1943-87	144
5.4	Possible event structure for the Kowai River	163

6.1	Areas of storage reservoirs and concentrations of dyed sand within them at 1690 minutes, Run 3	191
6.2	Conversion of volumes of dyed sand in different reservoirs to probabilities that input material will be located in each reservoir after one 4 hour time period	192
6.3	Exchanges of sediment between reservoirs from 1450-1690 minutes, Run 3	196
6.4	Flushing times computed from the transition matrix derived using Run 3 1450-1690 minutes data, Run 3	197
6.5	Modelled and measured sediment output and sediment storage changes, 1450-1690 minutes, Run 3	198
6.6	Modelled and measured outputs of sediment from the sand tray, 1450-2890 minutes, using the transition matrix derived from 1450-1690 minutes data	200
6.7	Modelled and measured outputs of sediment from the sand tray, 1450-2890 minutes, using transition matrices developed separately for each time period	202
6.8	Mean flushing times and residence times for different estimates of Q based on observed exchanges of sediment between reservoirs in 6 time periods	206
6.9	Sensitivity of the 1450-1690 minutes data and transition matrix to variations in redistribution probabilities	208
6.10	Estimated sources of sediment output from the sand tray	217
7.1	Types and scales of bed waves and bedload pulses in prototype rivers: modified version	221

LIST OF FIGURES

FIGURE	PAGE NUMBER	
2.1	Frequency distribution of median surface particle size	5
2.2	Spatial and temporal scales of bedload pulses and bed waves related to dimensionless water discharge	23
2.3	Spatial and temporal scales of bedload pulses and bed waves related to a dimensionless stream power index	24
2.4	A generic classification of bedload pulses and bed waves based on explanations suggested in the literature	26
2.5	Definition of types of sediment supply to a river	33
2.6	Definition of Total Sinuosity, ΣP (after Hong and Davies, 1979)	36
2.7	Estimated total bedload transport in the Rakaia River in a given time period (after Davies, 1988)	38
2.8	Classification of river channel patterns according to Carson (1984a)	43
3.1	Plan and elevation of the sand tray showing its principal features	55
3.2	Sediment feed apparatus and entrance to the model channel	57
3.3	Sediment collecting area	57
3.4	Particle size distributions of prototype and sand tray sediments	58
3.5	Initial channel cut into dry sand bed prior to the start of an experimental run	60
3.6	Calculation of alternative measures of bed relief using cross-section survey data	62
3.7	Idealised cross-sections and indices of bed relief associated with each	63
3.8	Definitions of sediment storage reservoirs	65
3.9	Dimensioned hydraulic geometry relationships for Runs 1 and 3	69
3.10	Examples of the different channel morphologies in Runs 1,2 and 3	71
3.11	Cumulative changes in mass of sediment stored (input-output) within the sand tray	72
3.12	Dimensionless hydraulic geometry data	76-77
3.13	Location of the Kowai River showing major tributaries and study reaches	79
3.14	Location of surveyed cross-sections within the study reaches of the Kowai River	81
3.15	Aerial photograph of the reaches shown in Figure 3.14	83
4.1	Sediment input and output rates for Runs 1, 2 and 3	86-87
4.2	Sediment output rates smoothed by a three-point moving mean for the model phases of Runs 1, 2 and 3	89
4.3	Autocorrelation (a.c.f.) and partial autocorrelation (p.a.c.f.) functions for the smoothed sediment output series of Runs 1, 2 and 3	91
4.4	Bed elevation, bed relief and sediment storage at the 13m cross-section, and sediment output rate from the tray	95- 96

4.5	Channel cross-sections and sediment storage reservoirs	98
4.6	Channel cross-sections and sediment storage reservoirs, Run 1 , 2530 and 2650 minutes	99
4.7	Comparison of measured bedload output with that predicted from the Bagnold (1980) equation	105
4.8	Cumulative frequency curves for mean stream power, ω , ($\text{Kg m}^{-1} \text{s}^{-1}$) for Runs 1 and 3	111
4.9	Bedload pulse periods measured in Runs 1-3 compared with data from other sources	114
4.10	Variation in shear stress, τ , slope, S, and hydraulic radius, R, during an aggradational episode (after Hey, 1979)	116
5.1	Sediment storage and cross-sectional morphology at all cross-sections in Run 1	120-1
5.2	Sediment storage and cross-sectional morphology at all cross-sections in Run 3	122-3
5.3	Channel morphology in Run 3 from 2.5m to 5m inclusive	126
5.4	Sediment output rate (g s^{-1}) and variation in bedload d_{50} (mm) in Run 1 from 2340 minutes to 2865 minutes inclusive	129
5.5	Channel and bar morphology through the bedload pulse depicted in Figure 5.4	131
5.6	Bedload transport capacity at cross-sections 6-13m inclusive, Run1	132
5.7	Schematic diagram to show the evolution of bar complex 7 and 8 on Figure 5.5a	135
5.8	Idealised development of a bed wave through time in a short reach as manifested in indices of cross-sectional and planform geometry, predominant morphological features, and sediment transport rate	138
5.9	Form of the bedload pulse input to Run 3a, and stream response	141
5.10	Cross-sectional morphology and sediment storage data for Run 3a	142
5.11	Active channel widths of Porters and Bridge Reaches, Kowai River	145
5.12	Active channel width (ACW) data from Figure 5.11 modified by dividing the ACW by the mean of all 5 ACW values for each section	146
5.13	Morphology of the active channels in Porters and Bridge Reaches based on aerial photographs	147-8
5.14	Width of the 1951 depositional surface and changes in the depth and volume of accumulated sediment, 1951-82 (after Beschta, 1983a)	149
5.15	Changes in unit volumes of stored sediment in Porters and Bridge Reaches, 1975-1987	151
5.16	View of the downstream edge of bed wave (6.4.1988) from the top of the terrace at the right bank end of cross-section 134	153
5.17	Bar face at the downstream edge of the bed wave (6.4.1988)	153
5.18	Morphology of Porters Reach in late 1987 showing the location of the leading edge of the bed wave	154
5.19	Cross-section surveys of Porters reach, 1987	155

5.20	Comparison of cross-section 133 in 1986 and 1987	157
5.21	Particle size changes along major complex bars in Porters Reach	159
5.22	Orientation of surface clasts in Porters Reach	162
5.23	Hypothetical evolution of the bed wave in Porters Reach during a flood event in March 1987	165
5.24	Idealised development of a bed wave through time in Porters Reach	167
6.1	Output of tracer sand and total sediment output from the tray, Run 3, 1515-2940 minutes	174
6.2	Surficial distribution of dyed sand as visually estimated in Run 3	177
6.3	Distribution of dyed sand at Run 3, 1690 minutes, derived from visual estimation and sediment sampling at 2m intervals along the tray	178
6.4	Distribution of dyed sand at Run 3, 2170 minutes, derived from visual estimation and sediment sampling at 2m intervals along the tray	180
6.5	Distribution of dyed sand at Run 3, 2650 minutes, derived from visual estimation and sediment sampling at 2m intervals along the tray	181
6.6	Distribution of dyed sand at Run 3, 2890 minutes, derived from visual estimation and sediment sampling at 2m intervals along the tray	182
6.7	Possible transfers of sediment between the four storage reservoirs, the source, and the absorbing state	187
6.8	Definition of transfers of material between reservoirs at times t and $t+1$, illustrated by the 5m cross-section at 1690 and 1930 minutes (Run 3)	194
6.9	Comparison of modelled and observed sediment storages, 1450-2890 minutes (Run 3) based on the 1450-1690 transition matrix	199
6.10	Comparison of modelled and observed sediment storages	203
6.11	Results of running the model with the 1450-1690 minutes transition matrix 10 times	210
6.12	Sediment storage changes during the 1450-1690 minutes period for the whole sand tray	216
7.1	Hypothetical model of responses of channel bed elevation and bedload transport rates to a concentration of flow in a single channel	224
7.2	Hypothetical model of responses of channel bed elevation and bedload transport rates to an avulsion which divides the discharge between three channels	225
7.3	Two dimensional representation of aggradation and degradation as a bed wave passes through a reach	229
7.4	Schematic representation of the controls over aggradation and degradation defined in terms of channel adjustments toward equilibrium	231
7.5	Active channel width, changes in the ACW 1980-1987, number of channels / cross-section, and channel condition for the Kowai River, 14.8.87.	234

LIST OF SYMBOLS

		Dimension
ACW	active channel width	L
b	channel width	L
b*	dimensionless channel width	-
BRI	bed relief index	-
d _A	grain size of maximum armour material size	L
d _p	grain sizes with p% finer - model	L
d _{10x}	mean b-axis of 10 largest clasts in a sample	L
e _t	error at time t in a time series	-
f	Darcy-Weisbach friction factor	-
Fr	Froude Number	-
g	acceleration due to gravity (9.81 m s ⁻²)	L T ⁻²
g _s	unit mass rate of sediment transport	M L ⁻¹ T ⁻¹
G _b	mass rate of bedload transport	M T ⁻¹
G _{bcap}	flow capacity mass rate of bedload transport	M T ⁻¹
G _s	mass rate of sediment transport	M T ⁻¹
h	flow depth	L
h*	dimensionless flow depth	-
l _b	submerged unit mass rate of bedload transport	M L ⁻¹ T ⁻¹
l _p	predicted increments of sediment volume in reservoir p	L ³
k	lag in a time series	T
k	transfer constant (Chapter 6 only)	-
k _s	roughness length	L
l _i	length of channel segment i	L
L	length of a specified object	L
n	number of values in a statistical sample	-
P	sinuosity	-
q	unit discharge	L ² T ⁻¹
q*	dimensionless unit discharge	-
Q	water discharge	L ³ T ⁻¹
Q*	dimensionless discharge	-
q* _b	dimensionless unit bedload discharge	-
Q _b	bedload discharge	L ³ T ⁻¹
Q _{bt}	total bedload discharge	L ³
r ²	correlation coefficient	-
r _k	autocorrelation function (a.c.f.) at lag k	-
R	hydraulic radius	L
Re	flow Reynolds number	-

Re_p	particle Reynolds number	-
RT_p	residence time for sediment in reservoir p	T
S	channel or valley slope	-
S_s	$(\gamma_s - \gamma_f) / \gamma_f$	-
t	single time period	T
t_e	event time	T
u	flow velocity	$L T^{-1}$
u_*	shear velocity	$L T^{-1}$
x_i	distance along a cross-section	L
x_i, \bar{x}	values and mean in statistical samples	-
z	channel bed elevation	L
D	redistribution matrix (elements d_{pq})	-
e	vector of volumes of source material being transferred to absorbing and non-absorbing states (elements e_p)	L^3
f	vector of flushing times (elements f_p)	T
I	identity matrix	-
N	fundamental matrix	-
Q	matrix of the probabilities of exchange of sediment between storage reservoirs (elements q_{pq})	-
r	vector of probabilities of stored sediment being transferred to the absorbing state in a single time period (elements r_p)	-
T	transition matrix	-
v	vector of volumes stored in reservoirs (elements v_p)	L^3
v'	vector of volumes stored in reservoirs after a single time period (elements v_p')	L^3
W	volume matrix (elements w_{pq})	-
α	statistical significance level	-
γ_f	unit weight of water (= $\rho_f \cdot g$)	$M L^{-2} T^{-2}$
γ_s	unit weight of sediment (= $\rho_s \cdot g$)	$M L^{-2} T^{-2}$
λ	wavelength of bed waves or meanders	L
λ_X	scale ratio for variable X	-
ν	kinematic viscosity	$L^2 T^{-1}$
ρ_s	density of sediment	$M L^{-3}$
ρ_w	density of water	$M L^{-3}$
σ_g	geometric standard deviation of a particle size distribution	-
σ_i	population standard deviation	-
ΣP	total sinuosity	-
τ	bed shear stress	$M L^{-1} T^{-2}$

ϕ_i	autoregressive coefficient at lag i	-
ϕ_p	proportion of sediment output derived from reservoir p	-
ω	stream power per unit bed area	$M L^{-1} T^{-1}$
ω_m	mean stream power	$M T^{-3}$
ω_o	critical value of ω for onset of particle motion	$M L^{-1} T^{-1}$
ω^*	dimensionless stream power index	-
ω^*_c	critical value of ω^* for onset of particle motion	-
Ω'	stream power index (= Q.S)	$L^3 T^{-1}$
σ	vector of flushing time standard deviations (elements σ_p)	T

ACKNOWLEDGEMENTS

This thesis was completed during tenure of a New Zealand Commonwealth Scholarship. The research was funded by grants from the North Canterbury Catchment Board and the University of Canterbury to Dr. J.B. Hockey.

Burn Hockey supervised the project from the outset, and his thoughtful criticism has been of immense value. During his period of leave in 1987, Dr. Ian Owens acted as interim supervisor. Dr. Alex Sutherland of the School of Engineering, University of Canterbury, has acted throughout as an unofficial associate supervisor, and facilitated the use of laboratory equipment in the Civil Engineering Department. His provocative questioning initiated many profitable lines of enquiry and the final manuscript owes much to his attention to detail.

During the formative stages of the project discussions with Dr. John Laronne proved invaluable. Dr. George Griffiths of the North Canterbury Catchment Board provided helpful criticism of the initial research outline and has remained supportive throughout. Numerous others have contributed ideas and thought provoking comments, including Prof. Michael Church, Prof. Olav Slaymaker and Dr. Murray Hicks. Dr. R.L. Beschta kindly enabled access to his own unpublished data from the Kowai River. Dr. John Hayward and Mr. Peter Ackroyd of the Centre for Resource Management, Lincoln College, have given unrestricted access to their data and aerial photographs from that river. Aerial photographs were also loaned by Ian Whitehouse of the (then) Ministry of Works and Development, and by the Department of Natural Resources Engineering, Lincoln College. A set of aerial photographs was taken for the present project by John Weeber of the North Canterbury Catchment Board.

The laboratory modelling work owes much to Peter Tyree who constructed equipment. Ian Sheppard and other staff of the Department of Civil Engineering assisted in the operation of the facility, and were always available to help when required. Chris Pennington helped with the photographic work. Staff of the Hydrology Centre (Ministry of Works and Development) willingly provided their information from work in the same facility. Considerable field assistance was provided by Ray Begg. Others who helped with this phase of the project were Vanessa Brazier, Juliet Brown, Burn Hockey, Jeff McDonnell, Andrew Nicholls, Ian Owens and Martin Single. Permission to work in the Kowai River came from the run holder at Brooksdale Station, Mr. Maurice Milliken.

Technical assistance in the preparation of the thesis came from Chris Pennington (photographs), and Tony Shatford and Alistair Dyer who drafted the figures. Juliet Brown assisted with proof reading and typing.

Those ultimately responsible for my interest in things geomorphological were David Rhodes and

Colin Nichols at Newcastle-upon-Tyne Royal Grammar School. This interest was expertly fostered by Dick Chorley, Martin Sharp, David Stoddart and Keith Richards, whose concern with sediment delivery inspired the 200 word research outline that developed into the following thesis.

To all the people mentioned above and others with whom I have shared geomorphological experiences I owe a great deal. Their responsibility for what follows is nil, but at least some will recognise their influence in the following pages.

1. INTRODUCTION

The first observations of temporal variability in bedload transport rates under steady flow conditions were made during the 1930's (Ehrenberger, 1931; Mühlhofer, 1933; Einstein, 1937; comprehensively reviewed by Gomez, Naff and Hubbell, 1989). Gilbert (1917) had previously speculated on the existence of larger scale bed waves developing as a consequence of mining activity and subsequently being transferred through the drainage network. However, it was not until the 1960's that this variability began to receive much attention, the intervening period having been dominated by attempts to develop universal bedload transport formulae, and by interest in the calibration of sampling devices (Gomez *et al.*, 1989). As technology for continuous recording of bedload transport rates has become available (e.g. Hayward, 1980; Reid, Layman and Frostick, 1980; Tacconi and Billi, 1987) so the frequency of reports of such phenomena has increased. This has been accelerated by a developing awareness of processes in gravel-bed rivers (e.g. Hey, Bathurst and Thorne, 1982; Thorne, Bathurst and Hey, 1987) in which processes of sediment sorting and bar formation encourage transport rate variability. Gilbert's (1917) initial description of bed waves has been re-examined at larger spatial and temporal scales in the light of similar examples of well documented increases in the rate of sediment supply to rivers (e.g. Beschta, 1983a; Pickup, Higgins and Grant, 1983; Macklin and Lewin, 1989), and in cases where there is no apparent acceleration of supply (e.g. Griffiths, 1979; Church and Jones, 1982; Ashmore, 1985, 1987; Nakamura, 1986).

The reports of variations in bedload transport rates and sediment storage volumes through time have come from a range of physical environments. There are numerous studies from laboratory flumes (e.g. Gibbs and Neill, 1973; Iseya and Ikeda, 1987; Kuhnle and Southard, 1988) and several from field examples with flume-like channel geometries (e.g. Meade, 1985; Reid, Frostick and Layman, 1985; Tacconi and Billi, 1987). Other river types from which bed waves have been reported include mountain torrents (e.g. Hayward, 1979, 1980), single-thread rivers of varying patterns (e.g. Jackson and Beschta, 1982; Nakamura, 1986) and braided rivers in both the field (e.g. Griffiths, 1979; Kang, 1982; Davies, 1987) and laboratory (e.g. Southard, Smith and Kuhnle, 1984; Ashmore, 1985, 1987, 1988). In view of recent work which has emphasised the interdependence of sediment transport and channel morphology (e.g. Brotherton, 1979; Carson, 1984a; Ashmore, 1987; Ferguson, 1987) there may be different processes associated with variability in transport rates and storage volumes in different river types. Further, variations in bedload transport rates within individual rivers have been suggested to correlate with variations in channel planform and / or cross-sectional morphology (e.g. Church and Jones, 1982; Ashmore, 1987).

As the review by Gomez *et al.* (1989) has illustrated, the mechanisms of bedload transport rate variation are best understood at smaller scales although many questions remain to be answered (Carson and Griffiths, 1987). It is at larger spatial and temporal scales that the processes remain

least comprehended. In particular, it is unclear to what extent bed waves can be developed by in-channel processes in the absence of variations in the rate of sediment supplied to the river. This question and many others are difficult to resolve in field studies on account of practical problems in obtaining sufficiently long records of the relevant data. This is inhibiting the development of analytical approaches to these issues although some progress has been made, for example by the model of Weir (1983).

An approach to these practical difficulties which has become increasingly popular in recent years is to use small scale physical modelling. Braided rivers can readily be simulated using sand sized material as a scaled down bed material. Such models have been used for investigations of channel patterns (e.g. Leopold and Wolman, 1957; Schumm and Khan, 1972), particular types of bedforms (e.g. Southard *et al.*, 1984) and channel form and sediment transport inter-relationships (e.g. Ashmore, 1985; Lee and Davies, 1986). The principles underlying such modelling are well understood, but it is impossible to produce uniform scaling of all aspects of sediment transport and channel shape simultaneously (Yalin, 1971a). Despite the excellent qualitative agreement between model and prototype (i.e. the system that is being modelled) form and process, it is presently difficult to produce reliable quantitative predictions from a model as to prototype behaviour. Modelling advantages including ease of measurement of several variables, rapidity of process, and potential for controlled variation of boundary conditions (Schumm, Mosley and Weaver, 1987) need to be offset against the difficulties of relating model results to prototype behaviour. Recent model studies, notably those of Southard *et al.* (1984), Ashmore (1985) and Davies and Lee (1988), have yielded results which have generated hypotheses that are amenable to prototype testing. Although the models have been unable to directly solve prototype problems, the hypotheses generated have been useful in improving understanding of prototype processes. This situation may change at some future time as understanding of prototype behaviour improves. For the present the use of small scale models can be recommended as a viable and useful approach to the study of gravel-bed rivers despite its limitations.

The primary aim of this study is to develop a greater understanding of the causes of variations in bedload transport rates and sediment storage patterns in braided rivers. The emphasis on this river type derives from its importance in New Zealand (Carson and Griffiths, 1987), but since gravel-bed channel patterns have been demonstrated to lie on a continuum (Richards, 1982; Carson, 1984a) some of the results from braided rivers should be transferable to other gravel-bed rivers. Care needs to be taken in doing this to isolate those processes which are entirely dependent upon the channel bifurcation and confluence processes that are unique to the braided river type.

For practical reasons the study emphasises the results of a small scale modelling approach. This is used to assess the controls over bedload transport rate fluctuations and the relationships

between bedload transport rate and channel morphology. Use of variations at-a-section through time and along a reach at a given time enables a descriptive model of these relationships to be developed.

As well as small scale modelling, the investigation utilises data collected from a small gravel-bed river. The problems of data acquisition mentioned above are tackled using conventional measures of channel pattern and by analysis of the sedimentary deposits of the river bed and their depositional history. These procedures enable some of the ideas developed from the small scale model to be evaluated.

Sediment routing methods have developed in recent years with an emphasis on stochastic modelling of sediment transfer (Dietrich, Dunne, Humphrey and Reid, 1982; Kelsey, Lamberson and Madej, 1987). Kelsey *et al.* (1987) were able to replicate a recorded bed wave using such methods, and their approach can be applied to the active bed sediments stored in braided rivers. In view of the data requirements of this stochastic modelling approach, it is only applied to data from the small scale physical model. Use of this method is aimed at providing insights into sediment transfer processes that are not available using other means, and its success should be judged by how well this is achieved.

The issues which are examined as ways of addressing the primary aim of the investigation are as follows:

1. the types of bedload transport rate and sediment storage variation, their spatial and temporal scales, generality of occurrence, and the variables which control each of these aspects;
2. the processes responsible for producing these features and their relationships with equilibrium river processes;
3. the ways in which sediment storage variations can be identified from channel morphology data;
4. the implications of the above for understanding of sediment transfer processes and the nature of sediment delivery by gravel-bed rivers.

These issues are addressed in the literature review contained in Chapter 2, at the end of which some more specific questions regarded as requiring further research are identified.

2. VARIATIONS IN SEDIMENT TRANSPORT RATES AND STORAGE, AND THEIR RELATIONSHIPS WITH CHANNEL PATTERN IN GRAVEL-BED RIVERS

The literature on fluctuations in sediment transport and storage in gravel-bed rivers contains a number of descriptive terms. Among the most common are waves (e.g. Mosley, 1978; Griffiths, 1979; Lekach and Schick, 1983), pulses (e.g. Reid and Frostick, 1984; Ashmore, 1987), slugs (e.g. Pickup, Higgins and Grant, 1983; Davies, 1987), and sedimentation zones (Church and Jones, 1982). Features occurring at many spatial and temporal scales have been described and are considered below. An attempt is made to maintain consistency throughout the discussion by using two scale-independent terms which are defined as follows:

- wave** a general term for an increase in the volume of sediment stored in a reach, relative to either the same reach at different times or adjacent upstream and downstream reaches; the emphasis on volume of sediment in storage implies that waves can be produced by changes in the width and / or depth of accumulation;
- pulse** a variation at a point through time in the rate of sediment transport (i.e. $\delta g_s / \delta t \neq 0$, where g_s is the unit mass rate of sediment transport); this has no spatial implications and being a dynamic concept is restricted in its usage to a process (sediment transport).

These two terms are used across the range of spatial and temporal scales defined in sub-section 2.2.1. Additional descriptive terms for waves and pulses are used at specific scales. These are also discussed in sub-section 2.2.1.

2.1 Rationale for separate consideration of gravel-bed rivers

There have been many studies of features peculiar to gravel-bed rivers over the past 15- 20 years (Hey *et al.*, 1982; Thorne *et al.*, 1987). Bed material size is one of a number of ways that river channels can be classified (e.g. Mosley, 1987) and as with many others it is a property that is continuously distributed. However, a distinction between sand and gravel bed rivers is not arbitrary (Parker and Peterson, 1980), since there is a gap between coarse sand and fine gravel in the frequency distribution of median surface bed material size (Figure 2.1). The gap in median sizes is mirrored by distributions within individual samples by the tendency for cover layer development in gravel-bed rivers, which concentrates coarser material at the surface, although the underlying material is often also deficient in the 1-4mm size range (Parker and Peterson, 1980). The size distributions of gravel-bed rivers are wider than those in sand (Simons and

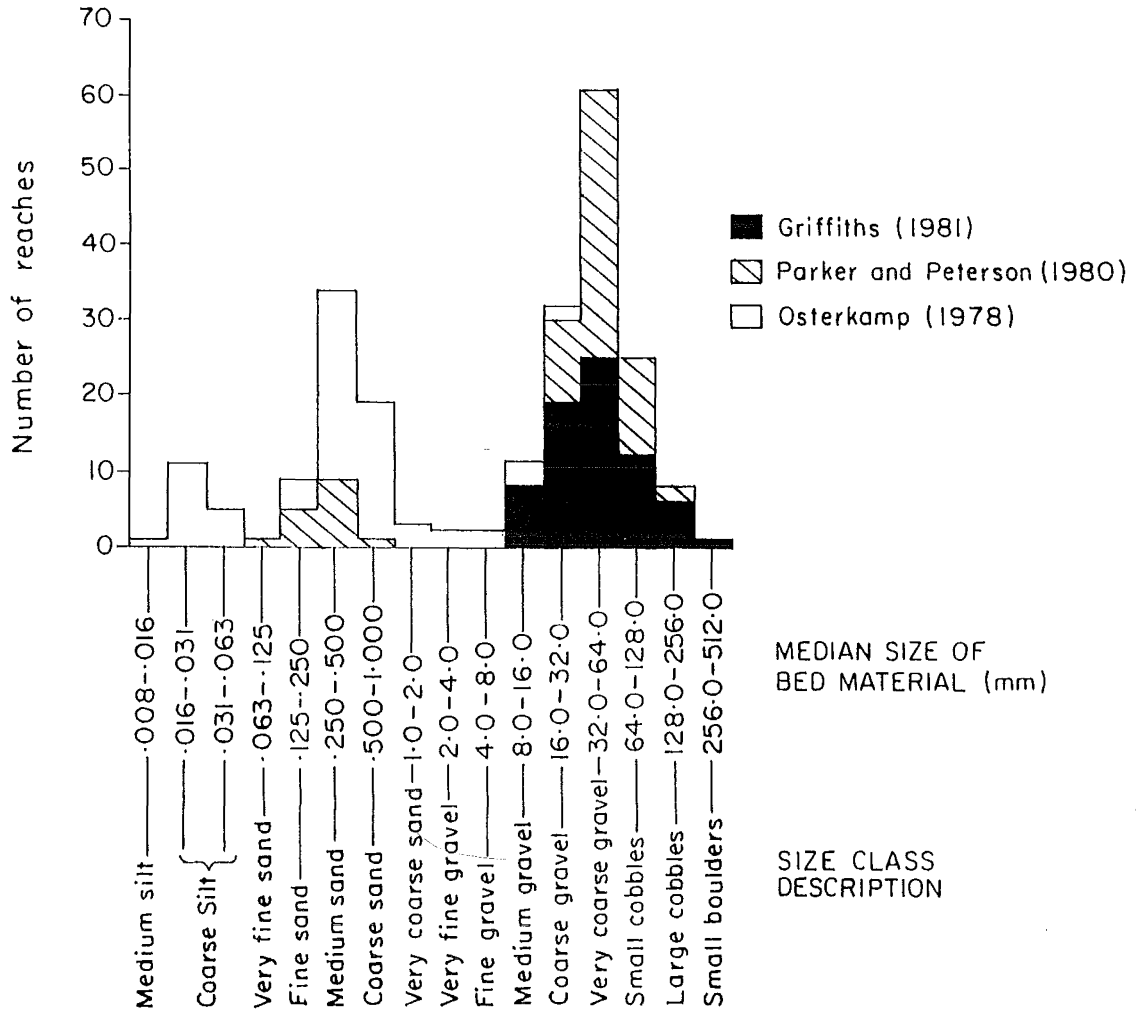


Figure 2.1 Frequency distribution of median surface particle size. Griffith's (1981) data are for 71 reaches of 46 New Zealand rivers, Parker and Peterson's (1980) for 78 Albertan river reaches, and Osterkamp's (1978) for 76 reaches on 59 Kansan rivers.

Simons, 1987 - discussion by J.C. Bathurst). Rivers with bimodal size distributions occur (e.g. the Tanana River - Bagnold, 1980) and may require separate consideration.

Parker and Peterson (1980) and Simons and Simons (1987) have detailed the qualitative differences between the behaviour of sand and gravel rivers. The major differences that they identify are as follows:

- a) bed mobility is greater in sand bed rivers and the occurrence of flows sufficient to mobilise gravel beds is limited to high stages; this is exacerbated by the development of cover layers (armouring);
- b) sediment supply events are more episodic in gravel bed rivers and sediment transport is more likely to be supply limited (Simons and Simons, 1987 - discussion by J.C. Bathurst);
- c) bedforms are only rarely present in gravel bed rivers and are weakly developed if at all, whereas dunes are the primary source of flow resistance in sand bed rivers; and,
- d) different bar types are found in sand and gravel bed rivers.

Numerous other effects are related to these and there are strong correlations between bed material size and other properties of river systems such as bed slope, flow regime and planform (Simons and Simons, 1987). Quantitatively these differences lead to separate equations for flow resistance and sediment transport. Few cobble and boulder bed rivers are included in the data in Figure 2.1, and there is no clear differentiation between this group and gravel bed rivers. When bed material is greater than about 64mm (median grain size) rivers are generally steep and have characteristic morphologies (e.g. Whittaker, 1987), and as such can be readily differentiated from other types of coarse bed river. Such rivers (often called mountain torrents) are not considered specifically herein, although some observations made in these situations have relevance to gravel bed conditions.

Because of process differences it is convenient to consider sand and gravel bed rivers separately. This is facilitated by the gap in the frequency distribution of median bed particle sizes. Numerous sub-classifications can be made within the gravel-bed river set, based on a range of variables. Sub-classifications based on channel patterns are considered in section 2.3.

2.2 Evidence for bed waves and bedload pulses in gravel-bed rivers

2.2.1 Spatial and temporal scales considered

Bed waves can be considered as bedforms, where these are defined as any bed feature with an elevation with respect to mean bed level that is in excess of the median bed particle size (Jackson, 1975). Smaller bedforms respond to the instantaneous fluid dynamic regime, whereas larger ones are sensitive to long-term variations in flow conditions and geomorphological regime

(Jackson, 1975). Three components are requisite in a model of bedform origin, namely a time element, a process regime element and a geomorphological regime element (Jackson, 1975). Such a scheme for all sedimentary environments was proposed by Jackson (1975) and has been refined for gravel-bed rivers by Church and Jones (1982). Their hierarchical bedform classification is reproduced in modified form in Table 2.1, along with the governing factors for the various scales identified by Jackson (1975). The spatial and temporal scales identified in Table 2.1 are closely interdependent. For gravel-bed rivers microforms can be disregarded as they only occur where material size is less than about 1.0mm (Jackson, 1975). A major process difference occurs between mesoforms and macroforms. Mesoforms are primarily dependent upon the local fluid dynamic regime and are largely independent of the geomorphological regime, with the reverse situation true for macroforms. This does not mean that the geomorphological regime has no influence on mesoforms, and the fluid dynamic regime no influence on macroforms, however. Rather, these are not their principal controls and can be regarded as defining the limits within which such controls operate. No equivalent change in the dominant process is apparent between macroforms and megaforms. The latter are composite features arising out of combinations of the former, along with erosional modification.

Bedforms can exhibit a range of types of superposition (Jackson, 1975). Mesoforms can be readily superposed upon macroforms and megaforms. It is also feasible that macroforms can be superposed on megaforms. Moreover, macroforms can combine in the horizontal dimension. If the resultant form is sufficiently large to begin to function as a single entity rather than as a set of semi-independent macroforms, then the result is a megaform. Macroforms and megaforms can thus be regarded as elements of a continuum.

The features which comprise different scales of bedform merit some comment here. Mesoforms are characterised by dunes and antidunes (which are rare in gravel-bed rivers), and by particle clusters (Naden and Brayshaw, 1987). Also included are riffles and pools, which are similar features to cluster bedforms, although at a slightly larger scale. Macroforms span two scales of channel bar, namely unit bars and complex bars in addition to gravel sheets. Unit bars are defined as bars that have remained largely unmodified since deposition, and which were initially deposited in response to a local change in hydraulic conditions (Smith, 1974). Their form and location relates to the geomorphic regime more closely than to the local hydraulic one. Bar complexes derive from unit bar erosion, superposition and lateral accretion. Bars can have both hydraulic resistance and sediment storage functions, which are often combined in single features (Church and Jones, 1982). Megaforms are extensive versions of macroforms, where numerous complex bars behave in an integrated manner.

Although bedform timescales are given in terms of flood event times, no direct phase relationship between the two is implied. Bedform change is a response to sediment transport processes that

Table 2.1 Hierarchical bedform classification for prototype gravel-bed rivers (adapted from Jackson (1975), Table 5, and Church and Jones (1982), Table 11.1.

t_e is the 'event time' i.e. the time for a flood wave to pass through a reach. Note that the upper wavelength for microforms and the lower limit for mesoforms are set at 10^{-1} m, rather than 10^0 m as in Church and Jones (1982). Regime time is the timescale over which the river system is in equilibrium (the form of which may be dynamic).

Bedform class	System scale	Wavelength (m)	Relaxation time	Typical features	Governing factors
Microforms	Particle size	$10^{-2} - 10^{-1}$	$\ll t_e$	Ripples, lineations Fine sediment only (< 1.0 mm)	Local fluid dynamic regime near bed. Independent of geomorphological regime
Mesoforms	Flow depth	$10^{-1} - 10^2$	$\cong t_e$	Dunes, antidunes, particle clusters, riffles	Variation of fluid dynamic regime of the entire boundary layer. Independent of geomorphological regime
Macroforms	Channel width	$10^1 - 10^3$	$\geq t_e$ $\gg t_e$	Gravel sheets, unit bars, complex bars	Geomorphological regime. Associated with bedload transport.
Megaforms	> several channel widths	$> 10^3$	Regime time	Bar assemblages	Geomorphological regime. Great variety of features.

operate at finite rates, so there must be a lag between flow changes and bedform response (Allen, 1983). The time taken for a bedform to attain equilibrium with a changed flow condition is the relaxation time (Brunsden and Thornes, 1979), which is broadly equivalent to the 'time span of existence' used by Jackson (1975; Table 5).

Table 2.1 has grouped a wide range of gravel bedforms into a single classification based on their spatial and temporal scales. Further, some differences in the dominant controls over the development of these bedforms are apparent between the different groups. The same terminology can be employed for the purpose of bed wave and bedload pulse identification i.e. meso-, macro-, and mega- scales are used as a basis for classification. The process differences between the meso- and macro-scales of bedform noted above suggest that there may be more than one type of generating mechanism for bed waves / bedload pulses dependent upon the scale of the phenomenon.

A further distinction is also made at the outset between endogenous and exogenous waves and pulses. Endogenous is used to refer to features produced from material located within the river system (i.e. it is reworked alluvial material). Exogenous refers to those features that result directly from inputs of material to the river system from outside (e.g. hillslope erosion, tributary inputs). Table 2.2 summarises the classification scheme used for bed waves and bedload pulses for prototype rivers. The wavelengths have to be altered by the appropriate scale ratio for small scale laboratory experiments.

Table 2.2 Types and scales of bedload pulse and bed wave in prototype rivers

Pulse/wave scale	Wavelength (m)	Relaxation time	Possible wave types
Mesoscale	10^{-1} - 10^2	$\cong t_g$	endogenous /exogenous
Macroscale	10^1 - 10^3	$\geq t_g$	endogenous /exogenous
Megascale	$>10^3$	Regime time	endogenous /exogenous

2.2.2 Sources of evidence for bed waves and bedload pulses

Identification of bedload pulses requires monitoring of the bedload transport rate, whereas bed waves are defined by volumes of stored sediment. Identification of bedload pulses from data on bedload transport rates requires that allowance is made for the relationship between water discharge and transport rate. Four types of technique which are briefly reviewed below have been used to estimate bedload transport rates.

A. Sampling. A range of bedload sampling devices is available, associated with which are sampling problems independent of the natural variability of the transport rates being measured (Carey, 1985; Hubbell, 1987). Sampled volumes of bedload require adjusting to get estimates of the actual transport rates, and the magnitudes of such adjustments are dependent upon both transport rate and particle size (Hubbell, 1987). Thus, obtaining reliable mean transport rates requires a long sampling period (Kuhnle and Southard, 1988) and / or a large number of samples; Pearson and Thompson (1986) suggested that 200 samples of up to 20 Kg are required in a braided gravel river, with water discharge $500 \text{ m}^3 \text{ s}^{-1}$. This causes considerable practical difficulties since flow conditions and transport rates change very rapidly in many gravel rivers, such that estimates to within +/- 100 % of the true value are as good as can be expected (Hubbell, 1987 - discussion by T.R.H. Davies). Sampling methods are not generally considered sufficiently accurate to enable precise specification of the magnitudes and periods of bedload pulses.

B. Continuous measurement. With the advent of continuous recording methods it has been possible to demonstrate that bedload pulses are not simply artifacts of a sampling procedure (Carey, 1985; Tacconi and Billi, 1987 - discussion by I. Reid and L.E. Frostick). Four types of such device have been used : vortex tubes; conveyor belt slots; pressure sensors; electromagnetic detectors. For practical reasons only rivers of up to about 15m wide have been monitored in this way.

C. Surrogate estimates. Bedload transport rates can be estimated from a range of surrogate variables. Examples include delta accretion survey (Thompson, 1985) and dispersion of tracer particle material (Laronne, Duncan and Rodley, 1986). The accuracy of such methods is variable, and they are difficult to repeat sufficiently often for reliable information about bedload pulses to be obtained.

D. Small scale physical modelling. Using a modelling approach the continuous measurement of bedload discharge becomes a straightforward procedure. Many studies of bedload transport have used laboratory methods, but only a few have allowed small scale rivers to self-form in the laboratory with bedload transport rate being continuously measured (e.g. Ashmore, 1987). The utility of this approach is dependent upon the ability of the modelling procedure to replicate prototype conditions. This is considered in Chapter 3. An advantage of this approach is that related data on volumes of stored sediment, channel patterns and bar morphology can be readily collected and used for interpretation of the patterns observed in the bedload transport rates. It is also possible to remove the effects of water discharge fluctuations by holding it constant.

Identification of bed waves requires either direct measurement, or an estimate of the volume of sediment stored in a river reach. Direct measurement has usually involved repeated surveys of river cross-sections. There are temporal and spatial sampling problems in this procedure, caused

by the time interval between surveys and the distance between adjacent sections. Also, the depth of bed activity in gravel rivers cannot be directly measured and requires other techniques, such as scour chains (Laronne *et al*, 1986). More dense networks of surveyed points can be used and total volumes stored within a reach estimated in some cases. Photogrammetric analysis may prove useful in this regard (Davies, 1987) but is presently expensive.

The easiest and most readily repeated method of river bed analysis involves use of aerial photographs, and methods have been suggested for using data that is readily obtained from such photographs to infer sediment storage volumes. The width of the active channel is the most readily measured parameter (Beschta, 1983b), and is closely correlated with the stored sediment volume (Magilligan, 1985; Nakamura, 1986). Alternatively, Davies (1987) has speculated that channel pattern could be used for this purpose. The understanding of links between channel patterns, sediment storage and sediment transport is examined in section 2.3. It is important to note that local effects, such as changing valley width and tributary inputs can cause the emergence of spurious patterns along a river. The critical element then becomes the change in sediment storage in a reach through time. Hence the temporal interval between measurements is important since it is not possible to draw conclusions about processes operating at any timescale smaller than this interval.

2.2.3 Types and scales of bedload pulse and bed wave reported in the literature

The classification of Table 2.2 is used as the basis for this discussion. Table 2.3 places studies from the relevant literature into this scheme, and Table 2.4 summarises the details of these studies. Gomez *et al.* (1989) used a classification of bedload pulses based on both timescales and suggested generating processes. With some exceptions their 'short-term' equates to mesoscale, and their 'long / intermediate term' to macro- and mega-scales.

A. Mesoscale. Exogenous mesoscale features are likely to occur every time there is a discrete input of material to a channel from bank erosion. Such features have not been explicitly described in the literature. Work at this scale has emphasised the endogenous nature of bedload transport rate fluctuations, although a variety of causal mechanisms has been proposed (see sub-section 2.2.4). Both field and laboratory studies have been undertaken and are described separately.

Reid *et al.* (1985) and Gomez *et al.* (1989) have reviewed some of the evidence for bedload pulses in natural rivers. The early data of Ehrenberger (1931), Mühlhofer (1933), Einstein (1937) and others (see Gomez *et al.*, 1989 p.135), although subject to sampling variability, are amongst the most detailed field data available. Solov'yev (1967) presented similar data. Mühlhofer's (1933) data exhibited regular fluctuations with 6-7 minute periods, and considerable cross-channel variation (see, Hubbell, 1987 p.90; Andrews and Parker, 1987 - discussion by M.

Table 2.3 Classification of the spatial scale and origin of bedload pulses and bed waves reported in the literature. Studies which reported bedload pulses are denoted * and bed waves +.

The studies are classified according to the methods described in sub-section 2.2.2.

Sampling: S - bedload sampled;

Continuous measurement: T - entire bedload trapped; R - bedload sensed electromagnetically;

Small scale modelling: F - flume study; P - physical model of self-formed rivers;

Bed waves: V - volumes of stored sediment measured; I - inferred from other data (bed elevation, channel pattern, dispersion of tracer material);

Other: M - mathematical model.

SCALE	ENDOGENOUS		EXOGENOUS			
MESO	Ehrenberger	1931	S *			
	Mühlhofer	1933	S *			
	Einstein	1937	S *			
	Solov'yev	1967	S *			
	Samide	1971	S *			
	Gibbs and Neill	1973	F *			
	Emmett	1975	S *			
	Hayward	1979	T *			
	Kang	1982	S *			
	Gomez	1983	S *	Occur frequently as sediment supply varies		
	Lekach and Schick	1983	S *			
	Carey	1985	F *			
	Reid <i>et al.</i>	1985	T *			
	Custer <i>et al.</i>	1987	R *			
	Iseya and Ikeda	1987	F *			
Naden	1987	M *				
Tacconi and Billi	1987	T *				
Kuhnle and Southard	1988	F *				
Whiting <i>et al.</i>	1988	S *				
Gomez <i>et al.</i>	1989	F *				
MACRO	Jackson and Beschta	1982	S *	Occur frequently as point inputs of sediment are redistributed		
	Kang	1982	S *			
	Southard <i>et al.</i>	1984	P,I +			
	Gomez <i>et al.</i>	1989	F *+			
MEGA	Romashin	1967	I +	Gilbert	1917	I +
	Thornes	1976	I +	Mosley	1978	I +
	Griffiths	1979	I +	Griffiths	1979	I +
	Church and Jones	1982	I +	Madej	1982	V +
	Beschta	1983b	I +	Beschta	1983a	I +
	Ashmore	1985	P *+	Pickup <i>et al.</i>	1983	V +
	Nakamura	1986	V,I +	Meade	1985	V *+
	Davies	1987	I +	Roberts and Church	1986	V +
				Kelsey <i>et al.</i>	1987	V +
				Macklin and Lewin	1989	I +

Table 2.4 Summary of the site characteristics, methods, and pulse/wave scales reported in the literature. The studies are grouped as in Table 2.3, along with additional work which doesn't fit into that classification. Note that at the megascale pulse timescale includes long periods of no bedload motion. The notation $2E-06$ is equivalent to 2×10^{-6} . Where wave spatial scale is given p.a., this is the estimated rate of annual migration of the wave form. w = standard channel widths ; m.a.f. = mean annual flood ; R.I. = recurrence interval; n.a.= not available.

Source	Location	Method	Bed material size d_{50} (mm)	Discharge (m^3s^{-1})	Sediment transport rate ($kg\ m^{-1}\ s^{-1}$)	Channel slope	Channel width (m)	Channel pattern	Pulse timescale (min)	Wave spatial scale (m)
MESOSCALE										
Ehrenberger (1931)	Danube	Sampling	20		0-1.5				18	
Mühlhofer (1933)	Inn	Sampling	gravel		0.3-2.5				6	
Einstein (1937)	Rhine	Basket sampler	28	200-1400	$0-10\ g\ s^{-1}$				1200	
Solov'yev (1967)	Mzymta and Ugam								12	
Samida (1971)	Elbow River	Sampling		62.3	< 0.3			Single thread	30	
Gibbs and Neill (1973)	Flume	Slot sampler in bed 30sec every 3 min	3.1	0.17	0.03-0.4	0.0035	1.22	Straight	30	
Emmett (1975)	Slate Creek 3.0	Helley-Smith sampler 30 sec. samples	43 (22- bedload)		$0.016 - 0.15\ kg\ s^{-1}$				30	
Hayward (1979,80)	Torlesse Stream	Vortex tube - continuous measurement	25	0.15-2.8	≤ 1.3	0.067	3.0	Straight	48-300	
Kang (1982)	Hilda Creek	Basket sampler	30	≤ 0.57		0.04-0.07	11-17	Braided	9-18 (mean 14)	
Gomez (1983)	Borgne d'Arolla	Helley-Smith sampler 30 sec. samples	1.2-3.6	≤ 1.83	0.035-0.521	0.03	10.25	Straight	< 60	
Lekach and Schick (1983)	Nahal Yael	Bucket sampler	0.15-2.5 (bedload)	0.03-0.115		0.044	1.5		25-30	
Reid <i>et al.</i> (1985)	Turkey Brook	Pressure sensors- continuous measurement	16 22 - armour 11 - bedload	0.7-16.6	0.0001-0.1	0.0086	3.0	Straight	84-120	
Custer <i>et al.</i> (1987)	Squaw Creek	Electromagnetic sensors	12	3.7	0.83	0.02	8.6	Straight	0.6-10	

Table 2.4 (Continued)

Source	Location	Method	Bed material size d_{50} (mm)	Discharge ($m^3 s^{-1}$)	Sediment transport rate ($kg m^{-1} s^{-1}$)	Channel slope	Channel width (m)	Channel pattern	Pulse timescale (min)	Wave spatial scale (m)
Iseya and Ikeda (1987)	Flume	Total load collected at 10 sec intervals	2.6 - gravel 0.4 - sand in varying proportions	0.0004	9E-07-2.9E-06 -gravel 7.3E-06 -total	0.019-0.042	0.1	Straight	1.7-3.3	> 1 dune wavelength
Naden (1987)	Mathematical model	Prediction from process theory					1-dimensional	Straight	60	
Tacconi and Billi (1987)	Virginio Creek	Vortex tube - continuous measurement	13 - bulk 27.9 - armour	1.25-7.1	0.00007-0.26	0.008	12	Straight	30	
Kuhnle and Southard (1988)	Flume	Total load collected at 30sec intervals	3.03 3.03 3.03	0.034-0.089 0.035 0.028	1.3-54.1 1.91 2.3-4.6	0.015-0.024 0.019 0.019	0.15 0.53 0.74	Straight Straight Straight	5-10 10-26 6-11	
Whiting <i>et al.</i> (1988)	Duck Creek Muddy Creek	Sampling Sampling	4.6 0.9	1.3- 3.0	< 2E-06	0.0015	5.0	Meandering	5	0.5-3.0
Gomez <i>et al.</i> (1989) (and Carey (1985))	Flume (SAFHL)	Continuous measurement	23.5	6.04	0.860	0.0032	2.74	Straight	0.47, 2.0 10.0, 100.0	
MACROSCALE										
Jackson and Beschta (1982)	Flynn Creek	Helley-Smith sampler	4 (bedload)	1.53	0.21	0.01	3.2	Meandering	\cong 720	
Kang (1982)	Hilda Creek	Basket sampler	30	\leq 0.57		0.04-0.07	11-17	Braided	50	
Southard <i>et al.</i> (1984)	Hilda Creek Laboratory model	Observation of morphology Observation of morphology	13-30	\leq 0.6			1-3 channels 2-3 channels	Braided Braided		
Gomez <i>et al.</i> (1989)	Flume (ERC)	Continuous measurement	4	0.54	0.115	0.0066	4.00	Straight	168.0	25-40

Table 2.4 (Continued)

Source	Location	Method	Bed material size d_{50} (mm)	Discharge ($m^3 s^{-1}$)	Sediment transport rate ($kg m^{-1} s^{-1}$)	Channel slope	Channel width (m)	Channel pattern	Pulse timescale (min)	Wave spatial scale (m)
MEGASCALE - ENDOGENOUS										
Romashin (1967)	Psezuane		260							500
Thornes (1976)		Channel width measurement				0.0045-0.0128	< 80			
Griffiths (1979)	Waimakariri R.	Cross-section surveys	34	1725 (m.a.f.)		0.0018-0.0041	900	Braided	Annual ?	1000 x 1 high
Church and Jones (1982)	Similkameen R.	Channel width measurement	Gravel	850			3 \underline{w}	Braided/wandering		42 \underline{w}
	Lillooet R.	Channel width measurement	Gravel	850			6.1 \underline{w}	Braided/wandering		37 \underline{w}
	Bella Coola R.	Channel width measurement	Gravel	565			3.9 \underline{w}	Braided/wandering		36.5 \underline{w}
Beschta (1983b)	Kowai R.	Channel width measurement	20	120 (2 year flow)		≤ 0.03	≤ 250	Braided/wandering		1300
Ashmore (1985)	Laboratory model	Collection of total load - 1 min every 15 min	1	0.0012-0.0045	0.002-0.02	0.01-0.015	0.38-1.06	Braided	240-480	
Nakamura (1986)	Furano R.	Width and sediment storage				0.10	34	Mountain torrent		300, 400, 1500
	Saru R.	Width and sediment storage				0.0036	151		850 - 2000	
Davies (1987)	Rakaia R.	Channel pattern	39	2291 (m.a.f.)		0.0036	1250	Braided		5000

Table 2.4 (Continued)

Source	Location	Method	Bed material size d_{50} (mm)	Discharge ($m^3 s^{-1}$)	Sediment transport rate ($kg m^{-1} s^{-1}$)	Channel slope	Channel width (m)	Channel pattern	Pulse timescale (min)	Wave spatial scale (m)
MEGASCALE - EXOGENOUS										
Gilbert (1917)	Sacramento									
Mosley (1978)	Tamaki	Tracer material dispersion	38	4.5		0.022	10-15	Meandering		< 2000 p.a.
Griffiths (1979)	Tarawera	Cross-section surveys							7 years	
Madej (1982)	Big Beef Creek	Sediment storage surveys	gravel	30 (10 year R.I.)		0.002-0.01	≤ 35	Meandering		800
Beschta (1983a)	Kowai R.	Channel width measurement	20	120 (2 year flow)		≤ 0.03	≤ 250	Braided/Wandering		≅ 1000
Pickup <i>et al.</i> (1983)	Kawerong R.	Cross-section surveys	6	4-6		0.02-0.071		Braided	4-6 months	6000-35000 p.a.
Meade (1985)	East Fork R.	Cross-section surveys	0.5-1.5 (bedload) 16-64 (pavement)	≤ 45		0.0007	20	Meandering		500-600
Roberts and Church (1986)	Queen Charlotte Ranges streams	Sediment storage surveys	gravel							100 (1 example)
Kelsey <i>et al.</i> (1987)	Redwood Creek	Sediment storage surveys	16-90			0.015		Meandering		30 years
Macklin and Lewin (1989)	River South Tyne	Channel width, natural tracer dispersion	gravel	400 (m.a.f.)		0.0055-0.0128	26-37	Wandering		1690

Church, p.319, for discussions of these data). Ehrenberger's (1931) and Einstein's (1937) data also reveal quasi-regular fluctuations (Hubbell, 1987 p.90). Einstein (1937) was able to correlate bedload particle size with transport rate (Carey, 1985). Sampling variability is also a problem with the Slate Creek data of Emmett (1975) where the bedload transport rate varied by up to 10 times over a 2.5 hour period in the absence of any bedform migration (Klingeman and Emmett, 1982). While this may reflect the occurrence of a bedload pulse, Klingeman and Emmett (1982) emphasised variability in the sampling technique in their discussion of these data.

Gomez (1983), using a Helley-Smith bedload sampler, obtained a similar pattern of cross channel variations, as well as temporal changes in bedload transport rates. At individual locations bedload pulses occurred with a period of less than 1 hour (Gomez, 1983. Figures 2 and 3), but it is unclear to what extent this is a sampling effect. Combining the data to obtain total bedload discharge for the section to try to reduce the influence of this effect, the pulse period becomes 1.5-2 hours. The sampling problem recurs in data from Hilda Creek, Canada, where a basket sampler was used in a straight reach of channel (Kang, 1982). Variations of 20 times in bedload transport over time periods of less than 10 minutes were recorded. Smaller pulses with a mean frequency of 14 minutes were also noted, and Fourier analysis revealed a broad peak over periods from 20 to 50 minutes. A further example of possible bedload pulses is the Elbow River data of Samide (1971) (cited by Carson and Griffiths, 1987), where order of magnitude variations in bedload transport rate occurred with discharge changes of less than 10%. Jackson and Beschta (1982) reported bedload sampling data which exhibits fluctuations that are uncorrelated with water discharge variations. Bedload pulses have also been recorded in Duck Creek, U.S.A. (Whiting, Dietrich, Leopold, Drake and Shreve, 1988) in a straight reach, and were inferred to be occurring in Muddy Creek by the same authors.

Bedload from the entire channel width was trapped by Hayward (1979, 1980) in the Torlesse Stream, New Zealand. A 3 m wide vortex tube sampler was installed in a straight reach of the Torlesse (Hayward and Sutherland, 1974), where the valley slope is 0.067. Bedload pulses over timescales ranging between 0.8 and 5 hours were recorded. A similar study on Virginio Creek, Italy (Tacconi and Billi, 1987) reported pulses occurring with periods of 20-30 minutes. Virginio Creek is 12m wide and has a slope of 0.008 where bedload was collected. The other major study of this type is that in Turkey Brook, United Kingdom (Reid *et al.*, 1985) where bedload was trapped in boxes and continuously weighed by means of pressure pillows connected to a transducer (Reid *et al.*, 1980). Turkey Brook is 3m wide, straight and has a slope of 0.0086 at the measurement site. Over a range of bedload transporting flow events, pulses occurred 1.4-2 hours apart (mean 1.7 hours). This pattern was repeated across the channel, although there were differences in the rates of bedload transport between adjacent samplers (Reid *et al.*, 1985). A different approach using electromagnetic detection rather than collection of bedload (Custer, Bugosh, Ergenzinger and Anderson, 1987) in Squaw Creek, U.S.A. recorded pulses at variable

intervals during a bedload transporting event, with 0.6 minute intervals early in the event, succeeded by more sustained pulses approximately 6 minutes apart.

All of the studies discussed so far have come from rivers with continuous or near continuous water flow. Lekach and Schick (1983) provided an example of similar behaviour from the ephemeral Nahel Yael in Israel. Bedload was sampled with a bucket sampler located in a small waterfall. As the water discharge varied through a five hour event several waves of sediment were recorded. The waves passed the sampling site about every 50 minutes and one longer feature was also noted. There are no data on associated bedform migration.

Whereas variable discharge has complicated the identification of mesoscale bedload pulses in field studies, constant flow rates in laboratory flumes have enabled clearer identification of the phenomena (Carey, 1985). In a test of sampler efficiency, Gibbs and Neill (1973) (cited by Carson and Griffiths, 1987; Figure 3.12b) found variations in bedload transport rate with constant flow conditions. Coefficients of variation (standard deviation of transport rate / mean transport rate) ranged between 44 % and 82 % (White and Day, 1982 p.190). A further set of observations originally collected for the same purpose have also yielded data on bedload pulses. Carey (1985), Hubbell (1987) and Gomez *et al.* (1989) discuss these results and Carey (1985) also considers similar data from a sand-bed river. The gravel-bed laboratory data contain oscillations with periods ranging from 28 to 6000 seconds (Gomez *et al.*, 1989). The ranges of variation are 0-3.3 and 0-4.5 times the mean rate, the former being associated with a shorter sampling interval than the latter. Iseya and Ikeda (1987) measured bedload transport rates every 10 seconds over a 5-6 minute period in experimental runs with a range of bed material mixtures. Variations in bedload transport rates with periods of 100-200 seconds were observed but only in runs where both sand (median grain size 0.4mm) and gravel (2.6mm) were fed into the flume. In a wide ranging set of experiments Kuhnle and Southard (1988) found pulses with a range of period of 5-26 minutes. Unlike the Iseya and Ikeda (1987) experiments, three dimensional bedforms were observed in these experiments.

B. Macroscale. In comparison with both meso- and mega-scales, there have been few studies of bedload pulses and bed waves at the macroscale. This is because of the relatively long monitoring period required for detection of bedload transport rate fluctuations at this scale, and the spatial scale being too small for sediment storage volumes to be readily measured or inferred. Nevertheless, some mesoscale studies have noted longer period fluctuations in bedload transport rates. Kuhnle and Southard (1988) noted more than one significant period of fluctuation in some of their runs. Gomez *et al.* (1989) used a 5-minute sampling interval in a 160m (long) x 4m (wide) flume. Bedload pulses with a period of 168 minutes were measured, and related to the migration of alternate bars. Kang (1982) observed a poorly defined peak in spectral density over periods of up to three times that of the smallest scale fluctuations in Hilda Creek

bedload transport rates. In a separate study of Hilda Creek, Southard *et al.* (1984) described a chute and lobe formation, giving rise to episodic downstream transfer of material. These features are single units that are too large to be considered mesoforms and can be classified as macroforms, although how they relate to other macroform features is unclear (Southard *et al.*, 1984). Similar features were replicated by the same authors in a laboratory model of braided rivers with low depth / grain size ratios (depth / d_{90} was usually < 1 , and rarely exceeded 3, where d_p is the grain size with p % finer).

The small number of studies at this scale reflects the difficulties of measuring bedload at such a scale. Unit and complex bars, which are the major morphological elements at this scale, are characterised by sudden and episodic changes in form during which sediment transport is also characterised by short bursts of activity (Smith, 1974). Thus, bedload pulses at this scale should be widespread where active bar growth and erosion are occurring. Similarly, exogenous pulses should be identifiable as material input to the river is redistributed.

C. Megascale. At this scale, river morphology has a relaxation time of the same order of magnitude as the river system as a whole (Table 2.1). It therefore becomes difficult to differentiate between truly endogenous bed waves and those occurring as responses to changed environmental conditions. The range of spatial and temporal scales contained within the megascale grouping is considerable, so this difficulty is more pronounced for some cases than for others. Some authors have argued that the megascale bed waves which they have identified have endogenous origins. Griffiths (1979) used the bed wave hypothesis to account for a considerable discrepancy between measured and predicted long-term bedload yields in the Waimakariri River, New Zealand. This hypothesis suggests bar assemblages up to 1km long which produce a rise in river bed level of about 1m. Davies (1987) suggested that similar waves may exist in the Rakaia River, New Zealand, based on downstream variations in channel pattern. Although both of these rivers would be considered to be unaffected by recent changes in environmental conditions, there is evidence that coastal erosion has caused the development of incised trenches in both rivers extending upstream from their mouths (Wilson, 1985). This trend could account in part for the discrepancy noted by Griffiths (1979), but seems unable to explain the regularity in channel patterns noted by Davies (1987) which is equally apparent in aerial photographs from other times.

Davies' (1987) correlation of channel pattern and sediment storage is based on the suggestion of Church and Jones (1982) and Church (1983) that 'sedimentation zones' and 'transfer reaches' characterise active gravel river morphology. Sedimentation zones in the Similkameen, Bella Coola and Lillooet Rivers, British Columbia are characterised by increased width of channel activity. A similar pattern is reported for the Psezuane R., USSR by Romashin (1967; cited by Church and Jones, 1982). Church and Jones (1982) related these features to sediment supply, and in

particular to the location of alluvial fans entering the rivers. The regular alternation of these two types of reach is preserved, although a reduction in supply has occurred in the last century as erosion of Neoglacial moraines has slowed down (Church, 1983). Channel width has been used in this regard by Beschta (1983b), who interpreted cyclic variations in widths of the Kowai River, New Zealand in terms of sediment storage variations. Similar patterns of channel width and braiding intensity were also noted in ephemeral streams in Spain by Thornes (1976), who also related them to the occurrence of active sedimentation. Width variations are also correlated with long wavelength peaks in spectral analysis of sediment storage volumes by Nakamura (1986), which are concomitant with cycles of erosion and deposition, and are interpreted as the sediment transport distance in past floods. Nakamura (1986) also reviewed other Japanese work which has reported wave-like behaviour of sediment, based on sediment storage patterns and river long-profile studies.

Ashmore (1985, 1987, 1988) used a recirculating flume with constant water discharge to investigate braided river processes. Bedload pulses developed and were associated with changes in channel and bar patterns (Ashmore, 1987). In most of his experiments more than one scale of bedload pulse was detected but the longer period ones fit into the megascale rather than the macroscale, due to their association with large scale bedforms. In order to maintain equilibrium the sediment feed rate at the head of the flume varied as the sediment was re-circulated, which could have the effect of preserving pulses once they initially developed in the system. Pulses of different scales, developed during the initial development of a braided channel in the early parts of the experiments, could be travelling at variable speeds, and superpose to give the sort of quasi-periodic bedload transport rates that were measured.

No studies have demonstrated unequivocally the existence of endogenous megascale bed waves. It is difficult to see this being achieved under field conditions since little is known about sediment supply variations and long term adjustments to environmental conditions in gravel rivers, and it is extremely difficult to eradicate the noise introduced by unsteady flow and sediment supply conditions (Nanson, 1974; Gomez *et al.*, 1989). The laboratory study of Ashmore (1985, 1987, 1988) provides the best available evidence that such features can be independent of sediment supply variations.

Other work has described bed wave characteristics in conditions where sediment supply is known to have varied. The idea that material introduced in such a way could migrate downstream as a wave was first mentioned by Gilbert (1917) following a study of mining debris dispersion in the Sierra Nevada, U.S.A. A similar situation was modelled by Pickup *et al.* (1983), using data from the braided Kawerong River, Papua New Guinea, where relatively fine debris from mining tailings overloaded a narrow, boulder-bed stream and promoted aggradation and braiding (Pickup, 1988). Macklin and Lewin (1989) measured channel width changes in the River South Tyne, U.K., and

noted the tendency for deposition to be concentrated in sedimentation zones. Sediment supply was accelerated due to lead and zinc mining in the 19th Century, and the pattern of subsequent storage changes has been complex. A related study of the effects of disturbance is that of Roberts and Church (1986). They identified sediment wedges produced during a phase of extensive logging in the Queen Charlotte Ranges, British Columbia. Channel width and slope change abruptly at the upstream and downstream limits of the wedges, which are persistent due to trapping material delivered from further upstream and adjacent slopes. The impact of logging was also noted by Madej (1982) who observed degradation in a logged reach of Big Beef Creek, Washington, U.S.A., and aggradation near its mouth. Aggradation was accompanied by rises in the number and size of mid-channel bars and a decrease in channel length. A second wave of sediment in the creek was due to a later logging episode. Kelsey *et al.* (1987) described the passage of a wave of sediment through Redwood Creek, California, which was introduced as a consequence of hillslope failure during a 60-80 year recurrence interval event. Similar patterns of material transfer occurred for material derived from bank erosion and mass movements. Bed level fluctuations in the Tarawera River, New Zealand, illustrate this (Griffiths, 1979), and Beschta (1983a,b) described downstream migration of a large bed wave following a major storm in the Kowai River in 1953. This wave has moved at less than 1km p.a. on average, and is identified by increased width of the active channel as it passes through a reach, followed by narrowing.

Only one study of waves at this scale, that on the East Fork River, USA, obtained detailed data on wave geometry and migration (Meade, 1985). Waves in the East Fork River are very well defined, and take the form of sand dunefields migrating across a gravel pavement. The source of material for the dunefields is erosion in a tributary, Muddy Creek, due to increased summer flow as irrigation water is discharged through it. The location of the dunefields is constant from year to year (Meade, 1985) suggesting that the storage zones are hydrologically determined. The continued adjustment of Muddy Creek to augmented discharge, and the supply of large amounts of sand to a gravel-bed river, suggest that this is not an equilibrium situation. Mosley (1988) reported a similar case from Antarctica where sand bedforms migrate across a gravel pavement, in which variability in sediment transport rates reflects availability of the sand sized material for transport.

2.2.4. Suggested mechanisms of wave and pulse development

A. Analysis in terms of dimensionless discharge and stream power. The classification used in Table 2.3 has provided an adequate basis for the description so far, although the boundary between the macro- and mega-scales is indistinct. Some of the studies classified as megascale may be better viewed as macroscale and within the megascale class, a wide range of scales cause further potential confusion. Revision of this scheme may be possible if the processes responsible for wave and pulse development were better understood. The wide range of scales

involved and the change in governing factors as bedform scale increases (Table 2.1) suggest that there may be more than one form of bed wave. Some studies (e.g. Ashmore, 1985; Nakamura, 1986; Kuhnle and Southard, 1988) have reported more than one scale of bed wave. This could reflect the addition of identical features, the existence of similar features at different scales, or the presence of distinctly different features at different scales. To attempt to identify different types of bedload pulse and bed wave, pulse timescale and wave spatial scale can be compared with dimensionless water discharge and a dimensionless stream power index. Dimensionless discharge, q^* , is given by,

$$q^* = Q / b ((S_s - 1) g d_{50}^3)^{0.5} \quad (2,1),$$

and the dimensionless stream power index, ω^* , by,

$$\omega^* = Q S / b ((S_s - 1) g d_{50}^3)^{0.5} \quad (2,2).$$

Q = water discharge ($m^3 s^{-1}$), b = flow width (m), $(S_s - 1)$ = the submerged specific gravity of sediment ($\cong 1.65$, usually), and S = channel slope. Pulse period was obtained from published studies by counting the number of peaks in sediment transport rate series and dividing by the measurement interval. Where the authors had identified significant periods by Fourier analysis or autocorrelation these data were used instead. The data are plotted in Figures 2.2 and 2.3 and are reproduced in Appendix 1. The minimum pulse period that could be identified depended on the sampling interval used, but there is no direct relationship between these two variables (see Appendix 1). For Ashmore's (1985) experiments the pulse period has been scaled by $\lambda_L^{1/2}$, where λ_L is the length scale of the model. This scaling is a consequence of using Froude number modelling (Yalin, 1971a).

Where the periods of bedload fluctuation are available there are distinctions between meso- and mega-scale studies. Hayward's (1980) data is the sole exception, plotting along with macroscale data in terms of q^* and ω^* (Figures 2.2b, 2.3b). Field and laboratory studies of the same scale overlap when period is plotted against either q^* or ω^* . The limited macro-scale data plot in the same region of the ω^* graph as Hayward's data. The longest period identified by Gomez *et al.* (1989) from their SAFHL data set also plots along with these data. This suggests that a different process mechanism is responsible for this scale of fluctuation than for the shorter ones, which confirms their own description of these data (see 2.2.4B. below). The paucity of macroscale and megascale data of this type prevents definite conclusions from being reached, but the distinction is sufficiently clear to suggest that different processes may be producing bedload pulses of different scales. This interpretation is subject to an adequate explanation for the anomaly of Hayward's (1980) data from Torlesse Stream which is regarded as mesoscale. Within the mesoscale data, there are order of magnitude variations in pulse period at given q^* or ω^* , and period can remain constant while q^* or ω^* themselves can vary by an order of magnitude. Thus, different scales of process may be operating within the mesoscale group. Ashmore's (1985) data plot separately from all of the other data. This study is the only one in the data set of braided

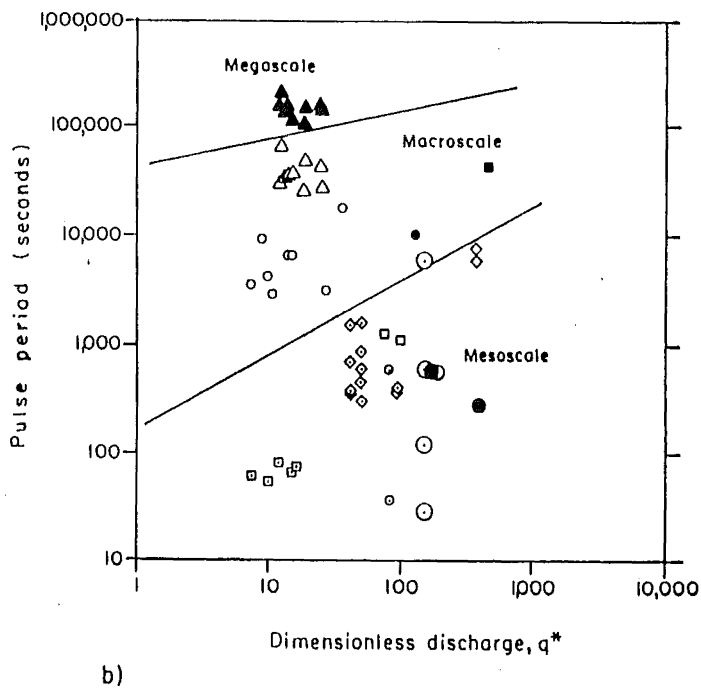
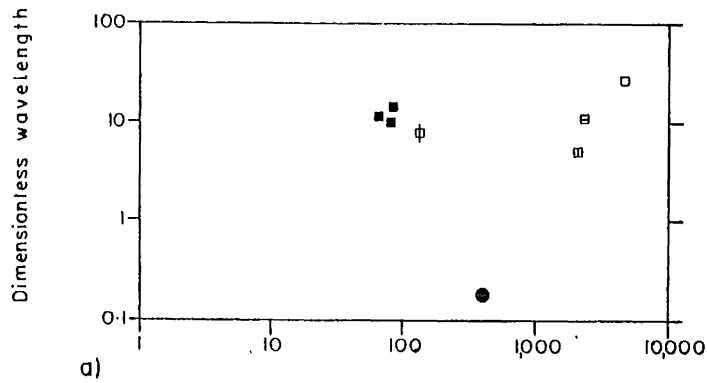


Figure 2.2 Spatial and temporal scales of bedload pulses and bed waves related to dimensionless water discharge. The data used in construction of the plots are presented in Appendix 1. Pulses of different scale were identified in the same experimental runs by Ashmore (1985), Kuhnle and Southard (1988) and Gomez *et al.* (1989). Custer *et al.* (1987) identified two temporal scales in one bedload transporting event in a prototype river. All scales identified in these studies are plotted.

- Sources: a) \boxplus Griffiths (1979); \blacksquare Beschta (1983a); \square Meade (1985); \boxminus Davies (1987);
 ● Whiting *et al.* (1988); ϕ Gomez *et al.* (1989) ERC Run (line shows the range of measured wavelengths)
- b) \circ Gibbs and Neill (1973); \circ Hayward (1979); \blacksquare Jackson and Beschta (1982); \diamond Gomez (1983); \triangle , \blacktriangle Ashmore (1985); \circ Custer *et al.* (1987); \square Iseya and Ikeda (1987);
 \square Tacconi and Billi (1987); ● Whiting *et al.* (1988); \diamond Kuhnle and Southard (1988);
 ● Gomez *et al.* (1989), ERC Run; \odot Gomez *et al.* (1989) SAFHL Run.

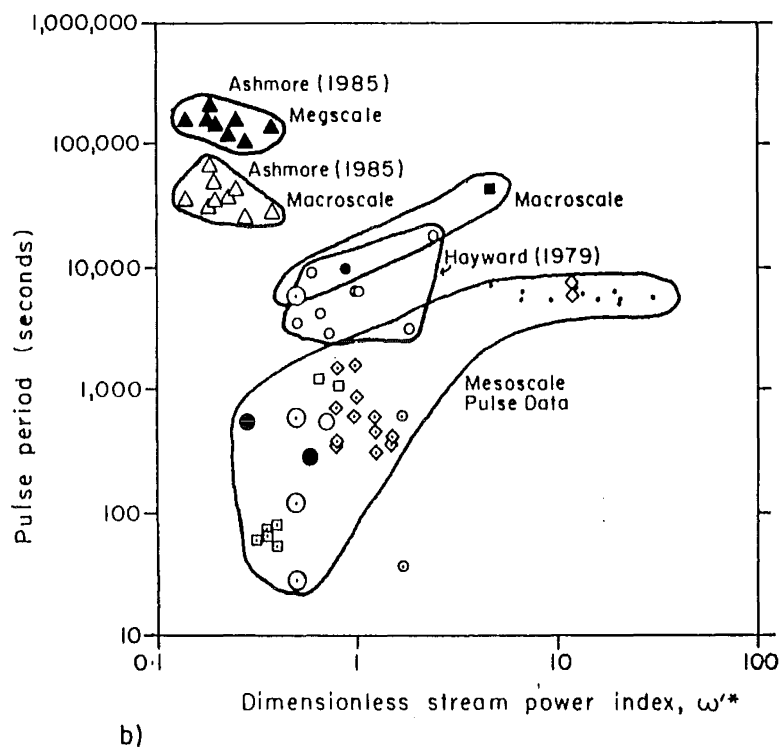
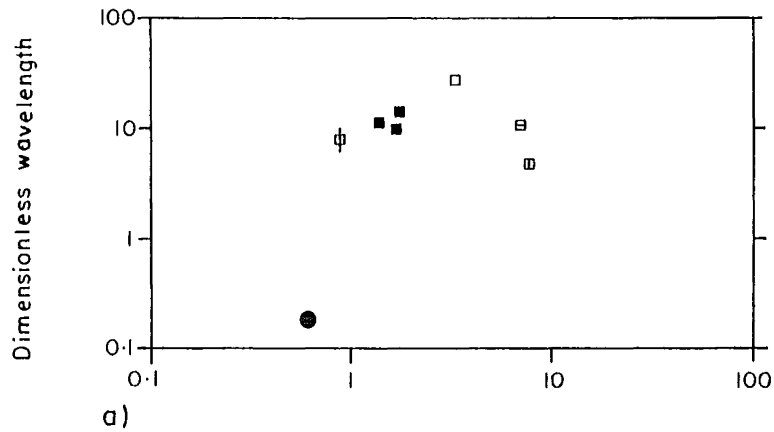


Figure 2.3 Spatial and temporal scales of bedload pulses and bed waves related to a dimensionless stream power index. The data used in construction of the plots are presented in Appendix 1. See Figure 2.2 for additional notes.

Sources: a) \boxplus Griffiths (1979); \blacksquare Beschta (1983a); \square Meade (1985); \boxminus Davies (1987); \bullet Whiting *et al.* (1988); \oplus Gomez *et al.* (1989) ERC Run (line shows the range of measured wavelengths)

b) \circ Gibbs and Neill (1973); \circ Hayward (1979); \blacksquare Jackson and Beschta (1982); \diamond Gomez (1983); \triangle , \blacktriangle Ashmore (1985); \cdot Reid *et al.* (1985); \circ Custer *et al.* (1987); \boxminus Iseya and Ikeda (1987); \square Tacconi and Billi (1987); \bullet Whiting *et al.* (1988); \diamond Kuhnle and Southard (1988); \bullet Gomez *et al.* (1989), ERC Run; \circ Gomez *et al.* (1989) SAFHL Run.

streams and the only one which used self-formed model streams. Either or both of these factors could be responsible for the position of these data on Figures 2.2b and 2.3b, but morphological evidence (Ashmore, 1985, 1987) suggested that these data reflect the existence of larger scale bed waves than have been reported from other studies.

Where bed wave length (λ) is the only available data, little emerges in the way of a clear pattern. Wavelength appears little changed as q^* rises (Figure 2.2a), except for the mesoscale data of Whiting *et al.* (1988). In terms of ω^* , the wide braided rivers (Rakaia and Waimaikariri) have wavelengths that are shorter than others with lower stream power. Again the paucity of data is a problem, but these patterns can be explained. The use of mean annual flood for the Rakaia and Waimaikariri Rivers may overestimate their dominant discharge. Davies (1988) calculated the dominant discharge of the Rakaia to be in the range $600 - 800\text{m}^3\text{s}^{-1}$, which yields a value of ω^* only 1/3 of that given by the mean annual flood. The inconsistency in definition of an appropriate representative flow magnitude is a further cause of the variability seen in Figures 2.2a and 2.3a.

Noteworthy on these plots is the good correlation between the data from the sand bed East Fork River and the gravel bed rivers, which suggests that the processes producing bed waves may transcend river classifications based on grain size. However, the previously noted fact that the East Fork River has a gravel pavement over which sand bedload moves complicates this issue.

In conclusion there is some evidence that bedload pulses and bed waves at particular scales occur with reduced frequency (increased period) as dimensionless discharge and stream power increase. Since bedload transport rate depends on stream power, the dimensionless power approach is preferred. This enables a distinction between meso-, macro- and mega-scale pulses to be drawn, although with one significant anomaly. This supports the assertion in Table 2.1 from Jackson (1975) that there is a change in dominant process between the meso- and mega-scales.

B. Suggested process mechanisms. As a consequence of the greater detail of observation and process measurements at that scale, the mesoscale studies have made the most comprehensive suggestions regarding the processes producing bedload pulses, although many are based on a small number of samples (Gomez *et al.*, 1989). Instantaneous fluctuations occur as a consequence of the mechanics of particle entrainment and transport. The development of an armour layer causes a decrease in bedload transport rate (Gomez, 1983). This need not be a unidirectional process, since armouring depends on previous flow event magnitude and on the relationship between prevailing flow conditions and the particle size of the surface material. Where armouring has developed, displacement of clasts leads to considerable erosion in the resultant gap in the armour layer. Such an effect could produce small scale bedload pulses (Custer *et al.*, 1987). Naden (1987) using a mathematical modelling procedure found that the erosion of certain particles from an armoured bed could have such an effect, and Kuhnle and

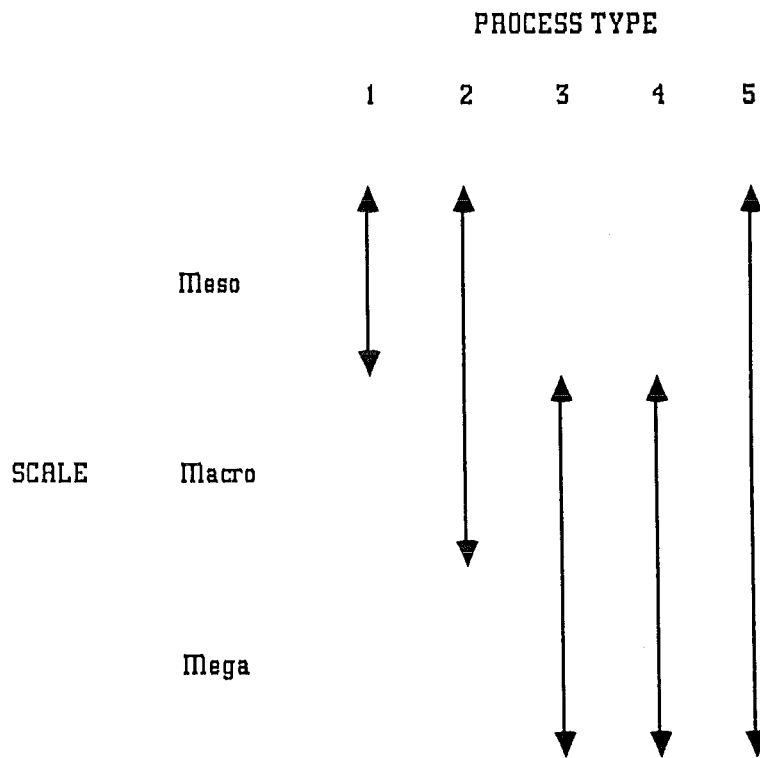


Figure 2.4 A generic classification of bedload pulses and bed waves based on explanations suggested in the literature. Arrows indicate the spatial and temporal scales over which the different process types have been suggested to operate. Process Type 1 is sediment sorting and hiding effects; Type 2 - bedload sheets; Type 3 - the effect of bar and channel formation and erosion; Type 4 - drainage network interlinkages; Type 5 - inputs of exogenous sediment to the river system.

Southard (1988) noted the episodic motion of large clasts in their flume experiments. The erosion of small scale cluster bedforms would have a similar effect on sediment transport rate. Such explanations can be used to account for small scale bedload pulses that occur irregularly in space and time. This category of sediment sorting and hiding effects are referred to as Type 1 processes (Figure 2.4).

More regular pulses have been noted in several studies and have been associated with low relief bedforms (bedload sheets; Type 2 processes in Figure 2.4: Kuhnle and Southard, 1988; Whiting *et al.*, 1988). These features have been described as one or two coarse (d_{70} - d_{90}) grains high, and at least two orders of magnitude longer than they are high (Whiting *et al.*, 1988). Similar features were found by Kuhnle and Southard (1988), and in both studies coarse material was observed to concentrate at the leading edge of the sheets. Gomez *et al.* (1989) identified three types of bedform each associated with bedload transport rate fluctuations of particular periods. The smallest were 'ripples' (1-2 grain diameters high), followed by 'primary dunes' (about 4m long, 6-9 grain diameters high, and migrating downstream), and 'secondary dunes' (0.4m long, 2-3 grain diameters high, superposed on the upstream faces of primary dunes). Their description of primary dunes appear similar to bedload sheets, which in turn may correspond to 'diffuse gravel sheets' (Hein 1974; Hein and Walker, 1977) in gravel rivers where active bar growth is occurring. These are a few grains high and can extend across the entire channel width (Hein and Walker, 1977).

Low sand and gravel sheets were reported by Iseya and Ikeda (1987) who described processes of longitudinal sediment sorting in detail. The longitudinal sorting is similar to the less detailed observations of Kuhnle and Southard (1988) and Whiting *et al.* (1988). The bedload transport rate was greatest in the 'smooth' bed state where sand dominated the bed. In the 'congested' state, bedload transport rates were reduced as a consequence of gravel particle interlocking (Iseya and Ikeda, 1987; their Figure 6). Bedload pulses resulted from the changing availability of material in response to longitudinal sorting. As discharge was constant, it can be assumed that the bedload transport capacity should increase with slope; the results of Iseya and Ikeda's experiments suggest the reverse trend, illustrating the importance of the sediment sorting effect. A similar sort of supply control over bedload has been postulated by Tacconi and Billi (1987).

In stressing the role of longitudinal sorting rather than the vertical dimension of small bedforms, Iseya and Ikeda (1987) have explained how bedload pulses can occur in the absence of obvious bedforms, although the small amplitude of such bedforms (e.g. Gomez *et al.*, 1989) may have prevented their identification in other studies. Such phenomena have been tentatively accounted for in terms of kinematic waves (Langbein and Leopold, 1968; Reid *et al.*, 1985). Longitudinal sorting may not always be so clearly developed as in Iseya and Ikeda's flume experiments. They found that the degree of sorting and development of bedload pulses, were

dependent on the sand: gravel ratio of the input material. Reid, Brayshaw and Frostick (1984) were able to show using an electromagnetic sensor that particles actually move in groups. A similar technique led to suggestion of the kinematic wave explanation as one of a number of possibilities for producing bedload pulses (Custer *et al.*, 1987).

In all of the explanations suggested above, sediment availability has been limited by the consequences of coarse particle interaction. Hayward (1979) suggested that bedload pulses in the Torlesse Stream are due to periodic evacuation of material stored in pools above the recording station. This is also a sediment supply related explanation for bedload pulses but is of a different type. Sediment sources in the Torlesse are restricted to certain locations along the river and change only infrequently, whereas in the other rivers described any part of the bed could serve as a sediment source. The explanation for bedload pulses in the Torlesse lies in its characteristic step-pool morphology (Hayward, 1980), and restricted locations of sediment storage. Step spacing then becomes the critical control over bedload pulse frequency, and it could be envisaged that pulses generated in this way would be less frequent than those generated by longitudinal sorting mechanisms. The Torlesse is therefore affected by structural elements (Whittaker, 1987) and does not have a purely gravel bed as do the other channels reported herein. This could explain the anomalous position of the Torlesse data in Figures 2.2b and 2.3b.

The explanation of bed waves at the macro- and mega-scales has generally had to rely on inference of processes in the absence of detailed process measurements at bedload transporting stages. An exception to this is the ERC run of Gomez *et al.* (1989) in which alternate bar migration was closely correlated with sediment output rate variations. Given that bar growth and erosion, and channel changes are continually occurring processes during bedload transporting events in many gravel bed rivers, variations in bedload transport rate over time would be expected. Jackson and Beschta (1982), for example, were able to relate bedload transport rate fluctuations to a scour-fill sequence. In braided rivers, even if the overall channel morphology was stable, variations due to channel division and confluence would cause differences in bedload transport capacities (Ashworth and Ferguson, 1986). The basic processes associated with braided rivers were suggested by Kang (1982) as the probable cause of measured bedload pulses. Southard *et al.* (1984) also demonstrated how the deposition and subsequent erosion of braided river bedforms leads to variation in the sediment output from a reach under constant flow conditions. Thus, at the macroscale bedload transport rate fluctuations would be expected as a consequence of the dynamic nature of river morphology in such rivers. These are Type 3 processes (Figure 2.4). Hein and Walker (1977) related diffuse gravel sheet behaviour to the growth of unit bars and thus provided a mechanism to relate the meso- and macro-scales of bedform. The bedload pulses that exist due to unit bar deposition and erosion can be related to the pulses occurring at a smaller scale and can be considered to be manifestations of the same processes. Gravel sheets

were considered to be macroforms by Church and Jones (1982) (see Table 2.1), but the temporal and spatial scales of bedload transport rate fluctuations led to bedload pulses produced by such sheets being classified as mesoscale. This inconsistency suggests that gravel sheets may exist at both the mesoscale and the macroscale with similar controlling processes operating at both. The controlling process difference between the meso- and macro-scales is therefore suggested to be an oversimplification of the controls over bedload pulses at these scales. Further, not all the mesoforms have macroscale counterparts (e.g particle clusters) and so at least two mesoform types need to be identified.

The occurrence of megascale bed waves has also been accounted for in terms of the basic processes of channel and bar change in braided rivers by Ashmore (1987). The only study which reports both detailed bedload transport rates and channel morphology is Ashmore's (1985, 1987) work. His conclusion that the large-scale wavelike movement of bed material is a fundamental element of braided river mechanics (Ashmore, 1987), suggests that the same processes which produce macroscale bedload pulses also produce megascale ones. This would be expected on the basis of the classification of Table 2.1. Although with less complete data than Ashmore's, other workers have postulated similar mechanisms for megascale bed waves. Griffiths (1979) suggested that the waves may take the form of groups of bars with plane bed sediment transport occurring across the upper bar surfaces. His emphasis on a process occurring at the macroscale to account for a megaform is further evidence of the links between these scales. A similar description is provided by Church and Jones (1982) who added that megaforms are likely to be self-sustaining, although possibly attenuating, once one such feature develops in a river. Thus, episodic supply of material to a river would be expected to produce megaform assemblages, which would become permanent features so long as supply events occurred sufficiently regularly. This provides a mechanism for exogenous bed waves to produce endogenous ones further downstream. Beschta (1983b) accounted for such development in terms of Schumm's (1977a) concept of complex response. This implies that a pulse of material introduced due to an infrequent event or a climatic change (e.g the erosion of Neoglacial moraines in the Bella Coola system - Church, 1983) can cause bed waves to develop for a considerable time afterwards, and these may be difficult to differentiate from truly endogenous waves. However, Macklin and Lewin (1989) regarded the complex response model as inadequate to account for the intricate pattern of storage exchanges within the River South Tyne.

The waves in the East Fork River have already been noted to be quite different from those in active gravel-bed rivers. Meade (1985) raised the question as to whether the wave forms could be a response to the transient conditions imposed by the increase in sediment input to the river. If the effects of disturbances such as this persist in river systems as Church and Jones (1982) suggested, localised events could cause the widespread occurrence of waveforms within a river system. In none of the megascale studies reported above has the river system been

undoubtedly in long-term static equilibrium, and all have had accelerated sediment input at some time in the historical past. In Ashmore's (1985, 1987) flume study, sediment input varied regularly as the flume operated a recirculating sediment system. Thus, all reported megascale waves could be viewed as exogenous features and there remains doubt as to what extent bed waves are inherent characteristics of river systems (Meade, 1985).

Briefly moving away from humid region rivers, two studies have identified bed waves in arid areas. Lekach and Schick (1983) rejected explanations for bedload pulses in the Nahel Yael that rely on bar accumulations or evacuation of material from pools, since these features are only present in a limited part of that catchment. They suggested that explanations may be sought in terms of the nature of slope-stream interactions (i.e the transfer of material from hillslopes into the river system), or discontinuities in drainage area that occur at channel confluences. Thornes (1976) made a similar suggestion to account for channel width changes in semi-arid streams in Spain. The stream lengths and basin areas above a particular point are held to be responsible for the channel width. This effect is augmented by transmission losses, which are especially great in areas of sediment accumulation (Thornes, 1976). This argument that bed waves are consequent upon drainage network structure may have application in humid area rivers also, especially where sediment supplying tributaries are widespread. Beschta (1983a) found a positive correlation between basin area and the length of aggradational zones in the Kowai River. This process Type is referred to as type 4 (Figure 2.4).

In conclusion, Figure 2.4 presents a wave type classification based on scale and process of formulation. Four process types have been identified in the preceding discussion, to which the role of external inputs to the river system is added as a fifth type. The simple scheme of Table 2.2 is shown to be inadequate as a basis for a generic classification of bedload pulses and bed waves.

C. Numerical modelling of bed waves. The simplest form of bed wave model is the kinematic wave concept used by Langbein and Leopold (1968), which has utility in the explanation of mesoscale bedload pulses. At this scale the modelling of wave phenomena has been little developed, but bedload pulses were one of the predictions of Naden's (1987) model of sediment entrainment and transport. A similar result has been obtained at the megascale by Hey (1979), whose dynamic process-response model of river channel development predicts alternating phases of degradation and aggradation, and river long profiles similar to those postulated to be associated with bed waves by Church and Jones (1982).

Several approaches have been taken to modelling bed waves. Griffiths (1979) produced a one dimensional kinematic model, which yields the bedload transport rate in terms of wave velocity and bed elevation. He demonstrated that total sediment transport rate depends upon both the wave geometry and essentially plane bed transport as predicted by equilibrium formulae. A similar one

dimensional approach was taken by Weir (1983) using linear stability analysis in combination with the Engelund and Hansen (1967) bedload equation to model sediment transport in the East Fork River. Using the quasi-steady approximation (i.e. assuming that local average water depth and velocity adjust instantaneously to changes in the bed profile), Weir (1983) concluded that a river in equilibrium which is transporting bedload should do so by a form of bed wave. In practical terms this method yielded a prediction of total bedload transport to within a factor of 2. Pickup *et al.* (1983) compared the results of two models with data from the Kawerong River, Papua New Guinea. Their sediment dispersion model depends on the velocity of sediment transport and a sediment dispersion coefficient. Little is known about the magnitudes or patterns of variation of either, so the effects of varying both were considered. Their second model assumed continuity of sediment transport using the Meyer-Peter and Müller (1948) equation to predict actual sediment transport. While both models predicted the total volume of sediment transported to within an order of magnitude, the pattern of downstream variations in deposition was reproduced only by the dispersion model. As noted above this model predicts wave attenuation, the magnitude of which depends on the value of the dispersion coefficient.

A different methodology has been utilised by Kelsey *et al.* (1987). They developed a stochastic approach to sediment transfer between storage reservoirs. In essence, their model assesses the probability of material from one location in the river bed (whether active or inactive sediment) moving to another location further downstream. This model successfully described the passage of a wave of sediment through a reach (Kelsey *et al.*, 1987). Moreover, it suggested that such waves are primarily confined to the active parts of the river bed, with material that is transferred from the active to the less frequently mobilised states being responsible for wave diffusion. This may account for the rapidity of wave diffusion in some cases, although Roberts and Church (1986) described how waves can be self-sustaining due to trapping coarse sediment.

The modelling of sediment waves has taken several forms. It is important to consider both sediment storage and transport processes in quantitative analysis of sediment transfer (Nakamura, Araya and Higashi, 1987; Richards, in preparation). Which method is most appropriate depends upon the scale of analysis and the aims of the modelling procedure. For the purpose of developing the understanding of bed waves the approaches described above all have utility. Small scale bedload transport processes (e.g. Naden, 1987) need to be understood to enable comprehension of bedload pulse generation, and larger scale consideration of transport rates and diffusion (e.g. Griffiths, 1979; Pickup *et al.*, 1983) helps to link bedload transport to channel morphology. The importance of sediment which is held in storage (Kelsey *et al.*, 1987) is useful for relating bedload processes to stored volumes of sediment, and hence to bed waves. Finally, models of channel evolution and process (e.g. Hey, 1979) enable bed waves to be put into the broader context of river geomorphology.

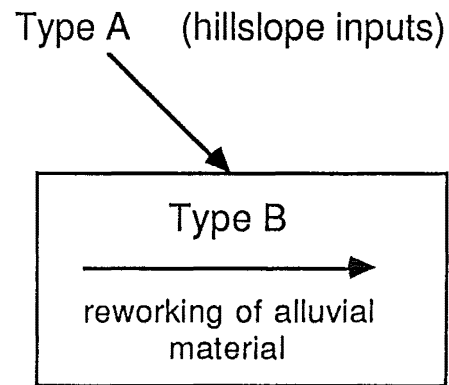
2.2.5 Sediment supply - transport capacity relationships in bed waves

The occurrence of a bedload pulse implies that sediment supply and / or the sediment transport capacity of the flow changes over time. There has been recent debate over the meanings of 'supply limited' and 'capacity limited' bedload transport (Richards, 1988). Church (discussion of Andrews and Parker, 1987) noted that equilibrium transport can still exist for the available sediment, but that the 'transport population' of grains may vary in a manner that is not simply dependent on instantaneous hydraulic conditions. Supply limitation is an appropriate concept for given particle sizes only i.e. " 'supply-limited' conditions... prevail when the amount of material of a given size range in transport is limited by its availability and not by the competence of the flow" (Pitlick and Thorne, 1987 - reply, p.183). Thus, the bedload pulses of Gomez (1983) represent an example of supply limitation caused by an armour layer reducing the availability of material of those sizes that the flow was competent to transport. In view of the exogenous - endogenous distinction made for bed waves above, material supply can be similarly categorised. Material that is input by exogenous processes has been called Type A sediment supply by Schumm (1977b). This represents input from hillslopes, terrace erosion, and other processes external to the river channel. Type B sediment supply is material that has been held in storage within the river, but which is re-mobilised, and is therefore endogenous. This is an adequate classification for a river system, but for a given river reach a third component of sediment supply needs definition, namely material input by the river from upstream. This is also exogenous to the reach under consideration and herein is defined as Type C sediment supply. These supply types are shown figuratively in Figure 2.5.

From the point of view of understanding bed waves, whether or not the transport : capacity ratio is constant is an important question. This ratio varies at the mesoscale (Hayward, 1979; Reid *et al.*, 1985), and there is evidence for similar variation at the megascale (Pitlick and Thorne, 1987). The interpretation of such variation has usually been in terms of supply limitation, which can be readily defined in some cases (eg Hayward, 1979; Gomez, 1983; Iseya and Ikeda, 1987). Little data is available on how the transport capacity of a river varies over time or downstream, although it has been speculated that capacity is not constant (Griffiths, 1979; Church and Jones, 1982; Ashworth and Ferguson, 1986). Care is needed in addressing this question since it is difficult to define capacity adequately. Simple application of an equilibrium bedload equation is an inadequate definition since the equations do not necessarily represent the flow intensity and entrainment conditions reliably (Richards, 1988). As bed waves are dynamic features which may enlarge or attenuate continuity of bedload transport cannot be assumed, especially over short time periods. Aggradation and degradation imply excesses of sediment supply over transporting capacity and the reverse, respectively.

At present it is difficult to assess the relative contributions of supply and transport limitation effects

a) Catchment scale



b) Reach scale

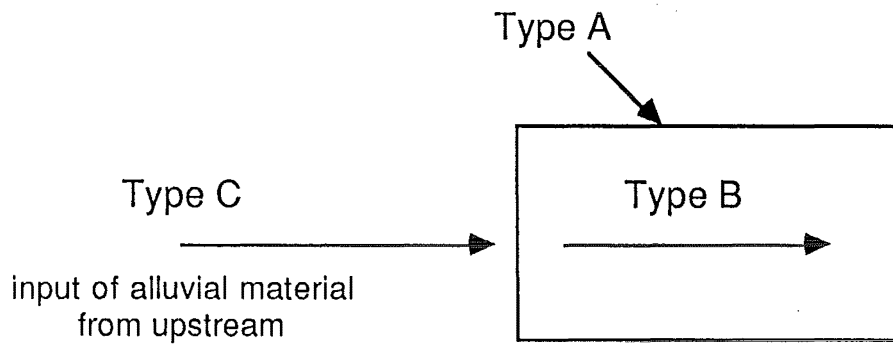


Figure 2.5 Definition of types of sediment supply to a river.

a) Catchment scale (after Schumm, 1977b)

b) Reach scale

to bed wave processes. Supply variations are known to occur and have been demonstrated to have significant effects in some cases. Bedload transport capacity variations are less readily defined, but are assumed to occur in many braided rivers where channel patterns vary downstream. The relationship between pattern and bedload transport is discussed in the following sections.

2.3 Interlinkages between channel patterns, and sediment storage and transport

The literature on channel patterns in gravel-bed rivers is extensive and has recently been reviewed by Carson and Griffiths (1987) and Ferguson (1987). This section does not attempt to review ideas on controls of channel pattern which are fully covered in these two references, but to identify those controlling factors which have direct implications for sediment storage and transport. Much of the literature has emphasised either hydraulic or sedimentary controls over channel pattern but few studies have produced contradictory results, suggesting that both flow intensity and sedimentary characteristics influence pattern development (Ferguson, 1987). The relationship between flow and sedimentary characteristics also determines sediment transport rates and hence patterns of sediment storage. This implies that there should be links between sediment transport and channel pattern. The nature of such relationships will be dependent upon the relaxation times of the two groups of processes. This is addressed more fully in sub-section 2.3.1.

The terminology used to describe channel patterns has become complex in recent years. Leopold and Wolman (1957) differentiated only three types: straight; meandering; braided. Their definition of braided was very broad (including any divided channel), and that of meandering unusually restrictive (encompassing only channels with sinuosity in excess of 1.5). This simple classification was taken to imply that the three groups were discrete by some subsequent workers. Recent developments have identified both different types of channel pattern, and transitional types between the major pattern groups (e.g. Carson, 1984a). Most authors now acknowledge that channel patterns lie on a morphological continuum and it is likely that a random sample of channel patterns would reveal that intermediate and transitional patterns are the norm rather than the exception (Ferguson, 1987). No particular classification is used herein and descriptive terms are defined where they are first introduced.

2.3.1 Hydraulic controls of channel pattern and their implications for sediment transport

The simplest suggested control over pattern is a combination of slope and discharge. The work of Lane (1957), Leopold and Wolman (1957) and Schumm and Khan (1972) suggested that for a given discharge there are threshold slopes between straight and meandering, and meandering

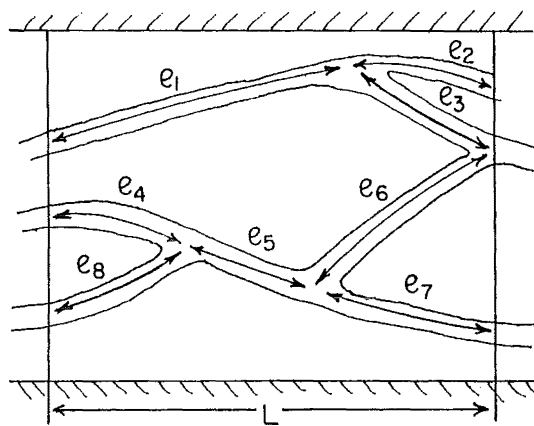
and braided pattern types. As discharge increases the critical slopes decrease. Ferguson (1987) described other studies which have yielded broadly similar results. Carson (1984b) noted that the thresholds are not so well defined as has often been suggested and that particle size has been omitted from the development of discharge-slope based thresholds. Even within individual bed material size classes, there is no clear discrimination between pattern types on the basis of slope and discharge alone, although braided rivers tend to have greater slopes and / or discharges. The combination of slope and discharge suggests that the thresholds may be based on mean stream power, ω_m , given by,

$$\omega_m = \rho_w g Q S / b \quad (2,3).$$

Ferguson (1981, 1987) has shown that inactive straight and sinuous channels have lower values of ω_m than active low-sinuosity ones, with actively meandering channels being intermediate. Carson (1984b) suggested that there is a threshold stream power for the onset of braiding but that this is not necessarily a discriminator from the meandering condition. The threshold between meandering and braiding is thus not as sharp as was supposed and Begin (1981) contended that it is gradational.

The empirical, hydraulically based controls over channel pattern discussed so far are not readily associated with a simple discriminator between pattern types, but may be able to be correlated with pattern if this can be quantified adequately. Thus far, only verbal descriptions of pattern have been used, which leads to the continuous nature of planform morphologies being replaced by an artificially discrete classification. The quantitative description of channel patterns is at an early stage of development, especially so far as multiple channel patterns are concerned (Davies, 1987). One promising approach involves the measurement of total sinuosity (ΣP) of a river (Ferguson, 1972; Hong and Davies, 1979; Richards, 1982; Maizels, 1983a; Robertson-Rintoul and Richards, in preparation), defined as the total channel length divided by the reach length (Figure 2.6). This measures channel pattern at a scale equivalent to macroforms or the first order channels of Williams and Rust (1969), and as such its application is restricted to sediment transport processes occurring at this scale. Total sinuosity appears at first sight to be strongly stage dependent, thus placing great significance on the selection of an appropriate discharge at which to measure it. However, limited field evidence suggests that ΣP is relatively stable over a range of discharges (Robertson-Rintoul and Richards, in preparation). This implies that a small number of channels dominate the channel pattern of braided rivers, much as bedload transport in such rivers is concentrated in dominant channels (Davoren and Mosley, 1986; Carson and Griffiths, 1987). This in turn means that the total sinuosity measured at low flows (which is when aerial photographs are usually taken) can be related to stream power and particle size.

For consistency, indices of both flow intensity and ΣP should be measured at the 'channel-forming discharge'. This discharge is readily apparent in laboratory experiments where discharge is constant but is more difficult to define in prototype rivers that are continuously



$$\begin{aligned} \Sigma P &= (e_1 + e_2 + \dots + e_8) / L \\ &= \left(\sum_{i=1}^n e_i \right) / L \end{aligned}$$

Figure 2.6 Definition of Total Sinuosity, ΣP (after Hong and Davies, 1979).

forming new channels at bedload transporting stages. Lee and Davies (1986) identified a flow exceeded approximately 2 % of the time as dominant (i.e. that which has the greatest impact on channel form over a long time period) in a series of laboratory experiments with both constant and randomly fluctuating discharges. This conclusion is based on channel width and bar surface area data with some support from long-term average sediment transport rate. Davies (1988) calculated the capacity of the Rakaia River, New Zealand, to transport bedload at various discharges using the bedload formula of Bagnold (1977). A flow rate of $800 \text{ m}^3 \text{ s}^{-1}$ was calculated to have the greatest total bedload transport in a given time interval (Figure 2.7) but the degree of dominance is not very pronounced (Davies, 1988). This result further suggests that ΣP may not be especially sensitive to the choice of discharge at which it is measured, since the dominant discharge curve is not strongly peaked.

Richards (1982) used a simple stream power index (Ω') defined as the discharge-valley slope product, QS, to show the existence of a continuum of channel patterns from single through multiple thread types. This approach has been refined for an expanded data set by Robertson-Rintoul and Richards (in preparation), by the addition of a sediment size term in the equation for ΣP . Separate equations are found for sand- and gravel-bed rivers, reflecting the fundamental differences in process between them (see section 2.1). For 40 gravel-bed rivers the result was;

$$\Sigma P = 1 + 5.5 d_{84}^{-0.14} \Omega'^{0.40} \quad (r^2=0.82) \quad (2,4).$$

The co-efficient 1 in (2,4) follows from the lower limit of ΣP being 1 (for a straight single-thread channel). Note that the slope used in calculation of Ω' is the valley slope, since channel slope is dependent upon channel lengths and hence ΣP . The data used to derive (2,4) exhibited no clear discontinuities so supporting the contention that channel pattern is a continuous variable if it is adequately described. Much the same point has been made qualitatively by numerous recent workers (e.g. Carson, 1984a; Ferguson, 1987). One of the implications of equation (2,4) is that for a given grain size, the braiding intensity of a river increases with stream power i.e. not only is a river with higher power more likely to be braided than single thread, but the degree of braiding is also power dependent. There is some supporting evidence for this from other sources. Howard, Keetch and Vincent (1970) reported correlations between a braiding index based on the number of channels in a reach, and combinations of slope and discharge ($0.31 \leq r^2 \leq 0.39$). A similar weak correlation ($r^2=0.34$) was reported by Mosley (1981) for a regression equation relating a braiding index to stream power, a flow variability index, and particle size.

The promising results obtained using the total sinuosity index suggest that channel pattern can be accounted for in terms of stream power and particle size. Ackers and Charlton (1970) used dimensional analysis to derive a similar result for meander wavelength which included sediment concentration, although its influence was noted to be weak. Other sedimentary factors are considered in sub-section 2.3.3. The implications of this result are now assessed. It is known that

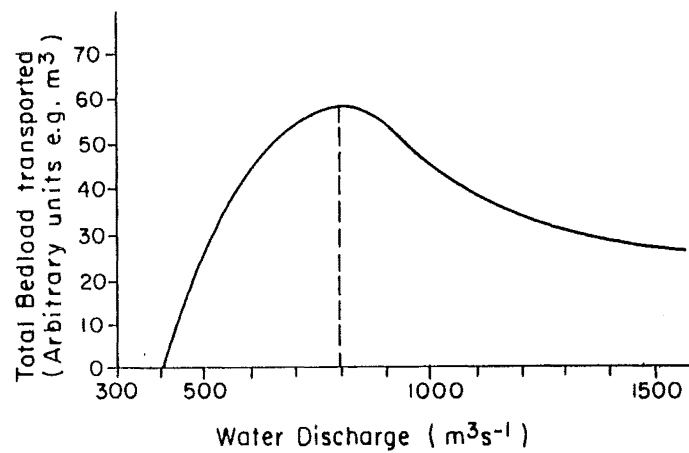


Figure 2.7 Estimated total bedload transport in the Rakala River, in a given time period (after Davies, 1988). Estimates were derived using the Bagnold (1977) equation applied to the full flow duration curve for the river. The minimum flow for the onset of bedload motion is about $400 \text{ m}^3 \text{ s}^{-1}$. The dominant discharge (i.e. that which transports the greatest volume of bed material; dashed line) is at about $800 \text{ m}^3 \text{ s}^{-1}$.

bedload transport rate can be expressed as a function of stream power (Yang, 1972). The same variables thus influence both the bedload transport rate and the complexity of channel patterns. Whether or not these exhibit correlations at any one time is entirely dependent upon the respective processes occurring at the same times, and with similar relaxation times. Should either of these conditions not be met, a lag would be introduced between the two processes which would prevent them from being in phase. In gravel bed rivers, channel formation can only occur when bedload is being transported. Ashmore (1985) identified three mechanisms by which braiding can be initiated as new channels develop, namely medial bar growth, chute cut-offs on bends, and proto-channel incision on bars. Other processes of channel pattern change, such as flow capture by an incising channel are also dependent on the existence of bedload transport. Thus there is an inevitable association between bedload transport and channel patterns. Whether or not the rate of bedload transport is correlated with the complexity of channel pattern is not so immediately obvious. Further, it is unclear what spatial and temporal lags exist between sediment transport and channel pattern.

An alternative approach to this linkage was provided by Schumm (1977a) in a synthesis of hydraulic geometry relationships which yielded a generalised relation between bedload discharge, Q_b , and channel morphology,

$$Q_b \cong b, \lambda, S / h, P \quad (2,5),$$

in which λ = meander wavelength, h = flow depth, and P = sinuosity. When bedload discharge is increased (+) or decreased (-), the following associated changes are qualitatively suggested by the hydraulic geometry equations :

$$Q_b^+ \cong b^+, h^-, \lambda^+, S^+, P^- \quad (2,6a)$$

$$Q_b^- \cong b^-, h^+, \lambda^-, S^-, P^+ \quad (2,6b).$$

The implication of equation (2,6) for channel pattern is that sinuosity is inversely related to bedload transport rate. This appears to contradict the findings of Schumm and Khan (1972) that as slope increases so both bedload transport rate and sinuosity increase (at least until the crossing of the meandering-braided pattern threshold). The relationship between stream power and sinuosity takes the same form as that between slope and sinuosity in these experiments (Schumm, 1977a), implying a positive correlation between sinuosity and bedload transport rate. Using the definition of total sinuosity introduced above, this correlation can be shown to extend into the braided pattern region.

The relevance of any relationship between sediment transport rate and channel pattern is dependent upon the coincidence of bedload and channel forming processes in both space and time. Although bedload transport is a necessary condition for the development of channels the processes responsible for producing the pattern of self-formed gravel-bed rivers are not necessarily those which move most of the bedload (Carson and Griffiths, 1987). However the two phenomena are undoubtedly related. Carson and Griffiths (1987) noted the importance of bank

scour of channel bars as sources of bedload material. They suggested that localised shoaling which promotes avulsion or proto-channel development, changes channel pattern and accesses new sources of bedload material by exposing additional banks to scour. Thus, processes of channel change increase the sediment supply to the flow and in 'supply-limited' channels actual bedload transport also increases. It seems reasonable to suggest that where the frequency of such channel changes is greater (i.e. in braided rivers as opposed to single thread ones), Type B sediment supply is greater, and local bedload transport volumes will be greater. The frequency of channel changes might be expected to correlate with the complexity of channel pattern such that a correlation between total sinuosity and bedload transport rate is not unreasonable. There thus seems to be some validity in the argument for this correlation in terms of gravel transfer processes.

Two other approaches to the explanation of channel pattern which have direct implications for sediment transport are those of Parker (1976) based on linear stability analysis, and various uses of extremal hypotheses. Parker (1976) used the ratios slope : Froude number, and flow depth : width which enabled both a discrimination between single thread and braided rivers and prediction of the number of braids to be made. These results were independent of the magnitude of bedload transport although they were dependent on its existence. However, the bedload transport rate covaries with all four parameters used in the analysis and its effect may consequently be masked within variations in these parameters.

Extremal hypotheses have been used to identify solutions to roughness and sediment transport equations. Davies and Sutherland (1983) demonstrated that the various extremal hypotheses reported in the literature (minimum energy dissipation rate; minimum unit stream power; maximum sediment transport rate; maximum friction factor) yield similar predictions. Kirkby (1972) found that the discharge-slope threshold for braiding of Leopold and Wolman (1957) is consistent with friction factor equations and the hypothesis that dimensionless shear stress is minimised.

ERRATA

Channel pattern is in part a consequence of the relationship between the maximum sediment transport rate and the imposed material load (Kirkby, 1980). Any situation where the imposed load exceeds the sediment output rate is associated with choking of the channel and changes of course, the degree of braiding increasing with the magnitude of the discrepancy. Kirkby (1980) argued that this process is self-limiting in that gradient increases associated with aggradation raise the sediment transport capacity. This is apparently a mechanism for the growth and erosion of bed waves and is similar to some of the suggested mechanisms noted in sub-section 2.2.4 above.

Bettess and White (1983) utilised a similar approach to Kirkby (1980) based on the assumption that channel pattern reflects a discrepancy between the valley slope and the equilibrium slope of the channel. The regime theory of White, Paris and Bettess (1982), in which specification of two out of five variables (discharge, width, depth, slope, sediment concentration) enables unique

determination of the other three, is used as the basis for their approach. For the example of $d_{35}=0.5\text{mm}$ (i.e. a sand bed river) the theory predicts that sinuosity is inversely related to discharge and sediment concentration, but that there is a high expectation that the channel will braid (Bettes and White, 1983). In terms of total sinuosity, therefore, the expectation is that ΣP increases with both discharge and sediment concentration which is consistent with the argument presented above. This is an encouraging agreement since it is a consequence of a theory of channel boundary shape which includes sediment concentration rather than being dependent upon empirical analysis of observed patterns. However, the approach fails to explain how different patterns develop (Ferguson, 1987) or to account for bank erodibility, the importance of which is undoubted (Carson and Griffiths, 1987).

2.3.2 Sediment supply effects on channel pattern

The hydraulic controls assessed thus far make the assumption of infinite availability of sediment for transport, although the role of sediment is acknowledged by the inclusion of a particle size term in some hydraulic descriptors of pattern. The role of sediment supply and type has been broadly identified by Schumm (1977a) who separated suspended load, mixed load and bedload channels. Within the gravel-bed river class (bedload channels), the role of sediment type has been investigated by Carson (1984a).

An excess of sediment input over transport capacity which induces aggradation has often been viewed as a cause of braiding. However, Leopold and Wolman (1957) suggested that braiding could be an equilibrium channel form, and the occurrence of braiding in degrading streams, such as the Donjek River, shows that there is no necessary link between aggradation and braiding (Richards, 1982). Carson (1984a) restated this point, noting that aggradation is particularly conducive to braiding but is not a prerequisite for its development. He suggested that rapidly aggrading rivers will usually braid, rapidly degrading ones usually meander, and that between these extremes channel patterns vary through a continuum largely controlled by bank erodibility. Inputs of Types A, B, and C sediment all affect channel patterns and influence the relationship between pattern and sediment transport.

Numerous examples of enhanced Type A sediment supply leading to increased braiding intensity are available (eg. Anthony and Harvey, 1987; Bradley, 1984; Carson, 1984a; Smith and Smith, 1984). In these cases braiding may only be a temporary response to the increased supply as has been suggested by Church (1983) for the Bella Coola River. Here increased lateral stability within the last century is due to diminution of the rate of coarse sediment supply to the river. As described in sub-section 2.2.4, this type of sediment input can initiate bed wave development and may be responsible for setting up disturbances in channel pattern which migrate downstream.

Type C sediment supply has a similar effect to Type A in terms of channel pattern, although the magnitude of its effects is likely to be less extreme since all of the sediment involved has to be fluvially transported into the reach. Carson (1984a) considered the effects of upstream sediment supply on channel patterns; especially notable is the contrast between the Rangitata River, New Zealand and the nearby Rakaia River, downstream of their bedrock gorges. Material transfer through the Rangitata gorge is limited whereas a much greater quantity of material is transferred through the Rakaia gorge. Thus, immediately downstream of their gorges, the Rakaia commences braiding whereas the Rangitata meanders and continues to do so until the sediment supply is augmented by a small tributary (Lynn Stream).

Brotherton (1979) concluded that the relative ease of transporting bank material (Type B sediment) determines channel patterns. Thus, meanders form where the bank material is easily transported and braids form where this is not the case. Both erosional and depositional causes of braiding are identified, although both involve local aggradation: in the erosional case, bank erosion and channel widening lead to local aggradation and braiding; for depositional braids, the deposition of material from upstream induces braiding, but also tends to promote bank erosion and hence erosional braiding. This argument has been refined by Carson (1984a,b) who produced a channel pattern classification based on the balance between bank erodibility and bed material supply rate (Figure 2.8). Moving from lower left to top right in Figure 2.8 channel pattern complexity increases, and total sinuosity would be expected to rise. Clearly a single index such as ΣP is an inadequate way of representing the range of channel patterns identified in Figure 2.8. Neither axis on the figure is a readily quantifiable variable, but the Figure can be used to assess the relative importance of sediment input from banks and upstream (Types A and C) against Type B sediment supply. Such information can supplement a total sinuosity (or similar) approach to estimating channel slope variations and bedload movement.

The utility of Carson's argument lies largely in his relating channel pattern to the actual processes of bedload transfer. Ferguson (1987) suggested that there are two mechanisms by which a high bed material load can encourage braiding. Firstly, medial bar growth due to supply exceeding transport capacity (Leopold and Wolman, 1957) encourages channel division. This mechanism has been observed by other workers (e.g. Krigstrom, 1962; Fahnestock, 1963; Ore, 1964). Secondly, dissection of and avulsion over low angle bars have been widely reported as initiators of braiding (e.g. Schumm and Khan, 1972; Ashmore, 1982, 1985; Ferguson and Werritty, 1983; Carson, 1984a; Rundle, 1985a). Church (1972) refers to the first mechanism as 'primary anastomosis' and to avulsive braiding as 'secondary anastomosis'. As a sub-category of the second group, cut-offs of features known as 'point dunes' (Hickin, 1969), which are associated with 'pseudomeandering' (Wolman and Brush, 1961), have been identified as causes of braiding (Ashmore, 1985). Such channels are classified as 'meanderthal' (i.e. meandering thalweg) by Carson (1984a). Carson further divided features due to the second mechanism by which braiding

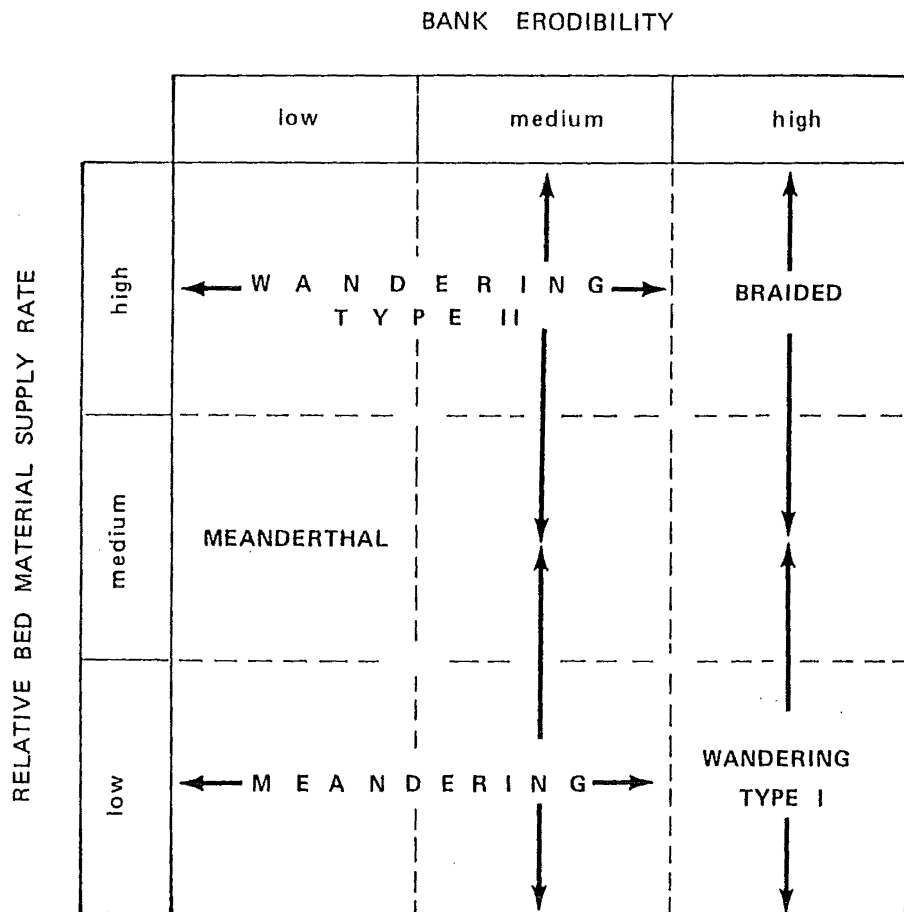


Figure 2.8 Classification of river channel patterns according to Carson (1984a). Wandering Type I rivers have irregular and rapid bend migration and wide, often dissected point bars. The Wandering Type II condition is associated with persistent avulsion of flow out of the main channel. Meanderthal rivers have a meandering thalweg in a relatively straight bed.

may be promoted by recognition of two categories of wandering channel. Wandering Type I channels occur where very wide point bars are dissected and are essentially very active meandering channels. Wandering Type II channels have frequent avulsion of flow out of the main channel. Ferguson and Werritty (1983) described such behaviour in the River Feshie, Scotland. Both the mid-channel bar deposition hypothesis, and the various avulsion / cut-off based causes of channel division would be expected to be facilitated by high sediment loads in relation to the transporting capacity of the river.

The classification of Carson (1984a) thus enables a direct link to be seen between sediment supply and channel pattern. This link is by no means simple or unidirectional since bank erodibility also serves as an important determinant of channel pattern. Thus, it is impossible to directly relate channel pattern, however described, quantitatively or uniquely to the rate of bedload transport or to the volume of material in storage. Care needs to be taken to allow for variations in sediment supply and bank erodibility when attempting to use a simple index such as total sinuosity for the prediction of relative sediment transport rates.

2.3.3 The sediment storage implications of downstream variations in channel pattern

Where channel pattern is observed to vary downstream independently of external influences such as tributary inputs and valley width variation, changes in one or more of three factors can be used to account for the variations:

- A. bed material type and supply rate;
- B. bank erodibility;
- C. hydraulic conditions.

For any given reach the bed material supply rate is dependent upon the hydraulic conditions in the reach immediately upstream (i.e. on Type C sediment supply) as well as on exogenous (Type A) sediment supply. If Type A supply and bank erodibility can be assumed to be constant (or their patterns of variation are known), then channel pattern changes can be accounted for in terms of hydraulic conditions. Beschta (1983b), for example, used equation (2,6) to argue that a change in bed material transport should cause an increase in the width of the active channel, in a wandering Type II gravel river. Where reliable empirical relationships between channel pattern and hydraulic variables exist, it should be possible to use the pattern information to estimate hydraulic conditions.

ERRATA

Without reliable quantitative information it is possible to use downstream variations in channel pattern to make a qualitative assessment of sediment storage patterns. Several such studies were noted in sub-section 2.2.3. The bases for these studies have been the relationships between sediment transport and channel pattern reviewed above. In general, only qualitative results have been obtained and explanations have been made in terms of all three factors

introduced at the start of this sub-section. Church and Jones (1982), for example, noted the influence of alluvial fans as periodic sources of large volumes of sediment in accounting for the locations of sedimentation zones. Beschta (1983b) and Macklin and Lewin (1989) have found that structural controls can determine the location of sedimentation zones by impounding material upstream. This refers both to bedrock gorges and artificial structures such as bridges. A similar result was presented by Magilligan (1985) who also regarded narrow valley reaches as transportational or erosional reaches, with deposition occurring in the wider valley sections. In cases where the valley width varies in this way, assessing downstream changes becomes more difficult than evaluating changes at-a-section over a time interval. Hence, Beschta (1983b) used changes in channel widths over 37 years to interpret the sediment storage patterns in the Kowai River, and Macklin and Lewin (1989) used changes over a 115 year period.

The work described in sub-section 2.2.3 showed the utility of downstream changes in river channel patterns for inferring sediment storage patterns. Davies (1987) expressed optimism about the future development of such approaches dependent upon the development of more useful quantitative measures of channel pattern than are presently available. Not only does this present a descriptive problem involving finding a suitable basis for the definition of pattern, but difficulties are also introduced by the comparatively poor understanding of the links between channel pattern and sediment transport processes. Sufficient is known, however, to enable qualitative evaluation of sediment storage patterns and in some cases quantitative estimates may also be possible. The reliability of these estimates remains to be tested.

2.4 Conclusions

The range of evidence now available suggests that bed waves and bedload pulses are common features in gravel rivers. It is important not to group all such features together. A range of process mechanisms have been postulated to account for their existence, and it appears to be possible to differentiate four discrete wave types based on process, and one based on the type of sediment supply (Figure 2.4). The first group are bed waves produced by the effect of particle interaction and sediment sorting. These may be independent of three-dimensional bedforms and occur at the mesoscale. The second type are manifested as channel bar assemblages and occur at the and macro- and mega-scales. This distinction is consistent with the hierarchical bedform classification suggested by Church and Jones (1982; Table 2.1), in which the governing factors change from the fluid dynamic regime of the boundary layer to the geomorphological regime as the scale increases from meso- to mega-scale. The third wave type is produced by bedload sheets of one form or another and as such could be closely linked to either of the first two types. There is some evidence that mesoscale bedload sheets are associated with the first wave type and macroscale ones with the second type. Recognition of the fourth wave type has largely been restricted to semi-arid areas thus far, and is a consequence of interlinkages between different

ERRATA

elements of the drainage network. This mechanism could readily be envisaged to also operate in humid areas although its effects may not be so pronounced. Figure 2.4 also distinguishes another group of waves due to external inputs of sediment to the river system, and is based on sediment source rather than process. In process terms such waves may fit into the four-fold classification described above or could behave differently under certain conditions.

As the scale of the phenomena increase, so the certainty of the evidence used for identification decreases. Continuous measurement of bedload transport has enabled a good understanding of the processes of mesoscale bedload pulses to be developed. At larger scales such an approach is impracticable (Gomez *et al.*, 1989) and the evidence used is usually indirect, with limitations on the precision of the inferences that can be drawn originating from uncertainty as to the details of the channel pattern-sediment storage linkages. Further, comprehensive quantitative description of channel patterns has yet to be achieved, although pattern is a readily obtainable variable (Davies, 1987). Even with advances in the quantification of pattern it is uncertain that it will prove possible to develop a descriptor that gives a unique value for each different pattern. Carson (1984a) illustrated how morphologically similar results can be produced by different combinations of the controls over channel pattern. Thus, sediment storage cannot be uniquely related to particular pattern types, but within a specified catchment the range of controls over pattern may be sufficiently restricted to enable such relationships to be developed. One way of circumventing some of the problems inherent to the macro- and mega-scales is to use small scale physical modelling. Although useful, uncertainties of scale still prevent quantitative predictions from being made on the basis of model results (Davies, 1987).

One of the important issues raised by studies of bed waves is the balance between sediment supply and bedload transport capacity. This issue has recently been debated (for example by Pitlick and Thorne, 1987, and discussion thereof), but it is complicated by the absence of a reliable definition of bedload transport capacity (Richards, 1988), which stems from incomplete understanding of sediment transport processes. Resolution of this problem requires further research into how bedload actually moves in gravel-bed rivers, rather than using 'black-box' explanations of transport rates (Carson and Griffiths, 1987; Davies, 1987).

For both sediment transport rate measurement and description of channel patterns, selection of appropriate spatial and temporal scales is critical. Where channel pattern alone is being investigated the question of long-term equilibrium of the river system is important. Werritty and Ferguson (1980) demonstrated different controls over channel pattern at different timescales. Over a 200 year timescale they were able to identify an equilibrium condition. Such graded time equilibrium is dependent upon the nature of changing environmental controls and may not always be so readily identified. Over 30 years the role of individual floods in changing channel pattern was important, with relaxation towards the longer-term equilibrium following the disturbances due

to these events. Carson (1984a) identified a similar sequence of disturbance and relaxation. Such disturbances are of importance for the study of bed waves and bedload pulses since they can input large amounts of material into the river system (e.g. Beschta, 1983a). Thus, pattern changes can be interpreted in terms of sediment supply and bed wave transfer once the effects of any longer-term trends are accounted for. These pattern changes have been assumed to involve regular fluctuation about a long-term average (Robertson-Rintoul and Richards, in preparation) which implies regularity of bed wave development. In such cases, care needs to be exercised to differentiate the long-term trends from cyclic variations (Ferguson, 1977), which is not always easy given that the timing of most of the evidence (aerial photographs) is fixed without reference to the needs of the study.

Bedload transport rate changes and channel pattern variations are not necessarily coincident in space and time. Although both occur only at high flows in gravel-bed rivers the processes responsible for the bulk of gravel transport and for the channel pattern are not necessarily the same (Carson and Griffiths, 1987). The volume of sediment in storage in a reach is more closely related to the channel pattern than to bedload transport rate. Both sediment volumes and patterns are determined by processes that affect the entire width of the river bed, rather than being as spatially concentrated as is bedload transport. So far as spatial effects are concerned it is apparent that the bedload transport rate past one cross-section will have an impact further downstream, and that a channel pattern change will also transmit effects, possibly upstream as well as downstream. It is important to select spatial scales appropriately to account for this, and more research into the characteristic length scales of the different processes is required.

Analysis of long-term river behaviour in terms of fluctuating variables raises the issue of the nature of river systems in general. Perturbations to a natural system can be damped or amplified over time, depending on the nature of the system. A single perturbation may lead to the initiation of an unsteady response further downstream and / or upstream, and unsteady behaviour over time at the site of the perturbation itself. Thus, a single input of sediment to a river could cause long-term bed wave propagation through the river system. This may or may not lead to the eventual establishment of a stable condition depending on the details of the system concerned. Thus, it may be impossible to identify truly endogenous bed waves since single exogenous inputs of sediment could produce long-term responses. The influences of tectonic events (e.g. Gregory and Schumm, 1987) or long-term base-level changes are important although generally poorly understood over long time periods. Such evidence as is available suggests that bed waves tend to attenuate as they move downstream, and that the persistence of disturbance in the river system may be finite. This question also requires much further investigation.

In conclusion, the review presented here has identified four main areas where clarification is required and which are addressed subsequently:

1. The relative importance of sediment supply and channel transport capacity in producing bedload pulses is unknown. This is especially poorly understood in braided rivers for which few detailed data sets on bedload transport rates are available. Related to this is the incomplete understanding of the processes of bedload transport and sediment deposition, which are critical for comprehension of bed wave behaviour.
2. The processes which produce bed waves in braided rivers are not fully understood, and the linkages between sediment transport, channel form and sediment storage require further elucidation.
3. In order to comprehend the linkages mentioned in Conclusion 2, patterns of sediment dispersion and redistribution require further investigation.
4. All of the above rely on specification of the spatial and temporal scales under consideration and of the range of behaviour that can be considered as 'normal'. This could provide a much better basis for evaluation of the impacts on river behaviour of natural or artificial changes in controlling variables .

3. METHODS USED IN THE PRESENT STUDY

The present study is based on two types of investigation, one involving a prototype river and one using scale modelling. The field study is described in section 3.2 after rationalisation and description of the scale modelling approach.

3.1 Physical modelling of gravel-bed rivers

3.1.1 The use of physical models in fluvial geomorphology

A range of studies commencing in the late 19th Century illustrates the potential uses of physical models for geomorphologists. Schumm *et al.* (1987) listed five of these:

1. physical models provide conveniently sized, rapidly evolving representations of landform development;
2. they serve as sources of hypotheses which can be tested on prototypes;
3. hypotheses generated under prototype conditions can be tested on the models;
4. measurements made in models can be used to estimate the types and rates of processes in prototypes;
5. difficult to observe physical processes may be discernible in the models.

A range of modelling strategies can be adopted to take advantage of one or more of these potential uses. Chorley (1967) defined three broad classes of physical model: analogue models; elements of unscaled reality, and; scale models. Analogue models have been widely used. Scale relationships are not necessarily preserved in such models, the aim of which is to reproduce aspects of forms and / or processes found under prototype conditions without faithful replication of the forces, materials, and / or processes occurring (Schumm *et al.*, 1987). Examples include studies of meandering using a thread of water on a glass plate (e.g. Gorycki, 1973) and a laminar flow model of braided river morphology (Hong and Davies, 1979).

Segments of unscaled reality can take two forms. Firstly, small scale prototypes can be used to assess processes that occur at larger scales. Thus, bedload transport rates have been recorded in flume-like sections of Oak Creek (Klingeman and Emmett, 1982) and Turkey Brook (Reid *et al.*, 1980) so as to assess general processes of bedload movement, which can then be applied to larger prototypes. Secondly, small scale physical models can be viewed as small rivers in their own right rather than as scale models of prototypes (Leopold and Wolman, 1957; Hooke, 1968). Application of the results of either approach to other scales requires specification of scale relationships. If these are not able to be precisely defined this approach can still have utility if the processes occurring are the same as at the larger prototype scale. Hooke (1968) doubted that hydraulic similarity in two-phase flows is a realisable goal given the state of knowledge about the mechanics of such flows. He suggested treating the models as small systems which can be

related to larger scales using 'process similarity'. This condition requires that gross scaling relationships are met, the model reproduces one or more morphological characteristic(s) of the prototype, and the processes responsible for this (these) characteristic(s) can logically be assumed to have the same effects in the prototype as in the model. As models of larger scale prototypes, process similar models have little quantitative value due to the absence of precise scaling relationships, and are one step further towards scale modelling on a continuum of model types than are analogue models. Considered as segments of unscaled reality, process similar models produce results that require explanation. These say nothing directly about the behaviour of larger scale prototypes, but may generate useful hypotheses for comparison with prototype observations (Mosley and Zimpfer, 1978).

In reply to Hooke's discussion, Bruun (1968) noted that a scale model can be regarded as both a model and a prototype at the same time. For models to become scale models rather than process similar ones hydraulic similarity must be achieved. This is described in sub-section 3.1.2. The aim of a scale modelling approach is to produce quantitative results, which is possible if the pertinent physical factors are correctly scaled (Bruun, 1966). Whether this is a realisable goal is in some doubt (Schumm *et al.*, 1987) as too little is known about scaling of sediment transport processes to enable their similarity to be reliably assessed. Although few geomorphological studies have used this approach it has had some application to the mechanics of gravel-bed rivers (e.g. Ashmore, 1982, 1985; Southard *et al.*, 1984). These studies have not attempted to model a specific site but to produce a generic model i.e. one in which the model river is self-formed and has mean characteristics similar to those in the prototype. This is not equivalent to strict hydraulic similarity, and as such lies between scale and process similar modelling (Ashmore, 1985).

Evaluation of the different approaches to modelling depends upon the aims of the specific study in question. Mosley and Zimpfer (1978) listed the advantages of small scale physical models in general terms. The most important of these are: the ability to control experimental conditions; the speeding up of evolutionary processes; potential combination of several processes in one study; possible observation of hitherto unidentified phenomena; the ability to assess the effects of boundary conditions. Disadvantages were also listed by Mosley and Zimpfer, most of which relate to problems in evaluation of the degree to which a model replicates nature. They concluded that model studies "cannot be the final step in the development of a theory." (Mosley and Zimpfer, 1978 p.458). Small scale models do not provide ends in themselves, but can provide insights that are unobtainable in other ways (Schumm *et al.*, 1987). The requirements of a specific study need to be defined before selecting whether a small scale model is an appropriate mode of enquiry, and if so which modelling approach should be used.

3.1.2 Application of scale modelling to gravel-bed rivers

The principles of hydraulic similarity are used where scale modelling procedures are applied to the study of gravel-bed rivers, and were fully explained by Yalin (1971a). Three types of similarity are important for hydraulic modelling; geometric, kinematic and dynamic. Geometric similarity requires that the length scale of the model is constant, although vertical and horizontal dimensions can be scaled differently. Geometric similarity is a prerequisite for kinematic similarity which requires that the patterns of fluid flow are the same in the model and prototype. This motion is consequent upon the action of forces, hence dynamic similarity under which forces are similar is also required.

The characteristic parameters for non-uniform flow in a non-prismatic channel can be grouped into the following dimensionless quantities (Yalin, 1971a): slope, S ; relative roughness, k_s/h ; Reynolds number, $\bar{u} h / \nu$; Froude number $\bar{u}/(g h)^{0.5}$. Here k_s is a roughness length (m), h = flow depth (m), \bar{u} = mean flow velocity ($m s^{-1}$), ν = kinematic viscosity ($m^2 s^{-1}$) and, g = acceleration due to gravity ($m s^{-2}$). Flow depth is approximately equal to hydraulic radius, R (m), for wide shallow channels. Defining the ratio λ_x as the model: prototype scale ratio, and referring to the four dimensionless quantities as $X_1 \dots X_4$ respectively, the condition for dynamic similarity is $\lambda_{X1} = \lambda_{X2} = \lambda_{X3} = \lambda_{X4} = 1$. Where water is used as the fluid in both model and prototype and kept at room temperature, $\lambda_\mu = \lambda_\rho = 1$, such that it is impossible for λ_{X3} and λ_{X4} to equal 1 simultaneously when $\lambda_L < 1$ (where L is length). The realisation of a small scale model ($\lambda_L < 1$) becomes possible only if the conditions of dynamic similarity are relaxed and the parameter ν is excluded from consideration (Yalin, 1971a). This is possible if the flow in both model and prototype is turbulent, the criteria for which are,

$$\bar{u} h / \nu > 2000, \text{ and}$$

$$u_* k_s / \nu > 70$$

where u_* = shear velocity ($= (g h S)^{0.5}$), and 70 is a critical value sometimes reported as being up to 100. Further, these inequalities need only be considered for the small scale model since the Reynolds number and particle Reynolds number ($u_* k_s / \nu$) are inevitably greater at larger scales (Yalin, 1971a). The second inequality can also be used to define a lower limit for the length scale, λ_L , which is determined by the prototype particle Reynolds number, $u_* k_s' / \nu'$. This lower limit is given by,

$$\lambda_L \geq [70 \nu' / u_* k_s']^{2/3}.$$

Minimum length scales can be calculated for gravel-bed rivers of the type to be modelled. Data are available from two such New Zealand rivers, the North Ashburton and the Ohau. Taking k_s' as $2d_{90}$ (following Parker and Peterson, 1980) and $d_{90}/d_{84}=1.11$ (Bray and Davar, 1987), the minimum value of λ_L can be calculated for a bedload transporting flow of $14.7 m^3 s^{-1}$ in the 'unconfined' braided reach of the North Ashburton River (Laronne *et al.*, 1986; Table 2c). With $R=0.33m$, $S=0.012$, $g=9.81 m s^{-2}$, $d_{84}=0.119m$, and $\nu=1.3 \times 10^{-6} m^2 s^{-1}$, the inequality becomes $\lambda_L \geq 1/69$. Lee and Davies (1986) suggested that the 'dominant' discharge in a model of this river

is the flow exceeded 2 % of the time, which corresponds to $28 \text{ m}^3\text{s}^{-1}$ in the prototype. This is an appropriate discharge at which to calculate λ_L since model conditions often use a constant discharge. For a flow of $29.2 \text{ m}^3\text{s}^{-1}$ (Laronne *et al.*, 1986; Table 2c), $R=0.40\text{m}$ and $\lambda_L \geq 1 / 73$. For the Ohau River (Thompson,1987) taking depth as equivalent to hydraulic radius, $R=2.7\text{m}$, $d_{84}=0.07\text{m}$ and $S=0.0044$, giving $\lambda_L \geq 1/70$. In another channel, $R=1.2\text{m}$, $S=0.0175$ and $\lambda_L \geq 1/84$. Thus a length scale of 1/60 or greater could be considered appropriate for this type of river.

When the condition for Reynolds number similarity is relaxed, the model is referred to as a Froude number model. Scaling based on the Froude number with geometrical similarity implies that the velocity scale is equal to the square root of the length scale. Thus the discharge scale, λ_Q is equal to $\lambda_L^{5/2}$.

The length scale of a mobile bed river model is determined by the sediment size scale ratio (λ_d). For uniform sediment this presents no problem, but for a natural size distribution there are several difficulties. Firstly, the best way to model a natural size distribution with small scale ratios is to use geometric scaling (Yalin, 1971a), since this avoids the problem of different properties of two-phase flow being associated with different effective grain diameters. Geometric scaling is defined as,

$$d_p' / d_p = \lambda_d,$$

where d_p' is model grain size, for all values of p . In practice this condition has to be relaxed at the fine end of the size distribution curve, since scaling down sand sized material would lead to the inclusion of cohesive silts and clays in the model material. Since the model sediment should have the same density and specific weight as the prototype, the only other relevant material property is shape. This is especially important for sediment entrainment (Komar and Li, 1986), and grain shapes in the model and prototype should be similar if sediment transport similarity is to be achieved.

Similarity of sediment transport is difficult to define precisely. Bedload transport is a combination of numerous processes; it is unclear whether a model which is process similar with respect to entrainment will also be so for saltation, and so on. Poor understanding of these processes makes similarity criteria hard to identify. Thus while hydraulic similarity can be precisely defined, process similarity is the most rigorous criterion that can presently be applied to sediment transport modelling, although the models may be more reliable than that in some respects (Ashmore, 1985).

The main hydraulic properties of a Froude number model can be summarised as follows (Yalin, 1971a; Ashmore, 1985):

1. grain size and flow dimensions are scaled by the same amount;
2. slope is identical in the model and prototype (i.e. $\lambda_{X1} = 1$);

3. the model fluid and sediment have the same density and specific weight as the prototype;
4. Froude number and the ratio h / k_s should be equal in model and prototype (i.e. $\lambda_{X2} = \lambda_{X4} = 1$);
5. Reynolds number and particle Reynolds number should exceed critical values for the elimination of viscous effects on the flow (i.e. $\lambda_{X3} \neq 1$); these values are about 2000 and 70, respectively;
6. flow shear stress should be sufficient for bedload transport to occur and the dimensionless shear stress ($hS / (S_s - 1)d$) should be equal in model and prototype. This is the case if Reynolds numbers exceed their critical values.

Having established these modelling criteria there are some practical problems which require consideration. The initial conditions at the start of an experiment affect the later development of a self-formed channel although the magnitude of these influences has not been fully assessed. Schumm *et al.* (1987) described studies of meandering in which the same results were obtained whether the flow was initially straight down the channel or introduced at an angle. A problem with modelling self-formed channels is that they evolve from a wide, shallow straight channel, which is selected as an initial condition for reasons of convenience and consistency. If natural rivers have never been in this condition it may be an irrelevant starting point. Carson and Griffiths (1987) use much the same argument to reject the use of stability analysis in studies of channel pattern. The effects of boundary conditions are difficult to assess given the natural variability in river behaviour under the same conditions.

This leads on to the issue of reproducibility of results. Schumm *et al.* (1987) suggested that establishment of unique, replicable relationships is a prime reason for using an experimental approach, and provided an excellent example of the reproducibility of meander patterns. Anderson and Calver (1981) conducted four sets of 30 experimental runs in which channels were allowed to form starting from the same initial conditions, and concluded that channel pattern variability in models is extreme and that multiple repetitions of experiments are required to ensure validity of results. Church (1984) suggested that experimental results should include a statement of the probability of observing the actual outcome which implies a need to conduct multiple tests. Except for under particularly restrictive conditions (the example used by Schumm *et al.* had water entering the flume at a 40° angle which may have served to fix the position of the meanders) there is evidence that qualitative similarity of channel forms can be produced under the same conditions, but that the details may differ (Ashmore, 1985, 1988). Experimental replicability has to be defined within the range of channel forms and processes that can occur under one set of controlling conditions. Further, this variability can be extreme (cf Runs 4a and 4b of Ashmore, 1988).

Part of the problem in defining replicability is the need to define when the model reaches equilibrium of process and form. Experiments have been run for time periods from 15 minutes (Anderson and Calver, 1981) to 35 days (Ackers and Charlton, 1970). Different investigators

have defined equilibrium in different ways. Wolman and Brush (1961) defined it as when the bedload discharge from their experiments became constant, changes in channel shape were negligible, and the longitudinal profile was regular and nearly constant. Kuhnle and Southard (1988) defined equilibrium as a condition in which the average sediment input and output rates were equal, and Ackers and Charlton (1970) and Schumm and Khan (1972) waited for the development of a stable channel pattern. Clearly, equilibrium and stability are not equivalent as equilibrium conditions can involve short term changes in channel forms and processes. Equilibrium needs to be defined according to the aims of a particular study. As a first step the requirements of Froude number similarity or process similarity must be met, depending on which type of model is desired. This may involve modification of the channel which is formed prior to the start of an experiment.

The final problem to be noted here concerns the variability of discharge. As timescale in a Froude Number model varies as $\lambda_L^{1/2}$ further compression of the timescale is usually used to speed up experiments. By using a constant water discharge model channels are in states of perpetual flood, which are by definition their dominant discharges. The role of fluctuating discharges in prototype rivers is complex with peak magnitudes, event inter-arrival times, and the order of occurrence of events all influencing channel response (Richards, 1982). The dominant discharges for sediment transport and channel morphology may be different, and separate aspects of these two groups of properties may be associated with different controlling flows. In view of this uncertainty the use of constant water discharge in laboratory experiments is often a necessary simplification, although a better understanding of the differences between constant and varying flows would assist result interpretation.

3.1.3 The experimental equipment

The experiments were performed in a sand tray 14.2m long and 3.0m wide (Figure 3.1). The depth of sediment averaged 0.15m, varying from 0.1m to 0.2m along the tray, the base of which was horizontal. The sand bed was given an initial slope by levelling with a wooden board mounted onto a beam which rested on rails along the edge of the tray. The slope of these rails could be altered and was set to that desired for the sand bed. Water was supplied to the head of the channel via a reservoir from a constant head tank. Discharge was regulated by means of a hand controlled valve and was measured using an orifice plate connected to a water manometer. It could be fixed by this method to $\pm 2.5 \times 10^{-5} \text{ m}^3\text{s}^{-1}$ which corresponds to $\pm 1.3 \%$ for the flow used. The reservoir at the head of the sand tray was sufficiently large to ensure that disturbances introduced where the water entered the reservoir were damped out. Two mesh screens helped to smooth the flow. Flow at the head of the experimental channel was transitional between laminar and turbulent ($Re \cong 1800$) as the water passed through a horizontal aluminium channel before entering the sand channel. Large ($\geq 100\text{mm}$) stones were buried in the sand at the end of this channel to dissipate flow energy and prevent scour of the bed. The distribution of water across

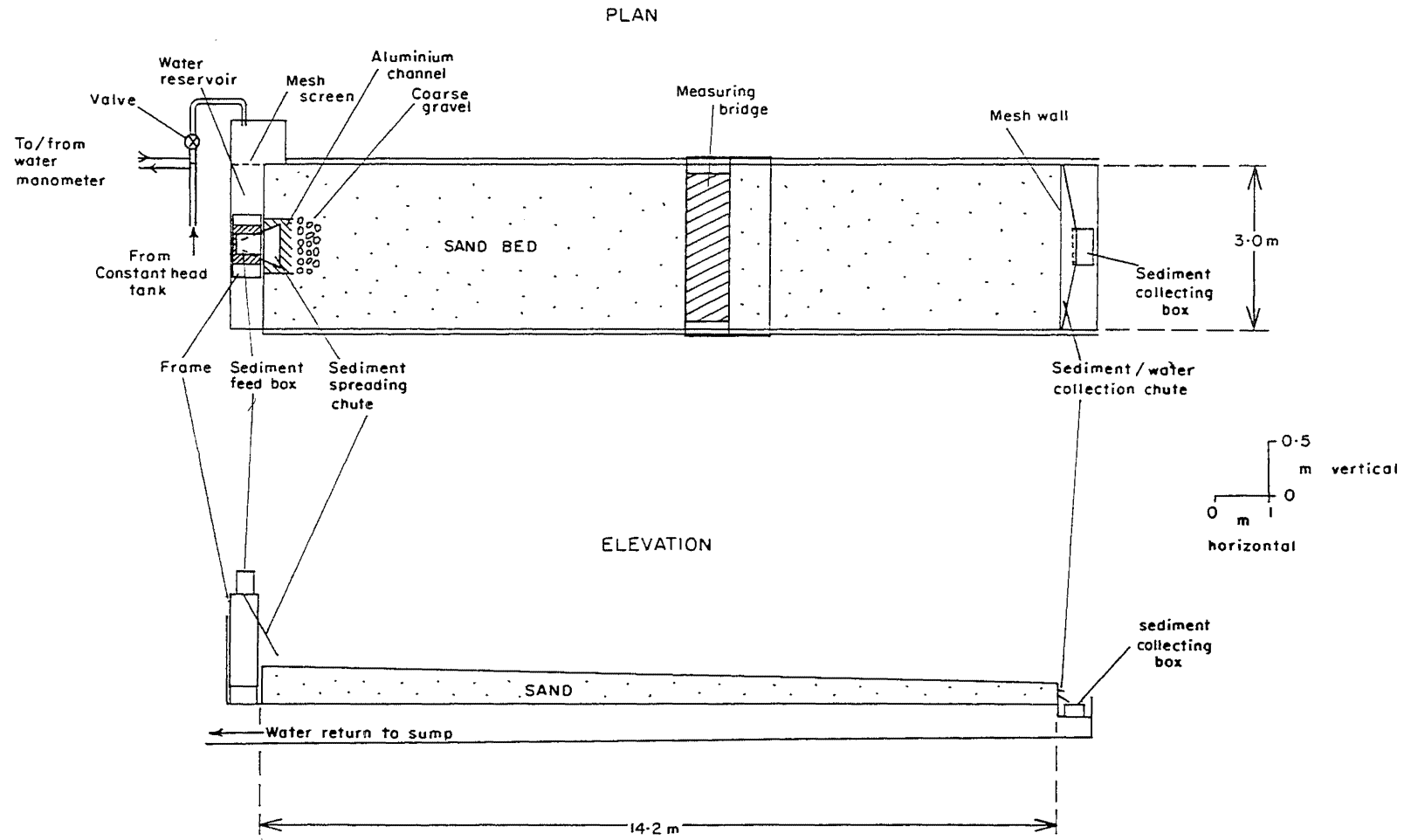


Figure 3.1 Plan and elevation of the sand tray showing its principal features.

the 1.0m wide entrance section was approximately even.

Dry sediment was added to the flow as the water passed through the aluminium channel. A spreading device (Figure 3.2) was used to ensure an even distribution across part or all of the width of the entrance section. Dry sediment was pre-weighed into appropriate amounts and fed into the spreader at 15 minute intervals. All of the sediment entered the chute within 1 minute and was removed by the flow within a further 3-5 minutes.

Bed elevation was varied at the downstream end of the tray by extending or shortening a wire mesh frame which held the sand in place. Subsurface water could penetrate this mesh but sediment could not so its surface acted as a base level. Sediment passing across the top of the frame was routed down an aluminium chute into a mesh collecting box (Figure 3.3). The water passing through the sediment collecting boxes was recirculated via a gravity system and sump. All material coarser than about 0.2mm was retained in the boxes. To allow for finer material passing through tests were performed during a preliminary experimental run whereby all of the sediment passing through was collected periodically. These suggested that $13.7 \pm 0.6\%$ ($n=2$) of material (by dry weight) was passing through the mesh. Some of this material accumulated in the floor of the area where the collecting box was located, the remainder collected in the water sump. Sediment transport rates were corrected accordingly. The transport rate was measured by leaving the accumulated sediment to drain for 5 minutes, weighing, and then converting to dry weight. The wet-dry conversion was calculated by oven drying samples to obtain dry weight, and was 0.74 ± 0.04 ($n=30$). Combining these two corrections gave a net correction factor of 0.85 ± 0.04 . 0.85 was used for all of the results presented herein.

The material used to fill the sand tray was sand from the Ashley River. Geometric scaling criteria as described in sub-section 3.1.2 showed that the distribution modelled that from prototype gravel rivers (Figure 3.4). Using d_{50} from the Ohau River gravel the scale ratio was 1:31.4. This exceeds the 1:60 maximum scale ratio estimated for this river in sub-section 3.1.2. The laboratory sediment was deficient with respect to the prototype material at both ends of the size distribution. To avoid the laboratory material becoming cohesive the fine tail of the grain size distribution could not be scaled down. The effects of this under-representation of fine material are not precisely understood, but sand is an important component of fluvial river gravels (Miall, 1977) and has a significant effect on gravel transport processes (Jackson and Beschta, 1984). The fine content increases bank strength and steepness enabling vertical or overhanging banks to develop, and width:depth ratios are smaller where the silt-clay percentage in the channel banks is greater (Schumm, 1960). The under-representation of the coarse end of the distribution may also effect sediment entrainment, armour development, and hence channel shape.

The laboratory material was generally sub-angular to sub-rounded in shape. These shapes are broadly similar to those reported by Blakely, Ackroyd and Marden (1981) for the Kowai River.

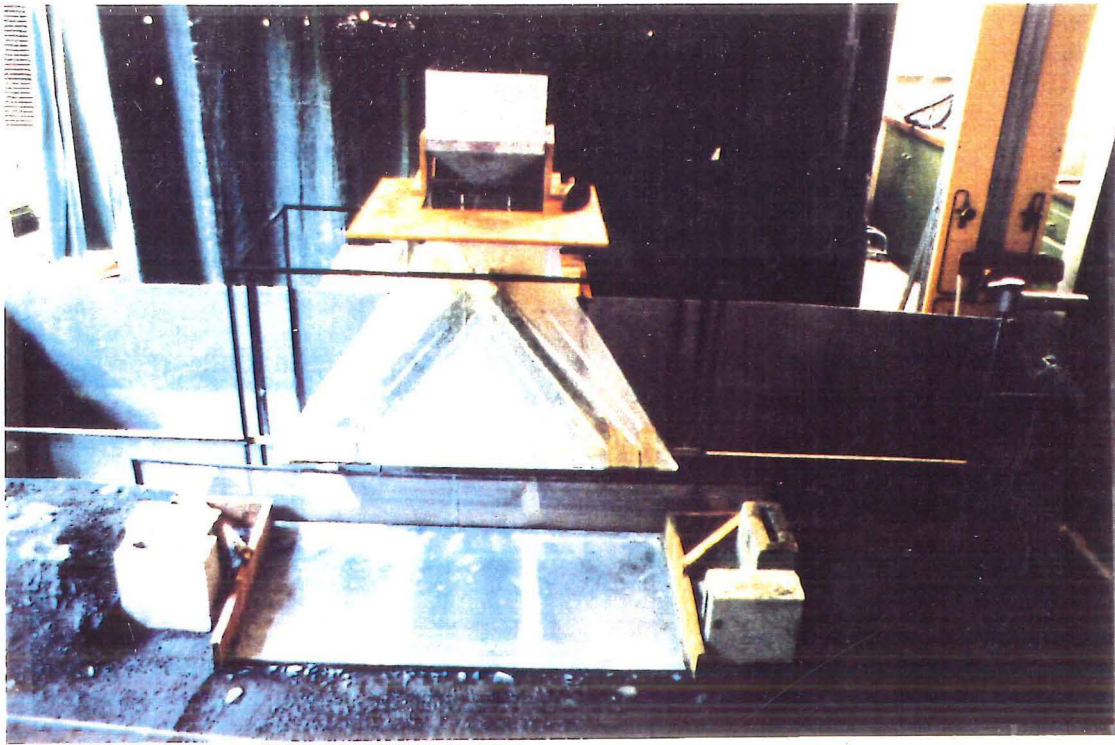


Figure 3.2 Sediment feed apparatus and entrance to the model channel. Sand passes through the aluminium box at the top and is spread across all or part of the head section by the perspex spreading chute. The sand mixes with water over a section of aluminium channel.

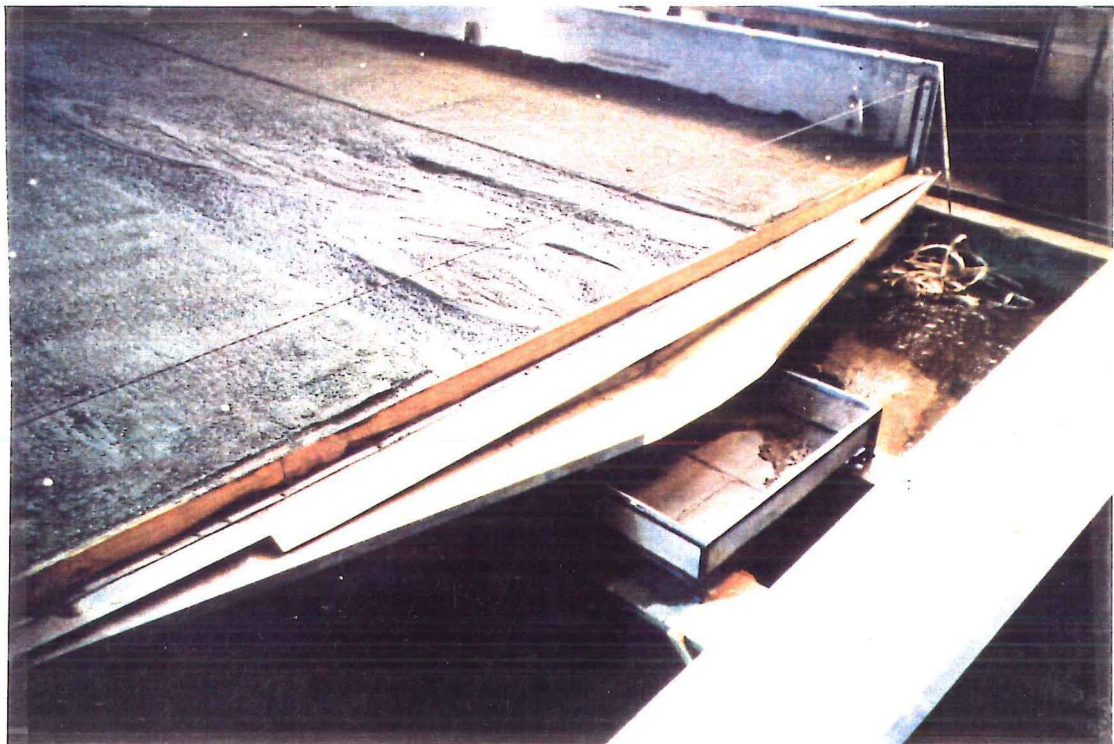


Figure 3.3 Sediment collecting area. Water and sediment pass out of the channel onto the sloping aluminium chute and into the mesh box (centre).

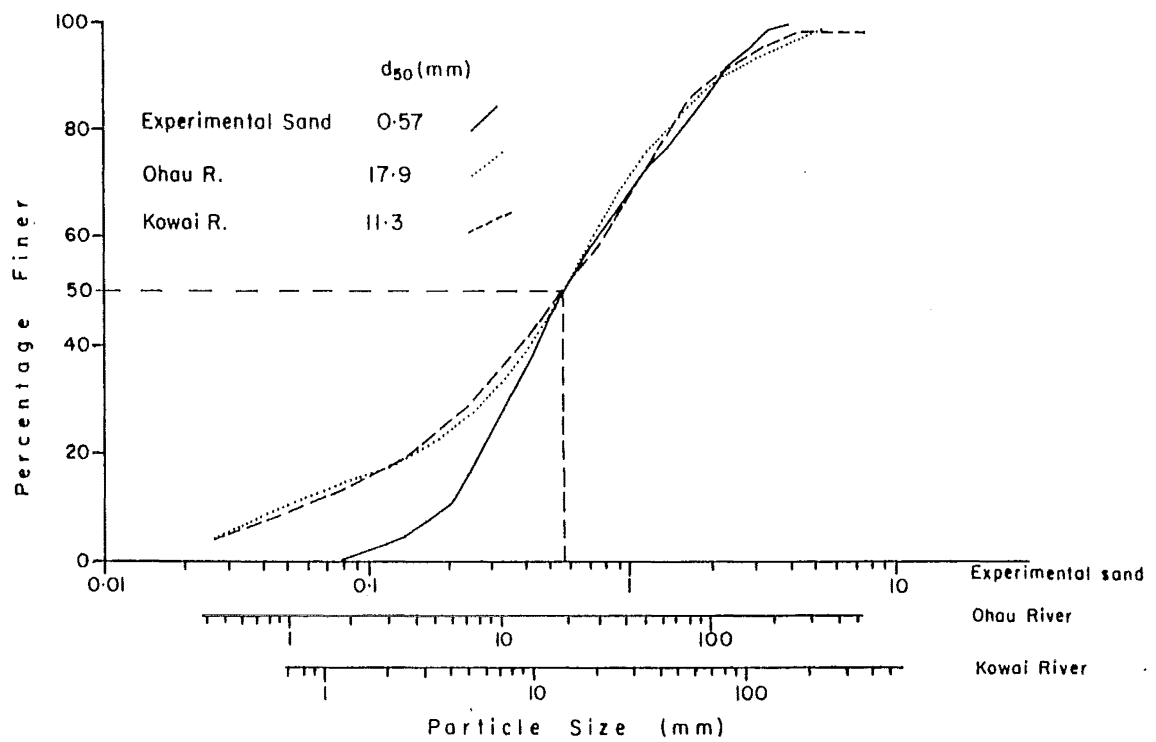


Figure 3.4 Particle size distributions of prototype and sand tray sediments. All are scaled by the d_{50} size. Ohau R. data is the average of 406 sub-surface bulk samples (from Thompson, 1985). Kowai R. data is the combination of 18 sub-surface bulk samples. Experimental sand data was obtained by dry sieving.

However, the particles are more spherical than is generally observed in prototypes, where high proportions of discs favour the development of imbrication (Bluck, 1982), and increase the shear stress required for particle entrainment (Komar and Li, 1986). Particle shapes vary with distance downstream and lithology but there are insufficient data from New Zealand rivers to enable detailed comparison of the shapes of sand grains used in the experiments with prototype material.

3.1.4 Standard experimental procedures

The sand bed was mixed with a garden rake prior to the start of each run to ensure its homogeneity. Rectangular channels of any desired width and depth (up to 3.0 x 0.1m) could be produced for the start of an experiment. Figure 3.5 shows the channel prepared for the start of a run. Before commencement of a run the sand tray was allowed to become fully saturated by running water into it at a very low discharge (about $1.0 \times 10^{-4} \text{m}^3 \text{s}^{-1}$). This usually took about 30 minutes. Discharge was increased to the value required for the run after this time. It took about 30 seconds for this to be completed at the upstream end of the channel, and a further 30 or so seconds for the increase to reach the downstream end. The equipment required constant monitoring so could not be left running overnight. At the end of each day the water input was turned off instantly; any sediment output from the channel after this time was not collected in the traps. As the water flow reduced, deposition occurred in some channels and bar faces were subject to localised slumping. The erosional effects were usually cancelled out when the flow was turned on again, although there were cases where channel changes which may have been induced by the shut-down occurred immediately after the resumption of flow

Each experiment was initially run for 20 hours spread over three days. Subsequently the flow was shut down every 4 hours (every 2 hours for part of Run 1) to enable measurements of cross-section and long profiles to be made. Occasionally parts of the initial channel banks collapsed and they were artificially rebuilt, care being taken not to exceed the initial bank elevation in this procedure.

Surveying of the channel bed and water surface was conducted using a beam mounted on a bridge across the sand tray (Figure 3.1). 3mm diameter aluminium rods of known length were lowered through holes drilled in the beam to rest on the channel bed, and the elevations of their tops read on a scale. Elevations relative to an arbitrary datum were then calculated. These calculations were corrected because the bridge and the rails on which it ran were not perfectly horizontal. At each shut-down in the flow 12 cross-sections located 1m apart, from 2m to 13m below the entrance to the aluminium channel at the head of the sand tray, were surveyed. Up to 50 elevations were measured on each cross-section, their precise locations depending upon breaks of slope. The minimum separation between measurement points was 0.01m. Long profiles of all channels were surveyed using the same apparatus. Successive data points were usually 0.3m to 0.5m apart. These long-profiles were repeated whenever possible with water

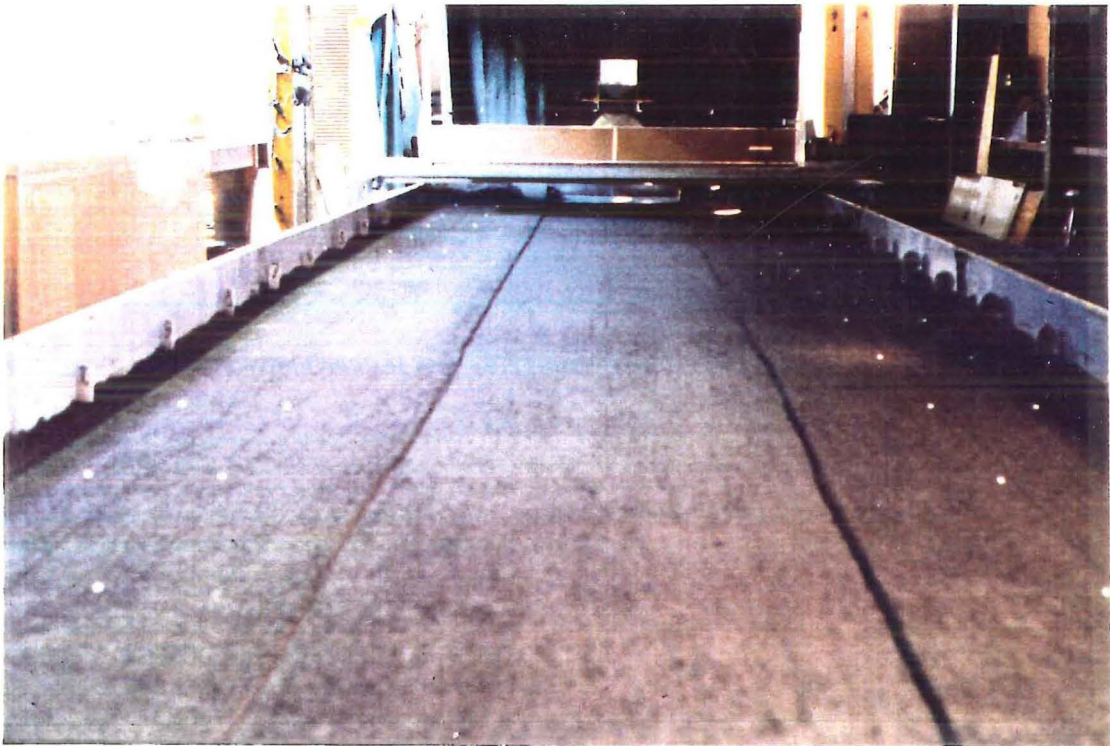


Figure 3.5 Initial channel cut into dry sand bed prior to the start of an experimental run.

surface elevations measured within 30 minutes of the recommencing of flow. Accuracy of reading the tops of the rods was estimated to be $\pm 0.5\text{mm}$ for all of the survey measurements, with the effects of slight bends in the rods being negligible.

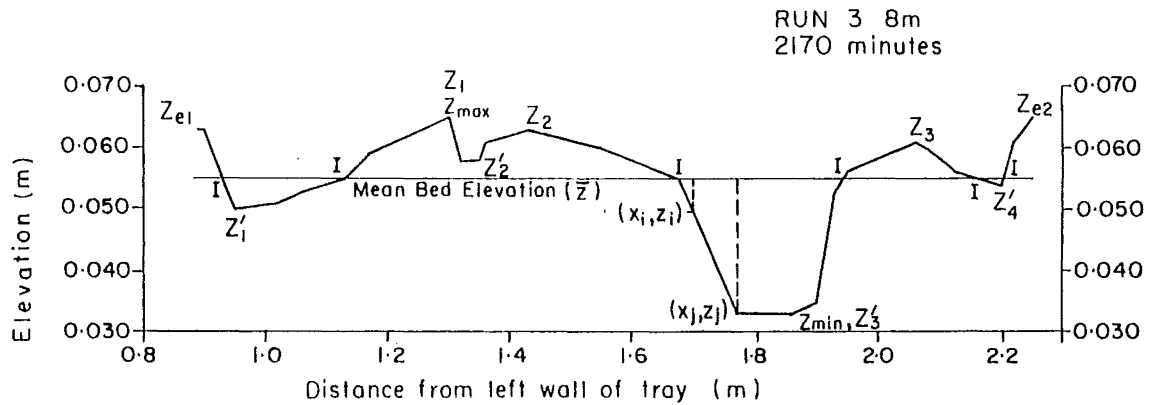
The data from a cross-section survey were used to calculate the mean bed elevation for that section. This procedure only applied to those parts of the channel that had been active at some time i.e. the pre-run channel banks were excluded. These mean elevations are also accurate to $\pm 0.5\text{mm}$. A bed relief index was calculated. Several such indices are available, ranging in complexity from a simple amplitude index (maximum elevation minus minimum elevation) to measures of the standard deviation of elevations about the mean. Three indices were computed for comparative purposes, examples of which are given in Figure 3.6. The bed relief index of Smith (1970) is also illustrated for comparison. This index was not used herein due to having neither the computational simplicity of the amplitude and dissection indices, nor making use of all the available elevation data. Only the bed relief index (BRI) is used in the subsequent discussion. It is defined as;

$$\text{BRI} = \left(\sum_{i=1}^n [(z_i^2 + z_j^2) / 2]^{1/2} [x_j - x_i] \right) / (x_n - x_1),$$

where z_i and z_j are successive bed elevations with respect to the mean, x_i and x_j their distances along the section, and x_n and x_1 the distances to the end points of the section.

The BRI has the advantage over the other indices that all of the available information on bed elevation is combined into a single index. This may create difficulties in interpretation, but in the comparative analysis the lack of information contained in the other indices reduced their sensitivity to changes in cross-section morphology. The amplitude index proved inadequate due to its overdependence on the depth of a single dominant channel or a small remnant of elevated bar surface in some cases. The dissection index produced discrete values which have insufficient resolution to describe a continuous range of morphological types. The BRI was only weakly correlated with the other two indices. Figure 3.7 presents examples of the BRI values associated with idealised cross-sectional profiles.

Cross-section data were also used to calculate the volumes of sediment located in different sediment storage reservoirs. An arbitrary datum was defined for the sand tray, this being 40mm below the pre-run channel bed and having a slope equal to the initial channel slope. The area of sediment between this datum and the surface of the cross-section was calculated. Each cross-section was sub-divided into different sediment storage reservoirs, namely active, semi-active, inactive and never active. This procedure is based on that used by Kelsey *et al.* (1987) although the definitions of the reservoirs are different. In their study the active reservoir was mobilised by flows with a recurrence interval (R.I.) of 1-5 years, semi-active by 5-20 year flows, and inactive by 20-100 year R.I. events. In the present study the reservoirs are defined as follows:



$$\text{Bed relief index (BRI)} = \left(\sum_{i=1}^n [(z_i^2 + z_j^2) / 2]^{0.5} [x_j - x_i] \right) / (x_n - x_1) = 0.00717$$

$$\begin{aligned} \text{Amplitude index} &= (\text{maximum bed elevation} - \text{minimum bed elevation}) \\ &= Z_{\max} - Z_{\min} = 0.065 - 0.033 = 0.032\text{m} \end{aligned}$$

$$\begin{aligned} \text{Dissection index} &= \text{Number of intersections between the mean bed elevation and the} \\ &\text{cross-section profile (I)} \\ &= 6 \end{aligned}$$

$$\begin{aligned} \text{Bed relief index} &= \{ 2[(Z_1 + Z_2 + \dots + Z_m) - (Z'_1 + Z'_2 + \dots + Z'_n)] \pm Z_{e1}, Z_{e2} \} \times 100 / L \\ \text{Smith (1970)} &\text{ where } Z_i \text{ are the elevations of height maxima between troughs, } Z'_i \\ &\text{ are minima between peaks, and } Z_{ej} \text{ are end elevations. } Z_{ej} \text{ are} \\ &\text{ added if they adjoin a trough, subtracted if they adjoin a peak.} \\ &= \{ 2[(0.065 + 0.063 + 0.061) - (0.050 + 0.058 + 0.033 + 0.054)] \\ &\quad + 0.063 + 0.065 \} \times 100 / 1.35 \\ &= 8.6 \end{aligned}$$

Figure 3.6 Calculation of alternative measures of bed relief using cross-section survey data.

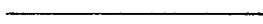
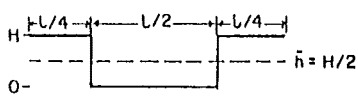
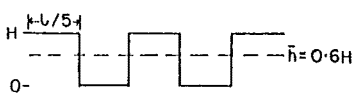
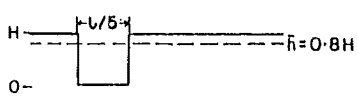
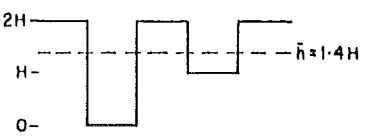
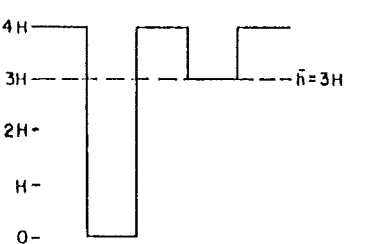
		B.R.I.	A.I.	D.I.
a) Plane bed		0	0	0
b) One channel occupying 50% of bed width		0.5H	H	2
c) Two equal channels, occupying 20 % of bed width each		0.48H	H	4
d) One channel occupying 20 % of bed width		0.32H	H	2
e) Two channels, each 20 % of bed width. One is double the depth of the other.		0.72H	2H	4
f) Two channels, each 20 % of bed width. One is four times the depth of the other.		1.20H	4H	2

Figure 3.7 Idealised cross-sections and indices of bed relief associated with each.

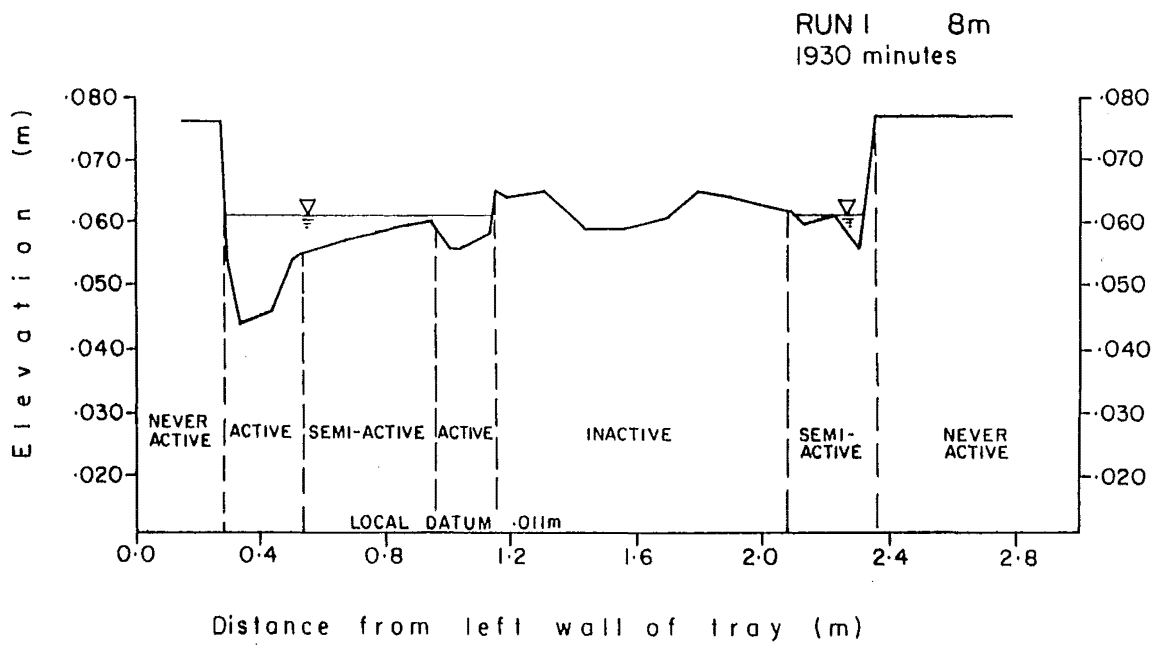
Active	sediment stored beneath bedload transporting channels;
Semi-active	sediment stored beneath bars and channels that are water covered, but which do not have appreciable bedload transport over / through them;
Inactive	sediment stored beneath bars which are emergent from the water;
Never active	sediment that remains beneath the banks of the initial pre-run channel.

The definition of these four reservoir types is illustrated in Figure 3.8a. Figure 3.8b presents the definition diagram from Kelsey *et al.* (1987) for comparison. Their active reservoir is broadly equivalent to the combined active, semi-active and inactive as defined herein. Their semi-active corresponds to the never active. The definition of reservoirs used here might appear to be comparable with the topographic levels in braided rivers defined by Williams and Rust (1969). The difference is that their levels reflect inundation frequencies in conditions of fluctuating discharge, whereas the reservoirs defined here are based on sediment activity with constant discharge. The two schemes are thus applicable to different conditions.

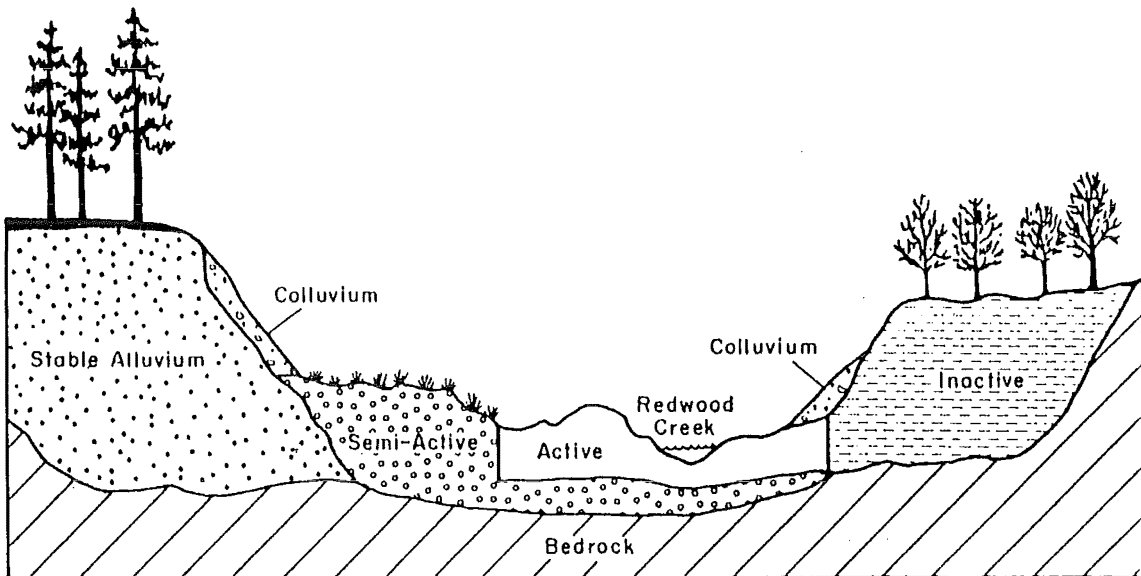
There are two processes by which reservoirs can receive or lose sediment. Firstly, deposition or erosion of material directly affects the volumes held in storage ('dynamic transfer'). Secondly, a change in water surface elevation can lead to a re-classification of sediment into different reservoirs ('static transfer'). Thus if bed and water surface levels rise during a phase of aggradation there would be a transfer of material from the inactive to the semi-active and active reservoirs. Similarly incision of a dominant channel with an associated drop in water level would cause these transfers to be reversed. Interpretation of changes in sediment storage over time or between reaches requires consideration of both of these processes.

The use of cross-section data is subject to sampling considerations. Drawing inferences about bed elevations and sediment storage patterns on the basis of such a sample requires a knowledge of the degree of sampling variability. No studies have been made of this variability and existing recommendations (Neill and Galay, 1967; Mosley, 1982) for the spacing of cross-sections in prototype rivers suggest that the number of sections should be appropriate to the form of the channel and the purpose of the investigation. The 1m spacing chosen for cross-sections in the sand tray was equivalent to ≤ 1 active channel width. Most unit bar forms and homogeneous channel reaches extended for more than one cross-section. Occasionally smaller scale features were located directly on sections. Most notable of these were confluence scour holes, the presence of which could significantly affect the indices of cross-sectional form and sediment storage. In the absence of more detailed information it is sufficient to note that the cross-section data represents a statistical sample of the bed of the sand tray, and that this imposes some limitations on data interpretation.

Vertical photographs were taken during the running of the experiments and after the flow was shut down. These were usually taken soon after flow was re-started following a shut-down so that



a)



b)

Figure 3.8 Definitions of sediment storage reservoirs.

a) Sand tray. Unit volumes stored in each reservoir in the example are: Active $0.018 \text{ m}^3/\text{m}$; Semi-active $0.034 \text{ m}^3/\text{m}$; Inactive $0.048 \text{ m}^3/\text{m}$; Never active $0.039 \text{ m}^3/\text{m}$.

b) As used by Kelsey *et al.* (1987).

the channel morphology on the photographs could be related to the cross-section data. Regular sketches of channel morphology were also made. To enable testing of the Froude and Reynolds number similarities the data necessary for calculation of these parameters were collected at various times during each run. Water depth was obtained using the survey equipment described above. Surface flow velocity was measured with polystyrene floats which were timed over a distance of 1.0m centred on the location where depth was measured. Surface velocity was converted to mean velocity by multiplication by 0.85.

A sediment sampling programme was carried out in each run. The data collected were used both directly and as a means of calibrating the sediment size variations visible on the vertical photographs. Sampling involved two methods: bulk sediment samples were taken using a small spatula from an area 0.02m x 0.02m, and to a depth not exceeding 0.01m; surface samples were scraped from the surface using the spatula. This meant that the thickness of the sampled layer was approximately equal to the size of the largest clasts in the surface layer. As such it is similar to the method recommended by Ettema (1984) for the sampling of armour layer sediments. This technique is specific to the present investigation and no attempt was made to compare its results with other methods for sampling coarse material. Because sample sizes were small the most reliable and simple technique for particle size analysis was to use a settling column. All samples were analysed using a Rapid Sediment Analyser (R.S.A.), which is suited to material in the 0.06mm to 2.8mm size range. Cross-checking of the results of this method with a standard dry sieve analysis showed them to be consistent for the sand used in the experiments.

A total of 24 samples were used to calibrate the textural differences visible on the vertical photographs. The sites were visually classified as fine, mixed, and coarse. These classifications are used throughout the following Chapters. The median particle sizes associated with each class were: fine $0.46 \pm 0.11\text{mm}$ (n=7); mixed $0.89 \pm 0.29\text{mm}$ (n=15); coarse $1.05 \pm 0.49\text{mm}$ (n=2). These are used throughout as estimates of the median sizes of sediment in each of the size classes.

The methods described above were used throughout the laboratory investigation. Other techniques that were used are described where they are introduced in Chapters 4-6.

3.1.5 The experiments

A. Operating conditions. Two series of experimental runs were conducted. The first, preliminary series consisted of five short (up to 720 minute) runs which were used for testing the survey equipment, the trapping efficiency of the sediment collecting baskets and other aspects of the experimental procedures. Three runs comprised the second series, and are designated Runs 1,2 and 3. Ashmore's (1985, 1988) data showed that when stream power and mean bedload transport rates are greater the patterns of temporal variability in transport rates became less clearly

defined. As the aim of the present study was to relate these fluctuations to channel processes, flow conditions which yielded lower values of stream power were selected. Using a slope of 0.01, a discharge of $2.0 \times 10^{-3} \text{ m}^3 \text{ s}^{-1}$ (2 l s^{-1}) was chosen. This gave a discharge-slope product of $2.0 \times 10^{-5} \text{ m}^3 \text{ s}^{-1}$, which lies towards the lower end of the range used by Ashmore (1988; his Figure 2). In practice the discharge used was $1.9 \times 10^{-3} \text{ m}^3 \text{ s}^{-1}$. Discharge and bed slope were the same for all three runs.

The initial channel was 1.0m wide for each run and depth was calculated so that $1.9 \times 10^{-3} \text{ m}^3 \text{ s}^{-1}$ represented the bankfull discharge condition. The channel depth was estimated using the following resistance equations for gravel-bed rivers from Bray and Davar (1987):

$$1 / \sqrt{f} = 1.9 (R / d_{84})^{0.25} \quad (3,1) \text{ and,}$$

$$1 / \sqrt{f} = 2.0 \log_{10} (R / d_{84}) + 1.1 \quad (3,2).$$

$1 / \sqrt{f}$ is given by,

$$1 / \sqrt{f} = \bar{u} / (8 g R S)^{0.5} \quad (3,3).$$

In the above, f is the dimensionless Darcy-Weisbach friction factor. For initial channel conditions equation (3,1) predicted a flow depth of $8.4 \times 10^{-3} \text{ m}$, and equation (3,2) gave $9.0 \times 10^{-3} \text{ m}$. The initial channel was therefore cut to $9.0 \times 10^{-3} \text{ m}$ (9mm) depth.

The sediment input rate for Run 1 was estimated using equation (3,4) which Ashmore (1985) fitted to a range of laboratory data. Dimensionless bedload transport, q_b^* , is related to a dimensionless stream power index by

$$q_b^* = 7.2 \times 10^{-4} (\omega^* / \omega_c^*)^{3.02} \quad (3,4),$$

in which ω^* is calculated using equation (2,2) and ω_c^* is a critical value of ω^* suggested by Ashmore (1985) to equal 0.1 for most laboratory conditions. Dimensionless bedload transport was converted to a mass rate of bedload transport, G_b (kg s^{-1}) using

$$G_b = q_b^* \cdot \rho_s \cdot b [(S_s - 1) g d_{50}^3]^{0.5} \quad (3,5).$$

For the initial channel conditions, $\omega^* = 0.351$, $q_b^* = 0.032$, and $G_b = 4.6 \times 10^{-3} \text{ kg s}^{-1}$ which is equivalent to 16.4 kg h^{-1} . Assuming that narrowing of the water surface would occur as the initial channel adjusted to equilibrium and that the sediment transport rate would also tend to reduce, an input rate of 15 kg h^{-1} was chosen. Using a sediment feed system, the input rate requires adjustment to ensure that equilibrium is maintained. In a study of the differences between sand feed and recirculating flumes Guy, Rathbun and Richardson (1967) concluded that there were no significant differences in flow or sediment transport parameters between the two system types. It is not clear to what extent these conclusions extend to cases where channels self-form in the sand tray, and in the present case care had to be taken in altering the sediment input since an object of the study was to measure the effects of constant flow and sediment supply conditions. In Run 1 the sediment input rate was adjusted during the first 1200 minutes (discussed in Chapter 4) after which a constant rate of 10 kg h^{-1} ($2.8 \times 10^{-3} \text{ kg s}^{-1}$) was used. For Runs 2 and 3 the input rate used was constant at $2.5 \times 10^{-3} \text{ kg s}^{-1}$ (9 kg h^{-1}).

The arrangement of the sediment feed system at the head of the channel was varied between the runs. In Run 1 sediment was evenly spread across the 1m wide input section until 1200 minutes, by which time severe aggradation was occurring in the upper 1m of the channel. The arrangement was then changed so that the central 0.4m of the input section received all of the material. This configuration was retained for Run 2. In Run 3 sediment was input to two 0.39m wide areas, with zero input to the central 0.22m of the input section.

Table 3.1 summarises the experimental conditions for the three runs. After 48 hours of Run 3 the sediment input rate was varied so as to simulate the input of a bedload pulse from upstream. This is described in detail in Chapter 5.

Table 3.1 Boundary conditions for the experimental runs. Times given in minutes after start of each run.

Run	Discharge (m^3s^{-1})	Initial Slope	Initial channel width (m)	Initial channel depth (m)	Sediment input rate (kg h^{-1})	Sediment feed configuration
1	1.9×10^{-3}	0.01	1.0	9.0×10^{-3}	varied until 1200 10 after 1200	across entire 1m width until 1200 all input to central 0.4m after 1200
2	1.9×10^{-3}	0.01	1.0	9.0×10^{-3}	9	all input to central 0.4m
3	1.9×10^{-3}	0.01	1.0	9.0×10^{-3}	9	input split into 2, 0.39m areas at the edges of the input channel

B. Preliminary observations. For practical purposes it is necessary to estimate discharge from channel width which is the most readily measured variable in the sand tray. Dimensioned hydraulic geometry relationships are given in Table 3.2 and are shown graphically in Figure 3.9. The data used in derivation of these relationships are given in Appendix 2. Scatter in the data for equilibrium channels is as great as in the data for all channels, and regression equations for the equilibrium channels alone are not statistically significant. The width and depth equations for the two runs are statistically dissimilar but within the range of data used these differences are small. The exponents compare reasonably well with the commonly reported values of 0.5, 0.4 and 0.1 for width, depth and velocity. Predictive equations for discharge in terms of width calculated from these data are :

$$Q = 2.15 \times 10^{-3} b^{0.92} \quad (r^2 = 0.39; \alpha = 0.01) \quad (3,6a)$$

for Run 1 and,

$$Q = 6.27 \times 10^{-3} b^{1.52} \quad (r^2 = 0.48; \alpha = 0.0001) \quad (3,6b)$$

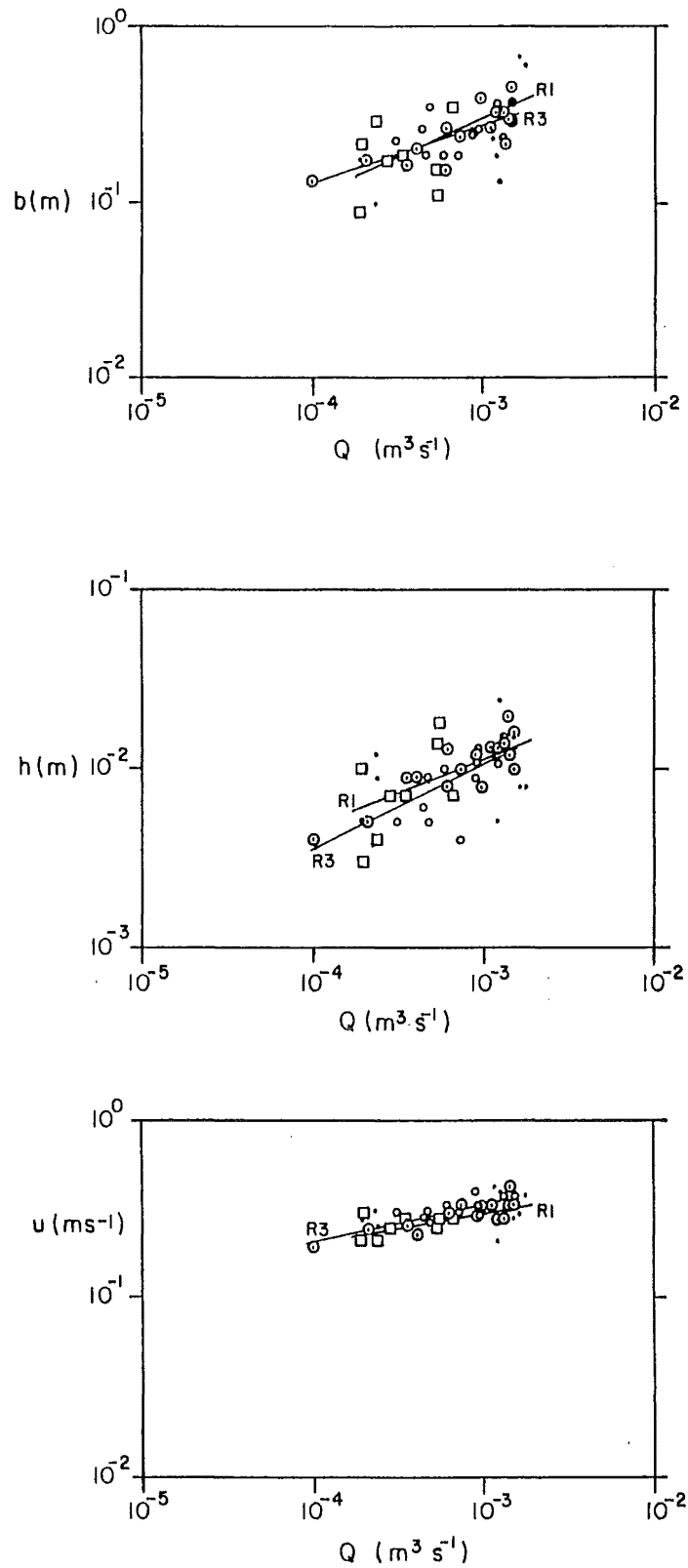


Figure 3.9 Dimensioned hydraulic geometry relationships for Runs 1 and 3.

Symbols are: \square Run 1 equilibrium channels; \bullet Run 1 non-equilibrium channels; \circ Run 3 equilibrium channels; \odot Run 3 non-equilibrium channels. Regression curves shown are described in Table 3.2.

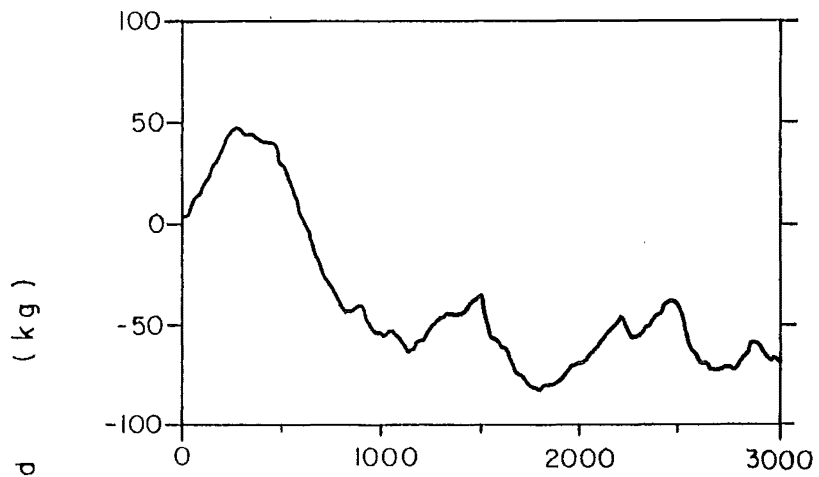
for Run 3.

Table 3.2 Dimensioned hydraulic geometry relationships for the experimental runs. Combining the data in the form $Q' = b \cdot h \cdot u$ gives $Q' = 0.98 Q^{1.00}$ for Run 1, and $Q' = 0.96 Q^{1.01}$ for Run 3.

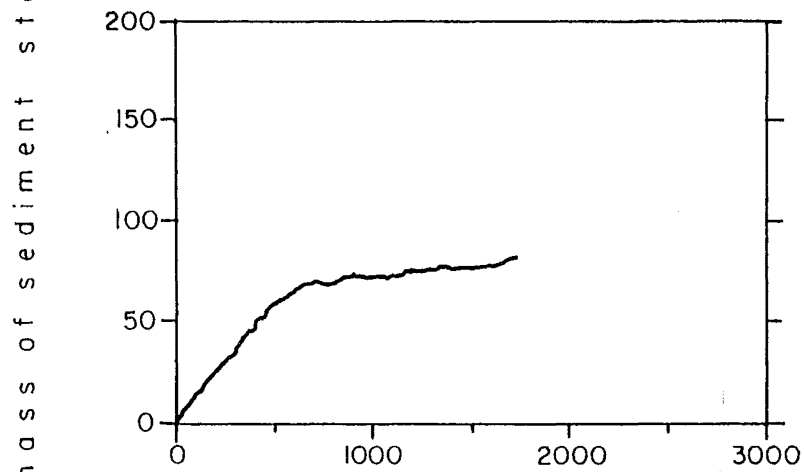
Variable	Run	No. of Observations	Equation	r^2	Significance level (α): F-test
width	1	17	$b = 5.36 Q^{0.43}$	0.39	0.025
	3	28	$b = 2.38 Q^{0.32}$	0.48	0.0001
depth	1	17	$h = 0.17 Q^{0.39}$	0.36	0.005
	3	28	$h = 0.31 Q^{0.49}$	0.59	0.0001
velocity	1	17	$u = 1.08 Q^{0.18}$	0.52	0.01
	3	28	$u = 1.30 Q^{0.20}$	0.58	0.0001

The hydraulic geometry data suggest that there are some differences between Runs 1 and 3. When sediment transport and channel morphology data are examined, further differences between the runs emerge. These are described fully in Chapter 4. Considering only the net change in volume of sediment stored within the sand tray (i.e. total input- total output) Run 1 is distinctly different from both Runs 2 and 3 (Figure 3.10).

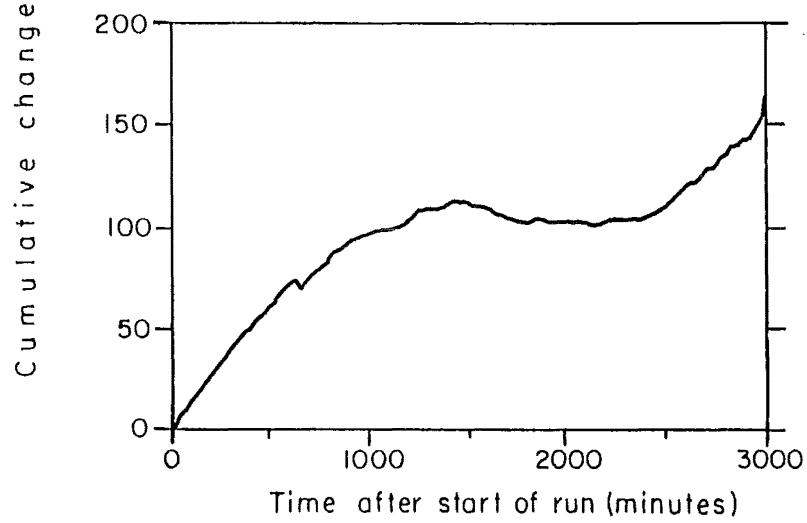
In Run 1 after an initial aggradation-degradation cycle phases of aggradation and degradation alternated in a quasi-rhythmical way. The initial aggradational phase consisted of a period of bar formation (both bank attached and medial types developed) and local channel widening. In Run 3, a prolonged aggradational phase was followed by a long period of equilibrium, and then by renewed aggradation with Run 2 replicating the first two parts of this sequence. Throughout the duration of Run 1 channel pattern changes were more frequent than in Runs 2 and 3, and widened more from the initial 1.0m wide channel (Figure 3.11). The reason why Runs 2 and 3 should be aggrading systems and Run 1 not so is not readily apparent given that they had the same water discharge, initial slope and channel conditions. There were two differences between the runs, namely the distribution of input sediment across the head of the channel, and the rate of input. Sediment input rate in Run 1 was varied until 1200 minutes, which could account for the change in amplitude of the fluctuations in volume change at about this time (Figure 3.10a). However, the reduction in sediment storage between about 500 and 1200 minutes was caused by bank erosion as the active channel widened and not by throughput of the material input at the head of the channel, most of which was deposited in the uppermost 2m of channel. After 1200



a) RUN 1



b) RUN 2



c) RUN 3

Figure 3.10 Cumulative changes in mass of sediment stored (input-output) within the sand tray.

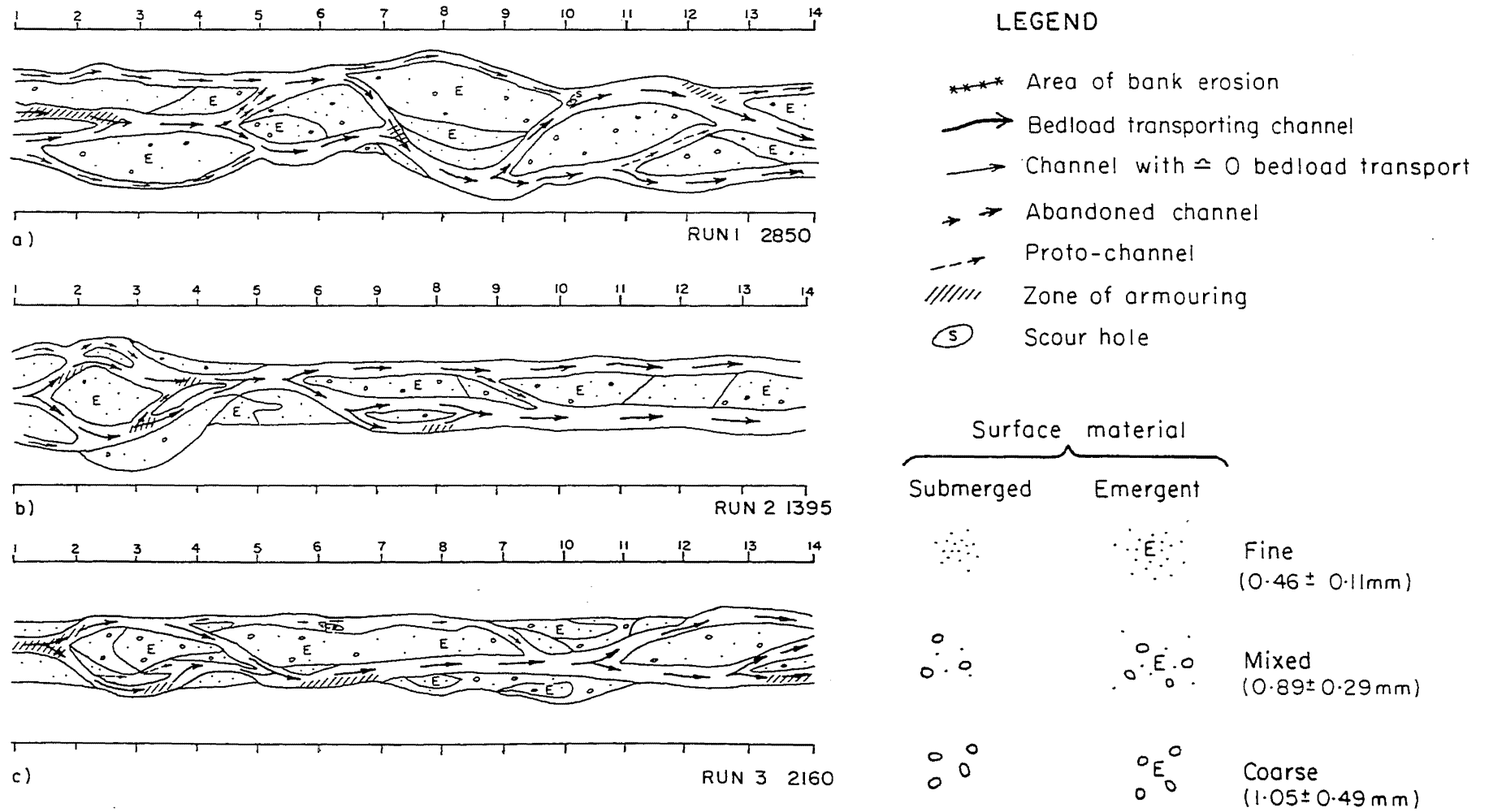


Figure 3.11 Examples of the different channel morphologies in Runs 1,2 and 3.

minutes sediment input was at constant rate and regular fluctuations in output continued until the end of the run. These are interpreted as being independent of the variation in sediment input over the first 1200 minutes, but the the initial variation may have set up an oscillatory response which persisted within the system.

The second difference was in the sediment input arrangement. In Runs 1 and 2 the input was entirely in the central part of the section, with areas adjacent to the edges of the 1.0m wide head section receiving all of the sediment in Run 3. The deposition of a large amount of sediment in the central area early in Run 1 undoubtedly encouraged water flow towards the initial banks, leading to erosion and then to the downstream progression of a meandering thalweg. In Run 2 this central deposition did not result in downstream progression of the thalweg. In Run 3, the channel remained towards the centre of the section upstream of about 4m, below which it diverted towards one or both banks from as early as 360 minutes. This was in response to deposition of a mid-channel bar. Why further bank erosion and pseudo-meandering did not occur downstream of this location is unclear.

Qualitatively the processes operating in the runs appeared similar, all apparently behaving as models of active gravel-bed rivers, and the magnitude of the differences in morphology and sediment transport is surprising. This may reflect the sort of variability in the patterns of such rivers suggested by Ashmore (1985). Pattern variability with the same conditions of slope and discharge is well known, and Begin (1981) proposed that for any value of excess shear stress there are different probabilities associated with different patterns, but only at extremes is one exclusive pattern possible. In the present case, two different types of river have developed with similar external controlling variables. Because there were some differences between these controls for the three runs it is not possible to say whether or not the differences in form and behaviour were caused by this variation. Without replication of the conditions in these runs it is not possible to determine the causes of the observed differences.

3.1.6 Tests of similarity and scaling

Dynamic similarity requires that Froude numbers and dimensionless depths are the same in laboratory and prototype situations, and that the Reynolds and particle Reynolds numbers exceed critical values. Measurements of these parameters were made at various times throughout each run at a range of locations within the channels. An appropriate roughness length, k_s , requires definition for these calculations. Two values of k_s are used herein, namely d_{50} and d_A which is equal to the largest material size present divided by 1.8. This is based on the suggestion of Chin (1985) that the maximum size of armour that can develop is equal to d_A . For the experimental sand $d_{50}=0.57\text{mm}$ and $d_A=1.99\text{mm}$. d_A lies between d_{84} (1.82mm) and d_{90} (2.44mm). Both estimates are conservative with respect to the roughness lengths recommended previously and so give a more rigorous test of dynamic similarity. Table 3.3 summarises the data

used for this test, which are detailed in Appendix 3.

Table 3.3 Summary of data used to test dynamic similarity in the laboratory channels. The Froude number, $Fr = u / (g h)^{0.5}$. Other parameters are described in the text. S.D. refers to the standard deviation of the observations. * indicates that only channels where bedload transport was occurring are included in the data.

Run	# of cases	Re		$Re_p (d_{50})$		$Re_p (d_A)$		Fr		h/d_{50}		h/d_A	
		mean	S.D.	mean	S.D.	mean	S.D.	mean	S.D.	mean	S.D.	mean	S.D.
1	80	3670	2270	19.0	5.3	68.1	18.0	0.90	0.22	22.1	10.2	6.3	2.9
2	22	3960	1530	19.7	7.6	68.8	26.7	0.81	0.14	25.1	7.6	7.2	2.2
2*	16	4470	1410	20.8	8.3	72.5	29.1	0.84	0.11	26.6	7.4	7.6	2.1
3	71	4140	2530	18.8	5.4	65.7	18.9	0.86	0.20	24.3	10.7	7.0	3.1
3*	36	5360	2590	20.4	5.2	71.1	18.1	0.88	0.18	28.7	10.4	8.2	3.0

In all runs mean Reynolds numbers were in excess of the critical value (2000) and no values below the onset of the laminar-turbulent transition (500) were recorded. Using d_{50} as the roughness length, particle Reynolds numbers lie well below the threshold value, but when d_A is used the mean values are close to the threshold of 70. Some channels have values of Re_p below this threshold and the influence of viscous forces cannot be ignored, although Re_p is slightly greater in the bedload transporting channels that are of most interest. During the experiments large areas of bar surfaces and abandoned channels were covered by thin water films retained in place by surface tension. Although not a phenomenon that occurs in prototype rivers these thin (1-2mm) films have little apparent effect on sediment transport processes. They may be significant where they develop towards the banks of bedload transporting channels and act to reduce the potential for entrainment of material from the channel banks.

The Froude numbers and dimensionless depths given in Table 3.3 appear broadly consistent with values reported from prototype gravel-bed rivers. Laronne *et al.*(1986) measured cross-sectionally averaged values of $Fr = 0.68 \pm 0.16$ (n=33), with maximum values on any one vertical of 0.94 ± 0.30 (n=32). This latter case is closest to the data collected in the laboratory experiments, although the standard deviation is greater in the prototype due to a few cases where $Fr > 1.4$ (Laronne *et al.*,1986 p. 234). Using Griffiths' (1981) hydraulic geometry data to calculate cross-section averaged Froude numbers gives mean values of 0.30 ± 0.14 (n=84) for channels with no bedload transport, and 0.61 ± 0.15 (n=52) where bedload transport was occurring. During flood conditions in the braided Butramo River, Ergenzinger (1987) measured Froude numbers with a mean of 0.93 ± 0.12 (n=63). A similarly reasonable agreement between prototype and laboratory is obtained for the ratio h/d_{50} . The two reaches of the Ashburton R. give mean values

of 11.2 ± 3.9 (n=20) and 5.1 ± 1.3 (n=13) (Larone *et al.*,1986), and Griffiths' data yield 29.4 ± 35.4 (n=84) and 34.9 ± 28.1 (n=52) for rigid and mobile bed data respectively. It is not possible to be more precise about the correspondence between these two quantities in the prototype and laboratory because comparable sampling procedures were not followed in the two situations. In general terms the agreement appears sufficient to state that the conditions for dynamic similarity are not violated by Froude numbers or dimensionless depths.

The similarity criteria which form the basis of the modelling approach are met by the model with the exception that surface tension effects are not negligible in certain locations within the experimental channels. A test of the scaling of channel dimensions can be made by analysing the hydraulic geometry of the channels in the sand tray. Three dimensionless quantities are used; dimensionless discharge $Q^* = Q / [(S_s - 1) g d_{50}^5]^{0.5}$; dimensionless water depth $h^* = h / d_{50}$; dimensionless width $b^* = b / d_{50}$. Parker (1982) used bankfull discharge and pavement particle size for the development of dimensionless hydraulic geometry relationships. The data used here include two channel types: equilibrium channels are those that were not aggrading, degrading or widening at the time of measurement, and were not armoured; non-equilibrium channels were undergoing one or more of these changes or were armoured. The equilibrium channels can be assumed to be conveying their dominant discharge but this assumption does not apply to the others. Equilibrium of channel boundary shape does not necessarily imply equilibrium of sediment transport. Calculations were based on bulk d_{50} of the laboratory sand in the absence of sufficiently detailed information on pavement material sizes.

As is usually the case with such data considerable scatter is present (Figure 3.12 a-c), and equilibrium and non-equilibrium channels show substantial overlap. The scatter is most marked for the channel slope data since slopes were not measured specifically for this purpose and insufficient elevations were surveyed for these estimates to be reliable. Prototype slope data also exhibit considerable scatter (Parker, 1982). Measurement problems contribute to the scatter in both width and depth data. There is some consistency between these results and the four data sets presented by Parker (1982; Figure 3.12d-f) and one from Ergenzinger (1987). Regression equations for the present study are presented in Table 3.4 (the data used in their derivation are in Appendix 2). Again width and depth equations for the two runs are similar within the range of data used (Figure 3.12d,e).

The measured dimensionless channel depths are lower than in the prototype rivers although consistent with laboratory data presented by Parker (1982) (Figure 3.12d). Channel width data for Runs 1 and 3 plot close to data from single channels with cohesive banks in the U.K. and are consistent with Parker's (1982) laboratory anabranches and Ergenzinger's (1987) prototype anabranch data. Both width and depth are less than in the Albertan data for both single thread channels and braided anabranches, and this is compensated for by greater slopes and flow velocities in the model channels (Figure 3.12f). The considerable overlap between the field and

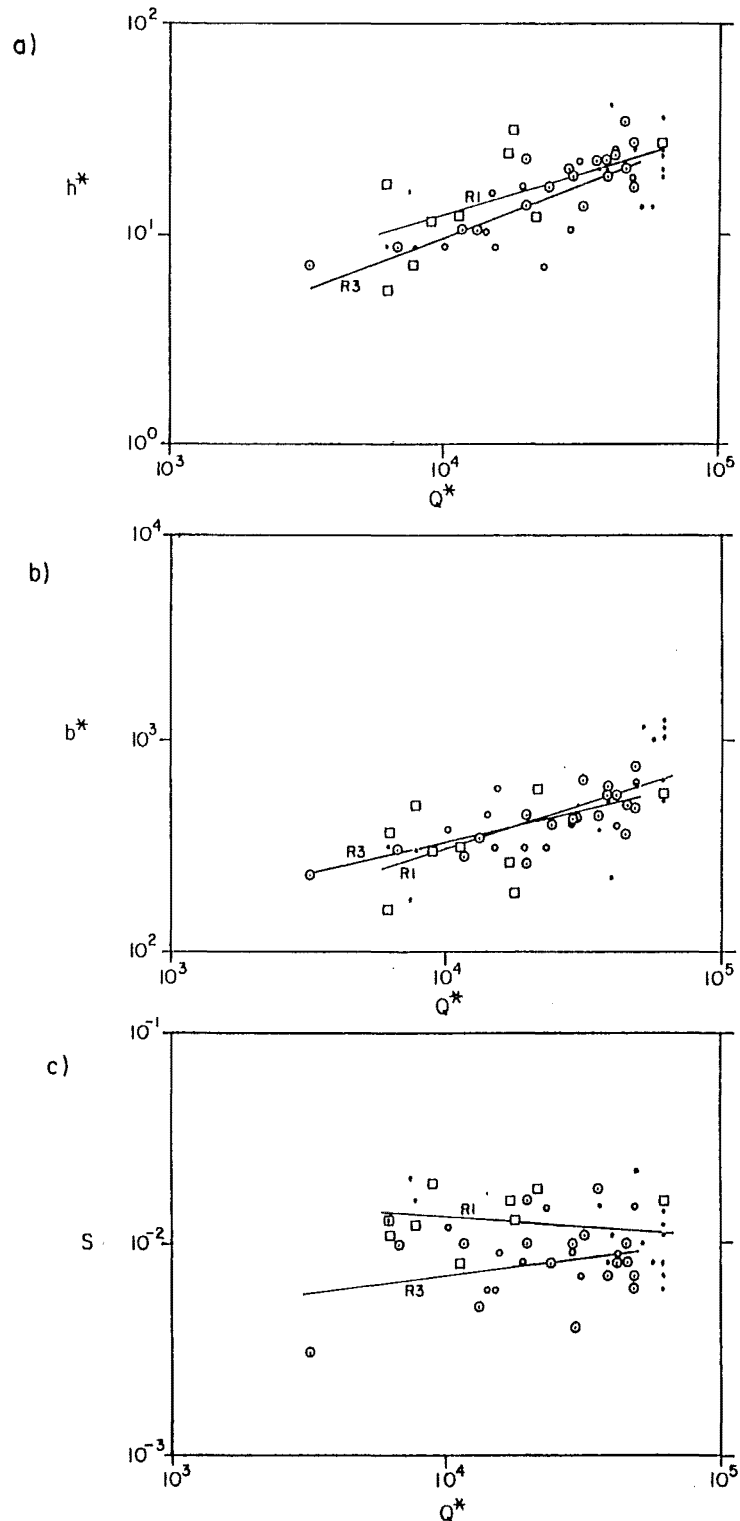


Figure 3.12 Dimensionless hydraulic geometry data. Regression curves on a)-c) are described in Table 3.4. Symbols on a)-c) are: \square Run 1 equilibrium channels; \cdot Run 1 non-equilibrium channels; \circ Run 3 equilibrium channels; \circ Run 3 non-equilibrium channels. Data sets on d)-f) are: 1. single channel U.K.; 2. single channel Alberta; 3. Sunwapta R. anabranches; 4. laboratory anabranches; 5. Butramo R. anabranches; \circ - Ohau R.; R1- Run 1; R3 - Run 3. Data sets 1-4 from Parker (1982), 5 from Ergenzinger (1987). Ohau R. data from Thompson (1987; Table 16.3).

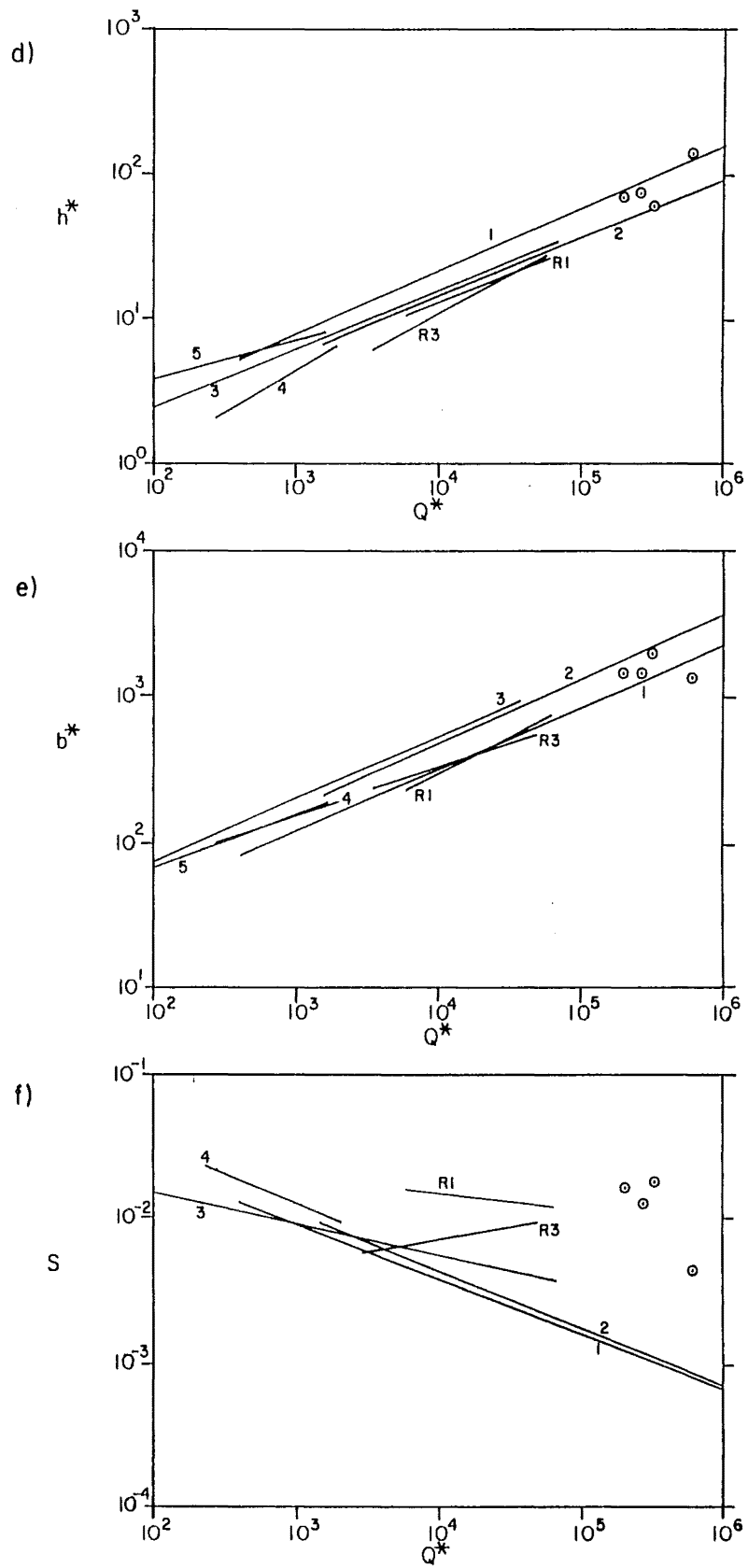


Figure 3.12 (Continued)

laboratory data in terms of depth and width suggests that geometric scaling is attained in the model although there are some differences between the data sets.

Table 3.4 Dimensionless hydraulic geometry relationships for the experimental runs. N.S. = not statistically significant.

Variable	Run	No. of Observations	Equation	r^2	Significance level (α): F-test
width	1	17	$b^* = 5.87 Q^{*0.43}$	0.37	0.01
	3	28	$b^* = 17.70 Q^{*0.32}$	0.61	0.0001
depth	1	17	$h^* = 0.32 Q^{*0.40}$	0.39	0.01
	3	28	$h^* = 0.08 Q^{*0.52}$	0.61	0.0001
slope	1	17	$S = 3.1 \times 10^{-2} Q^{*-0.09}$	0.05	N.S.
	3	28	$S = 1.5 \times 10^{-3} Q^{*0.17}$	0.07	N.S.

Application of the regime theory of White *et al.* (1982) to some of the laboratory data revealed that the channels are wider and shallower than theoretically predicted (Hoey and Sutherland, forthcoming). Thompson (1987) demonstrated the applicability of this theory to the braided Ohau R., data for which are included in Figure 3.12d-f. The Ohau data is consistent with the laboratory data in terms of b^* , h^* and slope (N.B. slopes for the Ohau R. are those predicted from the theory and were not measured). Thus the Ohau R. channels also exhibit geometric scaling with the laboratory channels but the regime theory applies much better to the former than to the latter. This casts doubt over the regime theory and/or the dynamic similarity between model and prototype. Given the apparent success of the theory in the Ohau R. case it is suggested that the results illustrate the inability of the model to faithfully replicate gravel-bed river processes. Further, this suggests that dynamic similarity between model and prototype may not be achieved. The model results cannot be expected to be quantitatively reliable, therefore, and the modelling procedure is closer to 'process similarity' than to full hydraulic similarity.

3.2 The prototype river study

3.2.1 The field site

Field investigation took place in the Kowai River, near Springfield, New Zealand (Figure 3.13). The Kowai basin lies on the eastern side of the Torlesse Range, the easternmost range of the

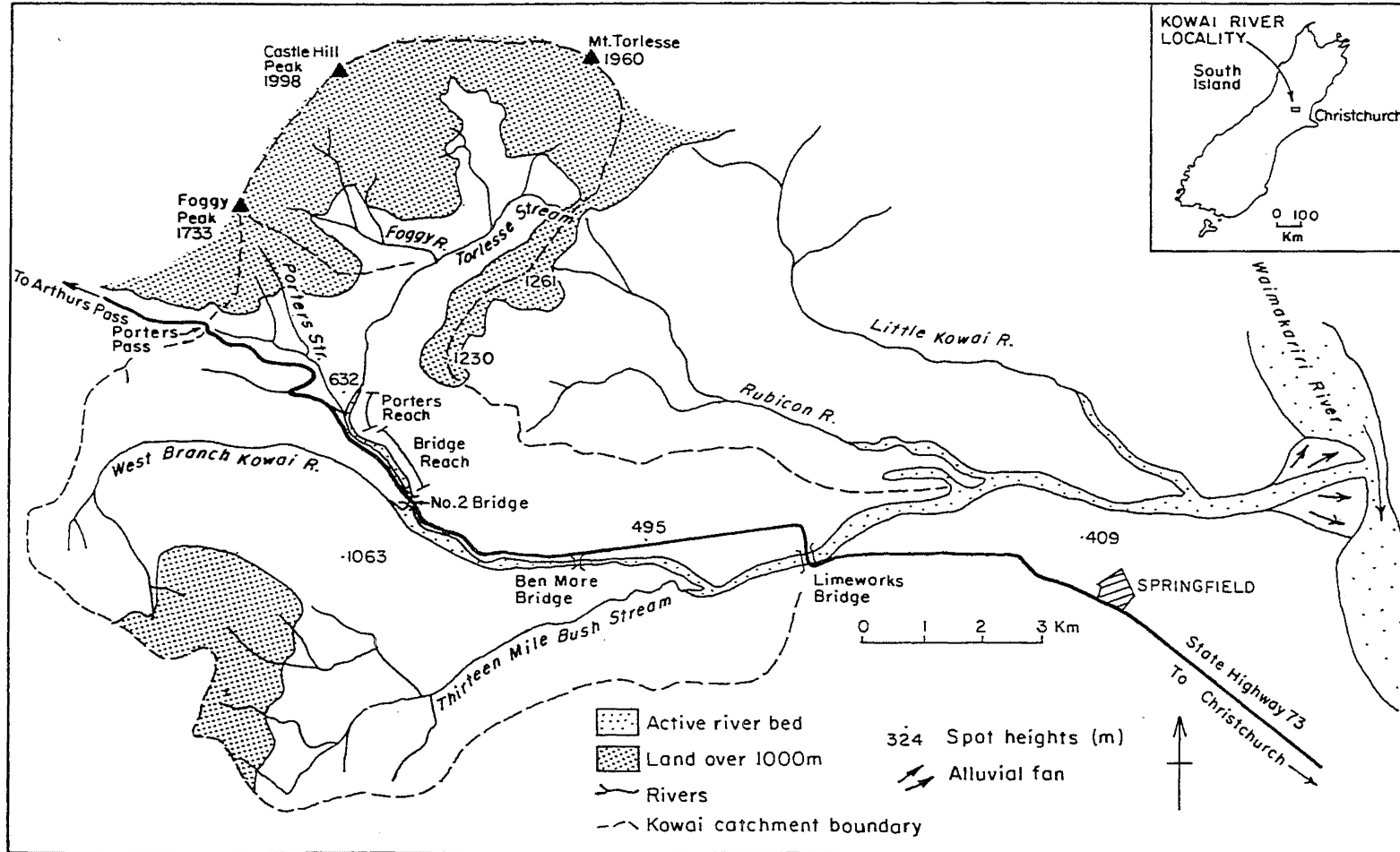


Figure 3.13 Location of the Kowai River showing major tributaries and study reaches.

Southern Alps in this vicinity. The basin is characterised by steep sided valleys infilled with fluvio-glacial gravels, and valley width increases rapidly towards the confluence with the Waimakariri River.

One of the Kowai tributaries, the Torlesse Stream, was studied extensively by Hayward (1980) from hydrological and geomorphological viewpoints. Blakely *et al.* (1981) and Beschta (1983a,b) have reported the results of work conducted within the Kowai catchment itself. Some of the cross-sections surveyed by Blakely *et al.* were re-used for the present study. Brunnsden (1973) presented a geomorphological map of part of the basin.

Outwash surfaces and terraces related to five glacial episodes have been identified within the valley (Blakely *et al.*, 1981). Below about 9km from its source the Kowai becomes a wandering gravel river, classified as Wandering Type II in the scheme of Carson (1984a), and having multiple channels at all except the lowest stages along much of its length. Reach averaged bed slopes range from 0.0238 at the start of this wandering reach to 0.0159 towards the confluence with the Waimakariri (Blakely *et al.*, 1981). The 'two year dominant flow' is estimated to be $120 \text{ m}^3 \text{ s}^{-1}$ at the Limeworks Bridge (Figure 3.13), and the fifty year flood = $373 \text{ m}^3 \text{ s}^{-1}$, based on data from similar gauged catchments. The hydrologic regime of the catchment is dominated by high magnitude rainfall events that can occur at any time of the year, and by snowmelt induced events in the Spring. Snowmelt is not always rapid and significant flood events do not occur every year. Seasonal mean flow variations in the nearby and similar Ashley and Selwyn Rivers show peaks in August and September (NCCB, 1982). Maximum discharges in the Ashley are greatest in March-September inclusive.

3.2.2 Methods used in the present study

Two adjacent reaches covering 3.5 km were selected for monitoring (Figure 3.14). Surveys of cross-sections, and bar and channel morphologies were made over a two year period. 17 cross-sections, separated by between 100m and 250m were used. They were divided into sediment storage reservoirs; in the absence of observations on bed activity during a flood event, the active and semi-active reservoirs were combined and are defined as being where the river bed was not vegetated (equivalent to the active channel width used by Beschta (1983b)). The inactive reservoir was represented by low vegetated terraces thought to be associated with the present discharge regime. Older fluvio-glacial terraces were not allocated to a storage reservoir, and are equivalent to the never active reservoir defined for the sand tray. Sediment samples were collected from bar and channel surfaces for particle size determination, and extensive use was made of the grid-by-number method of estimating surface material sizes (Kellerhals and Bray, 1971). The b-axes of samples of 100 clasts lying within a 1m x 1m square grid were measured. The grid was randomly located within a pre-determined morphological unit that was to be sampled, and particles for measurement were identified as being those that lay directly beneath the

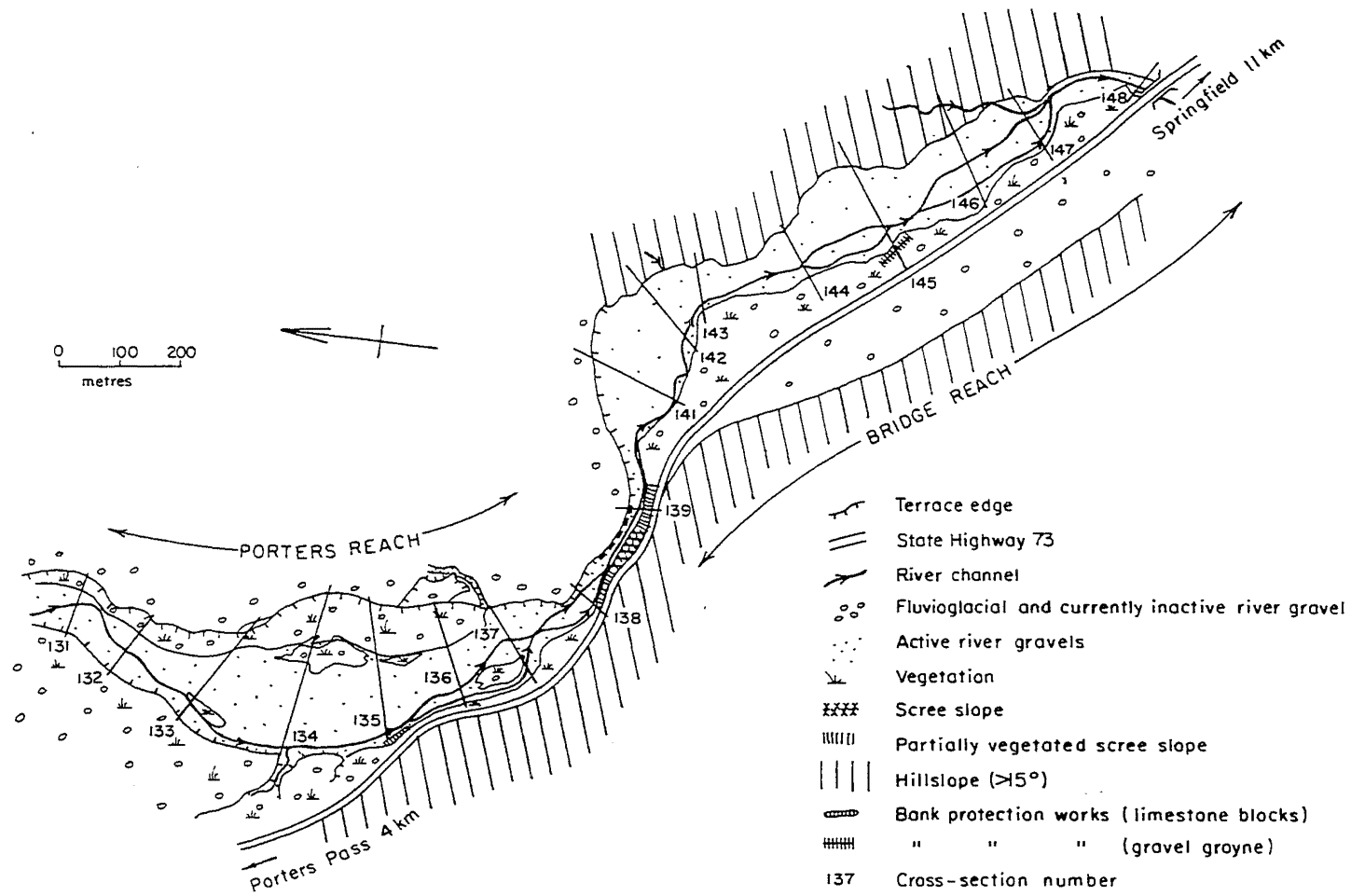


Figure 3.14 Location of surveyed cross-sections within the study reaches of the Kowai River.

intersections of the grid lines which were spaced 0.1m apart. Additional information was obtained from historical aerial photographs (see Appendix 4 for sources) and an additional set taken for this study. Figure 3.15 is an aerial view of the study reaches.

In the absence of major bedload transporting flows during the study period, channel morphology was little altered. To assess the origin of its different features and to try to obtain a history of the development of the contemporary river bed, palaeohydrological methods were used. These are fully described by Hoey (in press, 1989). The approach taken was to evaluate the critical tractive stress required to entrain river bed deposits. This is a standard procedure that has been used with some success elsewhere (Maizels, 1983b) although careful evaluation of the assumptions underlying the method are required. Three recent flow events were identified and an interpretation of river bed morphology based on these is presented in Chapter 5.

3.3 Synopsis

While laboratory modelling of gravel-bed rivers has been used increasingly in recent years doubts continue to be expressed regarding the transfer of laboratory results to natural channels, which Schumm *et al.* (1987) have argued to be the only full justification for performing small scale experimental work. Insufficient work has been carried out on scaling criteria for self-formed river models. Where a specific transport process is being modelled, Froude number scaling can be successful as Southard, Boguchwal and Romea (1981) demonstrated with sand ripples. In shallow gravel-bed rivers numerous processes occur which combine to produce the observed channel morphologies. Only if these all scale correctly could quantitative results be used to predict prototype behaviour. Similarity in sediment transport is imperfect and the scaling of the timescales of different sediment transport processes is variable (Yalin, 1971a). Such problems are magnified where modelling procedures involve modifications to complete similarity in a critical variable such as grain size. The utility of small scale models thus relates to the modelling of specific processes or to general morphologies. In the present case interest lies in bedload transport processes en masse, and it is the river morphology that holds most interest for the purpose of relating the model to prototypes. As yet few attempts have been made to test model-prototype similarity in anything but a preliminary way. The results of Hoey and Sutherland (forthcoming) are not encouraging in this regard since they suggest that Froude scaling over the gravel-sand size range is unable to replicate channel morphologies, although the qualitative agreement between the processes operating at the two scales was good.

SEE ERRATA

In the light of these comments the approach taken throughout the remainder of this thesis is as follows. Firstly, the model and prototype rivers are initially accepted as different systems, the behaviour of which require explanation in terms of their own conditions. This includes explanation of quantitative results. Secondly, results from the model and prototype are compared qualitatively. Thirdly, the transfer of quantitative model results to the prototype scale is made only to indicate

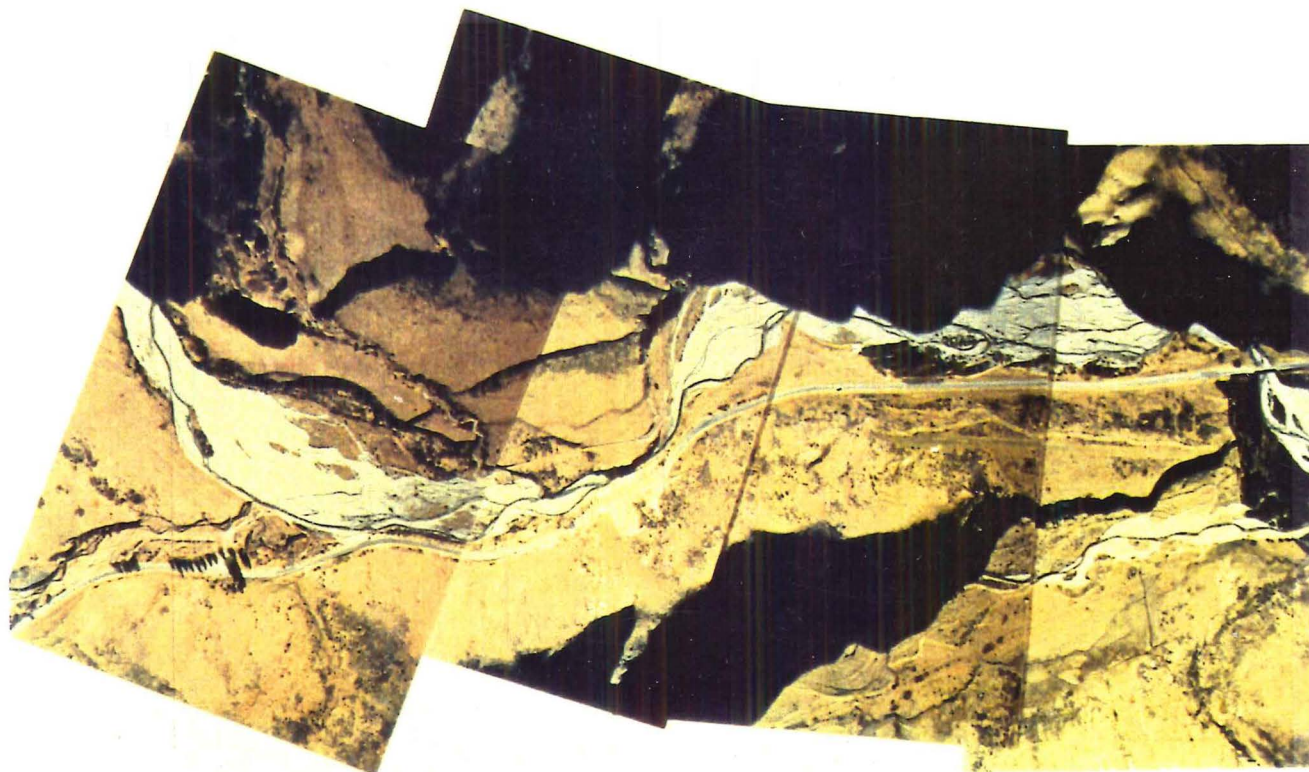


Figure 3.15 Aerial photograph of the reaches shown in Figure 3.14. Taken on 14.8.1987 by J. Weeber (North Canterbury Catchment Board)

the likely magnitude of processes at the larger scale. This approach appears at the present time to be as quantitative as is justifiable. Only in cases where a specific process is being investigated can quantitative results be compared between model and prototype scales.

4. TEMPORAL VARIATIONS IN SEDIMENT TRANSPORT RATES

Two of the topics that were identified as requiring further research in Chapter 2 are specifically considered in this Chapter. Firstly, the relationships between bed waves and channel form in both cross-sectional and planform dimensions are poorly defined; waves are believed to be associated with increased channel width (Beschta, 1983b; Church and Jones, 1982), reduced bed relief, and increased channel pattern complexity (Ashmore, 1987; Smith and Southard, 1982). These responses to wave development are intuitively reasonable consequences of aggradation, but little has been said about the processes that cause waves to form, and how these influence, and are influenced by, channel morphology and pattern. Secondly, the role of sediment supply versus transport capacity in producing bedload pulses remains to be clarified.

These two issues are approached using laboratory modelling results to demonstrate the existence of bedload pulses, which are described using time series analysis. Bedload transport rate fluctuations are related to changes in channel cross-section geometry and to the equilibrium transporting capacity of the channels. Finally, a possible control over wave development and erosion is investigated.

4.1 Sediment transport in the sand tray experiments

Experimental Runs 1, 2 and 3 described in sub-section 3.1.5 are used here. The three runs all exhibited variation in rates of sediment output although the patterns of variation were different. There was a time in each run from when the model river could be considered to be a reliable model of prototype gravel rivers. This required attainment of Froude and particle Reynolds number similarities which are necessary but not sufficient criteria for modelling reliability, and additional criteria defined with regards to the aims of the study. The time when the model river first represented in visual terms prototype gravel-bed rivers in planform morphology was the only such criterion used, in preference to alternatives based on the sediment output rate (see sub-section 3.1.2 for examples of alternative criteria), which were rejected as not being independent of the phenomenon under investigation, namely variation in sediment transport rate. Using the condition of visual appearance, the three runs are considered to have become faithful models of prototype gravel-bed rivers at 780, 600 and 780 minutes respectively. Prior to these times is referred to as the 'start-up' phase of each run, with the remainder being the 'model phase'. In Run 1 this is consistent with the onset of a phase of pseudo-meandering (Hickin, 1969, 1972) which gave way to braiding at about 1260 minutes. Runs 2 and 3 became braided at 600 and 780 minutes, and did not exhibit a pseudo-meandering phase.

Sediment output rates for the three runs are plotted on Figure 4.1 and detailed in Appendix 5. Ratios of maximum output rate : mean output rate were 3.48, 2.28 and 2.21, respectively for the entire runs. Considering the model phase only these become 3.63, 1.73 and 1.66. These ratios

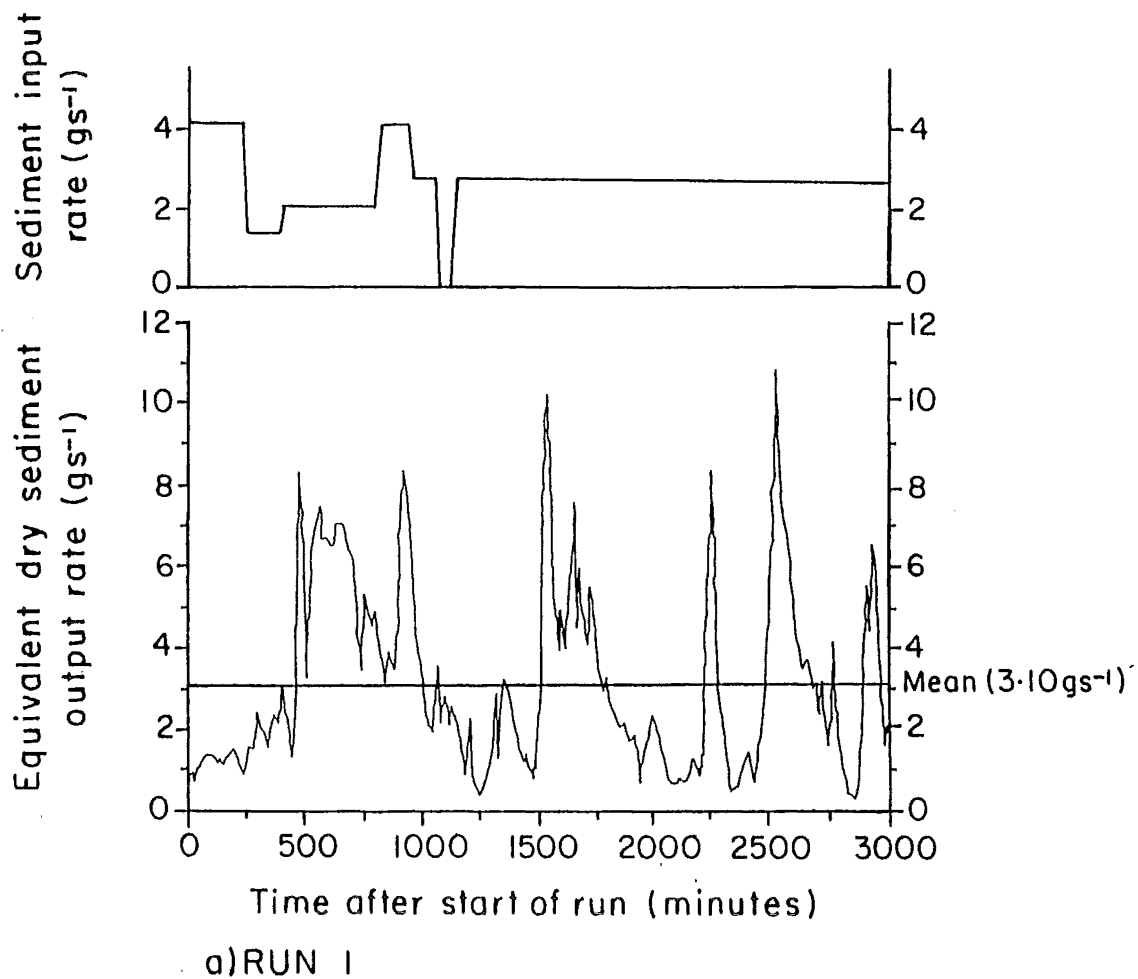
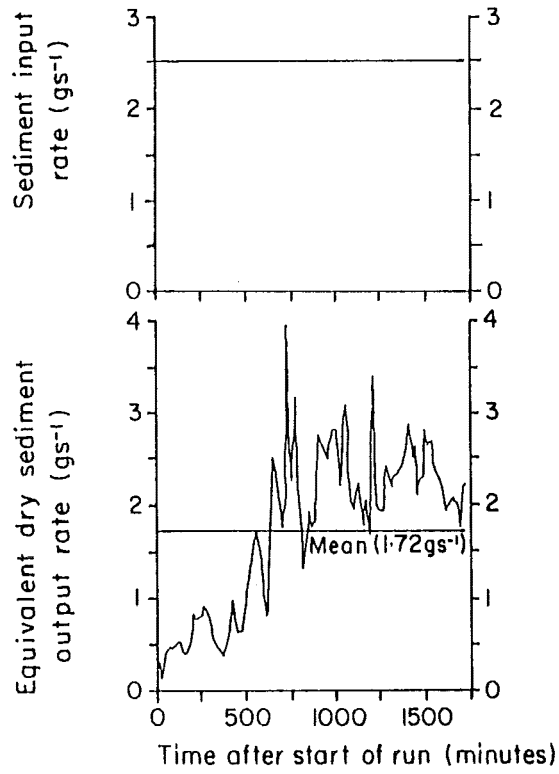
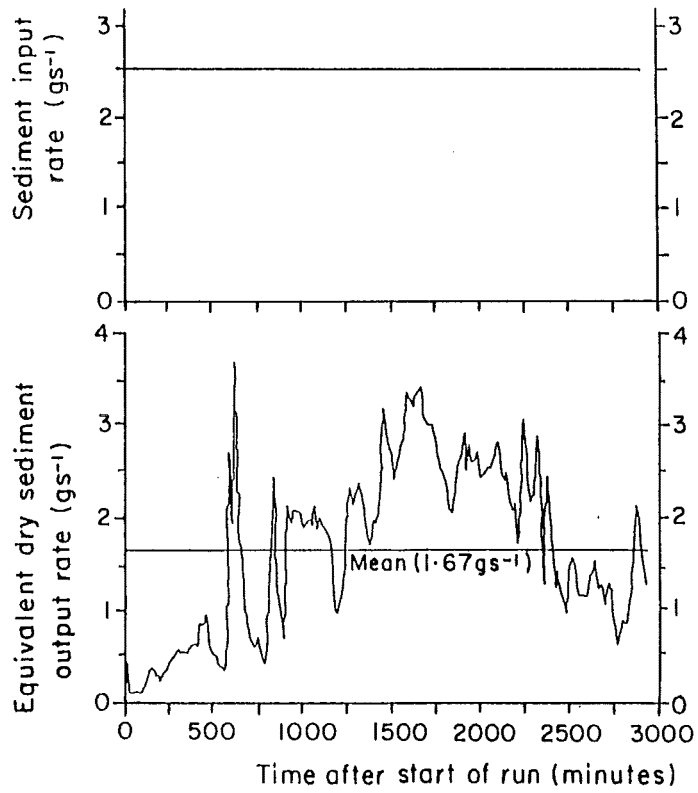


Figure 4.1 Sediment input and output rates for Runs 1, 2 and 3. Sediment output was converted from wet mass to equivalent dry mass. Note that sediment output is plotted on a different vertical scale for Run 1 than for Runs 2 and 3.



b) RUN 2



c) RUN 3

Figure 4.1 (Continued)

are consistent with Hubbell's (1987) suggestion that bedload transport rates vary between about zero and four times the mean rate. There was little consistency between the sediment output rate and the size of the output material in Run 1 (see Appendix 5 for data). The differences between runs reflect morphological dissimilarities that were described in sub-section 3.1.5 above. Within-run variation in sediment transport occurred at a variety of temporal scales, the smallest of which involved fluctuations between successive measurements. There is a sampling problem in interpreting these variations since changes in sediment output rate do not always occur within one measurement period. A three-point moving average smoothing was applied to the data to remove this effect (Figure 4.2). There appear to remain at least two scales of fluctuation. These are defined in Figure 4.2 by the identification of major and minor peaks and troughs, the frequencies of which are given in Table 4.1. From inspection of Figure 4.2, Run 1 had peaks of greater magnitude which were more clearly defined than in Runs 2 and 3. There were fewer short period oscillations in Run 1 than in 2 and 3, which had similar total oscillation frequencies (120 and 154 minutes). The major difference between Runs 2 and 3 was in the frequency of major peaks, but this could be a result of the short length of Run 2 causing some oscillations to attain exaggerated significance. The measured frequency of major peaks in Run 2 is thus not considered to be a reliable estimate of their actual frequency.

Table 4.1 Frequencies of oscillations in the three-point moving mean series of sediment output.

Run	Total time interval (minutes)	Number of cycles		Frequency of variation (minutes)	
		Major	Total	Major	Total
1	2220	5	9	440	247
2	1140	5.5	9.5	207	120
3	2160	4.5	14	480	154

Inspection of the sediment output series has revealed three scales of temporal fluctuation in bedload transport. These are at < 15 minutes, 100-250 minutes, and 400-500 minutes varying between runs. Before attempting to account for these in physical process terms the regularity of the oscillations and the statistical nature of the generating processes can be assessed using time series analysis.

The statistical nature of time series can be investigated by means of the autocorrelation function (a.c.f.) of a series, x_1, x_2, \dots, x_n , at different values of lag (k) (Box and Jenkins, 1970). The a.c.f. was estimated using

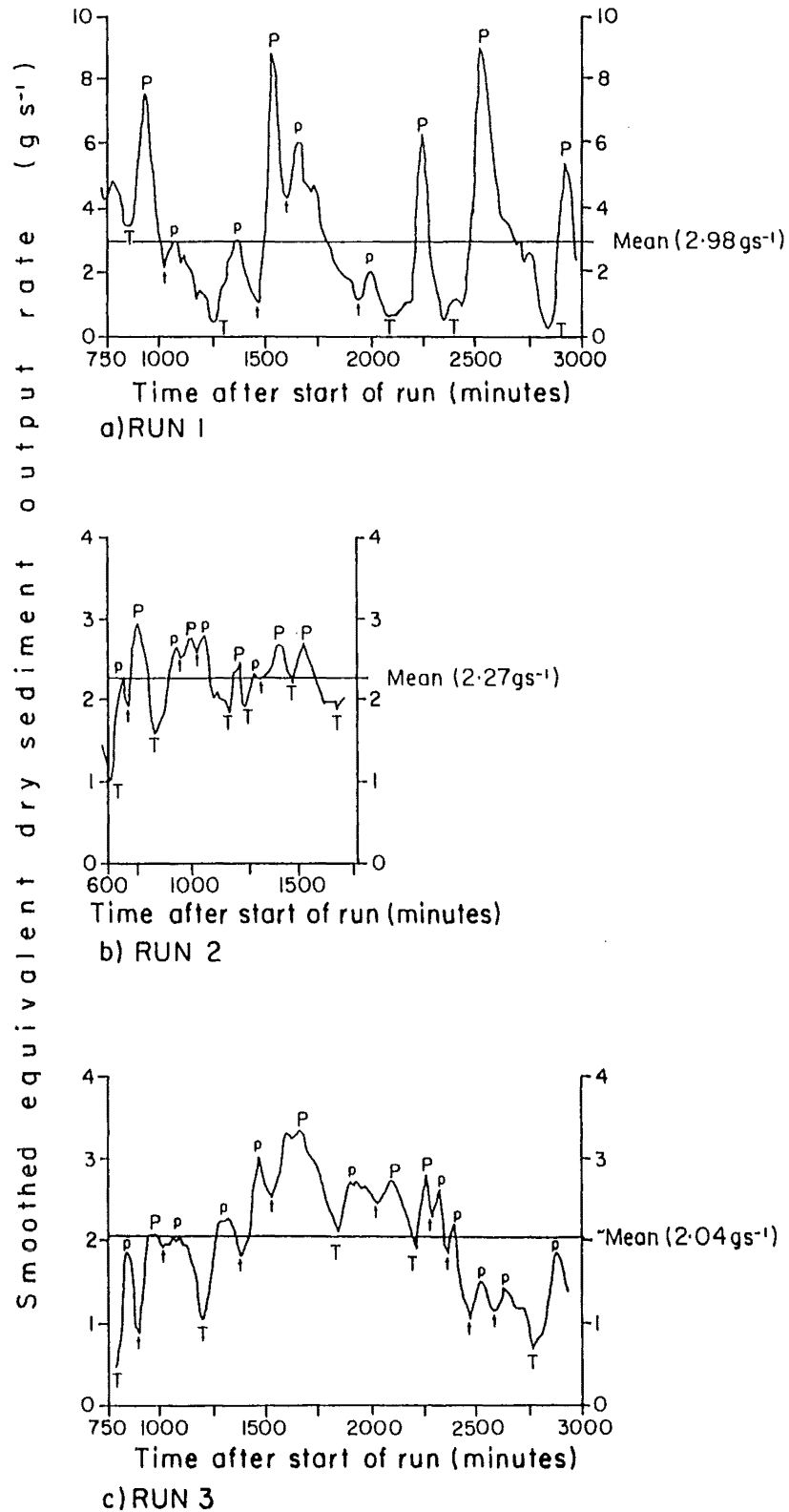


Figure 4.2 Sediment output rates smoothed by a three-point moving mean for the model phases of Runs 1, 2 and 3. P and T indicate major peaks and troughs in the sediment output rate series, and p and t minor peaks and troughs.

$$r_k = [n / (n-k)] \sum_{i=1}^{n-k} (x_t - \bar{x})(x_{t+k} - \bar{x}) / \sum_{i=1}^n (x_t - \bar{x})^2 \quad (4,1),$$

where \bar{x} is the mean of the series. Although simpler than some other available methods for calculating r_k , the values from equation (4,1) coincide with those from other methods under second order stationarity (Cox, 1983). This condition requires that the mean and variance of the population are time independent. The data must also be normally distributed. Using this method, values of r_k for k up to about $n/4$ are valid (Bennett, 1979). The 95 % confidence limits on the a.c.f. are given by twice the standard error of r_k (Anderson, 1976; Richards, 1979), where

$$\text{S.E.} (r_k) = [1 + 2 (r_1^2 + r_2^2 + \dots + r_q^2)]^{0.5} (n)^{-0.5} \quad (4,2)$$

in which $k = q + 1$.

The 3 point moving mean series (Figure 4.2) was used for the time series analyses in order to remove the effects of fluctuations with frequencies less than the sampling interval. Use of a higher order moving mean could introduce a spurious cyclicity to the series (Beschta, 1982). The sediment transport data from all three runs show two features of non-normality: a positively skewed frequency distribution and increasing variance with increasing mean. Both of these can be corrected for by using logarithmically transformed data. None of the log-transformed series showed any obvious time dependence of variance, so no further transformations of the series were performed. Table 4.2 gives the parameters of the transformed data series, which are broadly symmetrical with observations lying within +/- 3 standard deviations of the mean. Neither Run 1 nor Run 2 exhibited any linear trend in sediment output with time. Run 3 did have such a trend, significant at the 0.05 level, which was removed from the log-series before further analysis.

Table 4.2 Parameters of the log-transformed sediment output series.

Run	Mean	Standard deviation	Range if normally distributed	Actual range
1	0.341	0.363	-0.748 - 1.430	-0.585 - 1.034
2	0.348	0.089	0.081 - 0.615	0.009 - 0.593
3	0.272	0.182	-0.274 - 0.728	-0.367 - 0.530

The a.c.f.'s and partial autocorrelation functions (p.a.c.f.'s) of the three runs are given in Figure 4.3, where the significance of the results is shown by 95 % confidence limits. Only the first 4, 2 and 8 lags provide significant values of the a.c.f. for Runs 1,2 and 3, so the significant correlation lasted for 1, 0.5 and 2 hours respectively. Although negative correlations are observed at about 5 hours (Run 1) and 1.5 hours (Run 2), their magnitudes were not significant. The length of lag over which the a.c.f. is significant is similar to that reported by Ashmore (1987, 1988), but at

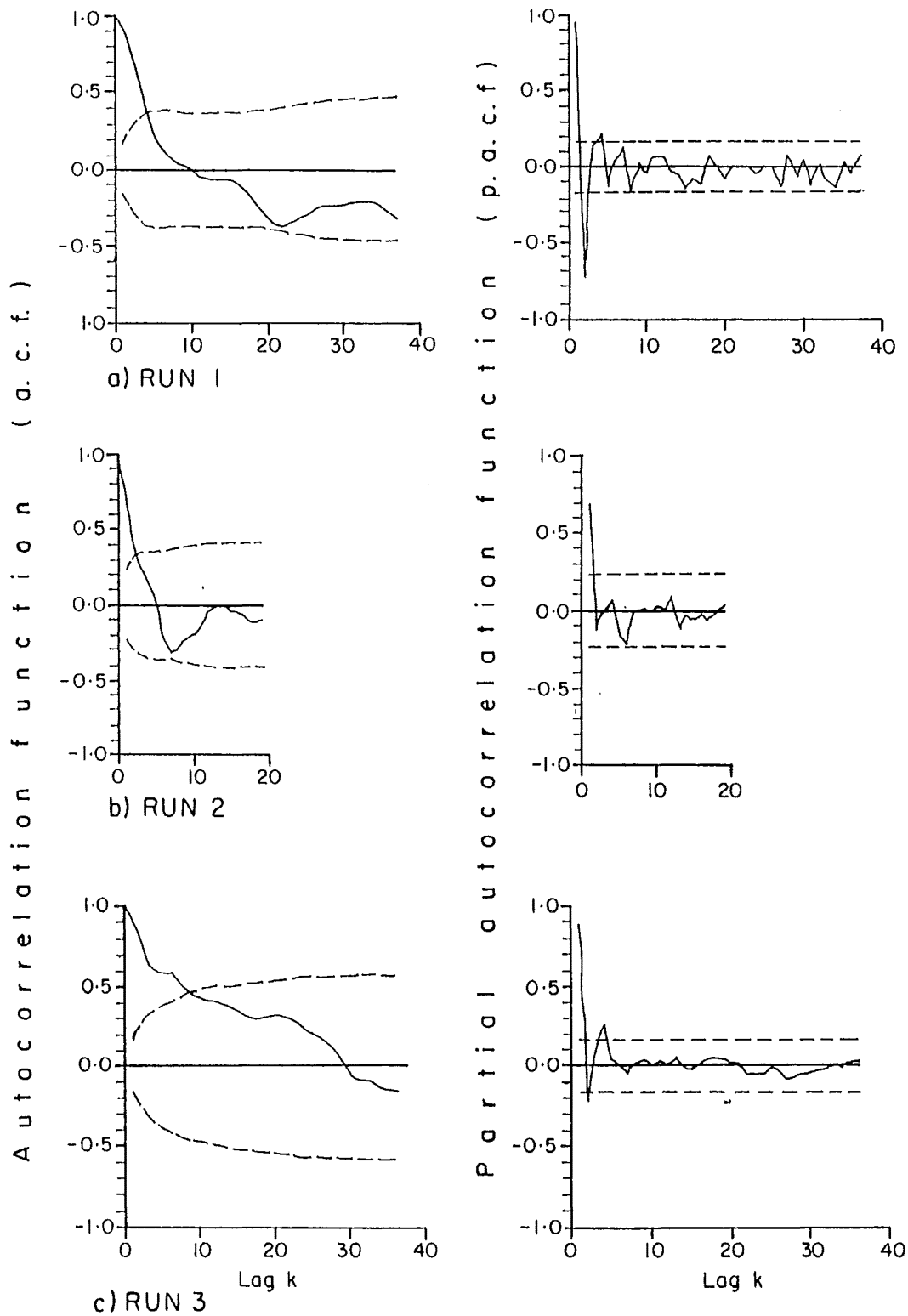


Figure 4.3 Autocorrelation (a.c.f.) and partial autocorrelation (p.a.c.f.) functions for the smoothed sediment output series of Runs 1, 2 and 3. The maximum lag, k , is at $n/4$. 95 % confidence limits (dashed lines) are at ± 2 standard errors. The time interval between data points was 15 minutes, hence 1 lag = 15 minutes.

greater lags the a.c.f.'s exhibit a more consistent decline than in Ashmore's data, where peaks in the a.c.f. at 4 to 8 hours were common. This reflects the greater degree of regularity of sediment transport rate fluctuations in Ashmore's experiments, which are apparent from a visual inspection of his sediment transport rate data (Figure 5 of Ashmore, 1988).

The patterns in the correlograms of Figure 4.3 suggest that there is no great degree of regularity in the sediment output rate fluctuations, but that the series are significantly non-random. The a.c.f.'s are characteristic of those generated by autoregressive processes (Chatfield, 1980; Richards, 1979). The p.a.c.f.'s are direct measures of the correlation between x_t and x_{t+k} that is not accounted for by the correlation of x_t with the series that have lags less than k (Richards, 1979). For a first order autoregressive process (designated AR(1)), the p.a.c.f. should cut off for lags greater than 1, with the cut off at lags above 2 for an AR(2) process. Thus, Run 1 is an example of an AR(2) process, and Run 2 of an AR(1) process. Runs 1 and 3 both have a significant value of the p.a.c.f. at lag 4. If these are significant values and not simply the result of one in twenty such values being significant with a random series, a mixed autoregressive moving average process (ARMA) would be suggested (Box and Jenkins, 1970). Such a model uses an additional parameter and was not found to fit the observed series significantly better than the AR(2) model for Run 1, or an AR(1) model for Run 3. Using the principle of parsimony (Anderson, 1976) the AR(2) process was selected as the best description of the Run 1 series, and the AR(1) process for Run 3.

Having identified that autoregressive processes can be used to describe the sediment output series the processes require definition. Autoregressive processes occur when each data point in a series is constrained by preceding value(s) in the sequence (Church and Jones, 1982), and as such produce relatively smooth output data series (Richards, 1979). The first order (AR(1)) process is given by,

$$x_t = \phi_1 x_{t-1} + e_t \quad (4,3)$$

where ϕ_1 is the autoregressive coefficient for lag 1, and e_t is an error term at time t . The second order (AR(2)) process is,

$$x_t = \phi_1 x_{t-1} + \phi_2 x_{t-2} + e_t \quad (4,4)$$

where ϕ_2 is analogous to ϕ_1 at lag 2. For stationarity, $\phi_1 + \phi_2 < 1$, $\phi_2 - \phi_1 < 1$, and $-1 < \phi_2 < 1$ (Richards, 1979). Both models imply that variation in the time series occurs over a time period longer than the chosen sampling interval.

The ϕ parameters were estimated for the experimental runs using a modified version of equation (4,1) with the factor $n/(n-k)$ removed. This is acceptable since only lags 1 and 2 are required for modelling, and the gross bias in the modified estimator of r_k can be ignored for very small lags (Cox, 1983). Model adequacy was checked by calculating population parameters and the correlogram for the series of residuals from the model. Non-significant a.c.f.'s suggested that the residuals were randomly distributed in time, and that they were approximately normally distributed.

The model parameters are given in Table 4.3, along with estimates of the degree of fit of the models (r^2), given by r_1^2 for AR(1), and by the equation of Nordin and Algert (1966) for the AR(2) process (Richards, 1976). For Run 1, the AR(2) model is a significant improvement over an AR(1) model, determined using an F-test method (Chayes, 1970; Richards, 1979). Further the AR(2) process satisfies the inequality, $4\phi_2 + \phi_1^2 < 0$ (Box and Jenkins, 1970; Richards, 1976) so that its realisation is a randomly varying cycle (Richards, 1979), which confirms the visual impression of the series.

Table 4.3 Parameters of the appropriate autoregressive models for the experimental runs.

Run	ϕ_1	ϕ_2	r^2
1	1.61	-0.73	0.97
2	1.00		0.48
3	0.89		0.80

Time series analysis of Runs 1,2 and 3 has described the two largest scales of fluctuation in the bedload output rate that were identified visually, in terms of AR(1) and AR(2) models. The visual differences between the sediment output series for the three runs are confirmed by the different forms of the models used to describe them. What remains is to try to identify the processes responsible for these fluctuations and to account for their characterisation by stochastic Markovian mechanisms.

The models detailed in Table 4.3 only serve to describe the bedload output series statistically, and say nothing specific regarding the physical processes involved. The adequacy of low order autoregressive models to describe geomorphological data is of more general interest. Ignoring purely hydrologic data for which time dependence of data series would be expected, studies of one dimensional spatial series have demonstrated the occurrence of phenomena that follow first or second order autoregressive generating processes. River bed profiles have been shown to be of this form. AR(2) models have been applied to sand waves and dunes (Nordin and Algert, 1966; Yalin, 1971b), riffle-pool sequences (Church, 1972; Richards, 1976; Church and Jones, 1982), oscillations at over 5 times the riffle-pool wavelength (Melton, 1962), and meanders (Yalin, 1971b). Correlograms presented by Beschta (1983b) for downstream channel width sequences appear consistent with the forms associated with autoregressive processes. It has sometimes been difficult to account for these statistical models in process terms, although Yalin (1971b) for example, argues that velocity pulsations and their effects on an erodible bed should both follow autoregressive processes.

It is of interest that low order autoregressive models are applicable to river morphology and

sediment transport studies, for this raises speculation as to whether temporal variability in river sediment transport is governed by this type of process, leading to statistically similar spatial patterns. The implications of this regularity should not be overstated, however, since moving average processes are naturally more dependent on random elements than deterministic ones, being based on the errors at different lags. This makes these processes less likely to operate in situations where deterministic physical mechanisms are operating, although with a random element imposed. The widespread applicability of AR models may thus be less remarkable than it appears at first. The need to find appropriate physical reasoning to account for the descriptive adequacy of the autoregressive models remains.

4.2 Channel form and sediment transport

The range of sediment output rates from the downstream end of the sand tray in the three runs could be accounted for in two ways:

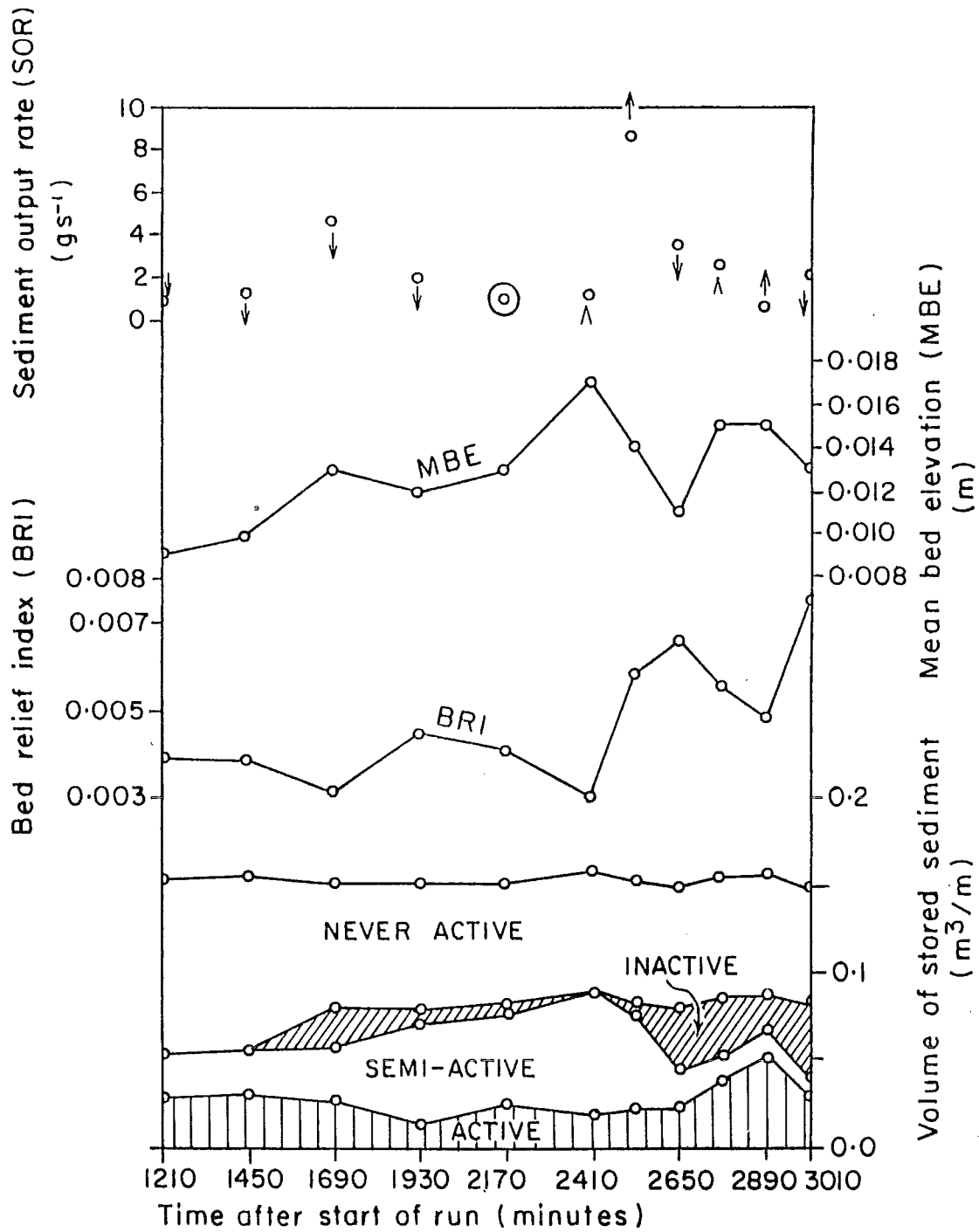
- a) transport capacity - changes in channel geometry lead to variation in sediment transport capacity and hence in sediment output;
- b) sediment supply - independent of channel geometry, the actual transport : transport capacity ratio changes through time.

A third possibility would comprise a combination of these mechanisms, neither of which implies anything about the processes causing such changes. The reasons why channel geometry or the efficiency of the sediment transport process might vary are not considered in detail here. The purpose of this section is to consider whether the sediment transport rate varies in response to a capacity or a supply mechanism, and to describe the channel geometry changes associated with this variation.

4.2.1 Channel geometry at the downstream end of the sand tray

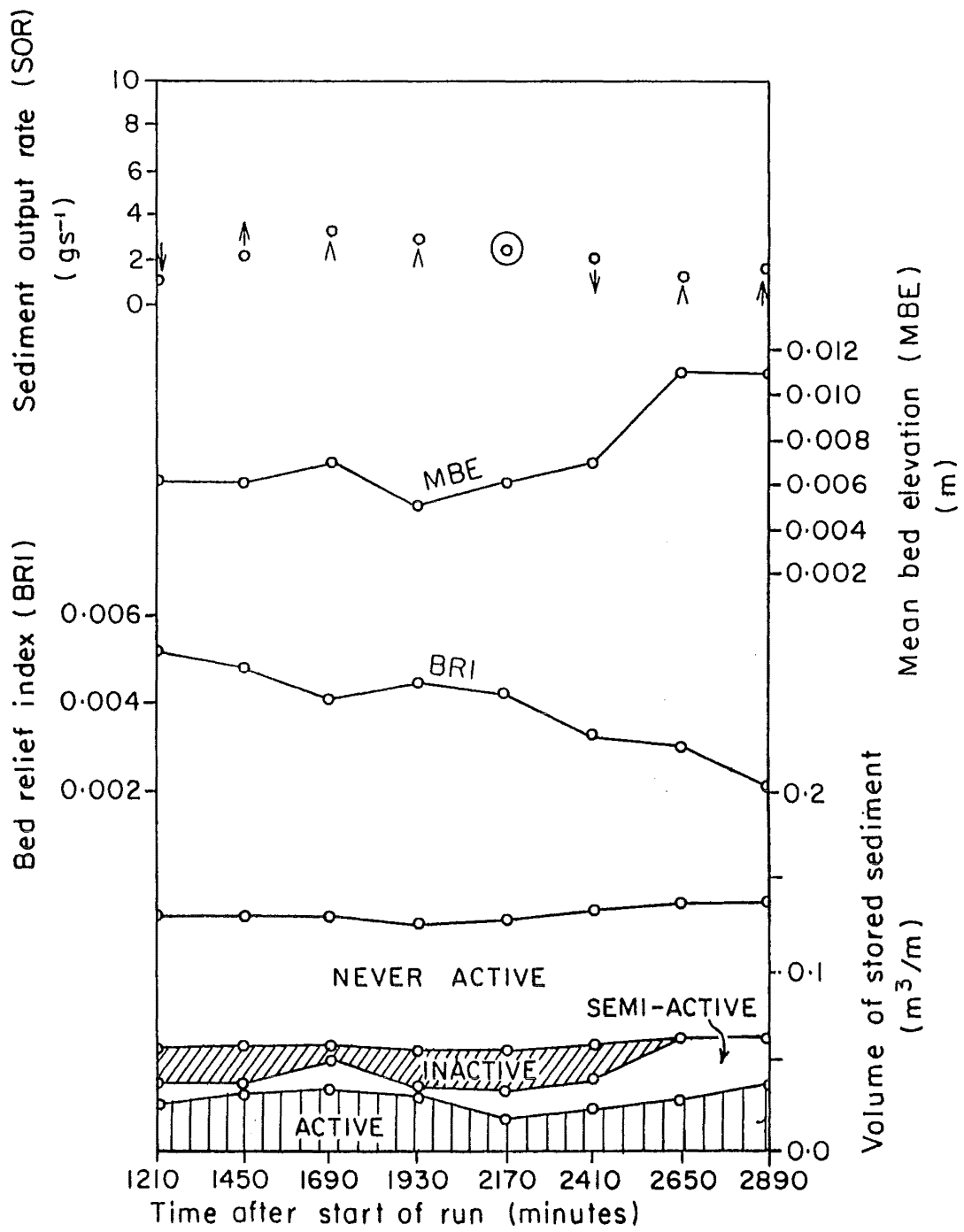
The surveyed cross-section closest to the end of the sand tray was at 13m, 1.2m upstream of the sediment collection trap. Channel geometry varied little over this 1.2m length, so an attempt can be made to relate geometry at 13m to sediment output. Only Runs 1 and 3 have a sufficiently lengthy record to merit further consideration. Figure 4.4 shows various indices of cross-sectional morphology, along with the sediment transport rate at four or two hourly intervals. The general relationships between these variables can be illustrated with reference to examples of conditions at specific times.

Mean bed elevation and the bed relief index (BRI) exhibited inverse trends but were not significantly correlated for Run 1 ($r^2 = -0.12$) but were for Run 3 ($r^2 = -0.76$). Sediment transport when mean bed elevation was relatively great and the BRI was low could be either relatively high (as at Run 1, 1690 minutes and Run 3, 1690 minutes), or low (Run 1 2410, Run 3 2650 and 2890 minutes). In both runs the absolute mean bed elevation in these contrasting examples was



a) RUN 1

Figure 4.4 Bed elevation, bed relief and sediment storage at the 13m cross-section, and sediment output rate from the tray. Sediment output is taken as the last 15 minute period before the flow was shut down. This period ended 10 minutes prior to the shut down. Vertical scales for Run 1 and Run 3 are identical. Arrows, \uparrow and \downarrow , show the direction of change in the sediment output rate. The symbol \odot indicates constancy, and \wedge and \vee the occurrence of a peak or trough in the sediment output series.



b) RUN 3

Figure 4.4(Continued)

greater where the sediment transport rate was lower, and there was sediment stored in the inactive (i.e. emergent) reservoir. Aggradation across the whole section was thus associated with reduced sediment transport through it as in-channel and bar top deposition occurred. Figure 4.5 shows two examples of where channel shoaling occurred, reducing water depth and spreading the flow more evenly across bar surfaces during times of low sediment output. Similar bed relief indices at times when the sediment output rates were different reflect the occasional dominance of one or two major channels cut into a previously aggraded surface in times of high output. The distribution of material between storage reservoirs reflected these changes, since aggradation and spreading out of the flow over bar surfaces caused static transfer of material from the inactive reservoir to the semi-active. Similarly, in-channel deposition led to the transfer of material from the active to the semi-active reservoir.

The reasons for bedload output variation can be further illustrated with reference to two occasions in Run 1. Conditions at 2410 minutes were described above (Figure 4.5a), and at 2530 minutes relatively high bed relief index and bed elevation were associated with a high sediment output rate (8.5 g s^{-1} ; Figure 4.6). By 2650 minutes mean bed elevation had dropped and the sediment output rate was falling (Figure 4.4a). Mean bed elevation declined as a result of incision of a major channel between 1.28 and 1.80m from the left bank (Figure 4.6) which evacuated previously accumulated material (Figure 4.5). This channel also eroded on its left bank side, but the remainder of the cross-section experienced only minor alteration. The high sediment transport rate at 2530 minutes reflected ongoing degradation and bank erosion, which continued for only another 15 minutes (Figure 4.1a) before the channel stabilised and started to act as a transfer channel (Church and Jones, 1982), followed by widening and some aggradation. From this time sediment output was reduced by the combined effects of bed armouring and reduced transporting capacity of the channel. The progression from 2410 to 2650 minutes can be viewed as an aggraded, low bed relief state with a low sediment transport rate, being succeeded by a phase of degradation, increased bed relief and an accelerated sediment transport rate. Finally a more stable condition was attained, and the channel morphology ceased to change. Such modifications to the channel form could be responses to controls external or internal to the channels themselves, with two possibilities being a change in the input water discharge to individual channels due to upstream changes, or exceedence of a threshold for the onset of degradation.

Similar situations to that just described can be identified elsewhere. In Run 1 from 2650 to 2890 minutes, increasing bed elevation (aggradation) was associated with decreasing bed relief and the associated transfer of sediment from the inactive reservoir to the active. Between 2890 and 3010 minutes, these changes were reversed, which suggests a phase of degradation and accelerated sediment transport. Inspection of Figure 4.1a reveals this to be the case with a general decline in the sediment transport rate just prior to 2890, followed by a significant peak before 3010 minutes. In Run 3, increased mean bed elevation from 2410 to 2650 was associated

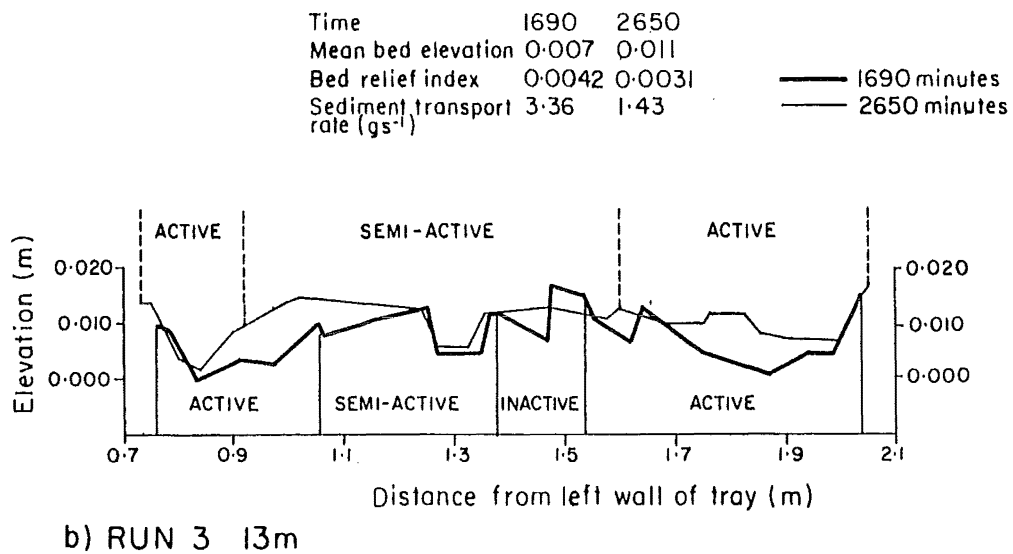
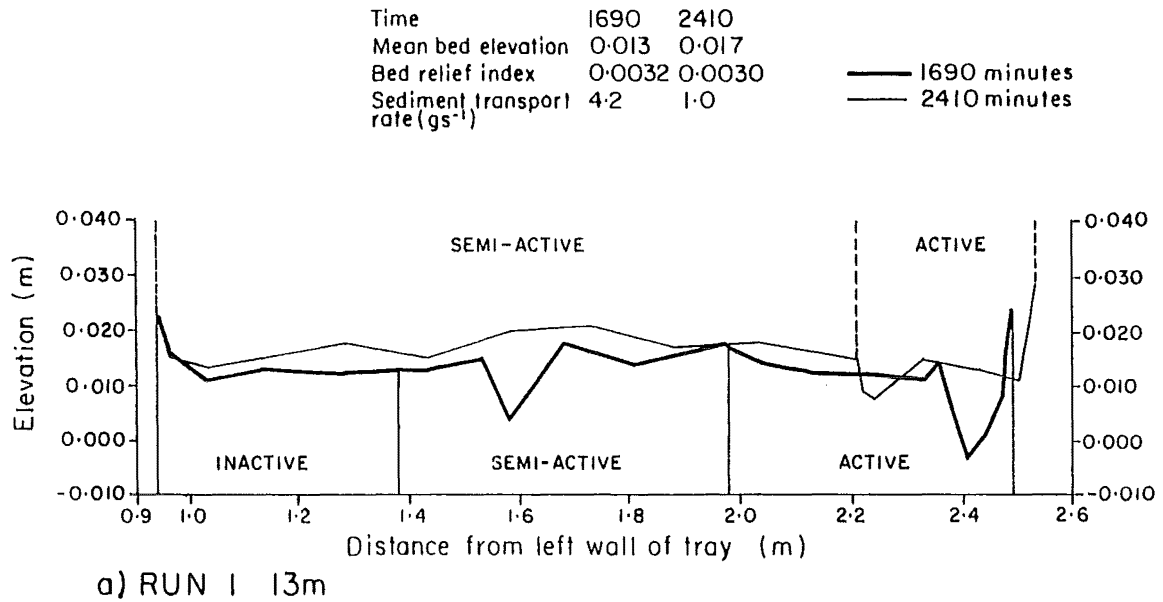


Figure 4.5 Channel cross-sections and sediment storage reservoirs. In both cases, the time of greater bed elevation was accompanied by reduced bed relief index and lower sediment transport rate.

Time	2530	2650	
Mean bed elevation	0.014	0.011	
Bed relief index	0.0058	0.0066	— 2530minutes
Sediment transport rate (gs ⁻¹)	8.5	3.4	— 2650minutes

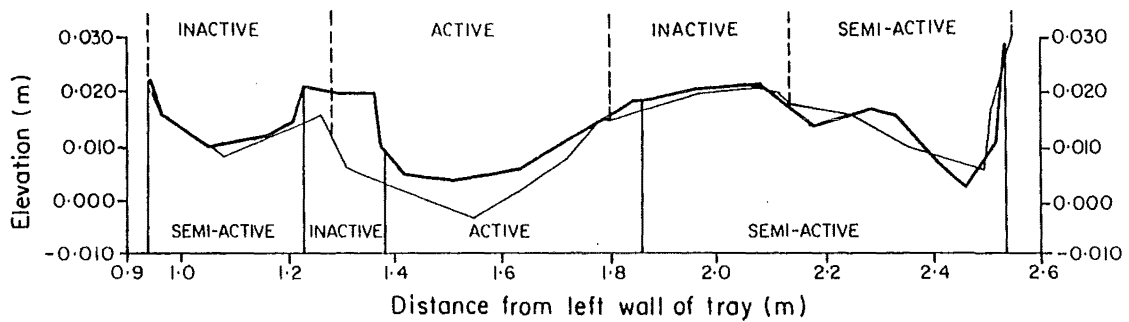


Figure 4.6 Channel cross-sections and sediment storage reservoirs, Run 1, 2530 and 2650 minutes.

with a lower magnitude of bed relief, and a larger volume in the active and semi-active storage reservoirs. Aggradation implies sediment deposition and a low sediment output rate would be expected, which was the case (Figure 4.1c).

These examples suggest some general principles that can be used to relate indices of cross-sectional morphology to sediment transport, which are summarised in Table 4.4. No single index is adequate alone and it is difficult to use the instantaneous sediment transport rate for this purpose. Relative changes over time in both morphology and sediment storage are easier to account for than are absolute values, due to their dependence upon the previous sequence of changes at the section. The relationships outlined in Table 4.4 should be applicable to other situations where periods of aggradation and degradation occur, but where there is no long-term aggrading or degrading trend. The uncertainty regarding the correlation between sediment transport rates and net aggradation requires further consideration of the controls over these rates.

Table 4.4 General relationships between channel condition, cross-section morphology, and sediment storage derived from the experimental runs. I = rate of sediment input to section; \emptyset = rate of sediment output from the section; z = bed elevation.

Case	Channel condition	Mean bed elevation	Bed relief index	Sediment storages
1	Degrading ($I < \emptyset$)	Decreasing ($\delta z / \delta t < 0$)	Increasing	Inactive: Increasing Semi-active: Decreasing
2	Aggrading ($I > \emptyset$)	Increasing ($\delta z / \delta t > 0$)	Decreasing	Active: Increasing Semi-active: Increasing Inactive: Decreasing
3	Stable ($I \cong \emptyset$)	No change ($\delta z / \delta t \cong 0$)	No change	No change

4.2.2 Comparisons of measured and predicted sediment transport rates

Precise prediction of bedload transport rates in braided gravel-bed rivers is not readily achieved (Carson and Griffiths, 1987; Davies, 1987). There are numerous reasons for this but variations in sediment availability have been suggested to be among the most important (Davoren and Mosley, 1986). The magnitude of this mechanism is the subject of the following discussion.

Many attempts at predicting bedload transport rates have made the assumptions that the channel

is in an equilibrium condition and sediment supply is unlimited. Equilibria of cross-sectional and long profile geometries are associated with process equilibrium, which implies spatial and temporal continuity of sediment transport (Richards, 1982). Hence river sections undergoing aggradation, degradation, bank erosion or bed armouring are excluded from consideration. Any definition of equilibrium is dependent upon the timescale of the analysis, and planform and cross-sectional morphologies have longer relaxation times (Brunsdon and Thornes, 1979) than sediment transport rate. Where channel geometry is in the process of adjustment to equilibrium following a change in one or more external controlling variables, sediment transport rate continually adjusts attempting to maintain equilibrium with the flow conditions. Instantaneous balance is not a realisable concept (Richards, 1982), but a form of equilibrium can be defined whereby channel morphology is unaltered over a time period which is sufficiently long to exceed the relaxation time of sediment transport.

The interval between measurements of sediment transport was 15 minutes. No data on the relaxation time of the process is available, but observations suggested that bedload transport adjusted to sudden changes in the water discharge within one or two minutes. This estimate was derived from visual observation of the time taken for the sediment transport rate to appear to stabilise when the water supply was turned on after an overnight shut down. The relaxation time is less than the measurement interval, and changes in the channel cross-sections were rarely observed to occur over such short time periods. A form of equilibrium can therefore be considered to exist, provided that the infinite availability assumption is met. The approach used was to relate 15 minute sediment output rates to the rates predicted from instantaneous channel geometry at the 13m cross-section (measured 10 minutes after the end of the sediment collection period).

Sediment output and channel cross-sections were measured by the methods described in section 3.1. Each bedload transporting channel was considered separately rather than using mean values for the cross-section, which had the effect of giving larger values of predicted bedload movement (Carson and Griffiths, 1979; Thompson, 1985). If mean values are used those parts of the section that have shallow flow and are not contributing to sediment transport have the effect of reducing mean depth and mean velocity and so distort the predicted transport rates. Discharge in the individual channels was estimated from empirical width-discharge relationships developed separately for each experimental run (Equation (3,6)). If the total discharge predicted in this way exceeded $1.90 \times 10^{-3} \text{ m}^3 \text{ s}^{-1}$, the flow in the individual channels was scaled down so that the total equalled this value. No scaling was performed when the predicted total discharge was below this value since the remaining flow can be accounted for as being over bar surfaces. Only those times when water surface slope data were available are considered subsequently.

The bedload transport equation used is that of Bagnold (1980) where stream power per unit bed

area is taken to be the primary independent variable. In using the equation d_{50} of the bulk material was used as the characteristic particle size. This is strictly incorrect for determination of the critical stream power, ω_o , in the equation, but was necessitated by the absence of adequate data on the particle size of the surface material at the times when bedload transport rate was measured. Bedload transport rate is predicted from,

$$i_b = (i_{b*}) [(\omega - \omega_o) / (\omega - \omega_o)_*]^{3/2} [h/h_*]^{-2/3} [d_{50}/d_*]^{-1/2} \quad (4,5),$$

where i_b = submerged unit mass rate of bedload transport ($\text{kg m}^{-1} \text{s}^{-1}$); h = flow depth (m); d_{50} = median size of the bulk bed material (m). The starred quantities are reference values. Stream power per unit bed area, ω , ($\text{kg m}^{-1} \text{s}^{-1}$) is defined as,

$$\omega = \rho_w q S \quad (4,6),$$

and ω_o is calculated from,

$$\omega_o = 290 d_{50}^{3/2} \log (12h / d_{50}) \quad (4,7).$$

The reference values used were those given by Bagnold (1980); $i_{b*} = 0.1 \text{ kg m}^{-1} \text{ s}^{-1}$; $(\omega - \omega_o)_* = 0.5 \text{ kg m}^{-1} \text{ s}^{-1}$; $h_* = 0.1 \text{ m}$; $d_* = 1.1 \times 10^{-3} \text{ m}$. This equation was used because of its relative simplicity and hence ease of interpretation of deviations from its predictions, its derivation from stable gravel-bed channels, and applicability to similar data sets to those used here (Ashmore, 1988). However, Carson and Griffiths (1987) found that it underpredicted actual gravel loads in prototype braided rivers although the magnitude of this error was reduced by specification of local flow parameters. Bedload transport was calculated from equation (4,5) and converted to a mass rate (G_b ; kg s^{-1}) using

$$G_b = 1.61 i_b \cdot b \quad (4,8).$$

Table 4.5 gives the data used in the calculations and the measured bedload transport rates, which are plotted in Figure 4.7. The mean discrepancy ratios (predicted output/ actual output) for the two runs are 2.88 and 2.40. This overprediction could have resulted from use of the bulk d_{50} for estimation of ω_o . Carson and Griffiths (1987) suggested the use of the d_{50} of the surface material to define whether or not any motion occurs. If ω exceeds ω_o calculated in this way, then ω_o from the subsurface material size is used to calculate the volume of material transported. The rationale for such an approach is that all particle sizes have approximately equal mobility once any surface cover layer is breached (Andrews, 1983; Parker, Klingeman and McLean, 1982). As an indication of the magnitude of any overprediction introduced by using bulk d_{50} in this procedure a total of 12 samples of surface material from Run 1 were used to estimate the surface material size. Taking all 12 gives $d_{50} = 0.89 \pm 0.32 \text{ mm}$. In only one channel which would have bedload motion using bulk d_{50} is zero motion predicted by this approach.

The overprediction could reflect the inapplicability of the equation to the types of channels studied, the presence of a large volume of throughput load (Carson and Griffiths, 1987), or non-equilibrium of the sediment transport process. A qualitative assessment of channel equilibrium is given in Table 4.6 which shows that 10 out of 28 channels were in a static equilibrium condition. Equilibrium was visually assessed, and no attempt was made to estimate the degree of non-equilibrium. Bank erosion and bed degradation were readily observed, but

Table 4.5 Measured and predicted bedload transport rates, using the Bagnold (1980) equation. $(d_{50}/d_*)^{-0.5} = 1.389$.

When there were multiple channels at the downstream end of the sand tray, successive channels from the left bank are labelled a,b,c.

G_b is the mass rate of bedload transport (kg s^{-1}). * indicates an estimated value of water surface slope (from bedslope and water depth data).

Time (minutes)	Water surface slope	Channel width (m)	Mean depth (m)	Measured G_b (kg s^{-1})	Discharge ($\text{m}^3 \text{s}^{-1}$)	ω ($\text{kg m}^{-1} \text{s}^{-1}$)	ω_o ($d=0.57\text{mm}$) ($\text{kg m}^{-1} \text{s}^{-1}$)	i_b ($\text{kg m}^{-1} \text{s}^{-1}$)	Predicted G_b (kg s^{-1})	Predicted/ Actual G_b
RUN 1										
2160a	0.008	0.15	0.0055	8.40×10^{-4}	3.75×10^{-4}	0.0200	0.0081	3.52×10^{-3}	8.51×10^{-4}	1.01
2160b	0.004	0.35	0.0130		8.18×10^{-4}	0.0094	0.0096	-	-	
2520	0.010*	0.37	0.0108	8.48×10^{-3}	8.61×10^{-4}	0.0233	0.0093	2.86×10^{-3}	1.70×10^{-3}	0.20
2640	0.010*	0.46	0.0126	3.47×10^{-3}	1.05×10^{-3}	0.0228	0.0096	2.38×10^{-3}	1.76×10^{-3}	0.51
2760a	0.011	0.61	0.0107	2.33×10^{-3}	1.36×10^{-3}	0.0245	0.0093	3.28×10^{-3}	3.22×10^{-3}	1.68
2760b	0.011	0.11	0.0128		2.82×10^{-4}	0.0282	0.0096	3.93×10^{-3}	6.95×10^{-4}	
2880a	0.011	0.52	0.0090	4.61×10^{-4}	1.18×10^{-3}	0.0250	0.0090	3.95×10^{-3}	3.30×10^{-3}	12.61
2880b	0.011	0.12	0.0028		3.06×10^{-4}	0.0281	0.0070	1.30×10^{-2}	2.51×10^{-3}	
3000	0.011	0.64	0.0160	1.91×10^{-3}	1.43×10^{-3}	0.0246	0.0100	2.34×10^{-3}	2.42×10^{-3}	1.26
RUN 3										
									Mean	2.88
									(disregarding 2880)	0.93)
1200a	0.006	0.33	0.0118	9.49×10^{-4}	1.09×10^{-3}	0.0198	0.0095	1.70×10^{-3}	9.04×10^{-4}	1.94
1200b	0.007	0.26	0.0116		8.09×10^{-4}	0.0218	0.0094	2.24×10^{-3}	9.38×10^{-4}	
1440a	0.006	0.33	0.0059	2.26×10^{-3}	9.50×10^{-4}	0.0173	0.0083	2.18×10^{-3}	1.16×10^{-3}	1.48
1440b	0.010	0.33	0.0126		9.50×10^{-4}	0.0288	0.0096	4.11×10^{-3}	2.18×10^{-3}	

Table 4.5 (Continued)

Time (minutes)	Water surface slope	Channel width (m)	Mean depth (m)	Measured G_b (kg s^{-1})	Discharge ($\text{m}^3 \text{s}^{-1}$)	ω ($\text{kg m}^{-1} \text{s}^{-1}$)	ω_b ($d=0.57\text{mm}$) ($\text{kg m}^{-1} \text{s}^{-1}$)	i_b ($\text{kg m}^{-1} \text{s}^{-1}$)	Predicted G_b (kg s^{-1})	Predicted/ Actual G_b
RUN 3 (Continued)								RUN 3 (Continued)		
1680a	0.009	0.19	0.0074		5.02×10^{-4}	0.0238	0.0087	4.08×10^{-3}	1.25×10^{-3}	
1680b	0.008	0.35	0.0074	3.37×10^{-3}	1.27×10^{-3}	0.0290	0.0087	6.39×10^{-3}	3.60×10^{-3}	1.44
1920	0.010	0.48	0.0157	2.89×10^{-3}	1.90×10^{-3}	0.0396	0.0099	6.81×10^{-3}	5.25×10^{-3}	1.81
2160	0.006	0.46	0.0116	2.48×10^{-3}	1.90×10^{-3}	0.0248	0.0094	3.10×10^{-3}	2.29×10^{-3}	0.93
2400	0.007	0.51	0.0109	2.29×10^{-3}	1.90×10^{-3}	0.0261	0.0093	3.68×10^{-3}	3.02×10^{-3}	1.32
2880a	0.007	0.20	0.0048		5.43×10^{-4}	0.0190	0.0079	3.41×10^{-3}	1.10×10^{-3}	
2880b	0.009	0.18	0.0042	1.82×10^{-3}	4.63×10^{-4}	0.0232	0.0077	6.12×10^{-3}	1.77×10^{-3}	2.53
2880c	0.008	0.24	0.0067		7.16×10^{-4}	0.0239	0.0085	4.47×10^{-3}	1.73×10^{-3}	
3120a	0.001	0.20	0.0057		5.43×10^{-4}	0.0027	0.0082	-	-	
3120b	0.011	0.24	0.0110	2.09×10^{-3}	7.16×10^{-4}	0.0328	0.0093	6.08×10^{-3}	2.35×10^{-3}	4.64
3120c	0.016	0.22	0.0050		6.28×10^{-4}	0.0457	0.0080	2.07×10^{-2}	7.34×10^{-3}	
3360a	0.006	0.30	0.0043		8.04×10^{-4}	0.0161	0.0077	2.40×10^{-3}	1.16×10^{-3}	
3360b	0.009	0.23	0.0155	7.00×10^{-4}	6.72×10^{-4}	0.0263	0.0099	2.81×10^{-3}	1.04×10^{-3}	5.25
3360c	0.009	0.17	0.0045		4.24×10^{-4}	0.0224	0.0078	5.40×10^{-3}	1.48×10^{-3}	
3600a	0.005	0.30	0.0157		1.01×10^{-3}	0.0168	0.0099	7.51×10^{-4}	3.63×10^{-4}	
3600b	0.008	0.21	0.0060	6.81×10^{-4}	5.85×10^{-4}	0.0223	0.0083	4.16×10^{-3}	1.41×10^{-3}	2.60
									Mean	2.40

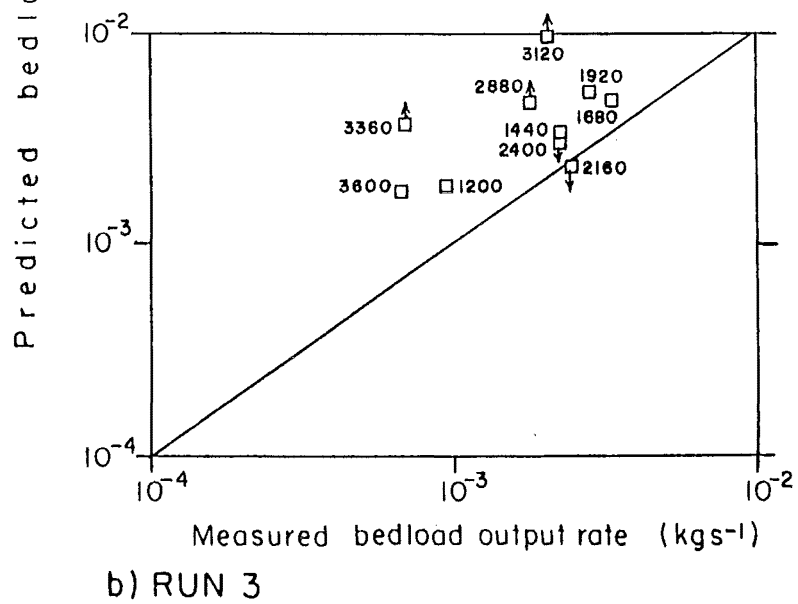
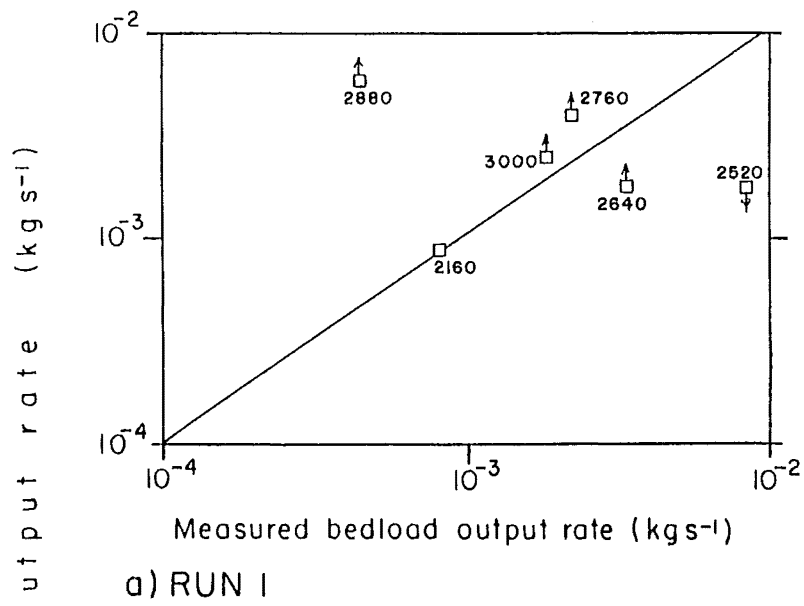


Figure 4.7 Comparison of measured bedload output with that predicted from the Bagnold (1980) equation. The observations are divided into stable (□), degrading and /or widening (▣), and aggrading (▤). Times (in minutes) of the observations are shown.

Table 4.6 Observed channel stability at the times of bedload transport rate calculation. The discrepancy ratio is predicted bedload output / actual output, using d_{50} of the bulk material to calculate ω_o .

Time	Discrepancy ratio	Static Equilibrium	Aggrading	Degrading	Eroding banks	Armoured	Notes
RUN 1							
2160a	1.32	x					Low input rate from upstream -may have been aggrading
2160b		x					
2520	0.41			x			
2640	1.23		x				
2760a	2.33		x			x	
2760b				x			x
2880a	18.93		x				
2880b					x		
3000	2.43		x				Starting to aggrade
RUN 3							
1200a	1.94	x					
1200b			x				
1440a	1.48		x				
1440b					x	x	
1680a	1.44		x				
1680b			x				
1920	1.81	x					
2160	0.93			x	x		
2400	1.32			x	x		
2880a	2.53		x				
2880b			x				
2880c			x				
3120a	4.64		x				
3120b				x			
3120c				x			
3360a	5.25	x				x	Previously degraded, armoured channels
3360b		x				x	
3360c			x				
3600a	2.60	x					Little activity - may have been slowly aggrading
3600b		x					

aggradation was more difficult to define visually. Where material was being deposited in the channels downstream of 13m aggradation was assumed to be occurring. Deposition was only readily observed when it involved material in excess of about 1mm. Armour layer development was also visually assessed and near continuous armouring is noted in Table 4.6. The channels considered to be in equilibrium are thus those that were not obviously in non-equilibrium. This is an unsatisfactory definition but is as precise a measure as is attainable in the absence of any data on channel geometry in the period immediately after the sediment transport rate measurements. Nothing is included in the definition of equilibrium about the timescale over which the equilibrium condition persisted. In some cases channel behaviour changed significantly within 15 minutes of the collection of the cross-section data but in others there were no obvious changes for several hours. It was not always possible to be definite that equilibrium existed (especially difficult was the distinction between slowly aggrading and equilibrium channels), and where uncertainty existed it is indicated in Table 4.6.

Considering Run 1 first, only at 2160 minutes were the channels in an equilibrium condition, and the equation only slightly overestimates actual bedload transport at this time. For the times when aggradation was occurring, predicted bedload transport rates exceed those measured (Figure 4.7a). This is especially obvious at 2880 minutes shortly after which there was a rapid increase in transport rate. The channel at 14m was armoured and there was a low rate of material supply from upstream, with much of what was supplied being deposited in the section. The only time when the channel(s) were degrading is associated with underprediction by the equation. In Run 3, the distinction between degrading and aggrading channels is less clear (Figure 4.7b). Four occasions when the channels were considered to be in equilibrium (1200, 1680, 1920 and 3600 minutes) have bedload overestimated by the equation. 1440 minutes is shown as equilibrium (Figure 4.7b), but had two channels of approximately equal discharge, one of which was degrading and one aggrading. The two occasions where channels were degrading plot to the right of the aggrading ones, as in Run 1.

The magnitudes of the discrepancy ratios are low compared with those of many attempts at bedload prediction (e.g. Carson and Griffiths, 1987 Table 3.2 where discrepancy ratios in the range $<0.1 - >16$ were noted), even though both equilibrium and non-equilibrium channels are included in the data set. The Bagnold equation overpredicted actual bedload transport rates in Run 3, and may also do so in Run 1 but only one data point from an equilibrium channel condition is available for this run. The pattern of deviation from the predictions of the equation can be accounted for in a qualitative way. Residuals from perfect agreement result in part from the relaxation time between a change in water or sediment input to a section, and channel geometry at the section responding to this alteration in external conditions (Andrews and Parker, 1987 - discussion by M.Church). Sediment supply effects, in the form of armouring, are apparently much less important than channel geometry changes in causing variation in bedload output. This was illustrated by the limited effect of introducing a bed material availability component to the bedload

equation, in the form of using surface material size to define the threshold for bedload transport.

Variation in bedload transporting capacity is apparent in Figure 4.7. Griffiths (1979) hypothesised that bed waves cause deformation of local hydraulic geometry and hence affect transport capacity. This is supported by data presented herein, but the poor correlation between actual and capacity transport rates requires one or more additional mechanisms. Supply limitation may be important in some cases but its influence is difficult to evaluate. The correspondence between channel equilibrium or non-equilibrium and the over- or under-prediction of actual transport rates suggests that non-equilibrium transport could be the major reason for actual transport rates adjusting to changes in channel geometry. This suggestion is examined in section 4.4.

4.3 Possible controls of bedload pulse generation

No attempt has thus far been made to identify the processes responsible for producing bedload pulses. Here an attempt is made to assess the immediate conditions relating to bed wave growth and erosion i.e. an explanation is sought in terms of cross-sectional parameters rather than with reference to reach scale processes. The latter type of explanation is considered in Chapter 5.

There are no simple relationships between the state of channel development (stable, aggrading, degrading) and measured hydraulic variables in the sand tray experiments (stable channels are those in which channel boundary shape was not changing; they may or may not be equilibrium channels depending on the presence of armouring). Since the bedload transport rate depends upon stream power per unit bed area, some relationship with this variable might be expected. When the channels at the 13m cross-section are considered (Tables 4.5, 4.6) no discrimination between channel state can be made on the basis of stream power per unit bed area (Table 4.7a). This is also the case when local 'valley' slope (i.e. the slope of all of the active bed) replaces channel slope, and the total water discharge is used in place of discharge in individual channels (Table 4.7b). The ability of stream power to discriminate between different channel states is reduced because the timing of the observations was fixed, and did not necessarily sample conditions at critical times, such as the onset of degradation.

The data set used in Table 4.7 was expanded by adding data from cross-sections 2-12m inclusive (see Appendix 6 for details). Discharge was estimated from measured channel widths, and slopes were measured directly. Channel stability was again visually assessed. Because of the difficulties in differentiating aggrading from stable channels, combined figures for these two states are included in Table 4.8. Data from Runs 1 and 3 using bed surface slope are supplemented by a smaller data set from Run 3 when water surface slopes were also available. Water surface slopes rarely attain either the upper or lower extreme values of bed slope so compressing the values of ω into a narrower range.

Table 4.7 Ranked values of stream power per unit bed area, ω ($\text{kg m}^{-1} \text{s}^{-1}$), associated with different channel conditions.

- a) using local water surface slope and discharge, for individual channels separately
 b) using 'valley' slope over the reach 12-13m, and total water discharge.

	Stable		Aggrading		Degrading and / or widening		
	Run 1	Run 3	Run 1	Run 3	Run 1	Run 3	
a)	0.0094	0.0161	0.0228	0.0173	0.0233	0.0248	
	0.0200	0.0168	0.0245	0.0190	0.0281	0.0261	
		0.0198	0.0246	0.0224		0.0288	
		0.0218	0.0250	0.0232		0.0328	
		0.0223	0.0282	0.0238			
		0.0263		0.0239			
		0.0290		0.0270			
		0.0396		0.0457			

	b)	0.0190	0.0190	0.0209	0.0190	0.0190	0.0190
0.0228		0.0190	0.0228	0.0190	0.0228	0.0209	
0.0266		0.0228	0.0228	0.0209	0.0247		
		0.0228	0.0260	0.0209			
			0.0266	0.0209			

Table 4.8 Summary of stream power per unit bed area data for experimental Runs 1 and 3. S.D. = standard deviation.

Channel condition	n	Run 1		Run 3 - bed slope			Run 3- water surface slope		
		Mean ω ($\text{kg m}^{-1} \text{s}^{-1}$)	S.D.	n	Mean ω ($\text{kg m}^{-1} \text{s}^{-1}$)	S.D.	n	Mean ω ($\text{kg m}^{-1} \text{s}^{-1}$)	S.D.
Stable	110	0.0233	0.0118	58	0.0290	0.0149	53	0.0301	0.0092
Aggrading	87	0.0265	0.0159	78	0.0265	0.0150	70	0.0282	0.0105
Degrading	37	0.0294	0.0132	28	0.0347	0.0196	26	0.0316	0.0112
Scour hole	10	0.0442	0.0144	3	0.0459	0.0268	2	0.0271	0.0074
Indeterminate	3	0.0145	0.0068	-	-	-	-	-	-
Aggrading + stable	197	0.0247	0.0138	136	0.0276	0.0151	123	0.0290	0.0099

In all three data sets the mean value of ω for degrading channels exceeds that for both stable and aggrading ones. The significance of these differences was evaluated using a t-test. All nine frequency distributions are not significantly different from normality enabling the application of this statistic. Table 4.9 presents these results.

Table 4.9 Results of t-tests to assess the significance of differences between stream power per unit bed area values in Table 4.8. Null hypotheses were $\omega_A \neq \omega_S$; $\omega_D \neq \omega_{S,A,A+S}$; where ω_A is the mean value of mean stream power for aggrading channels, ω_S for stable, ω_D for degrading, and ω_{A+S} for aggrading plus stable ones.

α = significance level; N.S. = not statistically significant

a) Run 1

	Stable	Aggrading	Degrading	Aggrading + Stable
Bed slope				
Stable	—	1.62 ($\alpha = 0.10$)	2.64 ($\alpha = 0.005$)	—
Aggrading		—	0.98 (N.S.)	—
Degrading			—	1.91 ($\alpha = 0.05$)
Aggrading + stable				—

b) Run 3

	Stable	Aggrading	Degrading	Aggrading + Stable
Bed slope				
Stable	—	0.77 (N.S.)	1.24 (N.S.)	—
Aggrading	1.05 (N.S.)	—	1.86 ($\alpha = 0.05$)	—
Degrading	0.63 (N.S.)	1.59 ($\alpha = 0.10$)	—	1.85 ($\alpha = 0.05$)
Aggrading + stable	—	—	1.19 (N.S.)	—
Water surface slope				

The t-test results from Run 1 suggest that the mean values of ω are greater for degrading channels than for the others, although this difference is not significant for aggrading ones alone. Using bed slopes in the calculation of ω , Run 3 data also reveal degrading channels to have significantly greater mean stream power than aggrading and stable ones combined. In this case stable channels have a greater mean value of ω than aggrading ones, which is not significantly lower than the mean for degrading channels. Using water surface slope data, degrading channels again have the greatest mean value of ω , but this is only statistically significant when compared with aggrading ones.

All three data sets show only small differences in average values of mean stream power with channel state. The cumulative frequency distributions of ω presented in Figure 4.8 have the stable and aggrading channel data combined due to their statistical similarity and the practical difficulties in distinguishing these channel states. The curves for degrading channels plot to the right of the other data in both runs when bed slope is used in the calculations. The water surface

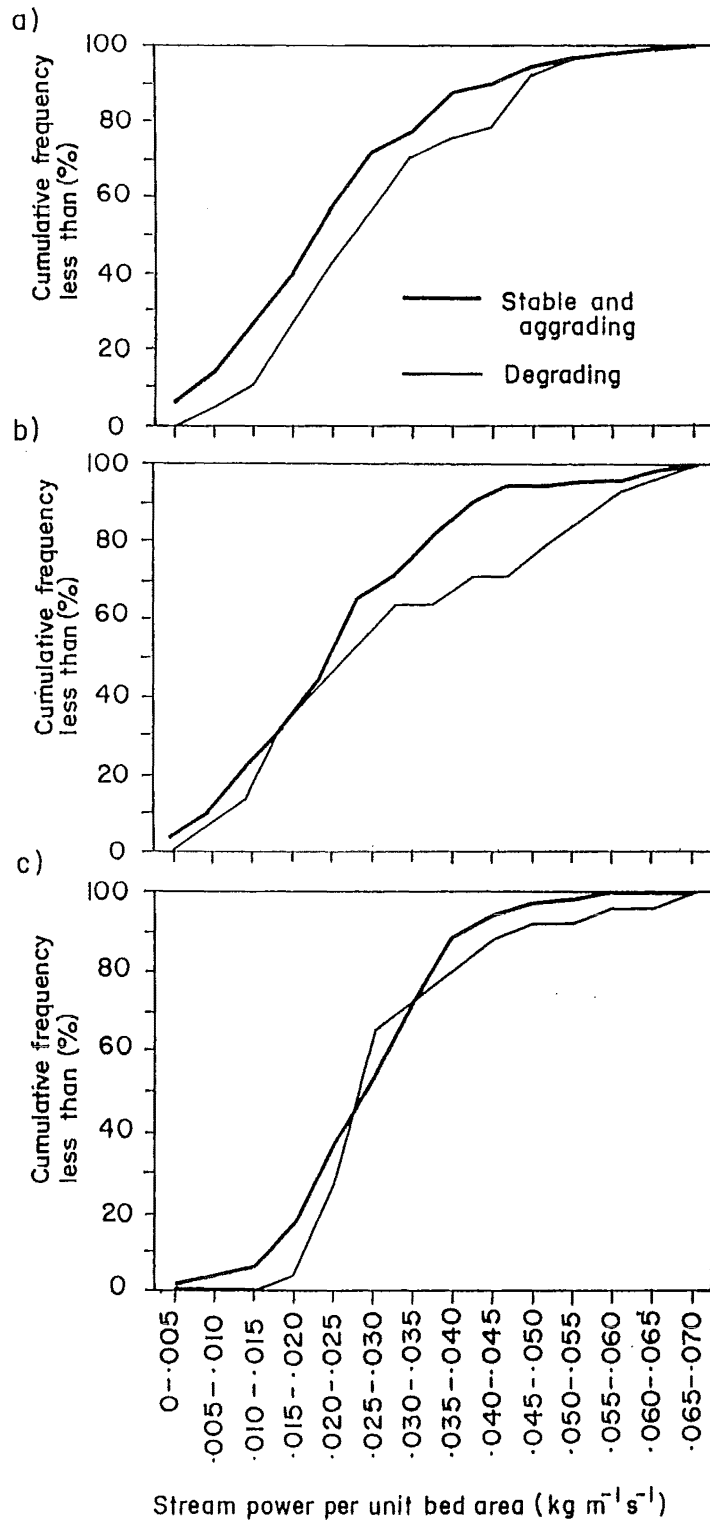


Figure 4.8 Cumulative frequency curves for stream power per unit bed area, ω , ($\text{kg m}^{-1} \text{s}^{-1}$) for Runs 1 and 3. Degrading channels are separated from aggrading and stable ones combined.

- a) Run 1- bed surface slope used to calculate ω
- b) Run 3 - bed surface slope
- c) Run 3 -water surface slope

slope data (Figure 4.8c) show the same pattern for $\omega < 0.020 \text{ kg m}^{-1}\text{s}^{-1}$ and $\omega > 0.035 \text{ kg m}^{-1}\text{s}^{-1}$. This reflects the compression of the range in ω referred to previously, which results from bed slopes less than about 0.004 generally being associated with greater water surface slopes (0.006 and above). Since water surface slope is closer to the energy slope of the flow than bed slope, the form of Figure 4.8c is regarded as the most reliable indicator of the shape of the distributions of mean stream power. In purely statistical terms these curves are indicative of a gradational threshold (Begin and Schumm, 1984) existing between the degrading and stable / aggrading channel states. Several reasons can be advanced as to why this threshold may be obscured in the data in Figure 4.8, the most important of which include:

1. mean stream power at the onset of degradation was rarely recorded due to the timing of sampling and would be expected to be the maximum ω ;
2. the most noticeable degradation was often restricted to short lengths of channel (<0.5m) but the measurement system used to determine slope was only able to detect slopes over lengths in excess of 1.0m; thus, maximum slopes may not have been recorded;
3. the value of the threshold for the onset of degradation depends on the degree of channel armouring that developed and this was spatially variable.

The indistinct nature of the gradational threshold between aggrading / stable and degrading channel states suggests that the control over bedload pulse generation is dependent upon additional variables. A stream power threshold may be applicable for a channel with constant water discharge, but this is rarely the case for sufficient length of time to enable any such intrinsic thresholds to be exceeded. Thompson (1987) suggested that channel shape evolves towards a theoretical equilibrium when external factors are constant, but that the spatial and temporal persistence of such conditions is limited by variation in these factors. These include variation in discharge due to avulsion or flow capture by the channel, and changes in sediment input and output. In the present experiments channels rarely remained stable (i.e. not widening, narrowing, degrading or aggrading) for more than 90 minutes. This is less than the period of any of the variations in bedload output from the experimental runs noted in Table 4.1. Thus, any intrinsic mean stream power threshold would only rarely be exceeded without being affected by variations in discharge or sediment supply to individual channels. The mean stream power threshold could still operate under circumstances where discharge varied but it is unlikely to do so in all cases. Discharge variations are associated with the renewed evolution of channel shape toward equilibrium which may under different circumstances increase or decrease mean stream power and could therefore accelerate or inhibit the onset of a phase of degradation. Some bedload pulses can be accounted for as the results of changes in channel geometry and others as consequences of an intrinsic mean stream power threshold between aggradation and degradation.

Another source of bedload pulses that is also related to channel geometry lies in the role of confluence scour holes. These cause local base level lowering and can promote upstream

migrating waves of degradation, an idea which has been reported in the literature (e.g. Pickup, 1977; Griffiths, 1979). Scour holes produced such a response on some occasions in the sand tray experiments but were not so regular as suggested by Ashmore (1985, 1987) and did not appear to be the dominant source of sediment for bedload transport. Carson and Griffiths (1987) suggest that most gravel in transport is derived from lateral erosion of the banks of bar tails and present a model of sediment transfer that is similar to that of Ashmore (1985, 1987). The results discussed above imply that the processes associated with confluence scour are only one of three mechanisms which can produce bedload pulses.

This discussion of mean stream power variations has suggested that any correspondence between this variable and channel equilibrium / non-equilibrium state that may be expected on the basis of the bedload transport rate results (section 4.2) is poorly defined. This results from the non-equilibrium conditions being consequent upon near continuous changes in discharge through each anabranch which occur more rapidly than channel form is able to respond. Mean stream power values thus reflect both the bed slope as a response to the aggradation / degradation which a channel undergoes as it relaxes towards equilibrium and the influence of changing the discharge through a pre-existent channel. This latter process can cause rapid rises in ω and hence in bedload transport rates, which are only detectable if measurements are made during relatively short periods of channel adjustment. Hence it is difficult to obtain representative data about the variation of ω with channel condition.

4.4 Discussion and conclusions

The variation in sediment output rate through time from the sand tray in the experiments described herein is similar to that reported by Ashmore (1985, 1988) in a comparable set of experiments. Figure 4.9 plots the data from these runs onto Figures 2.2 and 2.3 again illustrating the consistency of the present data with other information on bedload pulses.

The smallest scale fluctuations that were recorded (<15 minutes) are related to local short term effects such as progressive bed armouring (Gomez, 1983) and bedload sheet migration (Whiting *et al.*, 1988). The nature of sediment input in the experiments, which was effectively an instantaneous input every 15 minutes, could also produce such a result although it is unlikely that this effect would persist along the entire length of the sand tray (see Chapter 6). The larger scale bedload pulses can be regarded as including both macro- and mega-scale features. Which scale each pulse is classified under depends upon the channel processes producing it, and this aspect is described further in Chapter 5.

Bed wave development is associated with aggradation. Subsequent degradation does not necessarily remove all of the aggraded material since degradational processes are usually restricted to part of the active channel width. It is possible for bed waves to be superposed upon

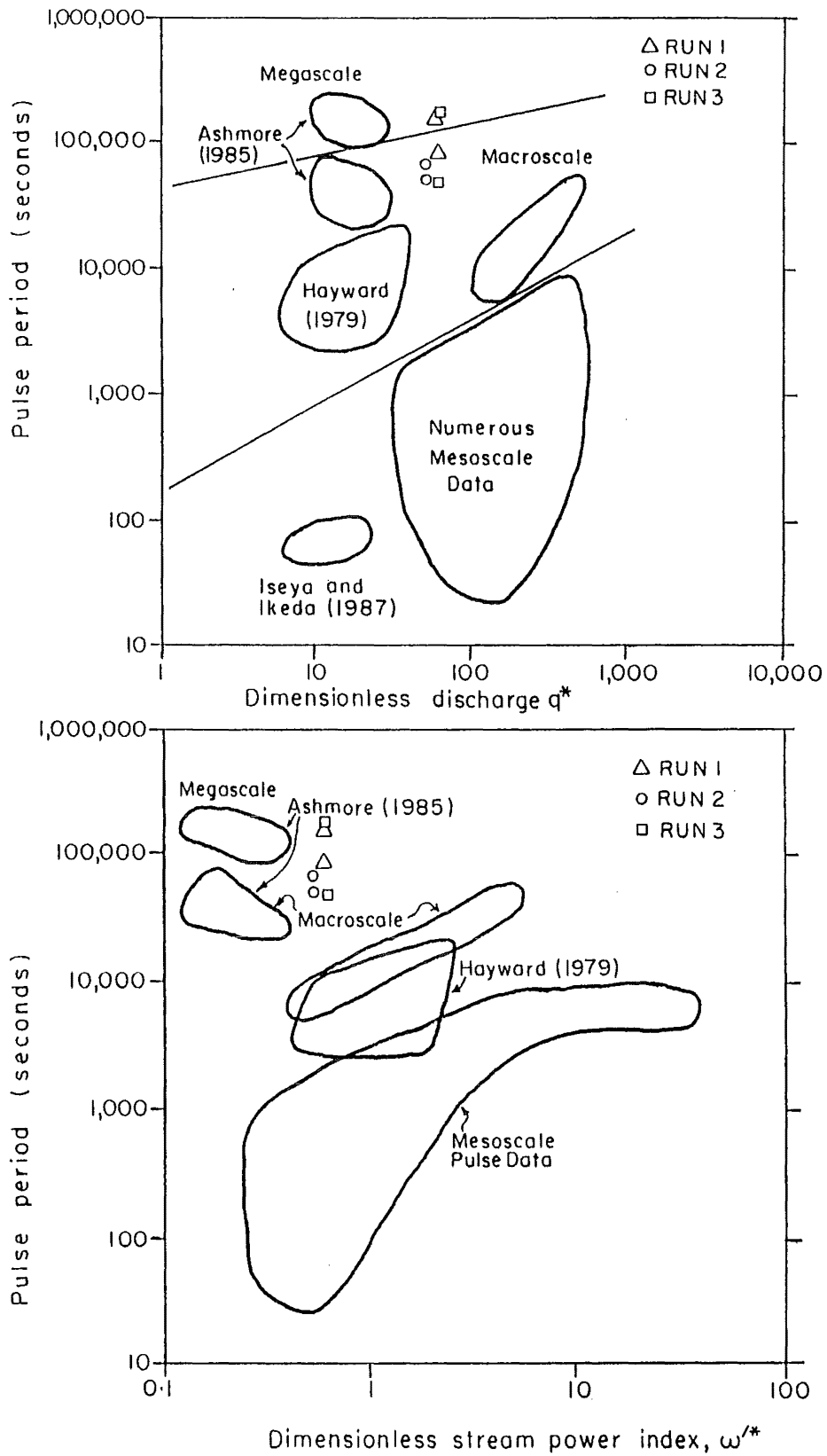


Figure 4.9 Bedload pulse periods measured in Runs 1-3 compared with data from other sources (see Figures 2.2 and 2.3 for details).

long term aggradational or degradational trends, as was observed in the experimental runs. The association of wave accumulation with decreasing bed relief and increasing storage of sediment in the active and semi-active reservoirs (Table 4.4) is consistent with previous work (Church and Jones, 1982; Smith and Southard, 1982; Ashmore, 1987). Inverse patterns are associated with degradation. Explanation of these patterns can be attempted either at the mega- and macro-scales, or at the meso-scale. At the former scales conditions are established which may directly produce wave accumulation and bedload pulses. The processes of aggradation and degradation are consequent upon meso-scale processes which have been described in the present Chapter as processes affecting single cross-sections.

Aggradation and degradation occur where there exists a non-equilibrium between water flow and the sediment input rate from immediately upstream. Under equilibrium conditions when sediment supply is unlimited by hiding effects, transport is at capacity. Equilibrium conditions are rarely attained in active braided rivers such as those of the experimental runs described herein. This reflects continually changing discharge in each branch channel and widespread armouring of the major channels. Under field conditions where total discharge also fluctuates, equilibrium may be even less frequently attained. Sediment transport rates in the experiments appeared to respond relatively rapidly to altered flow conditions, which supports the conclusion that there is a ". . . broad consistency between transport rates, hydraulic conditions, and channel morphology." (Davoren and Mosley, 1986 p.652). Also, Davoren and Mosley (1986) observed that where bed and bank erosion were not occurring, the sediment transport rate declined to zero, which reflects the importance of sediment supply in some conditions.

SEE ERRATA

Despite this adjustment measured transport rates were appreciably different from those predicted by equilibrium formulae (Figure 4.7). Overprediction of actual transport rates has been interpreted as implying supply limitation, but this assumes that the equation reliably represents both flow intensity and entrainment conditions (Richards, 1988) and that the non-equilibrium of the channels has no effect on transport rates. Assuming that the Bagnold (1980) equation is reliable under these conditions, the data of Figure 4.7 suggest that under conditions of aggradation this equation overpredicts actual transport rates. Hey (1979) presented a model for channel development in the context of a drainage basin and Soni's (1981) experimental results are similar but at a much smaller scale. Hey's model predicts that the balance between flow depth (hydraulic radius), slope and bedload transport rate varies during aggradation (Figure 4.10). Throughout this phase actual bedload transport is less than that predicted by the equilibrium equation because equilibrium conditions do not exist and bedload input to a section exceeds the output from it (by definition). Considering a cross-section at location x and another downstream at $(x + \Delta x)$, then aggradation implies that $\delta G_b / \delta x < 0$. Over a small distance Δx flow conditions can be assumed constant so that the bedload transport capacity remains constant. Thus at $(x + \Delta x)$ the transport rate must be less than capacity even if it is at capacity at location x . Extending this reasoning to a longer reach provides a rationale for the results of Figure 4.7. In the reverse case when

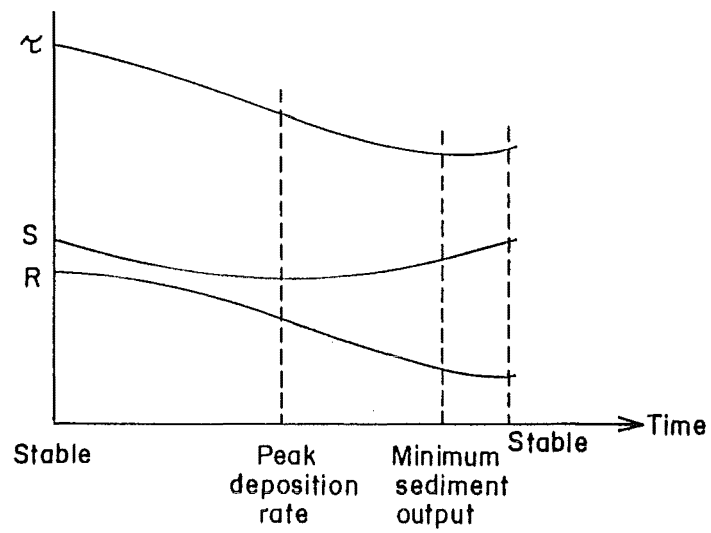


Figure 4.10 Variation in shear stress, τ , slope, S , and hydraulic radius, R , during an aggradational episode (after Hey, 1979). Bedload transport rate is proportional to τ^α where $\alpha > 1$.

degradation is occurring and $\delta G_b / \delta x > 0$, there is the additional component of gravity assisted entrainment from banks, so increasing the bedload transport capacity further. The discrepancy ratios are closer to 1.0 for degrading than aggrading channels due to more rapid relaxation of the channel shape toward equilibrium in the former case. This results from the nature of the processes; deepening a channel is rapid and not constrained by the requirement for sediment supply from upstream as is aggradation. ERHAT

These arguments apply only to the relatively unusual cases where discharge remains constant for sufficiently long to enable channel shape to relax toward equilibrium. The switch from aggrading to degrading states under such conditions may be controlled by a stream power threshold, the value of which is dependent upon development of armouring. A stream power threshold may also exist with respect to changing discharge, rather than slope or width, as avulsion or some other process of channel change upstream causes a discharge increase to which channel geometry adjusts. This can induce degradation and / or widening which leads to the evacuation of sediment. A third mechanism for producing a bedload pulse exists at confluence scour holes, upstream of which oversteepening leads to bed and bank erosion, sediment transport around the scour hole (Best, 1987) and deposition downstream (Ashmore, 1987; Carson and Griffiths, 1987).

The association between channel condition and the performance of the Bagnold (1980) equation suggests that the relationships outlined in Table 4.4 can be supplemented by a sediment transport relationship. Defining G_{bcap} as the equilibrium transport capacity, a degrading condition is associated with $G_b > G_{bcap}$, aggrading with $G_b < G_{bcap}$, and stable channels with $G_b \cong G_{bcap}$. All three mechanisms of pulse generation are associated with the possibility that channel pattern will be simplified in the zone of maximum transport rate. Essentially this is due to degradation enabling flow capture. Church and Jones (1982) have also suggested that the greatest rates of sediment transport are associated with pattern simplification. It is difficult to establish cause and effect in such systems (Richards, 1982) as the interdependence of channel form and sediment transport rate is complex (e.g. Ashworth and Ferguson, 1986). The way in which channel patterns continually changed and individual channel geometries responded to both internally and externally induced thresholds, produced the variations in sediment output over time shown in Figure 4.1. The irregularity of this variation is interpreted as resulting from these different processes acting in combination. There are certain constraints operating in this system - sediment needs to accumulate before a critical slope threshold can be exceeded, and once this is reached a certain time is needed for degradation to be completed. For given water and sediment input these constraints may serve to define the average spacing of peaks in the sediment output rate. In prototype rivers such regularity would be dependent upon there being similar regularity in the sediment input and water discharge. The major bed wave in the Kowai R., initiated during a storm in 1951 (Beschta, 1983a and b) is an example of an exogenous form which lies outside of the semi-cyclical patterns in sediment storage within the river. Other disequilibrating influences, such

as tectonic uplift (Gregory and Schumm, 1987) or base level changes (Wilson, 1985) will have similar effects. In addition variable valley width (Beschta, 1983b; Magilligan, 1985) and tributary locations (Church and Jones, 1982) are important.

To summarise, the principle conclusions of the sand tray study of bedload transport rates and cross-sectional channel morphology are as follows:

1. With constant water and sediment inputs, braided gravel-bed rivers have variable sediment transport rates through a cross-section. This supports the results of Ashmore (1985, 1988) and has demonstrated that bedload pulses can be produced with constant sediment input rate.
2. At-a-section variations in sediment storage and channel morphology can be correlated with bedload transport rates, although the morphology and transport processes have different relaxation times.
3. Equilibrium conditions are infrequently encountered and the application of equilibrium formulae for the prediction of actual transport rates is not always feasible. Deviations from these predictions are consistent with whether the channels concerned are aggrading or degrading.
4. The processes controlling the occurrence of bedload pulses include factors both internal and external to the channel under consideration. This prevents a simple explanation of pulse development in terms of a variable such as stream power per unit bed area.

5. THE FORM OF BED WAVES IN THE SAND TRAY AND FIELD

Chapter 4 has described bedload pulses and attempted to account for them in terms of instantaneous at-a-section conditions. The present Chapter extends this discussion both spatially and temporally, and examines the contrasts between bed waves in the sand tray and in the field. The channel and bar features which are associated with bed waves and their development through time have not been addressed thus far. This can be done in terms of surveyed snapshots of channel morphology and by looking at evidence for the evolution of these instantaneous morphologies. This discussion examines survey data taken at regular intervals during Runs 1 and 3, and uses examples of channel evolution to illustrate the nature of bed waves and their generating processes. Both endogenous and exogenous wave types are considered. A comparable approach is taken with field data from the Kowai River. Continuous data on channel and bar evolution are not available in the field example so the structure of sedimentary deposits is examined to enable interpretation of their evolution.

5.1 Bed wave characteristics derived from reach scale patterns of sediment storage and channel morphology in the sand tray

It was argued in Chapter 4 that sediment output rate variations can be accounted for in terms of channel geometry at the downstream end of the sand tray. These conclusions (summarised in Table 4.4) can be used for interpretation of variations in channel geometry along the entire length of the tray. There is little point in using aggregate data from the entire length of the tray since not all of the 13m length of channel underwent equivalent changes at the same times. Mean bed elevation, bed relief and sediment storage data for cross-sections 2m to 13m inclusive are presented in Figures 5.1 (Run 1) and 5.2 (Run 3)(see Appendix 7 for details). These data are considered under three headings: downstream consistency, temporal persistence, and downstream migration of bed waves.

A. Downstream consistency. Patterns in sediment storage and cross-sectional morphology persisted over reaches of variable length. Some patterns occurred contemporaneously over almost the whole length of the tray, such as the rise in mean bed elevation between 2650 and 2890 minutes in Run 3 accompanied by increased volumes of sediment stored in the active and semi-active reservoirs, which affected cross-sections from 3m to 13m inclusive (Figure 5.2). At most other times trends in the data were less consistent. At 1930 minutes (Run 1) the mean bed elevation was on a rising trend at 3-5m, and at minima from 6 to 13m. This pattern was not repeated by either the bed relief index or the sediment storage patterns (Figure 5.1). Run 3 at 2650 minutes provides a further example. Here the mean bed elevation was at a peak at 2m, a minimum at 3-8m, and was rising from 9-13m (Figure 5.2a). Again there was little consistency with the other indices.

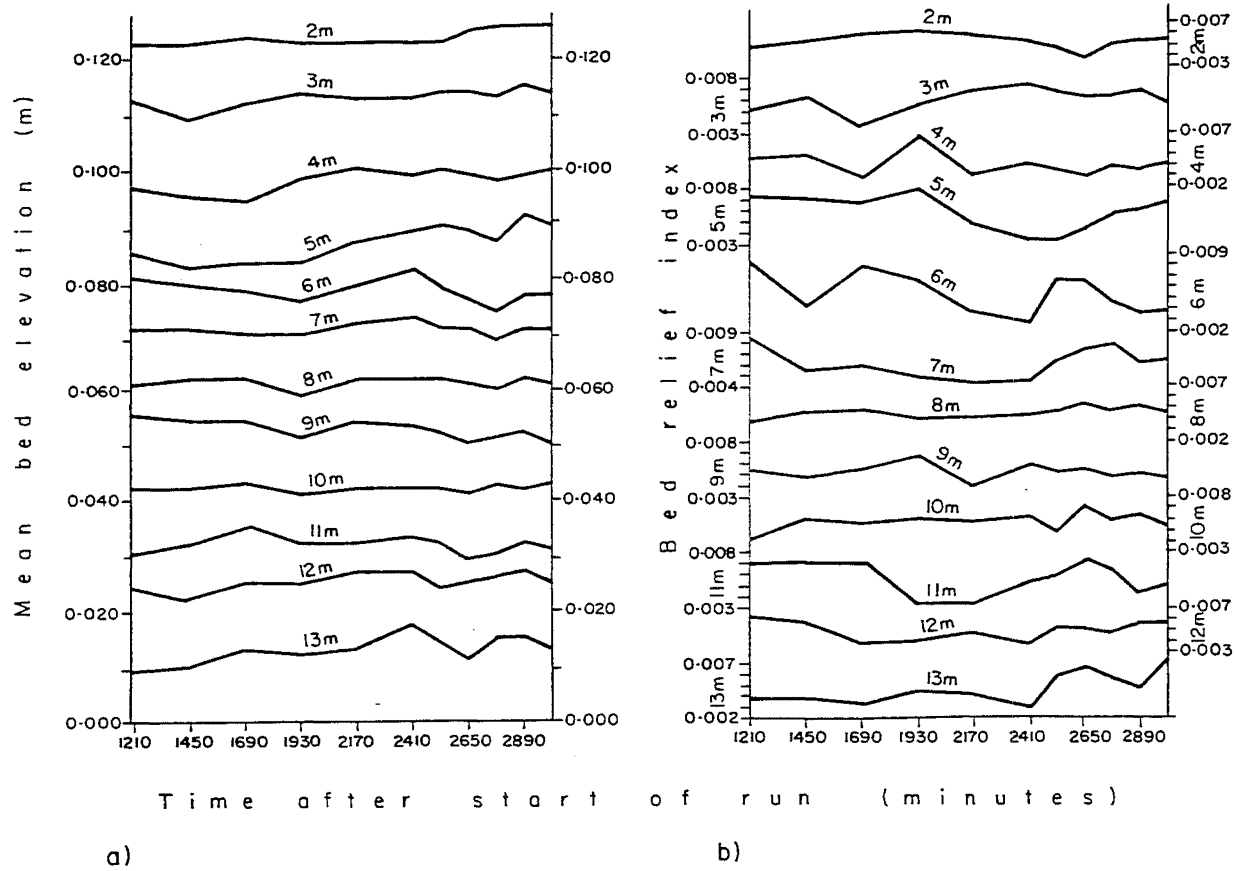


Figure 5.1 Sediment storage and cross-sectional morphology at all cross-sections in Run 1.

a) mean bed elevation (m)

b) bed relief index

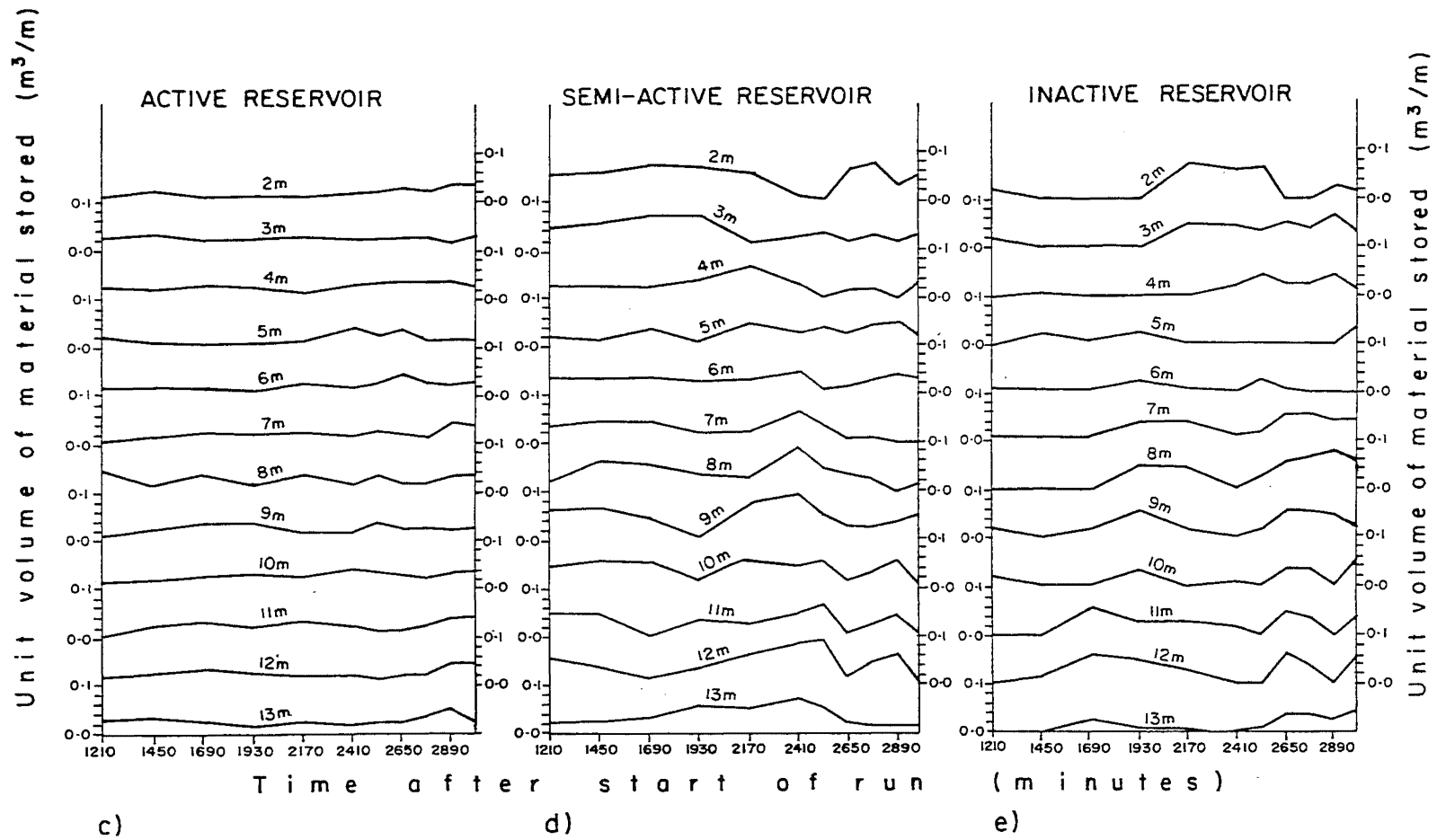


Figure 5.1 (Continued)

c) unit volume of material stored in the active reservoir (m^3/m)

d) unit volume of material stored in the semi-active reservoir (m^3/m)

e) unit volume of material stored in the inactive reservoir (m^3/m).

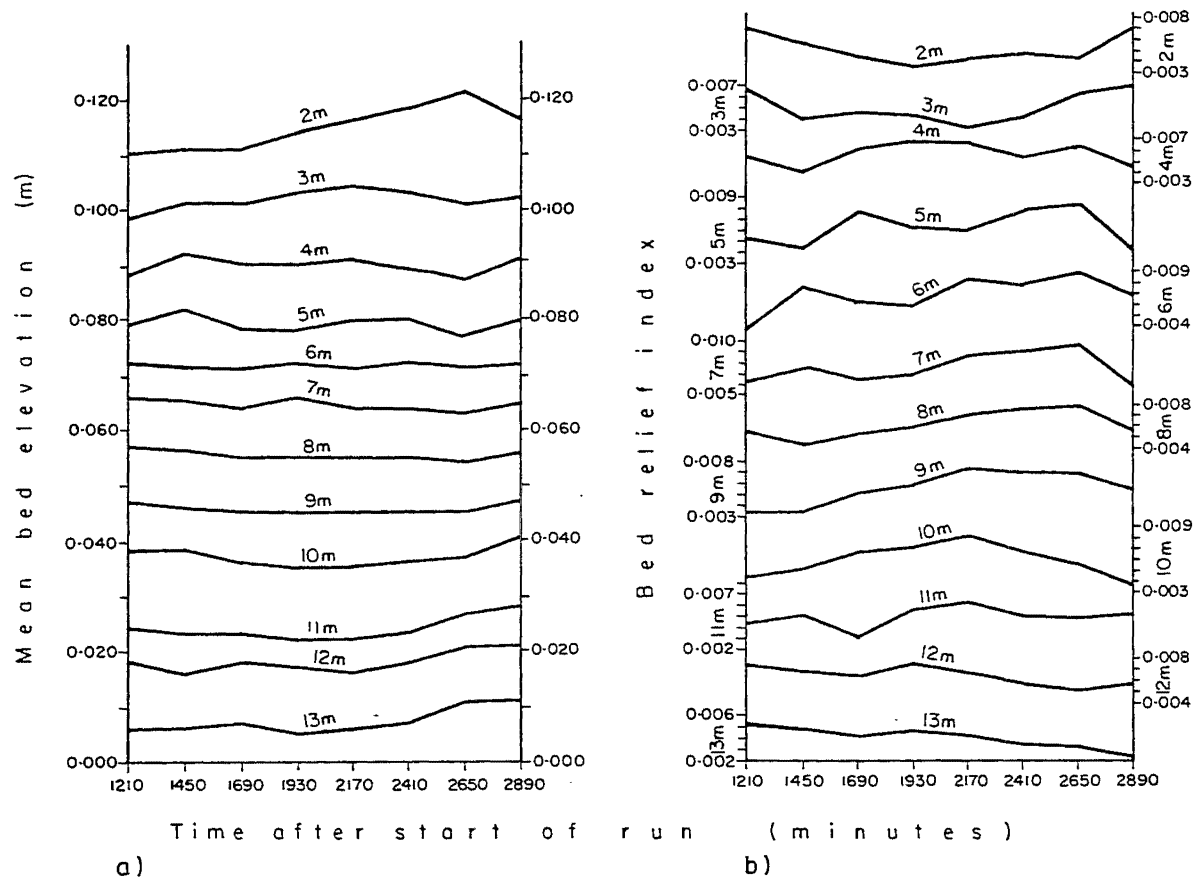


Figure 5.2 Sediment storage and cross-sectional morphology at all cross-sections in Run 3.

a) mean bed elevation (m)

b) bed relief index

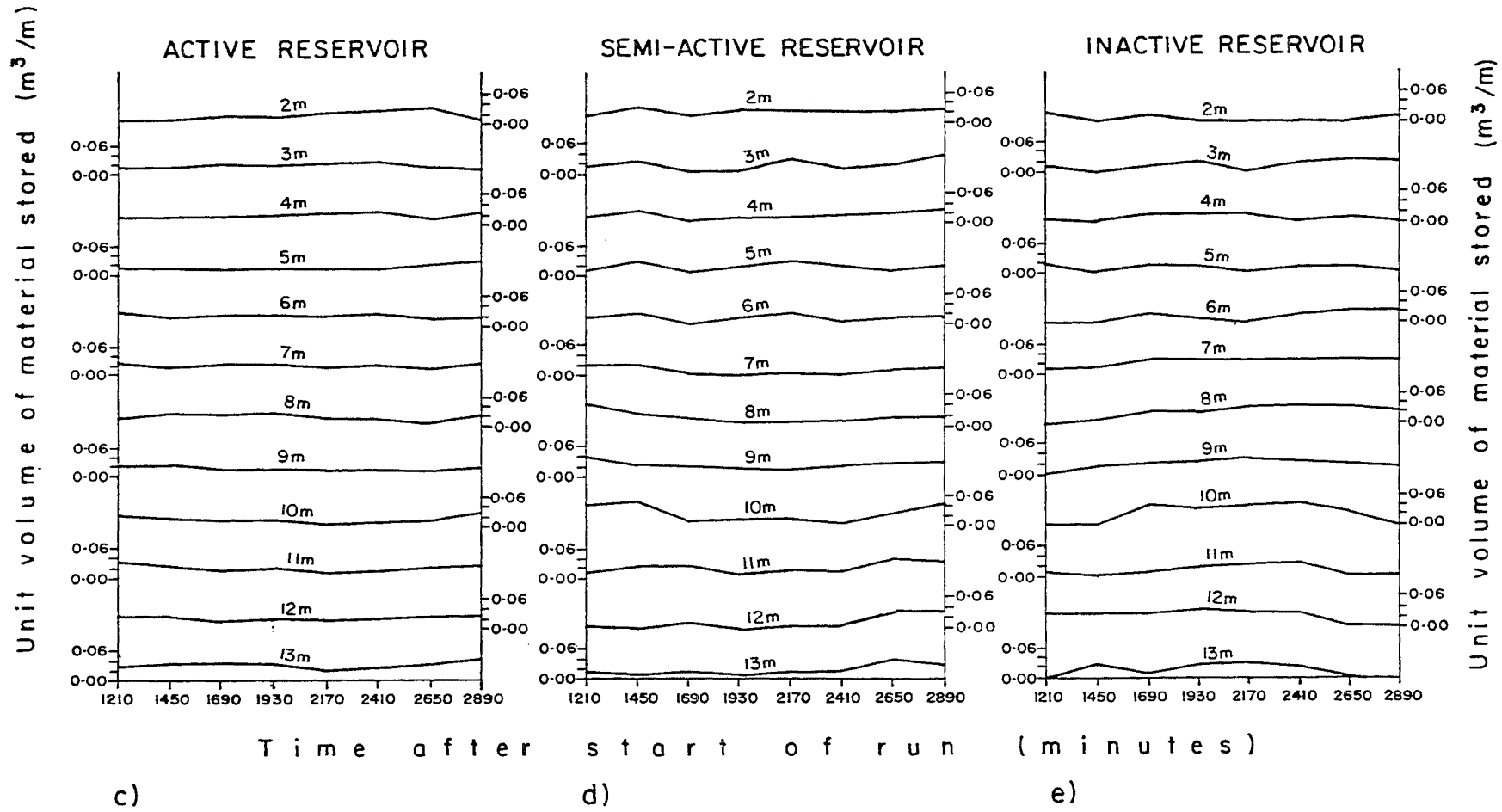


Figure 5.2 (Continued)

c) unit volume of material stored in the active reservoir (m^3/m)

d) unit volume of material stored in the semi-active reservoir (m^3/m)

e) unit volume of material stored in the inactive reservoir (m^3/m)

These illustrations suggest that the variability in the relationships between sediment storage and cross-sectional morphology that were identified at a single cross-section in sub-section 4.2.1, is accompanied by downstream variability in the same relationships. These can be accounted for at individual sections in the same way as was done for the 13m section by reference to the channel geometry and the direction and magnitude of the changes to channel form. The additional downstream variability reflects both spatial and temporal effects. Firstly, not all of the channel changes operated at the same spatial scale, and an indication of the lengths of reaches affected by simultaneous changes is provided by Table 5.1. Most patterns in the data were very localised, although trends in elevation and storage volume often affected 2m long reaches. Occasional synchronous patterns were visible over as much as 8m of the tray (about 6 active channel widths). Secondly, variability of process length was accompanied by temporal lag effects introduced by taking data for all cross-sections at one time. As was demonstrated for the 13m cross-section, channel changes are not instantaneous and channel morphology adjusts over a different timescale from sediment transport rate. Thus, if two adjacent sections are undergoing the same morphological and sediment storage changes diachronously they may be in different states at the time of sampling. Definition of a reach length affected by a given process thus requires temporal integration.

Table 5.1 Frequency of occurrence of synchronous peaks or troughs in mean bed elevation, bed relief index and volume stored in the semi-active reservoir over different reach lengths, for Runs 1 and 3. The definition of a peak was that the preceding and subsequent values of the quantity were lower than the value in question, with the reverse definition for troughs. The number of sections is the number of adjacent cross-sections where there were synchronous peaks or troughs.

Number of sections	Run1			Run3		
	Mean bed elevation	BRI	Semi-active volume	Mean bed elevation	BRI	Semi-active volume
1	15	19	22	6	14	6
2	3	5	8	7	2	4
3	3	7	4	-	3	5
4	1	1	1	-	-	-
5	-	-	-	-	1	1
6	1	-	-	-	-	-
7	-	-	-	-	-	-
8	1	-	-	1	-	-

B. Temporal persistence. Bearing in mind the constraints imposed by a 240 minute sampling interval (120 minutes for part of Run 1), the timescales of the processes of channel change can be considered. An example serves to illustrate temporal variability in sediment storage and morphological changes, and also refers to the question of the reach lengths affected by different processes.

Run 3 at 2.5-5m from 1210 to 1690 minutes provides this example. At 1450 there was a peak in mean bed elevation, a low bed relief index, and an increased volume of material in the semi-active reservoir, throughout this reach (Figure 5.2). This appears in Table 5.1 as a 2 section mean bed elevation peak (4m and 5m), a 3 section bed relief index peak (3m, 4m and 5m) and a 5 section peak in semi-active storage volume (2m-6m inclusive). This occurred without any major changes in channel pattern (Figure 5.3). At 1210 minutes, erosion of the left bank of the left channel had been accompanied by local degradation. Aggradation at the head of the tray affected the area of flow divergence (Figure 5.3b) and led to general aggradation in this reach as an increased proportion of the water discharge flowed over the large inter-channel bar. The material in this bar thus underwent static transfer to the semi-active reservoir (Figure 5.2d). By 1690 minutes, some degradation had occurred in the right channel. This was a response to aggradation partially plugging the head of the left channel and directing an increased volume of water into the right channel, which adjusted its cross-sectional geometry accordingly. Slightly more than one cycle of change is described here, although only one is apparent from the morphology data, reflecting the problems in interpreting data collected at a sampling interval of similar scale to the processes under investigation.

Because of the fixed sampling interval it is difficult to draw any precise conclusions regarding the frequency of morphological changes. By defining troughs in the various data series, some idea can be gained by measurement of inter-trough wavelengths (Table 5.2). This is not entirely consistent within Run 1 since the sampling interval was reduced from 240 to 120 minutes after 2410 minutes therein.

The data in Table 5.2 can be compared with the frequency of oscillation in the sediment output series (Table 4.1). For both runs the period (T) of major oscillations in the output series (440 and 480 minutes respectively) is mirrored by morphological variations with T=480 minutes. Minor oscillations in the Run 1 sediment output series (T=247 minutes) are picked up in Table 5.2 by fluctuations with T=240 minutes. No such fluctuations are found for Run 3 reflecting the shorter period (T=154 minutes) of the minor sediment output rate oscillations in that run i.e. the processes causing these occur at timescales that are too short to be detected by the 240 minute sampling interval for cross-sectional morphology. Table 5.2 also shows a number of variations with period 720 minutes or longer. No cycles of this period were detected in the sediment output data. High sediment output rates occur only during the degradational phase of a cycle of aggradation and degradation. Thus, the periods of aggradation-degradation cycles and the sediment output

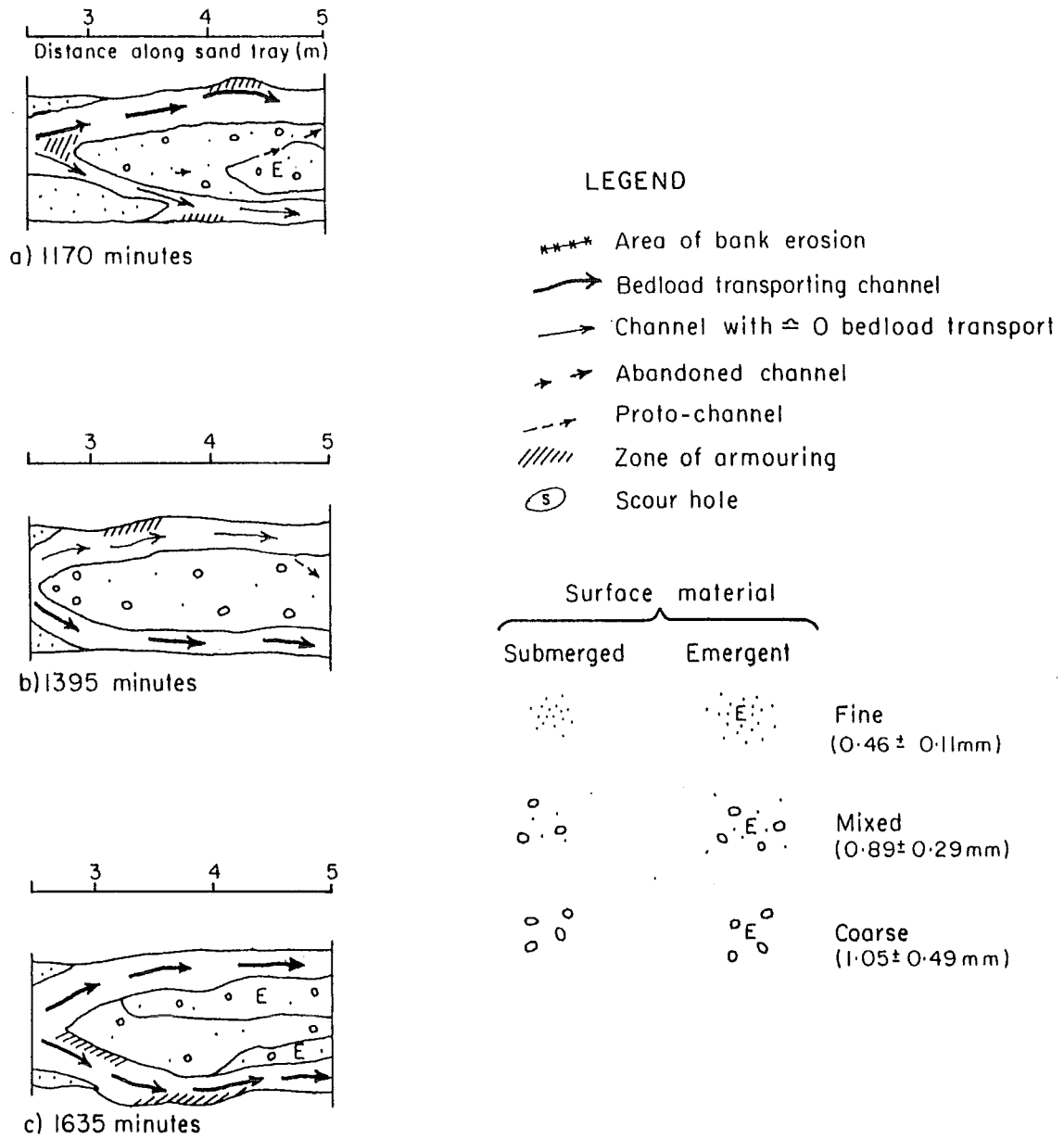


Figure 5.3 Channel morphology in Run 3 from 2.5m to 5m inclusive.

fluctuations should be similar. This suggests that the 720 minute periods identified in the cross-section morphology data are actually reflections of the sampling interval being too coarse to detect the timing of the oscillations precisely, and that they are combinations of variations at shorter timescales.

Table 5.2 Frequency of time intervals between successive troughs in the mean bed elevation, bed relief index and volume stored in the semi-active reservoir data series, for Runs 1 and 3. Troughs are defined as in Table 5.1. The time intervals are accurate to ± 60 minutes for Run 1 and ± 120 for Run 3 data. Note that 360, 600, 840 and 1080 minute intervals are likely to be under-represented due to the change in sampling interval for the latter part of Run 1.

Time interval (minutes)	Run1			Run3		
	Mean bed elevation	BRI	Semi-active volume	Mean bed elevation	BRI	Semi-active volume
240	1	3	2	-	-	-
360	2	2	2			
480	1	5	5	1	2	5
600	1	-	1			
720	6	6	2	3	3	1
840	4	1	2			
960	-	2	1	1	2	1
1080	1	-	-			

The aggradational and degradational phases were of different lengths. Taking degradational phases to be those when sediment output rate from the tray exceeded the input rate to it and aggradational ones as the converse, the ratios of times undergoing degradation : aggradation for the model phases of the 3 runs were 1 : 1.26, 1 : 3.00, and 1 : 2.45, respectively. The longer aggradational than degradational phases are also apparent in mean bed elevation data (Figures 5.1a, 5.2a) where reduction in mean bed elevation rarely persisted for more than one time period.

C. Downstream migration of bed waves. The problems of using a coarse sampling interval recur when an assessment of bed wave propagation (upstream or downstream) is to be made. If waves of material were migrating downstream and / or cycles of degradation moving upstream at an appropriate timescale, the effects should be most apparent in the mean bed elevation data. Figures 5.1a and 5.2a show no obvious patterns of this type, although there are cases when arguments could be advanced in support of an hypothesis of migratory behaviour (eg. Run1, 10m at 2770 minutes and 11m at 2890 minutes both had relatively high mean bed elevations). Any attempt to estimate the rate of wave migration and whether attenuation occurs downstream

would require a much closer sampling interval than was used here. This question is approached using a different technique, the dispersion of tracer material, in Chapter 6.

D. Summary. The data from both runs suggest that bed waves of different lengths occur, that their temporal persistence is variable and that they do not migrate in a way that is detectable with the sampling interval used herein. These first two conclusions are consistent with the variations in sediment output from the sand tray (Figures 4.1, 4.2). Applying a location-for-time substitution (Paine, 1985) this data in itself implies that wavelengths should be variable. Interpretation of the cross-sectional data was facilitated by use of information on the evolution of planform morphology. This has improved the understanding of changes in cross-sectional data.

Comprehension of the causes of bed wave genesis is still limited by uncertainty in relating known variations in sediment storage and channel morphology to the processes of sediment transport and channel change. Table 4.4 presented qualitative generalisations of these relationships at-a-section which have subsequently been used to aid interpretation of larger scale patterns. Improvement of this understanding requires more detailed information on the processes responsible for bed wave development and erosion. This is approached in the following sections.

5.2 Morphology of an endogenous bed wave / bedload pulse in the sand tray

As an example of the channel and bar morphologies associated with bedload pulses, the pulse in Run 1 between about 2350 and 2850 minutes is described subsequently. Figure 5.4 shows this pulse and the median size of bedload output from the sand tray during this period (see Appendix 5 for data). Figure 5.5 maps the morphology of bars and channels over the reach from 6m to 14m during the same period.

5.2.1 Sediment storage and transport during the bed wave cycle

A cycle of degradation and subsequent aggradation was associated with the bedload pulse arriving at the downstream end of the tray. From 2410 through 2890 minutes (the closest measurement times to the onset and end of this episode) mean bed elevations at all sections from 6m to 13m inclusive underwent a decrease and subsequent rise (Figure 5.1a). The time of minimum elevation varied from 2650 minutes at 9-13m, to 2770 minutes at 6-8m inclusive. In general terms the bed relief indices and the distribution of material between the different sediment storage reservoirs were consistent with the relationships presented in Table 4.4 at all of these locations i.e. as mean bed elevation declined so the inactive reservoir gained material from the semi-active and the bed relief index increased. Figure 5.1 shows that most of these changes were broadly synchronous over the entire 6-13m reach.

Changes in channel patterns during this period reflected the trends in the cross-sectional data. At

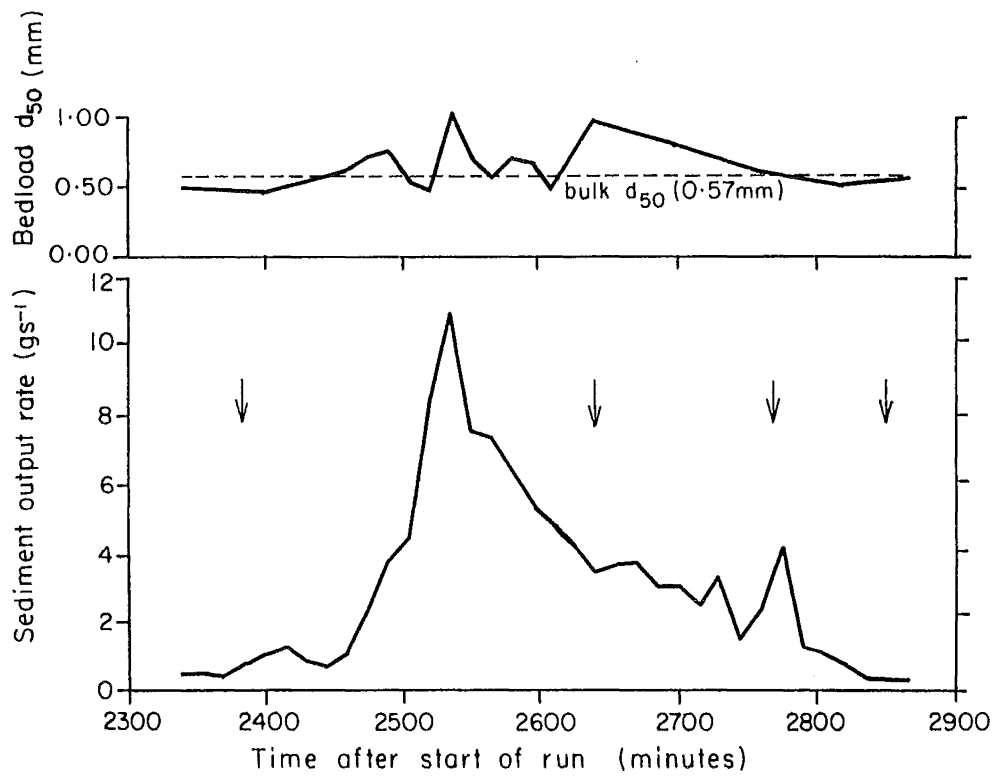


Figure 5.4 Sediment output rate ($g s^{-1}$) and variation in bedload d_{50} (mm) in Run 1 from 2340 minutes to 2865 minutes inclusive. Arrows show the times of channel morphology sketches in Figure 5.5.

the onset of the period (Figure 5.5a) channel pattern was complex with multiple sediment transporting channels and bar deposition occurring at several locations. Degradation of the main channel was preceded by bank erosion at B (Figure 5.5a) in response to the deposition of bar A. By 2500 minutes degradation was occurring between 8m and 14m leading to the development of a relatively straight channel taking most of the total flow (Figure 5.5b). Armouring developed as this channel stabilised and inhibited sediment transport. It is notable that bedload median size increased at about this time (2535 minutes) (Figure 5.4; Appendix 5) reflecting the hiding effect produced by the armouring which inhibited the transport of smaller particles. Bedload d_{50} remained above bulk d_{50} (0.57mm) until about 2800 minutes. The next phase of development involved bank erosion at A (Figure 5.5b) and the development of a meandering thalweg in the main channel throughout the reach. This was accompanied by avulsion into a former channel (A on Figure 5.5c). The re-occupation of this channel and its enlargement were responsible for the minor peak in sediment output at 2775 minutes (Figure 5.4). Pattern complexity continued to increase with the development of proto-channels (Moss, Green and Hutka, 1982) at A and B (Figure 5.5d) which later evolved into minor sediment transporting channels.

Considering the reach as a whole channel pattern complexity was inversely related to sediment output rate during this time period. It is difficult to quantify this relationship because of the different lengths of reaches undergoing synchronous changes. Using total sinuosity (ΣP) for the whole tray, rank correlation co-efficients between ΣP and sediment output rate are -0.19 and -0.18, for Runs 1 and 3 respectively, neither of which is significant. An indication of the nature of channel change is obtainable by calculating the bedload transporting capacity of the channels at different times. Transport capacity, designated G_{bcap} (kg s^{-1}) is readily calculated using the Bagnold (1980) equation (4,5) and the hydraulic geometry relationship (3,6a) for discharge estimation. As was noted in Chapter 4, the relationship between predicted and actual bedload transport rate is dependent upon the channel equilibrium or non-equilibrium state. At 2410 minutes, prior to the onset of the bedload pulse, the channels in the reach were either stable or aggrading. G_{bcap} varied downstream over an order of magnitude (Figure 5.6a) in response to changes in channel slope and cross-sectional geometry. As degradation commenced downstream of 10m, G_{bcap} had been reduced by the previous aggradational phase (Figure 5.6b; 11m, 12m). Degradation had raised the capacity at 13m by this time, as had the presence of a scour hole immediately downstream of the 10m cross-section which had increased local bed slope. At 2650 minutes, toward the end of the degrading phase, G_{bcap} was greatest at 9m and 10m where active erosion of lateral bars was ongoing. Further downstream, capacity was in the region $1 - 4 \text{ g s}^{-1}$ which was common for stable channels and is of comparable magnitude to the long-term average sediment output from the sand tray. Only at 7m where a confluence scour hole immediately upstream had the effect of reducing bed slope and hence stream power, was the predicted transport rate very low. The pattern at 2650 minutes was largely retained as the channel morphology changed through 2850 minutes except for an increase in G_{bcap} downstream of 11m due to the recently re-occupied right bank channel in this region (Figure 5.5d).

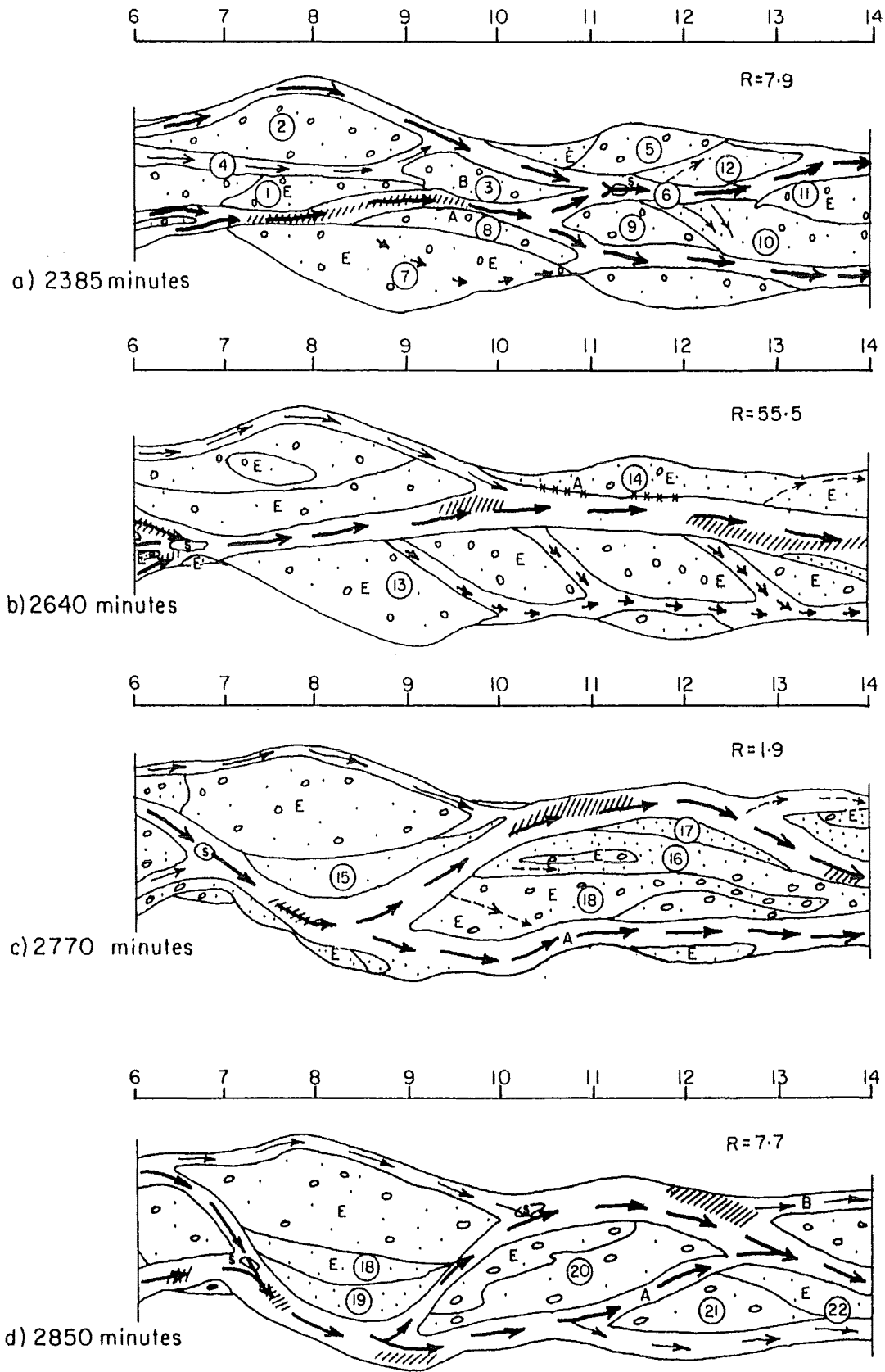


Figure 5.5 Channel and bar morphology through the bedload pulse depicted in Figure 5.4. See Figure 5.3 for legend. Locations marked with letters (A,B etc.) are referenced in sub-section 5.2.1. Depositional surfaces marked with encircled numbers (③ etc.) are referred to in sub-section 5.2.2. R is the ratio by surface area of complex bars to unit bars.

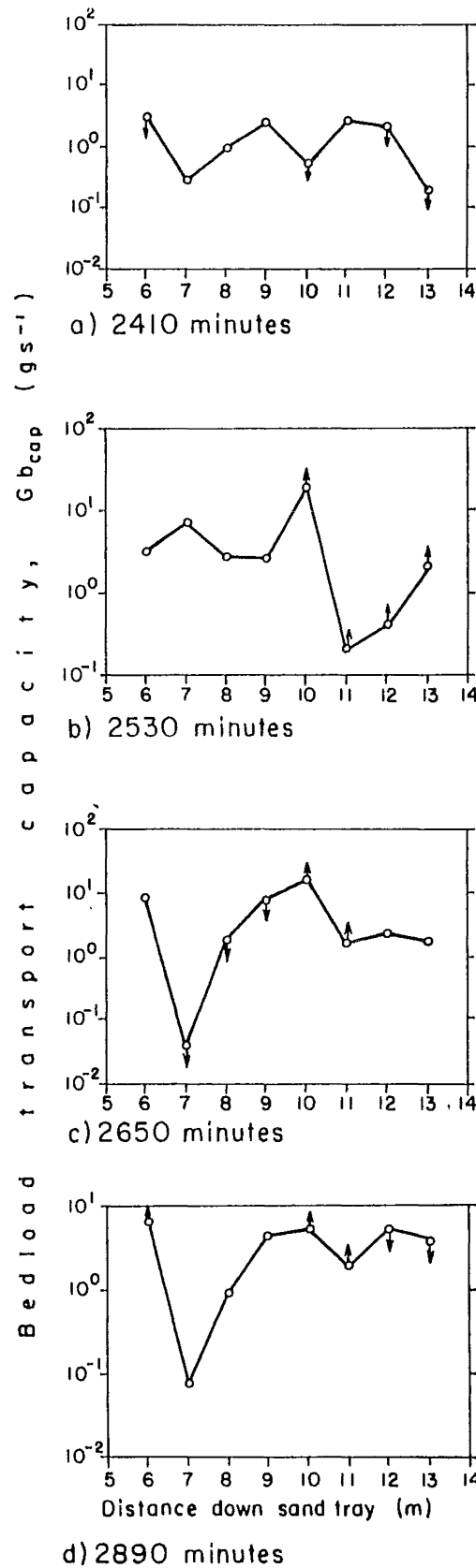


Figure 5.6 Bedload transport capacity at cross-sections 6-13m inclusive, Run1. Capacity was determined using the Bagnold (1980) formula, and converted to dry mass (g s^{-1}). \downarrow indicates that the channel was degrading (i.e. $G_b > G_{b\text{cap}}$), \uparrow indicates aggradation (i.e. $G_b < G_{b\text{cap}}$), and symbols without arrows are for stable channels (i.e. $G_b \cong G_{b\text{cap}}$).

Where one section has a substantially greater transport capacity than the next one downstream, aggradation may be expected to be induced at the lower section if sufficient sediment is being transported (this is dependent upon channel equilibrium or non-equilibrium). This provides a mechanism for the migration of bed waves within channels. In the present example it has been possible to identify the bed wave from the mean bed elevation, bed relief index and sediment storage data and to relate it to channel planform. Availability of the planform morphology data has enabled the processes involved in bed wave development to be described in a preliminary way. This can now be extended by a more detailed consideration of that morphology.

5.2.2 Bar and channel morphologies during the bed wave cycle

Before embarking on this discussion a note is needed regarding the terminology used herein. Ashmore (in discussion of Church and Jones, 1982) offered modified criteria for channel macroform classification. This scheme differentiates unit bars which are primary depositional features from bar complexes, and is used here to try to avoid the confusion of terminology noted by Smith (1978). The word surface is used for identification of morphological units and has no generic implications.

A. Bar and channel evolution during aggradational and degradational periods. During the period 2265-2385 minutes (Figure 5.5a) bar development had taken two forms. Firstly, pre-existing deposits were subject to erosion and dissection. Depositional surfaces 1,2 and 3 (Figure 5.5a) were remnants of a former complex bar which occupied most of the width of the active channel and was then subject to both dissection by channel 4, and lateral erosion by the main channel. Surface 5 was similarly a remnant of a previously more extensive complex. The second process involved bar growth and several types can be recognised. These included both unit bars (Smith, 1974) and bars formed by multiple overlaying of diffuse sand sheets (equivalent to the diffuse gravel sheets of Hein and Walker (1977)). Juxtaposition of these bars produced complex features which were subject to post-depositional dissection. Unit bars were commonly accreted onto pre-existent complexes. The resultant features do not fit readily into schemes for bar evolution such as those of Church and Jones (1982) and Ashmore's modification thereof.

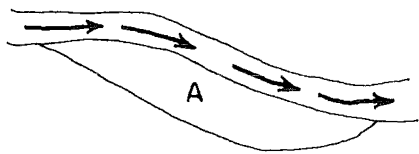
Surfaces 7 and 8 (Figure 5.5a) exemplify the depositional histories of the complex bars. It was initially composed of a former in-channel sheet of fine (<0.6mm) material which became emergent following degradation in the channel. As the channel migrated away from the right bank towards the position occupied at 2385 minutes, further sheets of material were added to the initial deposit so increasing its width. This bar growth ceased when the channel position stabilised, but as the channel began to erode at location B (Figure 5.5a) a new depositional unit (surface 8) was added. This development can be summarised as an initially eroded complex bar remnant being enlarged by lateral accretion of multiple sheets of material, and after a period of stability being further extended by addition of a bank-attached point bar. This sequence is schematically illustrated in

Figure 5.7.

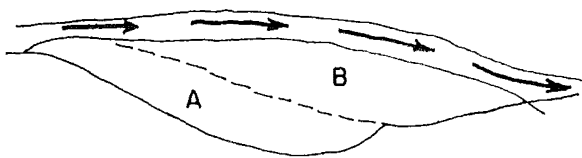
A further example, this time with deposits not attached to the initial channel banks, is provided by surfaces 9 and 11 (Figure 5.5a). Both of these developed as mid-channel bars during the phase of general aggradation in this reach, as a consequence of superposition of numerous diffuse sheets of material. By 2385 minutes the shallow, non-channelised flow between them was itself promoting vertical accretion and this surface (10 on Figure 5.5a) later became contiguous to, and almost indistinguishable from surfaces 9 and 11. Surface 10 was a form of diagonal riffle and the diagonal bar thus deposited could be regarded as a unit bar. Surface 12 (Figure 5.5a) was a similar feature. The resultant bar complex thus contained two remnants of successive accumulation of diffuse sheets of sediment, and a unit bar.

Moving from the aggradational to the degradational phase (Figure 5.5b) the depositional forms appear somewhat different. The main contrast is that most surfaces were emergent from the water and were thus experiencing none of the vertical accretion which was widespread during aggradation. Bar development at this time was restricted to lateral erosion on one bank of the dominant channel and deposition on the opposite side. The scale of these effects depended upon the magnitude of channel migration during this phase. In the case presented here there was little lateral erosion during degradation, and this is typical of the channel behaviour associated with other bedload pulses. Thus, although the degrading phase is important for net sediment transfer this can be accomplished without widespread modification of the bed morphology. Many deposits survive this period unaltered and are subsequently subjected to erosion and deposition once channel degradation ceases. This has important implications for the redistribution of sediment since it implies that the processes transporting most of the sediment are not those which have a dominating influence over sedimentary deposits. In prototype rivers, changes in channel and sedimentary deposit morphologies as the consequence of flood events may not indicate the magnitude of sediment transport during the event very accurately. Where aggradation and deposition dominate this can be achieved, but the visibility of the effects of degradation and erosion are dependent upon the timing of the end of the event being during the relatively short-lived degradational phase (see section 5.1B).

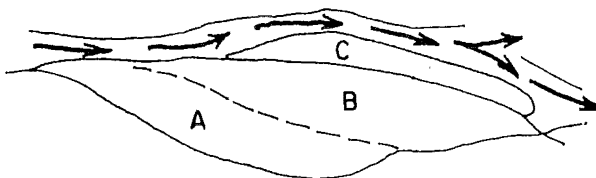
Post-degradational bar and channel behaviour is exemplified by developments after about 2650 minutes (Figure 5.5c and d). By 2685 minutes bank erosion at A (Figure 5.5b) and on the right bank side of the main channel between 7m and 8.5m, as well as longitudinal bar deposition downstream of 13m and general channel aggradation, had led to a substantial fall in bedload transport rates throughout the reach. As the thalweg developed a meandering form, previous complex bars were subject to either localised (e.g. surface 13 in Figure 5.5b) or complete (surface 14) erosion. Meandering was associated with point bar development (surfaces 15 and 16, Figure 5.5c). Both consisted of finer material that was transported in shallow over-bar flows (surface 15 had a surface d_{50} of 0.36mm compared with 0.78mm and 1.06mm for two samples from the



Bank attached bar remnant remained after erosion by main channel migrating toward its right bank



A unit bar, B, was deposited as the channel narrowed and migrated toward its left bank



Point bar C was added to surface B as the channel developed a bend in this area. The elevation of C was below A and B, which were at the same height.

Figure 5.7 Schematic diagram to show the evolution of bar complex (7) and (8) on Figure 5.5a.

adjacent main channel). Surface 15 took the form of a unit bar which was subject to later erosional modification. As the channel migrated further toward the right bank side an additional unit bar was accreted onto this (surface 19 on Figure 5.5d). This was noticeably lower than surface 18 which became emergent at about 2800 minutes as the main channel degraded. Surface 16 (Figure 5.5c) had a similar history to surface 15 except that it had some flow cutting across its surface and was less homogeneous in terms of sediment size. It too had an additional point bar joined to it (surface 17) but this was due to a reduction in flow in the main channel as avulsion occurred into channel A (Figure 5.5c).

Further development of the complex bar (surfaces 16 and 17; Figure 5.5c) involved their dissection and re-shaping by erosion (surfaces 20 and 21; Figure 5.5d) as well as some changes to their grain size composition. The fine material of the former point bar surfaces was replaced by coarser sediment as shallow bedload transporting flows developed across their surfaces. Again the composite nature of these depositional surfaces is well illustrated. Surface 20 contains elements of surface 13 (Figure 5.5b) which have survived since prior to the degradational phase, as well as two phases of point bar accretion and their subsequent modification by sheets of overriding coarser material. The plan shape of the surface was due to erosional modification. Viewed in isolation this could be classified as a longitudinal unit bar, but in reality has a very complex history and is better regarded as a detached medial bar. Surface 21 has a similar history to 20, but has additionally been accreted to by a lateral bar comprised mainly of finer material, surface 22 (Figure 5.5d).

The ratios of complex bar forms to unit bars by area are shown on Figure 5.5. The minimum value of this ratio occurred early in the aggradational phase as a consequence of deposition of unit bars. With erosional and depositional modifications of the types described above, this ratio increased as aggradation proceeded. Its peak (at 55.5 : 1; Figure 5.5b) was during the degradational phase as deposition ceased. The ratio fell as soon as degradation began to slow, the first indication of which was often when longitudinal medial bars were deposited in the main channel.

B. Summary. The discussions of sub-sections 5.2.1 and 5.2.2 have shown that channel morphology can be related to its sediment storage role at a particular time i.e. whether it is aggrading or degrading. During aggradation bars have a sediment storage function and are regularly modified as channels change course. During degradation the main channel(s) occupy a relatively small proportion of the bed and many bars have no contact with the flow. The role of those that do is primarily as hydraulic resistance elements (Church and Jones, 1982). Sediment throughput is considerable and high sediment transport rates through a reach do not necessarily imply large volumes of sediment removal therefrom. One of the consequences of the rapidity of channel change during aggradational phases is that bar complexes have involved histories and are of variable textural maturity. Some may attain the degree of particle size sorting suggested by Bluck (1982) but many more are affected by bedload transporting flows for insufficient time for this

to develop fully. In terms of a classification of bar types, Church and Jones' (1982- see also discussion therein by P.E. Ashmore) differentiation between attached and detached complex bars appears useful. Bar complex development often involves a range of unit bar types which could be individually classified into point bars, medial bars and the like. Their distinguishing feature appears to be their location relative to pre-existent bars and channels. For this purpose the simple attached-detached classification is valuable. It is unusual for unit bars to be deposited as detached forms except towards the end of degradational phases when major channels widen and often deposit longitudinal medial bars in much the way described by Leopold and Wolman (1957). The ways in which these morphological variations can be used to identify bed waves are discussed in the following section.

5.2.3 A model of endogenous bed waves derived from the sand tray results

The at-a-section conclusions of Table 4.4 can be combined with the results of this Chapter into a model of bed wave behaviour in a short reach through time. This is presented figuratively in Figure 5.8. The model makes the initial assumption that bed waves are defined in terms of aggradation-degradation cycles (Table 4.4; Smith and Southard, 1982). In line with the observations in section 5.1B regarding the short time period occupied by the degradational phase relative to that of aggradation, the former is shown as occupying 30 % of the total time. This fraction varied between runs. At this point it is worth re-stating one of the conclusions of sub-section 4.2.1 that relative changes in sediment storage, bed elevation and bed relief are more straightforward to explain than absolute values. Hence only relative quantities are suggested in the model.

In essence the model of Figure 5.8 is a period of aggradation and a more rapid degradational phase, which is mirrored by the variation in the bed relief index. Note though that this index has been found to be very sensitive to local conditions and so would be expected to contain a lot of 'noise' and not to change so smoothly as Figure 5.8 implies. Volumes of sediment stored in the semi-active and inactive reservoirs also follow the patterns suggested in Table 4.4, but attain their extreme values after the onset of degradation more rapidly than do mean bed elevation or bed relief. This is due to rapid lowering of water level during degradation leading to re-allocation of material from the semi-active reservoir to the inactive one. Changes in sediment storage due to dynamic transfers are considerably smaller than those due to static transfers. Sediment storage in the active reservoir exhibits fluctuations of lesser magnitude than do the less active reservoir volumes (Figures 5.1,5.2), and peaks at about the same time as the volume in the semi-active reservoir. Variation through time in this volume is more irregular due to its dependence upon the total width of the channels at a section as well as their elevations, so that it is related to both mean bed elevation and the number of channel segments. This last mentioned index shows a general pattern of variation similar to that in mean bed elevation although exhibiting a more rapid response to the onset of degradation. Its variation is stepped on account of it being sensitive to channels

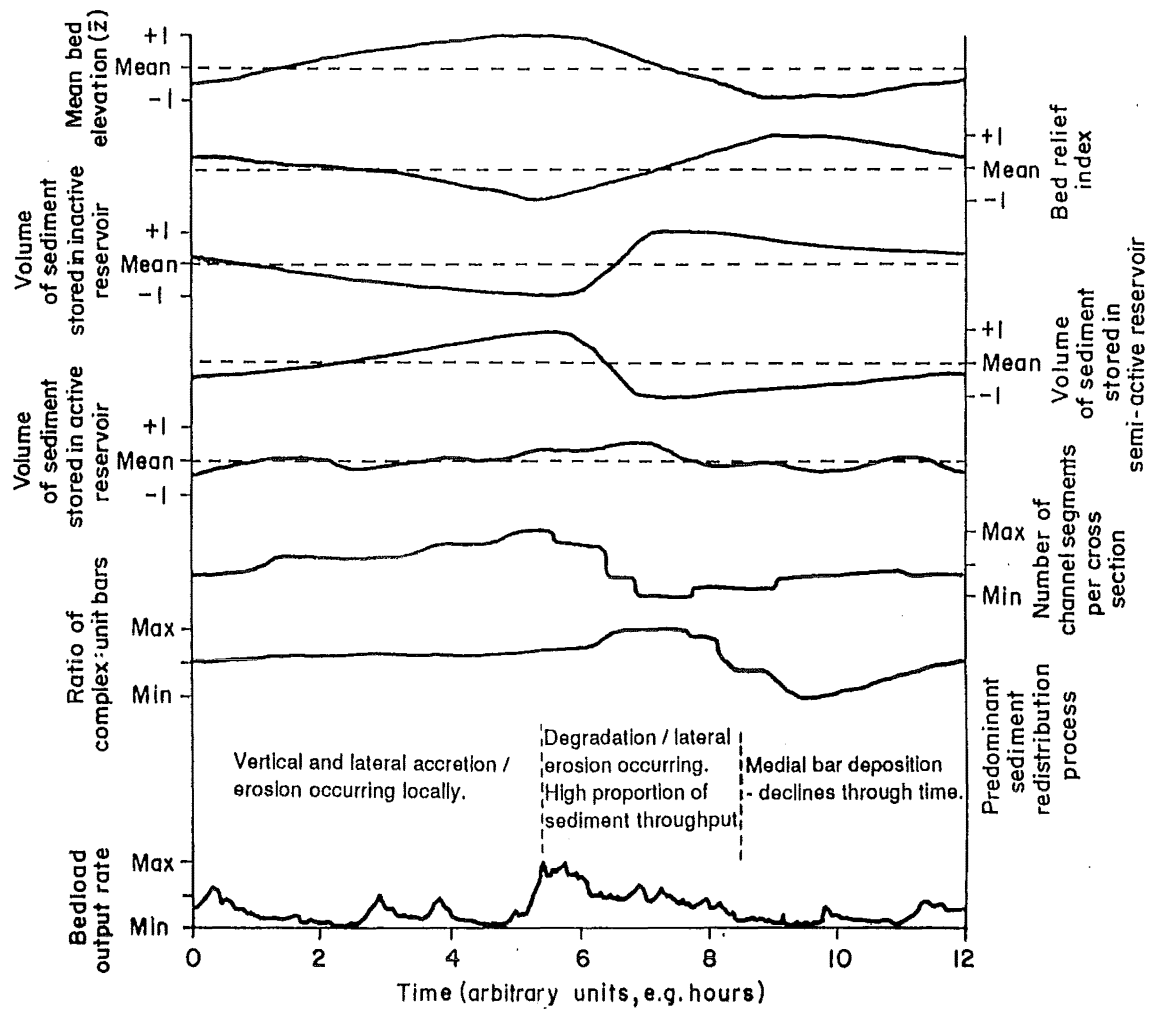


Figure 5.8 Idealised development of a bed wave through time in a short reach as manifested in Indices of cross-sectional and planform geometry, predominant morphological features, and sediment transport rate. All variables are plotted as dimensionless ratios. Note that the scales for the three sediment storage reservoirs are identical i.e. the magnitude of changes in the active reservoir is less than those in the other two.

being blocked or newly occupied, both of which tend to be sudden processes.

The next two elements on Figure 5.8 are of a different form from the readily quantifiable morphological indices described thus far. The ratio of complex bars : unit bars increases during the aggradational phase as described in sub-section 5.2.2. At the onset of degradation this ratio increases suddenly as channels are abandoned and channel deposits immediately start to function as resistance element bars. Once the rate of degradation begins to wane the first stage of deposition often takes the form of unit bars of longitudinal and point types. Thus the proportion of unit bars rises rapidly during the first part of the aggradational phase but soon starts to decline as these forms coalesce and are affected by channel migration and avulsion. The dominant processes of sediment redistribution vary through this cycle, although the planform type would tend to be regarded as constant throughout, whether braided or wandering. This is consistent with the suggestion of Brierley (1989) that as depositional processes are not planform dependent, fluvial facies models should not be expected to apply at the scale of channel planform. The passage of bed waves through a reach is one reason for this non-dependence of process upon planform type.

The final component of the model is an indication of the likely bedload transport rate from the reach during the bed wave cycle. Variations at a variety of timescales smaller than that of aggradation-degradation cycles were observed throughout this longer cycle.

This somewhat simplified model is applicable to a single reach through time. In practice, data are rarely available at a timescale sufficiently small to enable resolution of all components of such a cycle. Given that relative and not absolute trends are indicated by the model it would be difficult to locate such temporally coarse data within the model framework. In many cases the available data are spatial and involve repeated downstream measurement of the relevant variables. Application of the model of Figure 5.8 to this situation requires that location can be substituted for time on the abscissa of Figure 5.8. The data presented in Figures 5.1 and 5.2 suggest that this may be true within certain limitations. Similar patterns are visible over space and through time, but the distinctiveness of temporal patterns is much greater than that of their spatial analogues. This reflects the importance of at-a-section evolution and the historical development of bars and channels at individual locations. The significance of this effect in the sand tray, where initial conditions were identical at all cross-sections, suggests that the identification of spatial patterns in prototype rivers could be extremely problematical. However, the limited length of the reach in the sand tray may have obscured some patterns.

In the (unlikely) case of a pure location-for-time substitution being valid, the abscissa of Figure 5.8 could be changed to distance downstream. The laboratory data (Figures 5.1, 5.2) suggested that about 30-40% of total reach length is affected by degradational processes at any one time. The patterns of cross-sectional morphology, sediment storage and depositional processes are

likely to be subject to a greater degree of variability than in the temporal case. This may be removed by calculating the data as ratios relative to the long-term mean value for a particular section. Only bedload transport rate would be expected to vary considerably from the model of Figure 5.8 being subject to a lesser degree of spatial variability than temporal.

The model as outlined here is applicable to endogenous bed waves in the laboratory situation. Discussion of its likely strengths and weaknesses will be left until after its performance has been evaluated with respect to exogenous waves in both the laboratory and field.

5.3 An exogenous bed wave in the sand tray

At the end of Run 3 the sediment input rate at the head of the sand tray was varied. This is designated Run 3a. The scale of the pulse was chosen by identifying a cycle of accelerated and reduced sediment output relative to the mean value from Run 1. This period in Run 1 was from 2490 to 2895 minutes inclusive, and was input to Run 3 starting at 2940 minutes. Runs 1 and 3 were demonstrated in sub-section 3.1.5 to have certain different characteristics. Thus, the pulse was effectively of type A sediment (material supplied from outside the river system). This is shown in Figure 5.9 along with sediment output from the sand tray and the net storage change in the entire tray during this period. After completion of the cycle of input variation the constant input rate of 2.5 g s^{-1} was resumed. Figure 5.9 shows no apparent response to the pulsed input in terms of bedload output by the end of the run at 3600 minutes, and that except for a short period during which the sediment input rate was below 2 g s^{-1} aggradation continued as it had for most of Run 3 (Figure 3.11). The increase in total sinuosity to a value of about 2 is indicative of the channel multiplication which usually accompanied aggradation.

Figure 5.9 gives an idea of the aggradational response of the whole sand tray to the pulsed input. The spatial patterns in this aggradation are illustrated by Figure 5.10 which shows conditions prior to the pulse input (at 2890 minutes) and at three times afterwards (see Appendix 7 for details). The mean bed elevation indicates rapid aggradation upstream of 6m in the 200 minutes following the start of the introduction of the pulse, which continued although at a reduced rate when the input rate fell below 2.5 g s^{-1} and when a constant rate was resumed. Between 3130 and 3370 minutes, the aggradational zone moved between 1m and 2m downstream. In the lower half of the sand tray, both aggradation and degradation occurred in different places at different times reflecting ongoing sediment redistribution processes. The slowing of aggradation and then degradation (3370-3610 minutes) which affected this reach could have been a response to accelerated aggradation further upstream. The aggradation could have reduced sediment input to the next reach downstream (i.e. 8-13m) and caused the changes observed in this reach. Where aggradation was most pronounced, upstream of 7m, the bed relief index showed both increases and falls at different times (Figure 5.10b). The BRI was generally reduced between 2890 and 3610 minutes in the aggrading reach. As has previously been noted the BRI is very

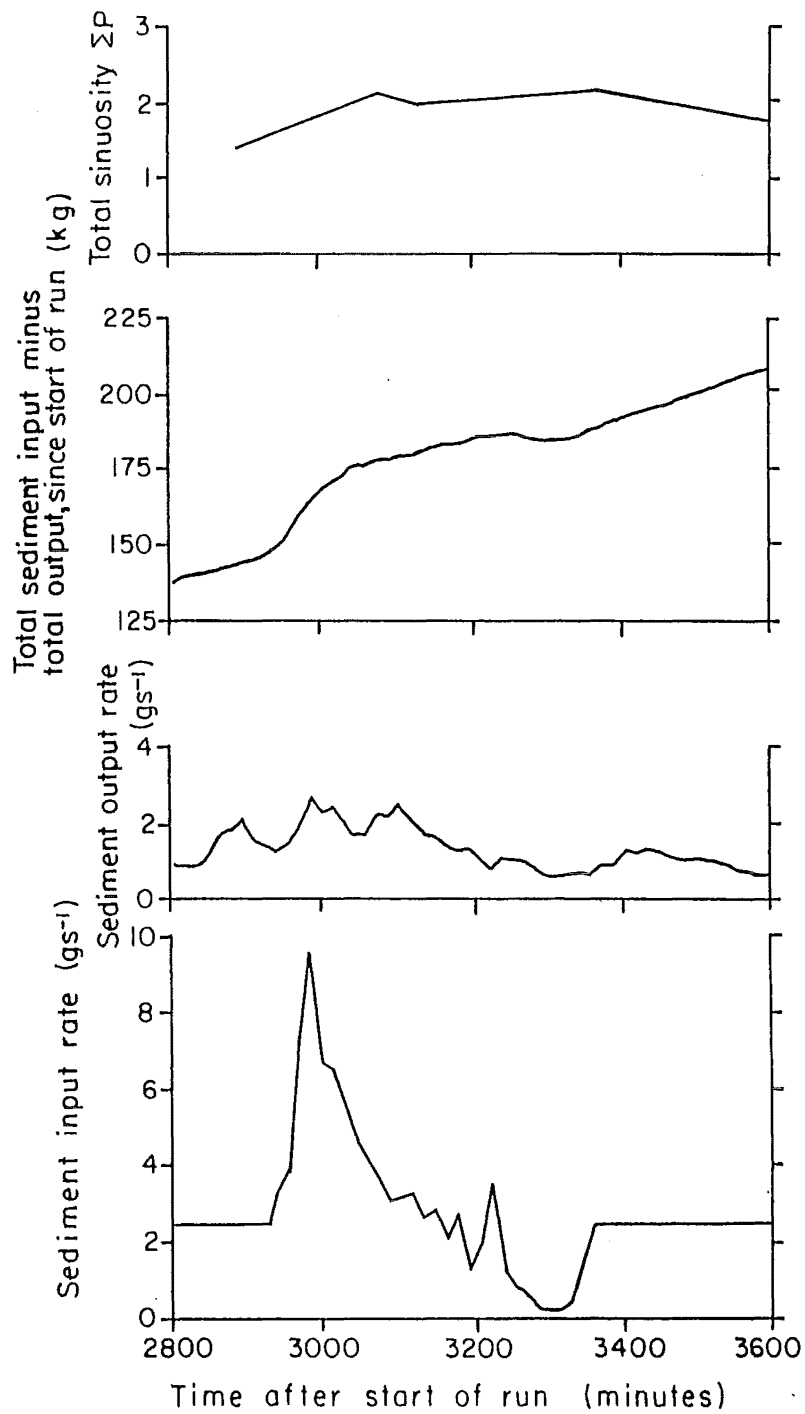


Figure 5.9 Form of the bedload pulse input to Run 3a, and stream response. Input and output rates are in $g\ s^{-1}$ of dry sediment.

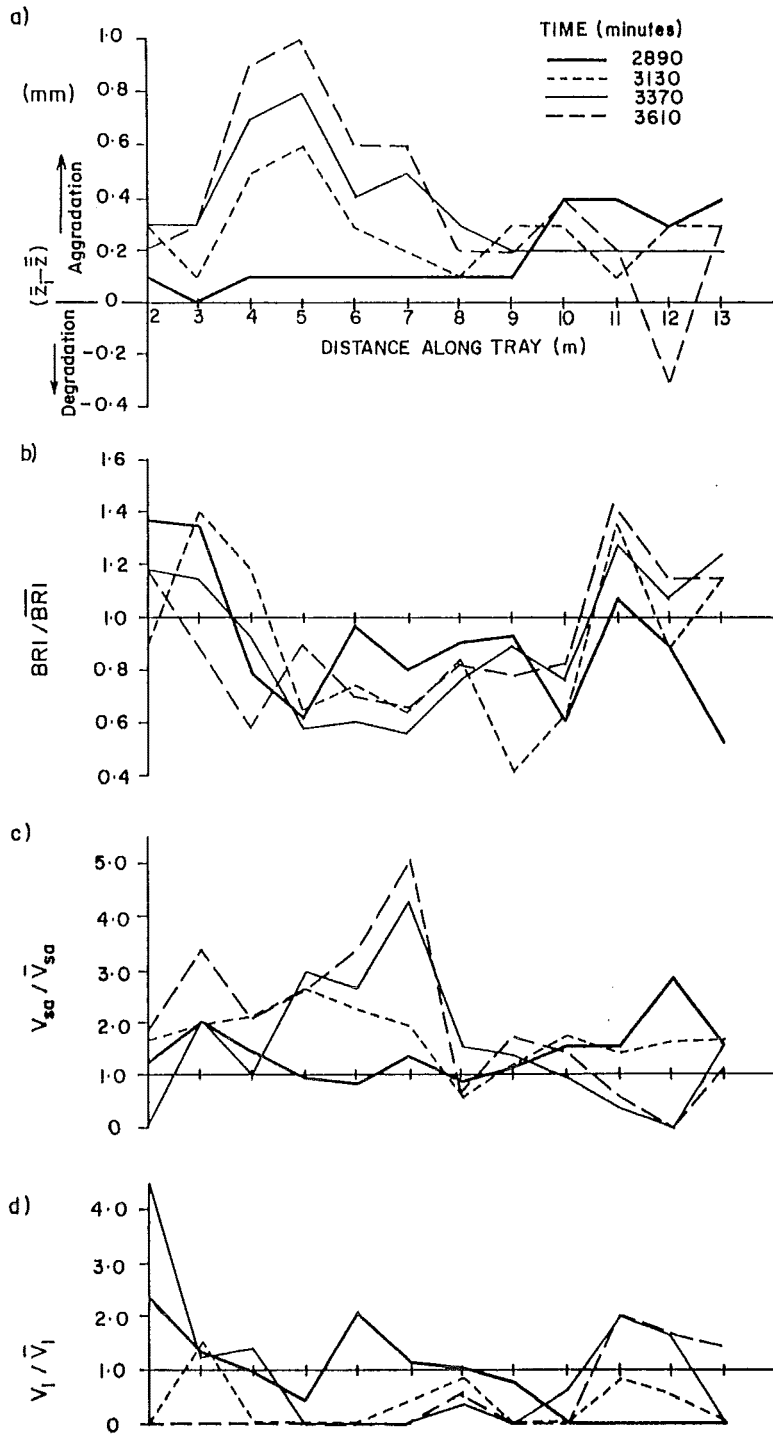


Figure 5.10 Cross-sectional morphology and sediment storage data for Run 3a. Mean bed elevation (\bar{z}) is shown as differences from the mean values for Run 3 ($\bar{\bar{z}}$). Other data are in the form of a ratio of instantaneous values divided by the mean values. Mean values are indicated by bars. This latter method for transforming the data is inappropriate to the mean bed elevation, values of which decrease systematically downstream.

- a) mean bed elevation (mm)
- b) bed relief index
- c) volume of sediment stored in the semi-active reservoir
- d) volume of sediment stored in the inactive reservoir

sensitive to small scale, short lived processes and to the past development of particular cross-sections. The patterns that it exhibited here are not so well defined as in the case of endogenous bed waves which led to the model of Figure 5.8. This index appears less sensitive than the mean bed elevation or sediment storage patterns to changes in the rate of aggradation or degradation.

Changes in the distribution of sediment between storage reservoirs are also indicative of the pattern of aggradation (Figure 5.10c and d). As would be expected from the earlier model, the semi-active reservoir contained much of the material during the aggradational phase with the inactive losing sediment as aggradation proceeded. Where degradation occurred, as at 11-13m, the reverse patterns predominated. Note from Figure 5.10d that at 3370 minutes the reach 2-4m had an increase in material in the inactive reservoir at the expense of the semi-active. This presumably reflected local degradation, which is confirmed by visual observations of channel changes at this time that showed degradation occurring in the main channel upstream of about 4.5m, possibly as a response to the low sediment input from 3240 minutes. Aggradation had resumed in this reach by 3165 minutes.

It would have been instructive to continue Run 3a in order to see if the aggradational wave was transferred downstream, and whether it ultimately produced a pulse in the sediment output rate of similar form to the input pulse. From the limited available evidence there do not seem to be any major differences between the behaviour of this wave and that suggested by the model of sub-section 5.2.3 (Figure 5.8). Only the patterns in the BRI data differ markedly from the model predictions, and there are reasons why this could have been anticipated.

5.4 Exogenous bed waves in the Kowai River

Figure 3.14 showed the locations of two reaches of the Kowai River. This discussion is concerned primarily with Porters Reach between cross-sections 131 and 139 (XS131-XS139). Prior to analysis of the present morphology of these reaches an overview of their historical development is presented.

5.4.1 Development of Porters and Bridge Reaches prior to 1987

Blakely *et al.* (1981) have suggested that the Kowai River changed from meandering to braided form in response to sediment influxes and an altered hydrologic regime following widespread forest destruction between 500 B.P. and 1000 B.P. Further forest removal in the mid-19th Century caused a resumption of this process. Stabilisation of the river bed was due to tussock grasses and matagouri until about 1930, since when broom, blackberry and gorse have been influential. These last mentioned species have had an especially notable influence during the past 30 years.

The history of Porters and Bridge Reaches can be evaluated from aerial photographs dating from 1943, 1960, 1966, 1975 and 1987. Channel width data from these times are presented in Figures 5.11 and 5.12. Figure 5.13 shows the channel morphology in 1943, 1966, 1975 and 1987. The active channel widths (ACW's) shown in Figures 5.11 and 5.12 were defined following Beschta (1983b) as the total width of channels and exposed bed material at a cross-section. This excludes vegetated island and berm areas. Absolute channel widths are strongly influenced by valley shape in these reaches, particularly the bedrock gorge at 2.3-2.5 km., and the narrow section where the road bridge is located at 3.7km (Figure 5.11). Changes in channel width, such as the general narrowing of Porters Reach between 1965 and 1975, can be identified from these data. The statistical significance of changes in the mean widths of the reaches was assessed using a paired t-test (Beschta, 1983b). These results (Table 5.3) suggest a significant increase in width in both reaches over the period 1943-1960, and a significant decrease in Porters Reach between 1965 and 1975.

Table 5.3 Mean width changes in Porters and Bridge Reaches, 1943-87. Δb = change in mean width during the time interval indicated (m). >0 indicates widening, < 0 narrowing; s.l. = statistical significance level; N.S. = not statistically significant at the $\alpha = 0.05$ level.

Reach	1943-1960		1960-1965		1965-1975		1975-1987	
	Δb	s.l.	Δb	s.l.	Δb	s.l.	Δb	s.l.
Porters	+ 34	0.01	+ 7	N.S.	- 42	0.05	+20	N.S.
Bridge	+ 32	0.05	- 2	N.S.	- 6	N.S.	+ 7	N.S.

The widening between 1943 and 1960 was interpreted by Beschta (1983b), on the basis of a similar data set, to be the consequence of a large volume of sediment input to these reaches during a flood event in 1951. Widening and sediment accumulation are most evident in the upper part of Porters Reach where low vegetated berms were eroded and / or buried by sediment during the event, and in Bridge Reach where similar berm erosion occurred (Figure 5.13a and b). By reconstructing the 1951 depositional surface, Beschta (1983a) concluded that the material accumulated further up the Kowai catchment in 1951 is being eroded, as is the material that was deposited in Bridge Reach, but that Porters Reach is undergoing aggradation (Figure 5.14). From Beschta's data it can be suggested that Porters and Bridge Reaches both act periodically as sedimentation zones (Church and Jones, 1982). An interpretation of the aggradation in Porters Reach is that it had a greater volume of sediment temporarily stored within it during the event than at the end of it. This accumulation may have induced the exceedence of a threshold condition which initiated evacuation of sediment from the reach. Porters Reach may thus have functioned as a transfer channel (Church and Jones, 1982) for the latter part of the 1951 event. It can be

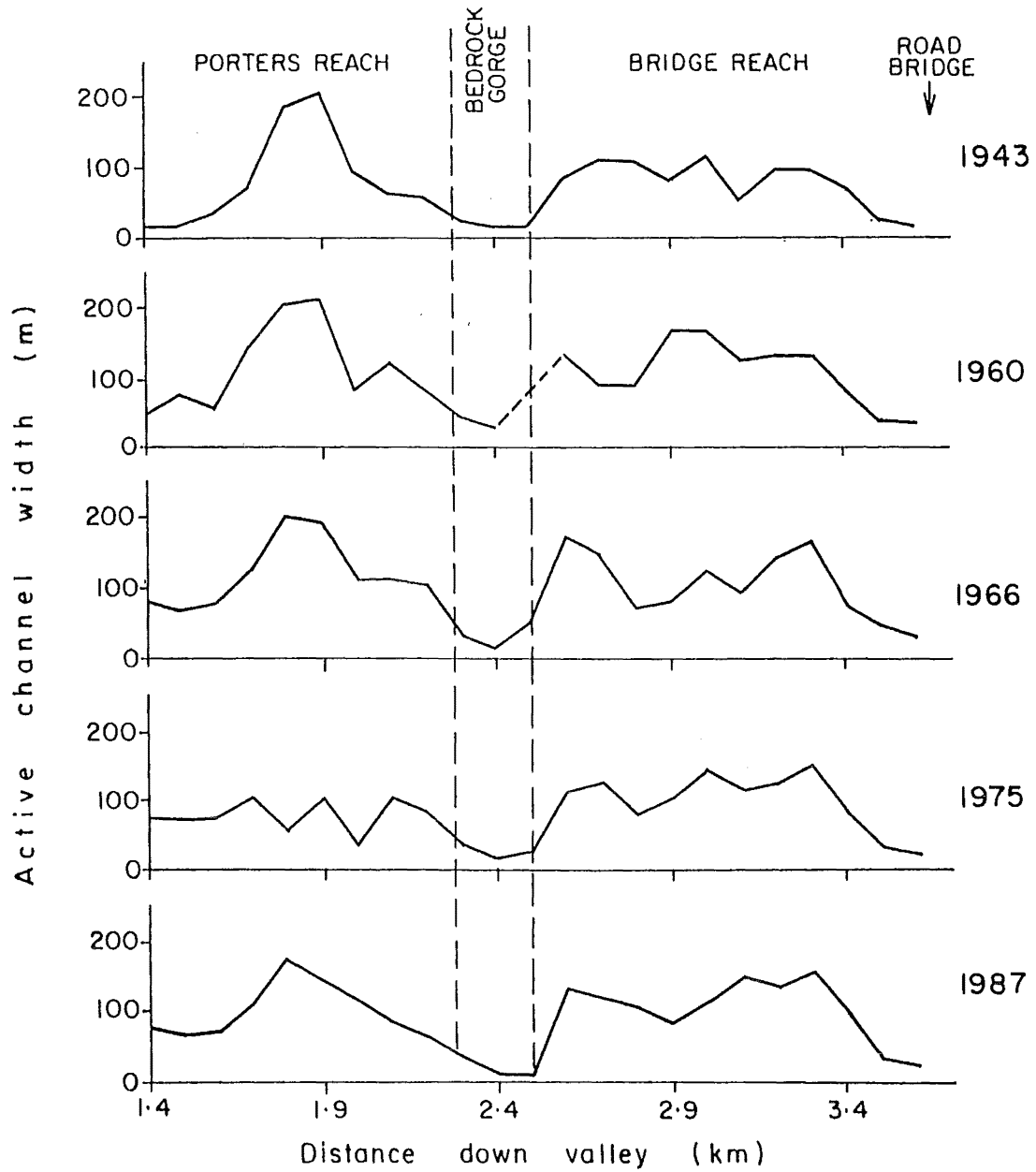


Figure 5.11 Active channel widths of Porters and Bridge Reaches, Kowal River. Data taken from aerial photographs and Beschta (1983b; personal communication, 1988).

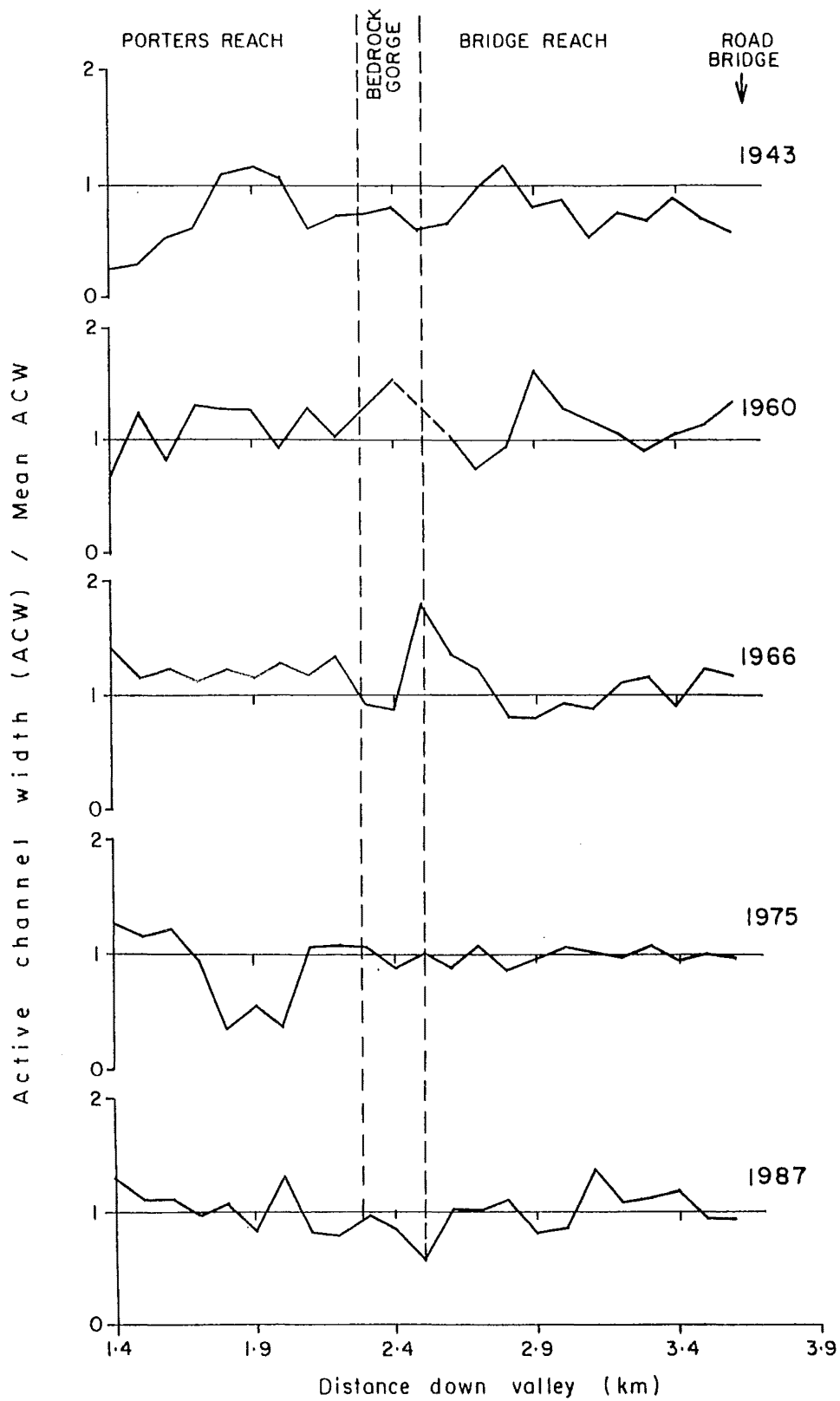


Figure 5.12 Active channel width (ACW) data from Figure 5.11 modified by dividing the ACW by the mean of all 5 ACW values for each section. Data sources as for Figure 5.11.

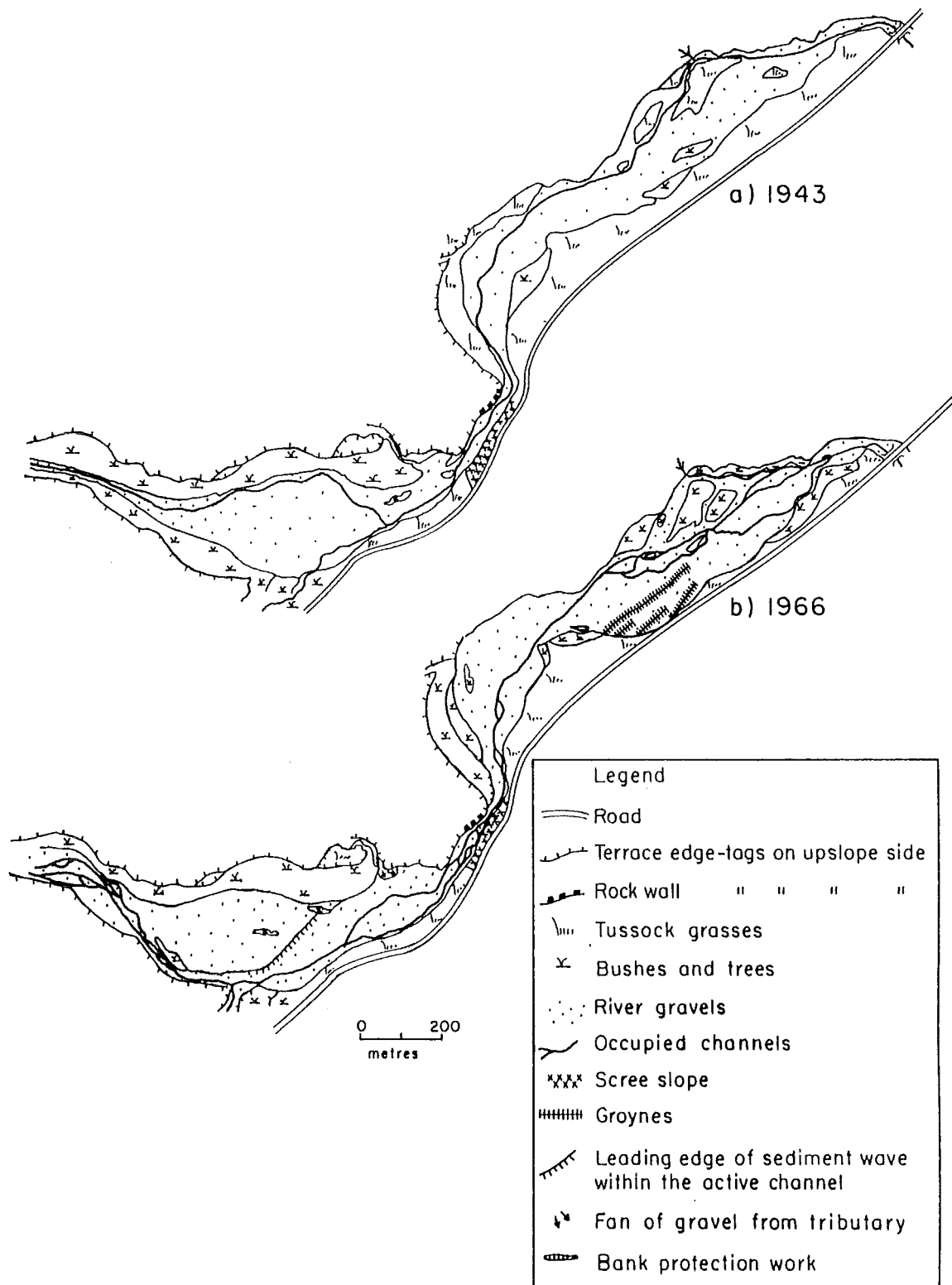


Figure 5.13 Morphology of the active channels in Porters and Bridge Reaches based on aerial photographs.

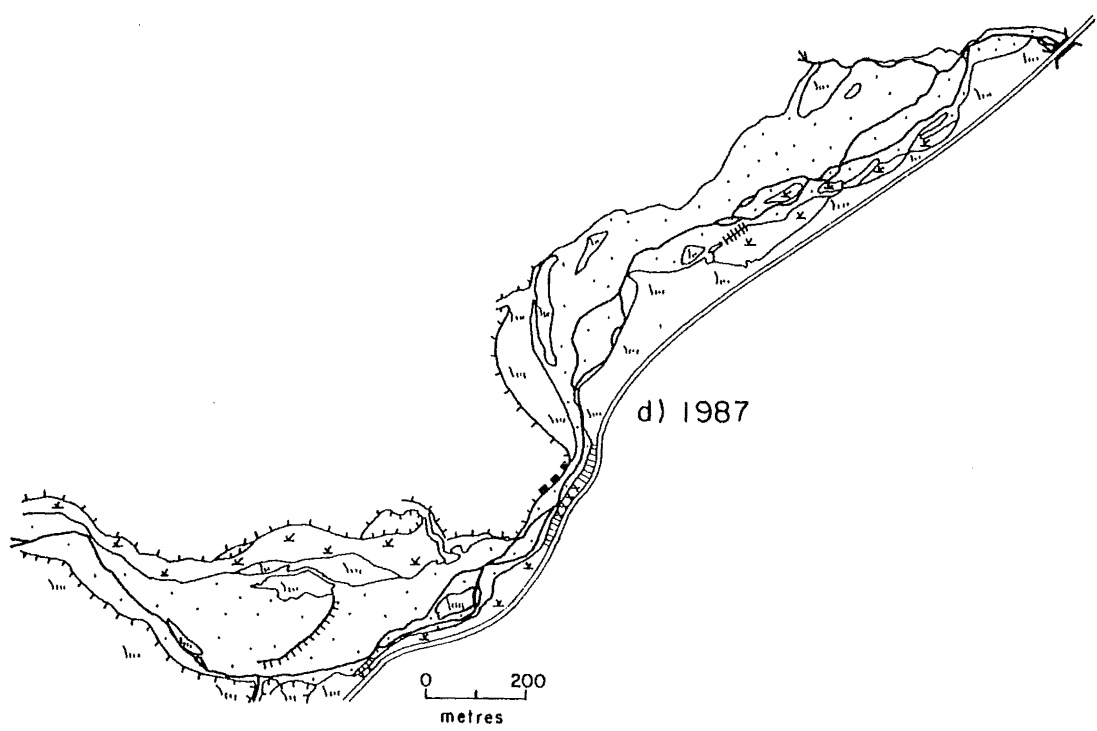
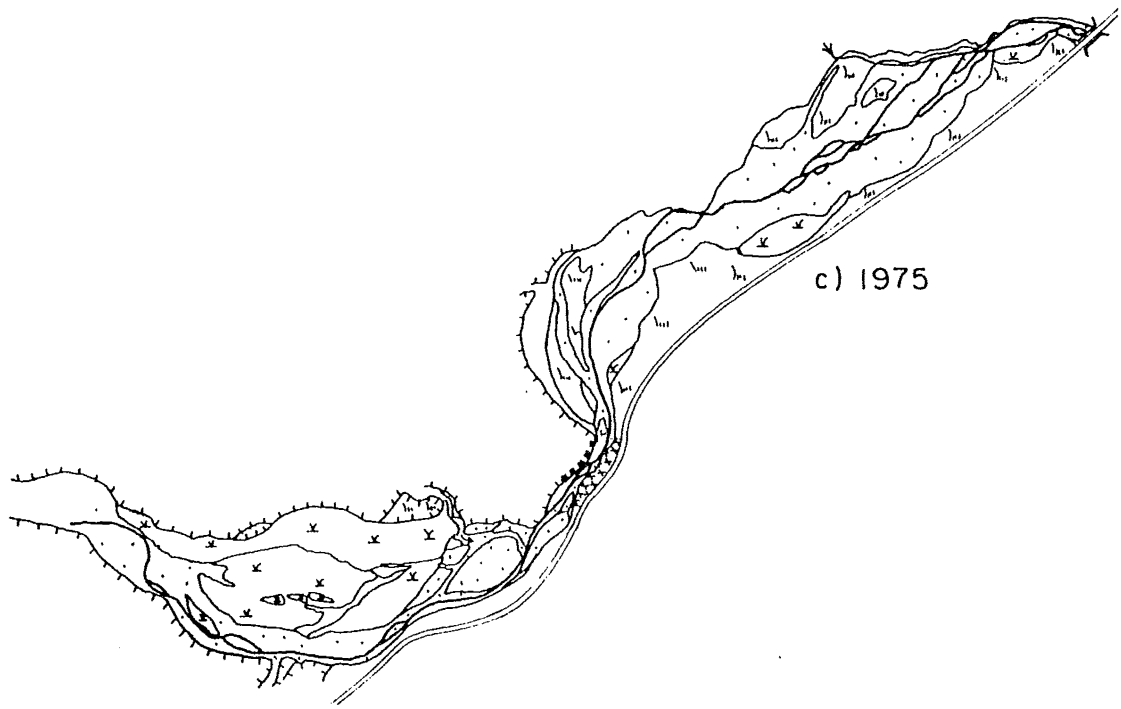


Figure 5.13 (Continued)

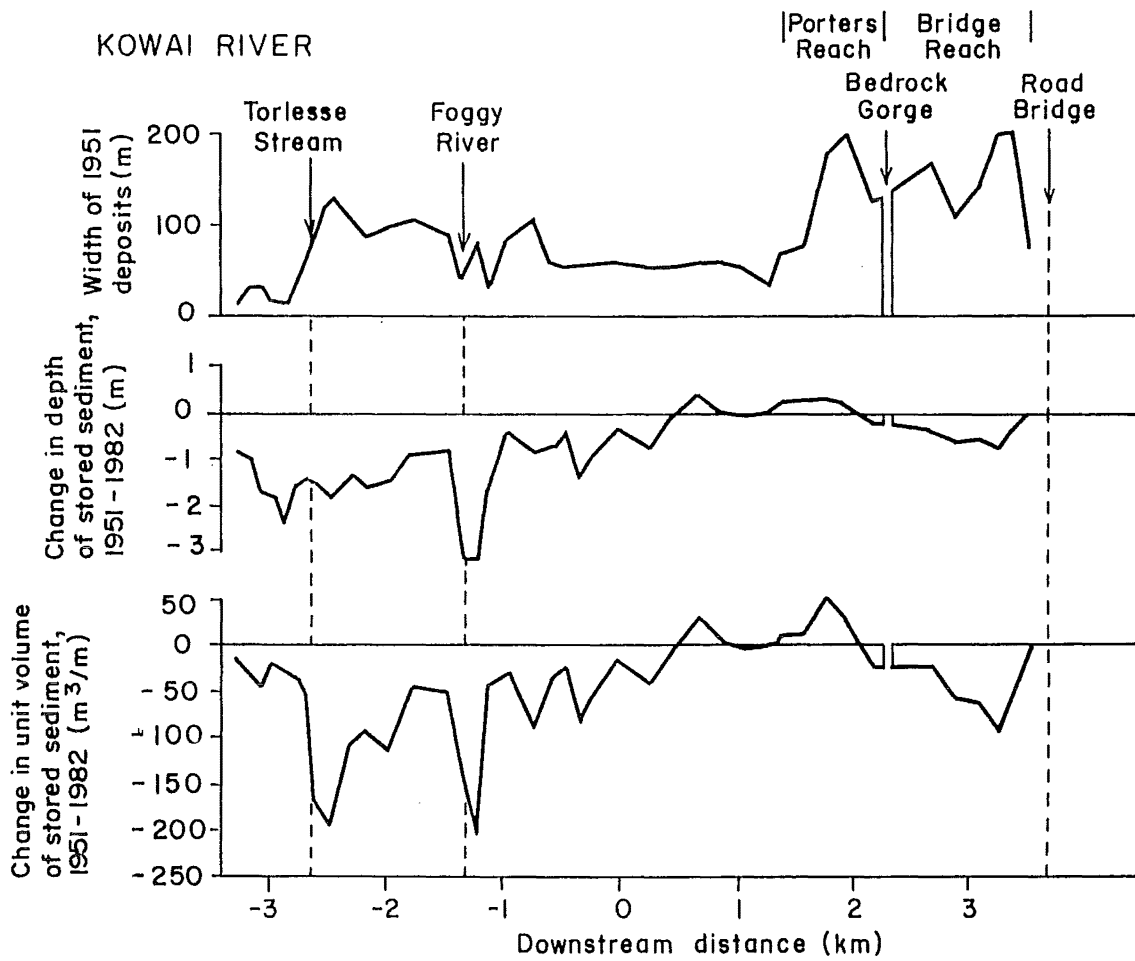


Figure 5.14 Width of the 1951 depositional surface and changes in the depth and volume of accumulated sediment, 1951-82 (after Beschta, 1983a).

considered that the 1951 disturbance to this part of the Kowai River system has subsequently been followed by relaxation towards an equilibrium state (Brunsden and Thornes, 1979). Beschta (1983b) illustrated how dispersion of sediment stored in Porters and Bridge Reaches as well as further upstream led to widening of the active channel further downstream after 1972.

Within the constraints imposed by the effects of this one major event, other smaller scale processes have been operational. Although not clearly visible in the width data of Figure 5.11, they show up when channel widths are divided by the long-term mean values at a given section (Figure 5.12). Widening in Bridge Reach between 1943 and 1960 shows clearly on Figure 5.13 (a and b). By 1966 (Figure 5.13b) groynes had been constructed to protect the road and may have prevented further widening in this area. Figure 5.12 also documents the narrowing in Porters Reach between 1.7km and 2.1km over the period 1966-1975, with widening re-occurring by 1987. The narrowing was due to vegetative stabilisation of berm areas on the inside of the bend which forms Porters Reach (Figure 5.13c). By 1986 this area had been eroded and the main low flow channel was located towards the left side of the active channel, in much the same position as in 1943 (Figure 5.13a). Further erosion occurred between January and April 1987 when the low flow channel again switched toward the right bank (Figure 5.13d).

Between 1975 and 1987 total sediment storage in this reach was little altered, but material had been redistributed between the semi-active and inactive storage reservoirs (see Appendix 8 for data). The net changes in Porters and Bridge Reaches are small compared to the magnitudes of exchanges to and from the inactive and active plus semi-active reservoirs (Figure 5.15). These reflect the changes in the active channel width referred to in the preceding paragraph and illustrate how significant changes in the distribution of sediment between reservoirs, and hence in availability for transport, can be of greater importance than the total volumes stored in particular reaches. Blakely *et al.* (1981) surveyed the net changes in mean bed level between 1975 and 1979 for a longer reach and inferred a damped periodic downstream oscillation in mean bed level changes, which they interpreted as representing attenuation of sediment pulses introduced in the stream headwaters. The 1975-79 patterns in net storage reflect a continuation of those identified by Beschta (1983a; Figure 5.14). Changes post-1979 appear to have reversed this trend with little net change through most of Porters Reach and aggradation in the lower part of this and in Bridge Reach.

The post-1943 development of these reaches has been strongly influenced by a single flood event in 1951, responses to which are ongoing. Smaller scale processes have also operated and have been responsible for the bidirectional changes in channel width that have occurred since 1951. The remainder of this discussion focusses on this smaller scale.

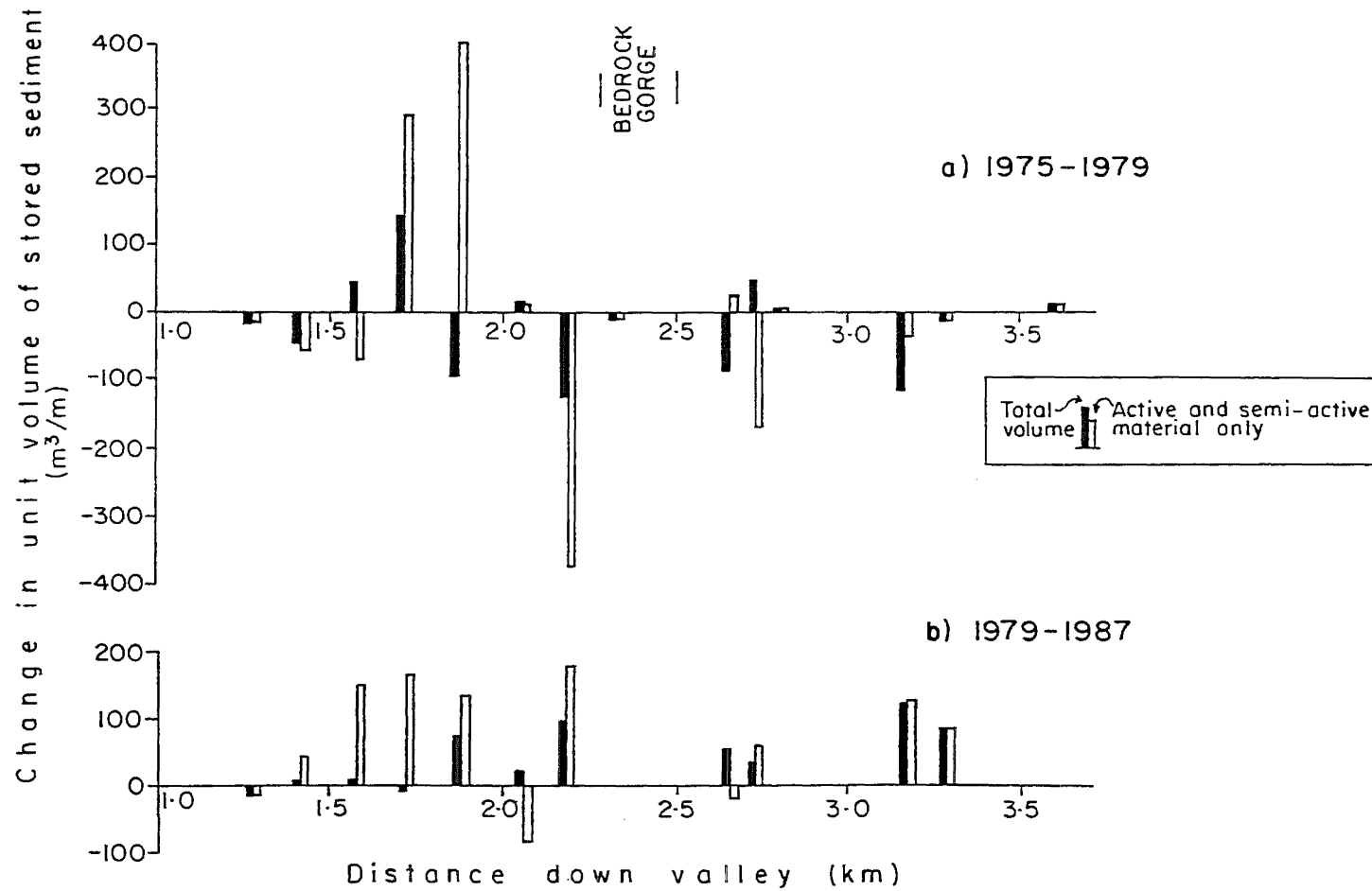


Figure 5.15 Changes in unit volumes of stored sediment in Porters and Bridge Reaches, 1975-1987. The differentiation of material into active / semi-active and inactive reservoirs is explained in sub-section 3.2.2. The total volume is the sum for all three of these reservoirs.

5.4.2 Morphology of a bed wave in Porters Reach

The model of channel morphology and sediment storage patterns associated with a bed wave developed from the sand tray data (Figure 5.8), can be compared with data from the Kowai. The following discussion describes the data required for this. Sediment storage patterns and the nature of bar complexes in Porters Reach are described. The depositional history of these deposits is then investigated using palaeoflow reconstruction.

A. River bed geometry. A flood event that occurred early in 1987 when the main channel switched from near the left bank to close to the right bank of the active channel in Porters Reach, was associated with the accumulation of a distinctive wave of sediment within the reach. The leading front of this wave is especially discernible (Figures 5.16 and 5.17). The position of the leading edge is also indicated on Figure 5.18 which shows the locations of bars and formerly occupied channels within the active gravel bed. Downstream of where the confining fluvio-glacial terraces become further apart (between XS 132 and XS 133) surfaces G and M (Figure 5.18) are formed by a large complex bar which has undergone both dissection and lateral erosion. At high stage this would take the form of a transverse bar complex. Erosion of the downstream edge has been achieved by a channel between surfaces G and N (Figures 5.17, 5.18). It is not clear how much further surface G extended prior to this erosion. Lateral erosion (by channel I) produced the lower surface, H. Numerous small channels dissected the surface, some such as C and P being as large as the 1987 low flow channel. Channel C is approximately the course that was taken by the low flow channel prior to early 1987, and may have survived the phase of deposition without being completely in-filled.

The cross-sections located in Figure 5.18 were surveyed in 1987 (Figure 5.19). Upstream of where the active channel bed widens, a series of depositional units was cut into by the low flow channel and others of similar size (Figure 5.19; XS 131, XS 132). The cross-sections 133, P3, P4 and 135 include the deposits that are identifiable as a bed wave. The low flow channel at XS 133 is perched above parts of the active bed closer to the left bank (Figure 5.19). The existence of a perched channel creates the potential for avulsion, subject to further aggradation of the presently occupied channel or degradation of the inactive one during a flood event (Werritty and Ferguson, 1980). In this case channels Q and R (Figure 5.18) were blocked by accumulations of coarse material at their heads. This plugging mechanism as a cause of flow avulsion was also observed in the sand tray experiments described previously. Downstream of XS 133 the general cross-valley slope of the active channel changes direction toward the right bank (Figure 5.19). This reach can be regarded as an overwidened meander bend (Carson, 1986) at high stage, and as such a slope towards the outside of the bend (i.e. the right bank) would be expected. The counter slope at XS 133 implies either that the flow at the time of deposition was close to the left bank at XS 133 and the right bank at XS P3, or that the flow remained close to the right bank and was perched during the deposition of surface G at this location. Comparison with a survey of XS 133 in 1986 (Figure



Figure 5.16 View of the downstream edge of bed wave (6.4.1988) from the top of the terrace at the right bank end of cross-section 134. The channel flows through the bedrock gorge located at X. Note the low flow channel adjacent to the right bank.

SEE ERRATA



Figure 5.17 Bar face at the downstream edge of the bed wave (6.4.1988). In the foreground is a shallow abandoned channel assumed to have been responsible for eroding the leading edge of the wave. Pole is 1m long.

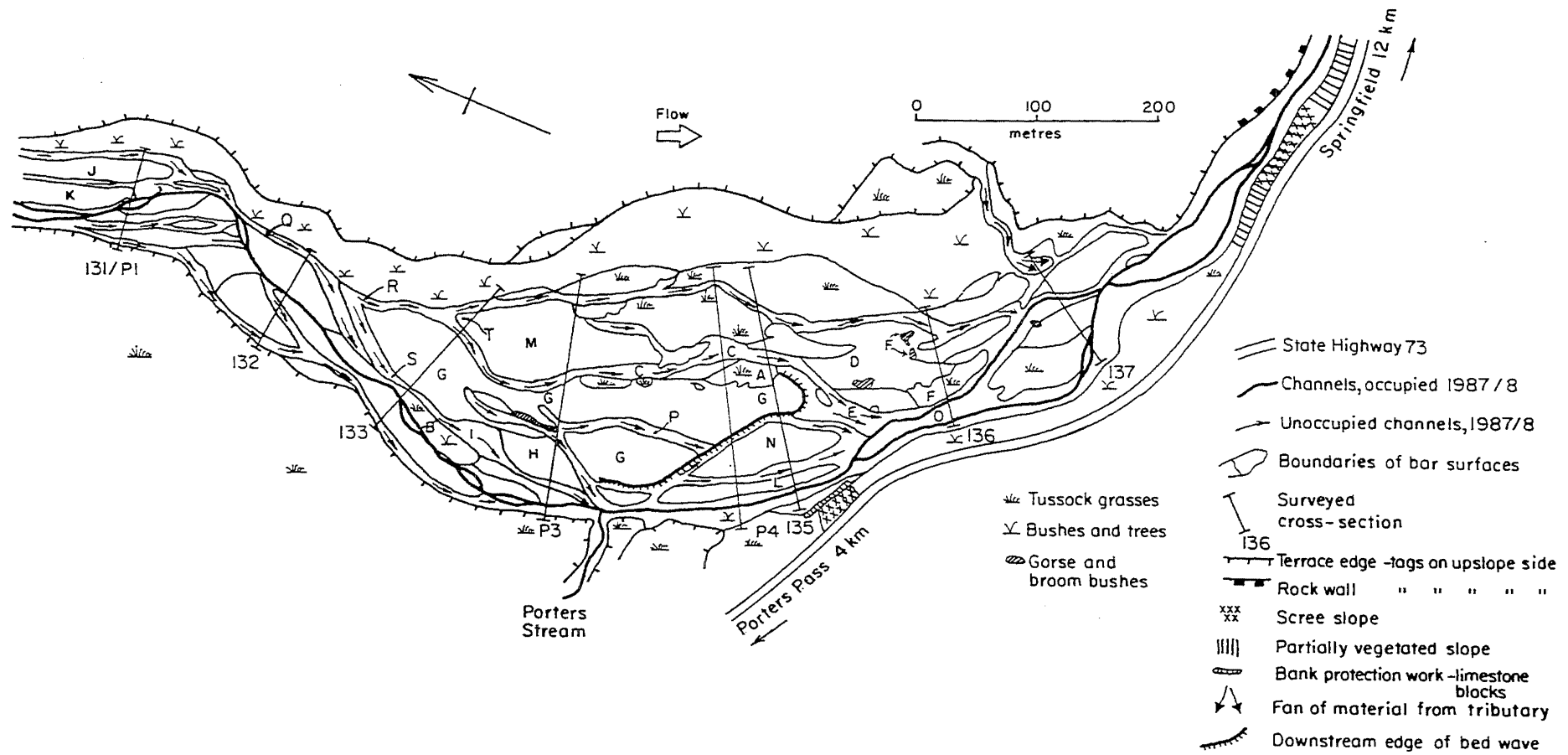


Figure 5.18 Morphology of Porters Reach in late 1987 showing the location of the downstream edge of the bed wave. Cross-sections referred to in the text are shown.

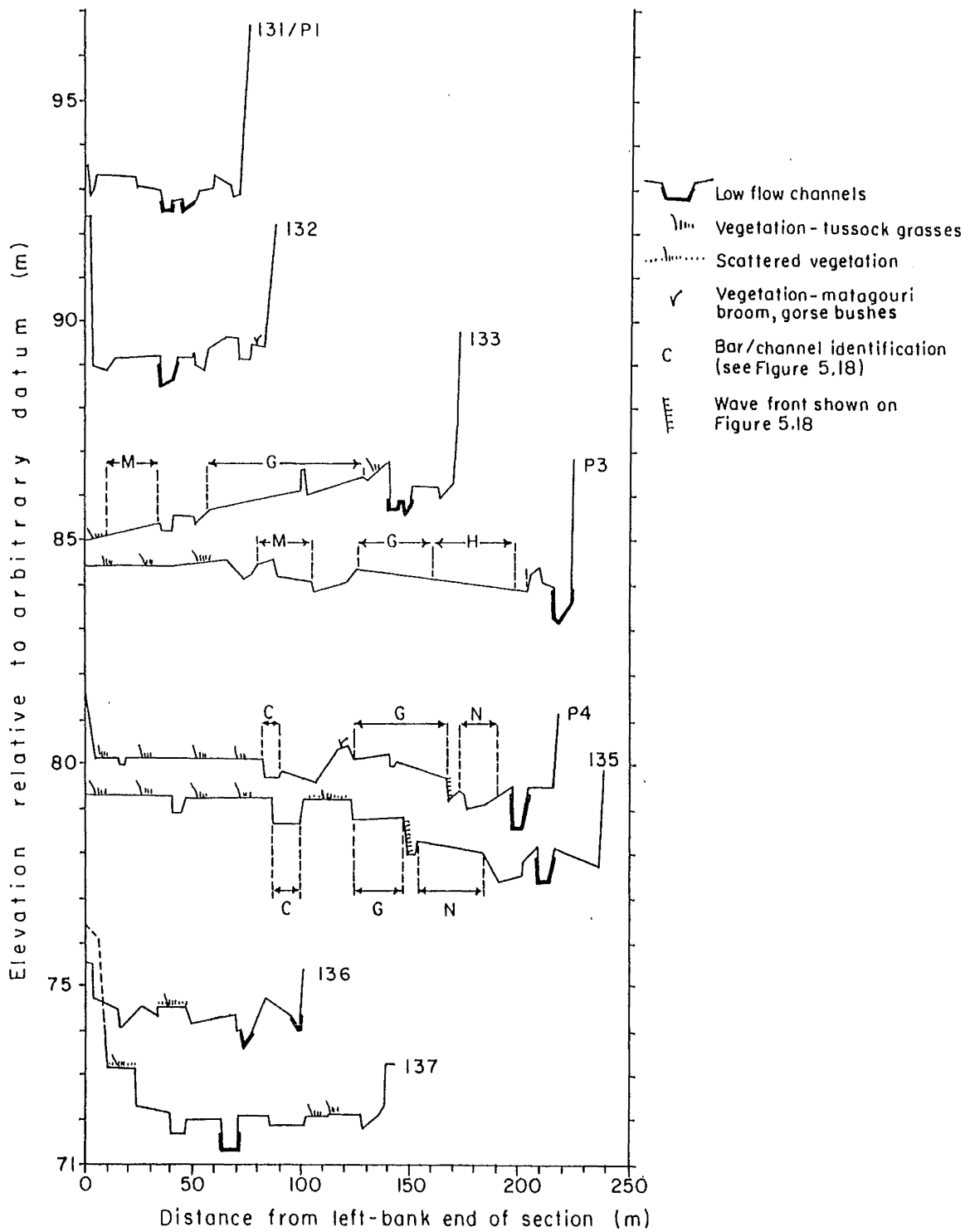


Figure 5.19 Cross-section surveys of Porters reach, 1987. See Figure 5.18 for the locations of the sections.

5.20) shows that although the overall bed level was little altered, the previous two main channels had been in-filled and the 1987 main channel was incised below the level of the 1986 deposits. The location of the channel at XS 133 is suggested to be a result of the channel location further upstream, coupled with the influence of the very stable vegetated island in this area, and the plugging of channel I at location S (Figure 5.18).

The wave front on XS P4 and XS 135 is not as distinctive as it appears in the field. Other features with comparable relief show up in the cross-sections although these are usually either channel banks or the edges of vegetated islands that exhibit longer term stability. Downstream of the wave front the active channel width decreases rapidly although it is not until near XS 137 that the fluvio-glacial terraces and bedrock force this reduction. XS 136 and XS 137 resemble XS 131 and XS 132 in that they are relatively narrow sections into which channels have incised. Whereas between XS 133 and XS 135 the completely vegetated islands and bar fragments stand at least 0.5m above the surrounding bar surfaces, this is not the case downstream of XS 135, and there are several islands of vegetation on the bars in this area. The most distinctive of these are indicated (F) on Figure 5.18. Persistence of these vegetated areas suggests that the gravel bed has not been generally active in the XS 136 / XS 137 area as recently as further upstream. Sediment transport through these sections was therefore largely confined to the present low flow channels during the event(s) which deposited the wave. Further, this implies greater channel stability than upstream. Towards the bedrock gorge this is unsurprising, but in the area between XS 135 and XS 137 there is no obvious reason for such stability. One possible explanation would be that the channels here had attained an equilibrium condition. There is no evidence for avulsion or channel plugging processes operating on surface D or downstream thereof but some minor channel incision is visible.

B. Bed sediments and bars. Particle size variations cannot be used to differentiate the bed wave (surfaces G and M) from the remainder of the reach. Neither d_{50} , d_{10x} (the mean of the 10 largest clasts in a sample) nor the geometric standard deviation (σ_g) show any significant differences between bar units (Appendix 9). Further, no downstream trends are observed in these parameters for Porters Reach. Care was taken to locate the particle size samples on constructional surfaces only, avoiding small channels cut into the bar surfaces. This procedure eliminated the effects on sorting of re-working by channels. No attempt was made to avoid or include cluster bedforms, or to adopt a consistent location with respect to diffuse gravel sheets. Restriction of sampling sites in this way would have proved difficult to achieve because of the apparently chaotic juxtaposition of gravel sheets and irregular distribution of cluster bedforms. Features which could be interpreted as cluster bedforms were incorporated into all samples (some were as small as three clasts in association) and their influence upon the results depends upon their scale. Obstacle clasts in the clusters were generally of size d_{90} , which is broadly equivalent to d_{10x} , or greater.

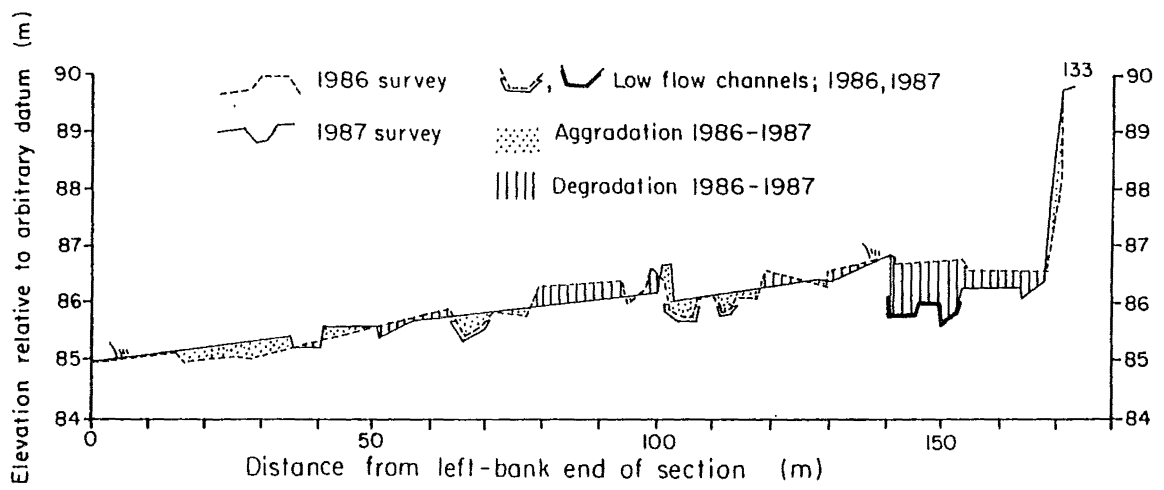


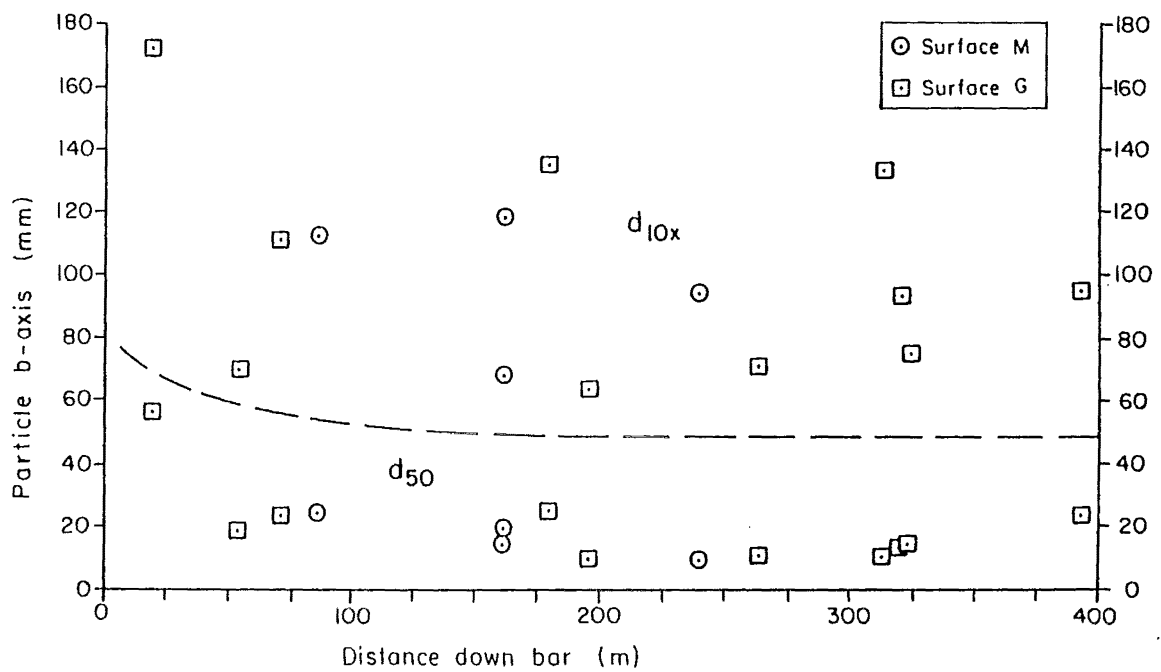
Figure 5.20 Comparison of cross-section 133 in 1986 and 1987.

Downstream fining of the coarsest material present has been reported over short (< 700m) reaches by Bluck (1982) and Ashworth and Ferguson (1986). Both studies also detailed downstream fining within individual bars. This is most marked for the coarsest material present (Ashworth and Ferguson (1986) used d_{10x} , and Bluck (1982) defined the maximum clast size (MCS) as the mean diameter of the largest 30 clasts in a 3m x 3m square). Bluck (1982) identified this trend on major bars despite lateral and vertical accretion of smaller unit bars.

The mechanism for longitudinal size sorting that Bluck (1982, 1987) has proposed is dependent upon the largest material sizes that are present. This model submits that bars act as templates which select and reject clasts by a turbulence controlled mechanism (Bluck, 1987). Coarse clasts induce sufficient turbulence to prevent deposition of finer material (other than very fine material which can be trapped between larger clasts). A similar explanation was proposed by Kirkby and Statham (1975) for the development of size sorting on scree slopes. However the absence of perfect sorting led them to suggest that a 'random stopping process' also exists. In rivers, such a process may take the form of the development of cluster bedforms which alter turbulent flow structures around them so as to encourage both lee and stoss side deposition (Brayshaw, Frostick and Reid, 1983).

Bluck's model deals only with the surface of a deposit and would not necessarily be expected to apply to situations where transport layers more than one grain thick were being emplaced. Meland and Norrman (1969) illustrated how sediment sorting in this situation is a complex process which can lead to coarser material overlying finer, finer over coarser or a broadly homogeneous mixture. This results from larger particle sizes having greater transport velocities, and so despite being more difficult to entrain tending to arrive at depositional sites before slower moving finer material. Thus, from a homogeneous sediment source coarse material may move downstream to a depositional area and then be buried by slower moving finer material. Subsequent erosion of this deposit could remove the slower moving sizes first so that they could arrive at the next depositional site before, with or after the faster moving coarse fractions. Size sorting of the bulk material then becomes dependent on the distances between successive depositional zones. Given that these mechanisms appear to suggest that size segregation would not be universal, which is supported by Parker *et al.* (1982) who proposed that all grain sizes in a mixture have approximately equal mobility, size sorting in bulk gravels would not be expected to be commonly encountered. However, falling stage sorting of surface material should be possible given that a wide range of grain sizes will be present near the surface of the transport layer and that the coarse fraction is generally over-represented in this material (Parker and Klingeman, 1982). Size sorting by the selective rejection mechanism is therefore possible notwithstanding the implications of Meland and Norrman's (1969) results.

In a complex bar such as surface G in Porters Reach, the size of the largest clasts (d_{10x}) should decline downstream according to Bluck's model. Figure 5.21 shows that this is not the case. Data



SEE ERRATA

Figure 5.21 Particle size changes along major complex bars in Porters Reach. These are identified as surfaces M and G in Figure 5.18. d_{10x} is the mean b-axis of the 10 largest in a 1m x 1m surface sample of 100 clasts. d_{50} is the median size from the same samples.

for surface G exhibit considerable scatter. Surface M data are included in Figure 5.21 as M and G are morphologically similar and are hypothesised to represent one depositional surface. When median surface particle size is examined, a poorly developed trend for down bar fining is observed. This result is surprising given the absence of such a trend from the d_{10x} data. The sample from closest to the bar head (located at T in Figure 5.18) was appreciably coarser than all of the samples from further downbar. This sample is not necessarily derived from the same depositional unit as the others, being located immediately downstream of a channel diffluence on a gravel sheet that may have been produced by the loss of flow competence as it spread out over the bar, rather than to the primary depositional processes which formed surface G. The particle size evidence suggests limited downstream sorting of median particle size but no sorting of the larger clasts. An explanation for this pattern requires understanding of the structure of surfaces G and M.

The structure of these surfaces comprises four main elements that can affect size sorting. The first of these is the complex bar which forms the core of the depositional surfaces and which may have had greater extent at the time of deposition. Superposed upon this are smaller forms described as diffuse gravel sheets by Hein and Walker (1977). In their initial definition, Hein and Walker regarded these as permanently submerged channel features, but they can also be recognised on bar surfaces. They are smaller features than the unit bars of Smith (1974) and Bluck (1982) being only one or two grains thick. They possess diffuse lobate fronts (Hein and Walker, 1977) where coarse material congregates. Sheets of this type can be recognised widely on surfaces G and M. Also identifiable are particle clusters, which are also widespread across both diffuse gravel sheets and bar core areas. In the Kowai, the type of particle cluster that is present is intermediate between linear, flow parallel clusters (Brayshaw, 1985) and transverse clast dams (Bluck, 1987), being either wide versions of the former or narrow ones of the latter (Hoey, in press 1989). Cluster bedforms have implications for sediment entrainment (Naden and Brayshaw, 1987) and also serve to inhibit sorting processes. The clasts retained in linear clusters are considerably finer than the obstacle clast (Brayshaw, 1985), whereas with transverse clast dams groups of material of similar size form the dam with finer particles in the inter-dam spaces (Bluck, 1987). The clusters in the Kowai contain elements of both these forms with the obstacle produced by a group of similar sized clasts and the stoss and lee accumulations consisting of finer material. Whether such bedforms occur in bar head or tail regions they disrupt the turbulence structures responsible for size sorting. The clusters in the Kowai often exhibit imbrication and a consequent increase in the flow shear stress required to initiate particle motion facilitates their preservation. Finally, dissection by shallow channels has occurred across both surfaces G and M with distinct levee deposits in some locations.

Sediment sorting of the surficial element of the bar core deposits would produce down-bar fining according to the results of Bluck (1982) and Ashworth and Ferguson (1986). When smaller depositional units accrete to the main bar they tend to have a finer grain size than the parent bar,

but Bluck (1982) has only recorded minor changes through time in the grain size at fixed locations on major bars. This suggests that new accretions are modified *in situ* until their grain size is equivalent to that of the parent bar. Once this is achieved longitudinal size sorting should occur as it would for the parent bar alone. Attainment of this mature state depends upon four general factors (Bluck, 1982), namely: relative rates of grain size selection and vertical accretion causing reduced water depths and hence flow competence; rates of lateral accretion which causes the flow to be diverted away from earlier deposits; availability of material of different sizes; the rate of channel migration which can induce erosion or burial of earlier deposits. Bluck (1982) suggested that in braided rivers undergoing rapid sedimentation small unit bars are relatively immature with respect to grain size uniformity. This conclusion is supported by the Kowai data which demonstrates this immaturity at the scale of a major complex bar. The first two of the factors listed previously can be invoked to account for this pattern. These both imply that the deposit has been exposed to competent flows for insufficient time to enable size sorting to develop. This is partly a consequence of rapid sediment deposition in part of the active channel (near Q on Figure 5.18) causing concentration of the flow into one dominant channel. Incision of this channel in response to flow concentration could have induced a reduction in flow competence over surfaces G and M. Sediment sorting may also have been inhibited by deposition of the surficial material on these bars occurring close to the end of the flood event which produced the major bar forms. This potential explanation is external to the sediment deposition process whereas the former one is consequent upon that process.

The irregular pattern of down bar variation in d_{10x} is interpreted as reflecting the influence of cluster bedforms on the samples, combined with the absence of sufficient time for complete size sorting to develop. The trend in d_{50} data, although weakly developed, can be taken as evidence that longitudinal sorting of particles of lesser diameter than d_{10x} had commenced. However it seems likely that the lack of well developed sorting in terms of either d_{10x} or d_{50} reflects the effects of rapid aggradation and flow reduction.

C. Depositional history of the bed wave. The morphology of the deposits in Porters Reach may indicate a recent depositional episode upstream of surface D (Figure 5.18) with the channel remaining stable between there and the bedrock gorge at the downstream end of the reach. Particle size data imply that this depositional surface is immature. The suggestion is made of an advancing wave of sediment coming to rest somewhere downstream of XS 135, and then being subject to limited lateral erosion and dissection. Rust (1975) and Tandon and Kumar (1981) have demonstrated that AB-axis orientation is parallel to flow direction in braided river deposits. AB-axis orientations were measured (Figure 5.22). In the upper parts of surfaces G and M clasts are oriented parallel to the nearest channel, orientations becoming more variable further away from the channels. By XS P4 orientations are between 45° and 90° to the nearest channels. Clast alignments suggest flow almost perpendicular to the wave front and directed towards the low flow channel. This is assumed to represent a primary depositional feature given the immaturity of the

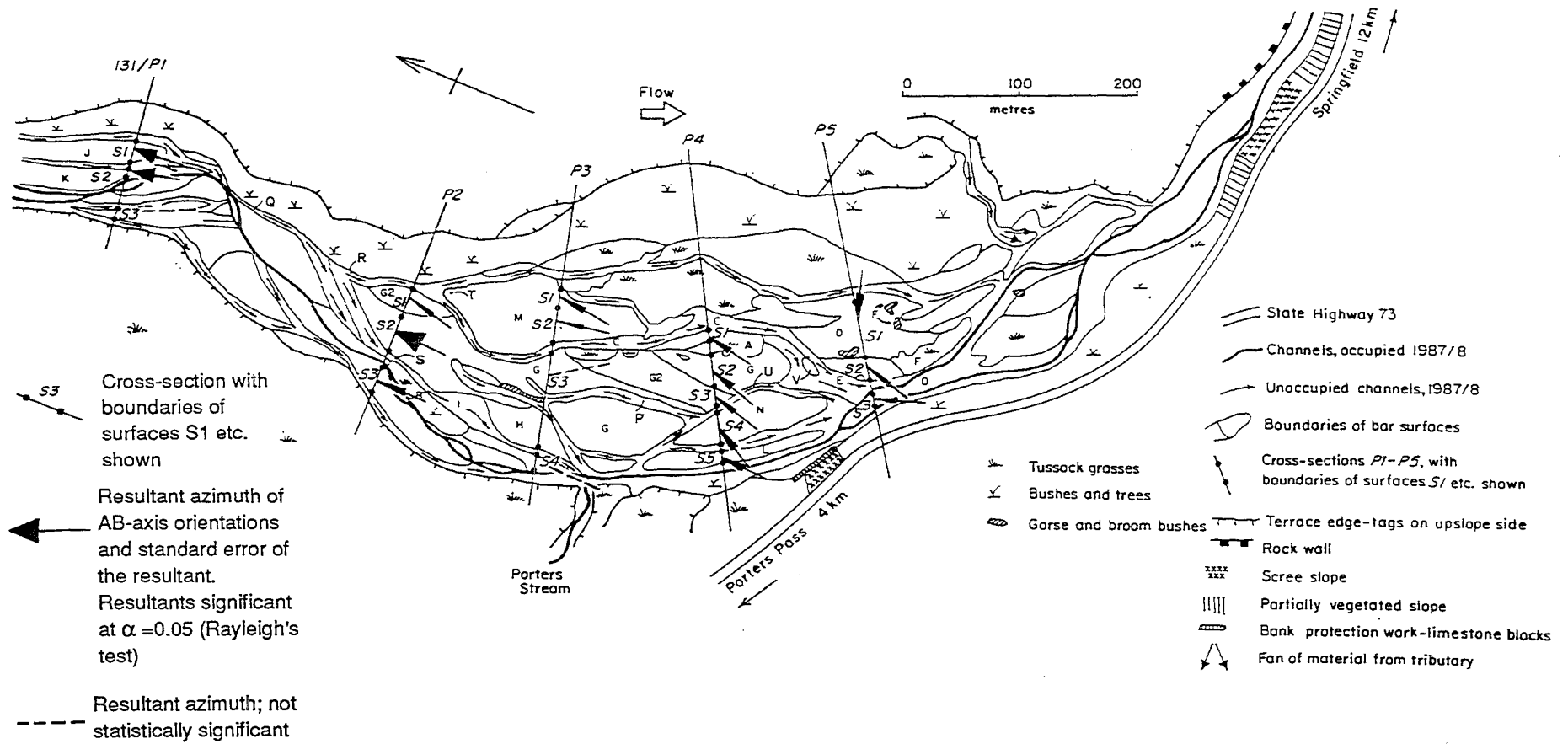


Figure 5.22 Orientation of surface clasts in Porters Reach. Cross-sections P1-P5 were used for the palaeoflow analysis.

deposits with respect to size sorting. Had the orientation been the result of falling stage modification of the initial depositional alignment, better development of size sorting would have been expected. The reason for the flow alignment seems to be topographical. Downstream of XS P3 (Figure 5.18) the active channel starts to constrict due to stable vegetated terraces attached to the left bank (Figure 5.19; XS P3, XS P4, XS 135). At XS P5 (Figure 5.22) clast orientations are controlled by the main channel except for close to the left bank where flow appears to have been normal to the previously active channel. This may indicate the inactivity of surface D during the most recent flood event(s), which would support the interpretation of this surface given earlier.

The depositional history of this reach was further investigated using palaeoflow reconstruction (Hoey, in press 1989). The cross-sections and depositional surfaces used for this purpose are shown on Figure 5.22 (P3/S2 refers to cross-section P3, surface S2 etc.). Table 5.4 summarises the results of this analysis. Note that some of the previously referenced depositional surfaces have been sub-divided, and that not all of the surfaces identified on Figure 5.22 appear in Table 5.4 for reasons discussed fully elsewhere (Hoey, in press 1989).

Table 5.4 Possible event structure for the Kowai River. N.A. - not available

Event	Surfaces formed in event	Approximate discharge ($m^3 s^{-1}$)	Possible time of occurrence	Water surface slope
1	P2/S3	7 +/- 1.5	July-Sept. 1987	N.A.
2a	P2/S1, P4/S3 P4/S4, P5/S3	22 +/- 12	March 1987 - falling stage	0.031
2b	P1/S1,P1/S2,P2/S2 P3/S1,P3/S2, P4/S2,P4/S5,(P5/S2)	55 +/- 23	March 1987 -peak flow	0.027
3	P1/S3,P5/S1	104 +/- 26	March 1986 (or later 1986)-peak flow	0.026
4 ?	P3/S4	142 +/- 28	Pre-March 1986	N.A.

Table 5.4 identifies three flow events responsible for the deposits in Porters Reach. Event 4 is tentatively postulated and is not further considered herein due to being based solely on surface P3/S4 which is located in an hydraulically unusual location in the lee of a vegetated island (B on Figure 5.22). The largest flow event, 3, is assumed responsible for deposition of P1/S3 and P5/S1. P5/S1 is representative of surface D which has previously been suggested to be an earlier deposit than surfaces G and M. Event 2 comprises the major depositional phase in the

reach with some falling stage modification of these deposits. Surface N lies within event 2a and suggests that G may have extended further downstream than at present before being eroded as a channel bend developed along the line of channel U (Figure 5.22). The bar remnant V also implies a former greater extent of the depositional surface. Some falling stage modification of surface G is also suggested (surface G2 on Figure 5.22) as shallow channels cross its surface.

The postulated evolution of the bed wave is illustrated in Figure 5.23. Only the approximate position of the low flow channel is known for the period leading up to the flood event in March 1987 (Figure 5.23a). As deposition occurred, the flow may have concentrated into one or more channels upstream of the leading edge of the wave. Channels developed during the latter stages of the event and were responsible for erosive modification of the wave form as illustrated in Figure 5.23c. During this phase the channel changes that were referred to above (in the river bed geometry section) occurred, producing the dissected appearance of the deposit. Close to the low flow channel some modification has occurred during later events.

Aerial photographs from 1966 show a distinct depositional unit terminating in a bar face at about the same location as the 1987 position of the leading edge of the wave (see Figure 5.13b). The location of the deposit is controlled by the shape of the between-terrace channel in this vicinity. Where the active channel width increases downstream of XS 132, deposition is promoted at times of high flow by decreasing flow depth associated with the width increase. This location of valley widening thus acts as a sedimentation zone (Church and Jones, 1982). At the downstream end the transition into a transfer reach is controlled by the bedrock gorge which effectively prevents deposition in Porters Reach downstream of about XS 137. The shape of the downstream edge of the depositional surface could be due to flow orientation being controlled by the location of the gorge and / or the additional discharge from Porters Stream causing erosion immediately downstream of the confluence.

5.4.3 Bed waves in Porters Reach: conclusions and a model

Werritty and Ferguson (1980) have proposed a cyclic model for channel changes in this sort of river. Major overbank floods produce an unstable braided channel pattern which is then rationalised as reworking occurs during subsequent events. In the Porters Reach example this rationalisation was well underway by the end of the last major event in 1987. In the River Feshie studied by Werritty and Ferguson (1980) the primary control over channel pattern was hydraulic. The case in the Kowai is somewhat different with major channel changes initiated by large volumes of sediment entering the river system. Single events which transport considerable volumes of material are responsible for inducing changes in channel and sediment storage patterns that are only slowly reworked. Not all events involve the delivery of large volumes of sediment from the upper catchment. The major control over sediment supply to Porters reach appears to be the Foggy River fan at its junction with the Kowai River some 2km. upstream

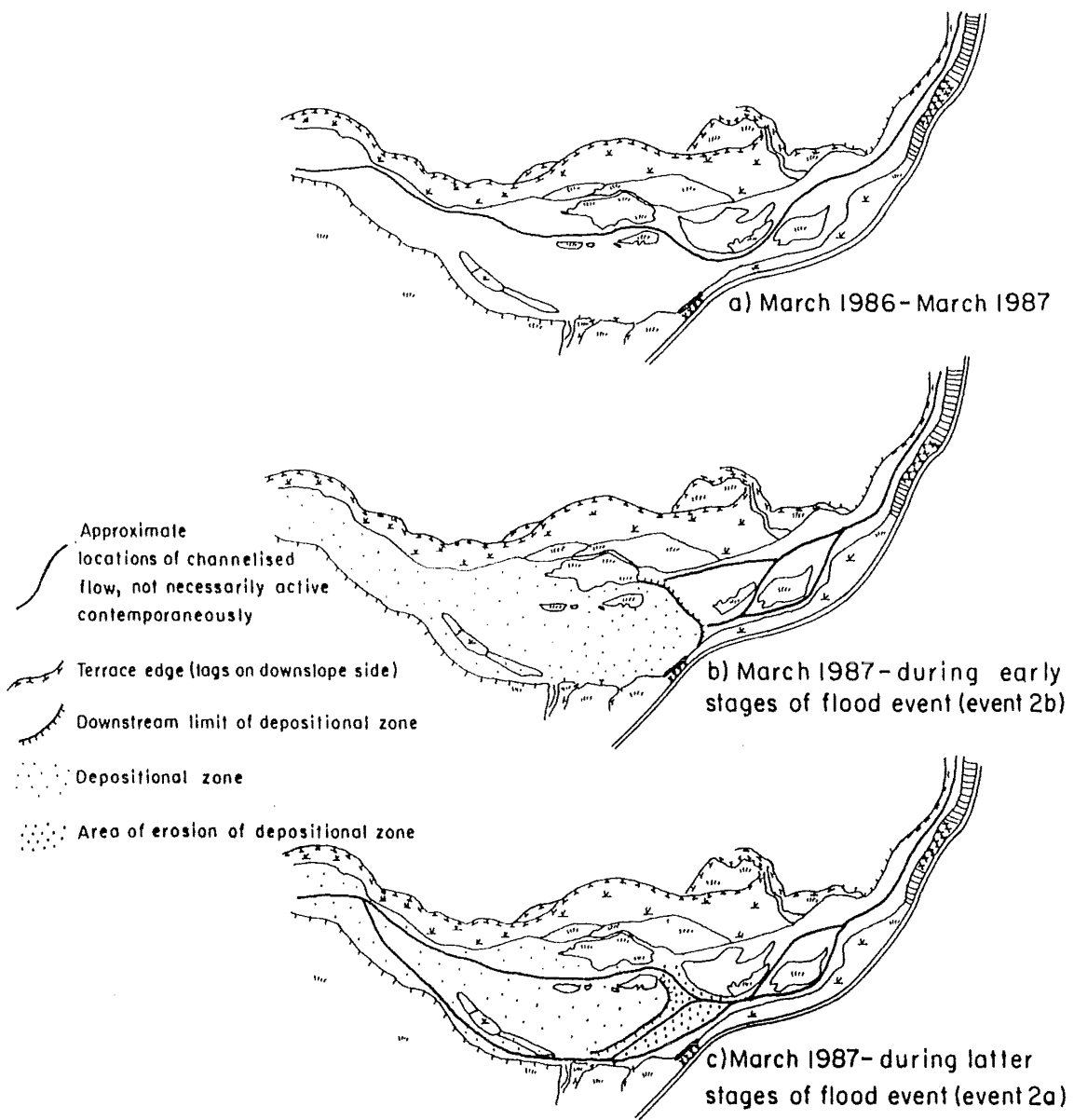


Figure 5.23 Hypothetical evolution of the bed wave in Porters Reach during a flood event in March 1987. Note that channel positions are approximate and that their continuous occupation for the duration of the event is not suggested.

(Blakely *et al.*, 1981). Periodic erosion of the Foggy fan causes the input of large quantities of material to the Kowai. Between the fan and Porters Reach there are few potential sediment storage locations, so that the first manifestation of this increased sediment load is as a deposit within this reach. Bridge Reach serves as a second sedimentation zone and there are numerous others further downstream.

Beschta (1983b) concluded that sediment loads exert a greater influence on active channel widths in the Kowai than do water discharges. This is reinforced by the behaviour of Porters Reach which is strongly controlled by the sediment supplied to it. Over a longer timescale this reach is still adjusting to the effects of the 1951 flood event and the 1987 deposition has to be seen in this context. Long term aggradation is continuing in Porters Reach (Figure 5.14) and shorter cycles of aggradation and degradation contribute to this. One consequence of the long-term aggradation is that the deposits are texturally immature and exhibit poorly defined particle size sorting.

These conclusions can be used as the basis for a model of bed wave behaviour in Porters Reach, analogous to and based upon that suggested for the sand tray in sub-section 5.2.3. Figure 5.24 presents this model figuratively. Note that it assumes zero long-term aggradation or degradation. Because of the types of available data, the variables included in this model are not identical to those used in sub-section 5.2.3 but are closely related.

The primary difference between this and the sand tray derived model is that discharge was not constant in the field situation and that bedload transporting events are infrequent. Changes are thus episodic and there are long periods of inactivity. These are shown by dotted lines on Figure 5.24. The aggradation-degradation cycle is defined by changes in the mean bed elevation. The shape of the mean elevation vs. time graph is based on that measured in the sand tray experiments (Figure 5.8). The model assumes that most of the degradational phase occurs within a single event, but this need not be the case and this phase could be extended. There is no evidence available to define the relative lengths of the aggradational and degradational phases. The active channel width tends to increase during periods of aggradation (Beschta, 1983b) although this relationship is not necessary. It is decreased due to vegetative stabilisation transferring material to the inactive storage reservoir during prolonged quiescent periods.

The total volume of stored sediment follows an identical pattern to mean bed elevation, by definition, but the magnitude of changes therein are much less than those in the active plus semi-active storage reservoir. This reflects the transfer of material into these storages as a consequence of increased active channel width. Channel pattern complexity, as measured by the number of channels at a cross-section, increases most during the aggradational phases. This is also based on the sand tray results as there are no aerial photographs available for the Kowai for other than low flow conditions. During these periods there are reaches with relatively complex

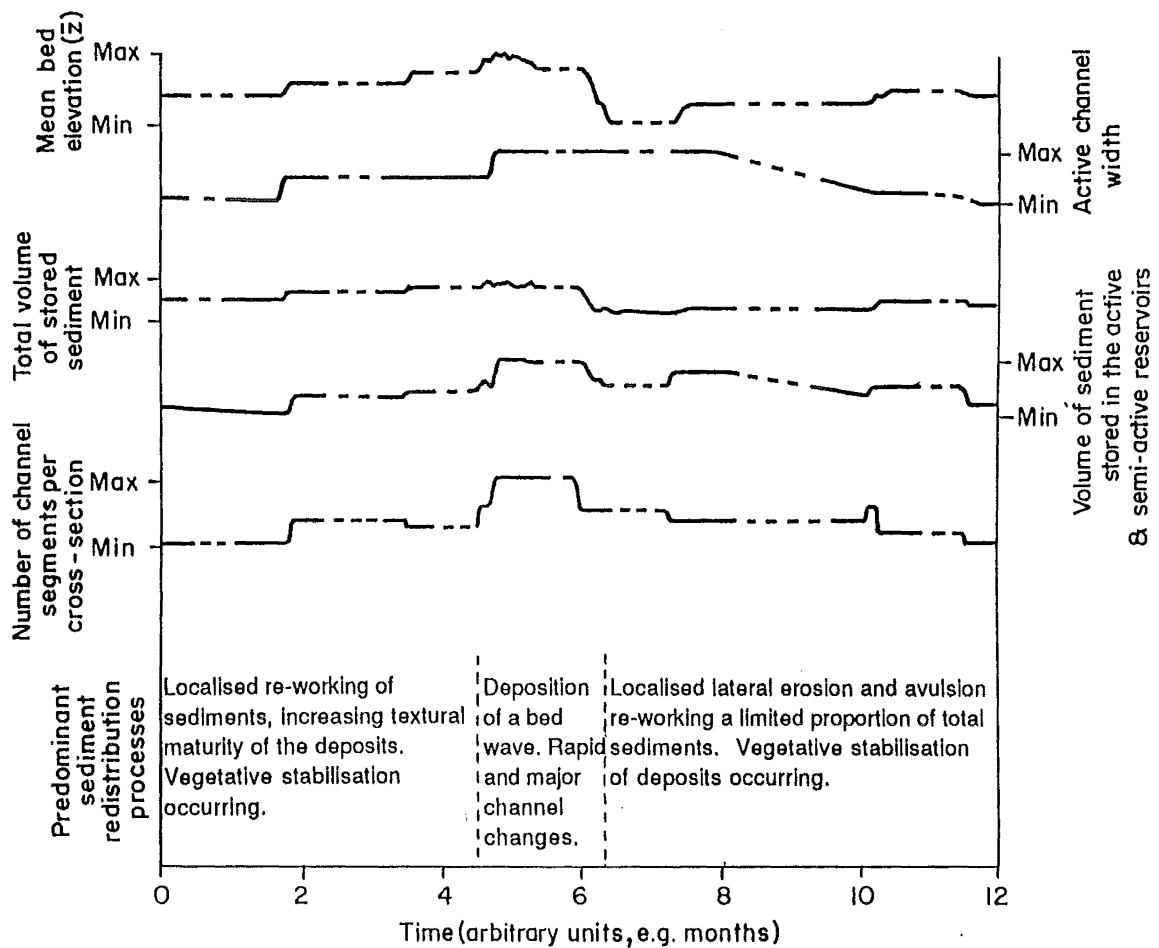


Figure 5.24 Idealised development of a bed wave through time in Porters Reach. All variables are plotted as dimensionless ratios. Dashed lines indicated periods of inactivity (i.e. no bedload transporting events occurring) which are of indeterminate length.

channel patterns which may correlate with aggradational zones. The complexity of unoccupied shallow channels in Porters Reach (Figure 5.18) gives an indication of how complex the pattern in this reach would appear at a moderately high stage. This has been observed in the field and is consistent with the aggradational nature of this reach. Subsequent decreases are due both to incision of major channels and the tendency for smaller events to rationalise patterns.

This model is somewhat more tentative than the earlier one due to the comparative paucity of data used in its construction. It is specific to cases where the upstream supply of sediment is episodic. Where this supply is more constant, cycles of aggradation and degradation may have less abrupt extremes and could resemble more closely those found in the sand tray.

5.5 Discussion and conclusions

The bed waves discussed in sections 5.2, 5.3 and 5.4 exhibit many similarities and some important differences. These could reflect differences between laboratory and prototype systems, and / or between endogenous and exogenous wave forms. The major differences between the models of Figures 5.8 and 5.24 are the episodic nature of changes and the occasional reversal of long-term trends in the Kowai model, neither of which is as significant in the laboratory case. Both of these reflect the episodic nature of water and sediment inputs to the Kowai system. In particular the data used in the development of the Kowai model came from the deposits of a flood event of about 2-year recurrence interval (Blakely *et al.*, 1981; Hoey, in press 1989) and a sediment supply event of uncertain magnitude and frequency. Inputs of sediment in larger volumes could produce quite different responses. The 1951 event produced aggradation throughout much of the Kowai catchment, responses to which are ongoing (Beschta, 1983a). The impacts of large scale events have been widely noted as causes of increased sediment storage and braiding intensity, which reduce over time (e.g. Church, 1983), but a similar pattern of change may occur with more frequent events (e.g. Werritty and Ferguson, 1980). Church and Jones (1982) and Church (1983) have questioned whether single events may introduce non-equilibrium forms to river systems, the responses to which involve oscillation between different forms of channel behaviour. Their example of the increased sediment supplied to the Bella Coola River by erosion of Neoglacial moraines causing oscillations in sediment storage, the magnitude of which has declined through time, provides a possible model for river response to the episodic input of large volumes of sediment. Schumm (1977a) illustrated how sediment yield following local uplift in experimental basins follows the same sort of damped oscillatory response. In the Kowai this type of behaviour can be identified with reference to the 1951 event. Subsequent events have supplied additional material to the river system at intervals, and these have themselves been of variable magnitude. These sediment parcels may be transferred through the river system in the form of bed waves, and so superposed upon the ongoing response to the 1951 event. The evidence from Porters and Bridge Reaches tends to support this superposition hypothesis as against an alternative view that additional sediment is

incorporated into the post-1953 bed wave(s). There is a lower limit to the volume of sediment supply required to initiate a distinctive bed wave, the magnitude of which depends upon the scale of the system concerned. Smaller volumes of sediment could be incorporated into existing storage patterns without inducing appreciable change.

It could be anticipated that larger bed waves would migrate downstream more slowly than smaller ones because of the greater volumes of material involved, or that the reverse could occur if waves migrate as coherent forms. This complicates superposition of waves of variable size from sources located at different positions in a catchment. In a catchment where sediment storages were restricted to the active river bed this could lead to a complex pattern of waves of different scales passing through reaches together. This is illustrated by the lack of regularity in either time or space of sediment storage and channel morphology trends in the sand tray. The Kowai has two characteristics which serve to reduce this complexity. Firstly, considerable volumes of sediment are stored in Foggy Fan which is only occasionally eroded. This regulates the introduction of waves to Porters Reach and ensures that intermediate sized waves enter the reach on a quasi-regular basis. Smaller (macro-) scale waves can readily by-pass the fan as they are transported through the Kowai itself. Larger events such as that in 1951 can circumvent storage in the fan. The present study found evidence for continuing recovery from the effects of the 1951 event in Porters and Bridge Reaches in the form of changes in sediment storage patterns, and multiple macro-scale bed waves associated with unit bars and diffuse gravel sheets. The bed wave upon which much of the model in sub-section 5.4.3 is based was of intermediate size and is assumed to represent the result of one erosional episode at the Foggy fan. The role of tributary fans in storing sediment both directly and as a result of trapping material in the main channel behind them has previously been identified by Church and Jones (1982) and Church (1983). The second characteristic is the variability of valley width which restricts the locations where sediment is able to accumulate. This tends to exaggerate changes in slope, bed elevation and channel pattern, and restricts them to specific locations.

In terms of a model of bed wave behaviour, the role of sediment storages further upstream is to limit the spatial and temporal variability of sediment supply. In many ways the situation in Porters Reach is similar to that in the sand tray experiments. Sediment supply from upstream (Type C) is episodic in both; in the tray due to aggradation / degradation cycles (except at the head of the tray), and in the field due to episodic erosion and temporary sediment storage. Both of these are regulated by channel processes and are independent of Type A supply events. Thus, although the waves in the Kowai were classified as exogenous they are actually introduced to Porters Reach in an endogenous manner, except for the large scale events that exceed the capacity of sediment storage in Foggy Fan in a single event. Both models are therefore applicable to Types B and C sediment supply and neither truly accounts for Type A. Their similarity in many respects is therefore less surprising than it may appear at first. The limited evidence from the introduction of a Type A wave to the sand tray (Run 3a) suggests that the model of endogenous wave behaviour

applies reasonably well to this situation also.

The model developed from the Kowai data is derived from a situation close to the sediment sources. Downstream attenuation of bed waves would be expected on the basis of work in this river (Beschta, 1983a) and elsewhere (Gilbert, 1917; Pickup *et al.*, 1983). Beschta (1983a) extrapolated aggradational zone length vs. basin area data from the Kowai to the Waimakariri R. and suggested that depositional zone lengths of order 40-60 km would be expected in the latter. However, Griffiths (1979) estimated bed wavelengths of the order of 1km in that river. This discrepancy implies that Beschta's extrapolation is unjustified and that there may be a limit to the length of bed waves, which could be defined as a certain number of channel widths. The limited data on Figures 2.2 and 2.3 imply that this limit is at about 20-30 channel widths, and that it may decrease above some indeterminate value. This is supported by Church and Jones (1982) data which showed no clear reduction in bed wavelength as channel width decreases downstream i.e. the number of channel widths in a bed wave increases as width decreases. At small widths in headwater areas this correlation seems to be reversed if it is assumed that width varies as drainage basin area in Beschta's data. If the wavelength of bed waves is limited in this way they should remain detectable downstream although their attenuation may make this more difficult. It is anticipated that the model developed from Porters Reach will remain broadly applicable further downstream although the magnitudes of differences between reaches may be reduced. Where attenuation occurs there will be a tendency for other influences to obscure the wave forms and superposition effects, for example, may obscure patterns that would be distinctive further upstream.

The models discussed in this Chapter have focussed primarily on the sediment load of the rivers, and have emphasised the role of sediment supply in producing wave forms. In Chapter 4 waves were analysed in terms of water flow conditions and the hydraulic factors underlying their growth and erosion were considered. The hydraulic variations that are important for sediment redistribution in wave forms are themselves dependent upon the existence of those forms. At the meso-scale sediment is nearly always available for transport and bedload pulses can be explained in terms of hydraulic behaviour and the interaction between flow and sediment properties (e.g. Iseya and Ikeda, 1987). At the mega-scale the effectiveness of given hydrological events is dependent upon the location of stored sediment in the river system that is available for transport and redistribution during the event. Beschta (1983b) concluded that sediment availability rather than water flow controlled the variation in channel width in the Kowai R. There are numerous examples of sediment supply influencing the behaviour of river channels (e.g. Lewin, Bradley and Macklin, 1983; Bradley, 1984; Nakamura, 1986). River behaviour at this scale can therefore be primarily related to sediment redistribution factors, but hydraulic interactions with the accumulated sediment are necessary to produce bed waves and so remain significant.

To summarise the conclusions of this Chapter, the following are the main points to emerge:

1. Bed waves exhibit a range of spatial and temporal scales even under conditions of constant water and sediment inputs. This variability is likely to be amplified in situations where these are themselves variable.
2. Sediment storage patterns and the processes responsible for them can be represented by a model of changes occurring during the passage of a bed wave. This model has potential to be used diagnostically.
3. Similar models can be applied to the sand tray and prototype data on waves of Type C sediment. Limitations on data availability in the prototype case prevent the degree of this correspondence from being precisely evaluated.
4. Processes of sediment redistribution observed in the sand tray have been used to infer the processes that may have produced similar morphologies in the prototype to those in the tray. This has been aided by use of prototype data that would be more difficult to obtain from a small scale model. The potential for integrating studies which combine these two approaches has been demonstrated.

6. PATTERNS OF SEDIMENT REDISTRIBUTION ASSOCIATED WITH BED WAVES

Bed waves have been conceptualised as simple moving wave forms which may or may not attenuate as they migrate downstream. Pickup *et al.* (1983) suggested a range of processes by which bed material dispersion in braided rivers is facilitated, so enabling attenuation. Dispersion is caused by interaction between any sediment supplied to a reach and the existing bed material within the reach, which Mosley (1978) has also illustrated. This is further encouraged by interaction between active bed and floodplain sediments (Kelsey *et al.*, 1987; Macklin and Lewin, 1989), but its rate is dependent upon the characteristics of the river system. Church (1983), for example, argued that dispersion in a wandering, predominantly single-thread river is limited because sediment storage is concentrated in deposits that may be stable for time periods comparable with the transit time of sediment along several kilometres of channel. Rapid dispersion need not imply wave attenuation if sediment added by local erosion offsets the attenuation effect (Roberts and Church, 1986). The dispersion patterns associated with bed waves are thus likely to vary between river systems.

Some studies of small gravel-bed streams and rivers have addressed the question of dispersion using natural or artificial tracer materials, but as Hassan, Schick and Laronne (1983) have noted many have had low rates of material recovery. This severely limits the value of information that can be derived from the data (Kelsey *et al.*, 1987). In laboratory studies it is possible to monitor the dispersion of tagged material reliably (e.g. Meland and Norrman, 1969; Iseya and Ikeda, 1987).

In the present study, part of experimental Run 3 was used for the investigation of redistribution processes by introducing a quantity of fluorescently dyed sand at the upstream end of the sand tray. The following discussion considers the dispersion of this dyed material within the tray and attempts to relate this to processes of channel change. An attempt is then made to model sediment transfer between bed material storage reservoirs as a stochastic process.

6.1 Sediment dispersion processes and channel morphology

6.1.1 Sand tracing techniques

The entire 2.25 kg of sand input to the tray in Run 3 at 1500, 1515, 1530 and 1545 minutes was dyed. Its distribution was equivalent to that of the sand filling the tray, and was not modified significantly during the dying process. Dying was accomplished with a red fluorescent dye applied using the method of Kirk, McLean, Burgess and Reay (1974) whereby curing and crushing of the labelled sand are performed concurrently. Introduction of the dyed material in four scheduled sediment inputs gives a median input time of 1522.5 minutes. During the 45 minute period between the first and last such input channel pattern remained essentially stable, especially in the

upper 2m of the tray.

In the following discussion the sand is considered as being divided into two size fractions: coarse ($\geq 0.6\text{mm}$) and fine ($<0.6\text{mm}$). 0.6mm was the closest sieve size to the median particle size of the material filling the tray (0.57mm) that was available. Two sets of samples were collected to evaluate dispersion of the dyed sand. One set came from the material collected in the sediment collecting boxes at the downstream end of the tray. Samples were taken every 15 minutes until 1600 minutes and every 30 minutes thereafter. The second set were bulk samples collected to a depth of 10mm from cross-sections located at 2m intervals along the tray. Sampling sites were randomly selected from within the morphological units into which each section was divided. The sediment storage reservoir in which each of these sites was located was noted. The samples were taken when the flow was shut down at 4 hourly intervals. During the first 3 hours after the dyed sand was introduced regular sketches were made of its surficial distribution and were supplemented by vertical photographs.

The concentration by weight of dyed sand in each sample was measured in the following way. A 1.5-4 gm sub-sample was obtained using a sample splitting device. The coarse and fine fractions were separated and weighed to a precision of 1×10^{-7} kg. All dyed grains were removed from the larger size fraction and weighed. This procedure was quite straightforward under ultraviolet lighting as the dyed grains emitted a distinctive orange glow. A direct measure of the percentage by weight of dyed material was thus obtained. For the finer fraction such a procedure was impracticable. A further sub-sample of this fraction was weighed and the number of dyed grains within it counted. These sub-samples contained up to about 1000 grains. The number of dyed grains was converted to a weight by assuming that each grain had the same mass as the median grain size of all material $< 0.6\text{mm}$ (This mass is 4.63×10^{-8} kg for a spherical grain of diameter 0.322mm and density 2650 kg m^{-3}), thus enabling a percentage by weight of dyed sand to be derived. The percentage of dyed material in the total sample is readily calculated from the data for the two size fractions. For the samples collected from the sediment output from the tray, the percentage of dyed sand was multiplied by the total sediment output to obtain a mass of dyed sand exported during the time period represented by the sample.

The masses of all material in the coarse and fine fractions were used to obtain an index of median particle size (the equivalent diameter index). This is defined as $0.6 \times (\text{Mass} \geq 0.6\text{mm} / \text{Mass} < 0.6\text{mm})^{1/3}$ and is useful for comparative purposes but cannot be compared with any sizes obtained by different methods.

6.1.2 Output of dyed sand from the tray

The outputs of dyed sand and total sediment are shown in Figure 6.1 (see Appendix 10 for details). From 1515 minutes (the first sediment output measurement after the input of tracer

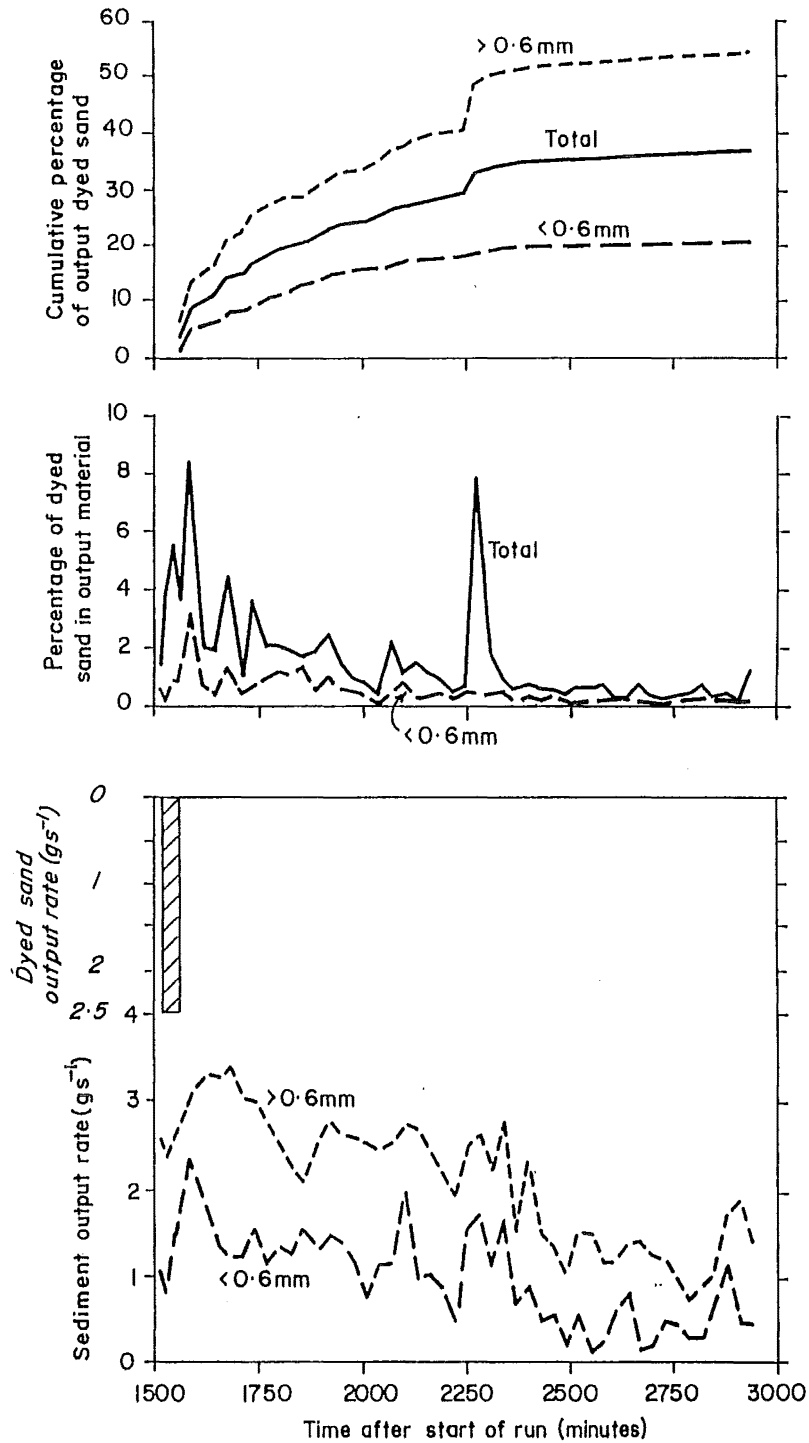


Figure 6.1 Output of tracer sand and total sediment output from the tray, Run 3, 1515-2940 minutes. The interval between measurements was 30 minutes, and the sediment output series plotted in Figure 4.1 has been adjusted to give a 30 minute sampling interval

- a) output of dyed sand as a cumulative percentage of the total input
- b) output of dyed sand as a percentage of total sediment output
- c) total sediment output and input of dyed sand

material) until the end of Run 3 at 2940 minutes, total sediment output rate exhibited a declining trend about which there were minor fluctuations. The percentage of total sediment output <0.6mm averaged 44 ± 15 % (n=50). As a percentage of total sediment output, the export of dyed sand from the tray also declined through time. About this approximately exponential trend there were several small deviations and a larger one at 2280 minutes. The percentage of output dyed sand which was in the < 0.6mm fraction has a mean value of 33 ± 23 % (n=50) which is significantly less than the value for all of the sediment output (t-test; $\alpha = 0.01$). This may be a consequence of the different procedures used to obtain the estimates of concentrations of dyed sand in the two size fractions.

By the end of the run (1440 minutes after the first input of dyed sand), 36.5 % of the tracer material had been output from the tray. This included 20.2 % of the input in the fine fraction and 54.2 % of the coarser fraction. Together these accounted for 36.5 % of the dyed sand input; 63.5 % therefore remained in storage within the tray. During this period 84.2 % of the material entering the tray was accounted for by export from it (i.e. the sediment delivery ratio of the stream was 84.2 %). To explain the discrepancy between this figure and the 36.5 % delivery ratio for the dyed sediment requires exchanges of sediment from the input material into storages within the tray, and from these storages into the output sediment.

The rate of output of dyed sediment slowed appreciably after the peak at 2280 minutes (Figure 6.1a). The mean output of dyed sand as a percentage of the total input prior to and including 2280 minutes was 1.24 %, declining to 0.16 % afterwards. It seems likely that the majority of the remaining output of dyed material would take the form of short peaks such as that at 2280 minutes, associated with erosion of an area of storage of such material. The peak at 2280 minutes could have been produced by bank erosion or the breaching of an armour layer which included a significant number of dyed particles ≥ 0.6 mm in its composition.

Prior to 1750 minutes the rate of dyed sediment output exhibited considerable variability (Figure 6.1b). Most of the material output by this time had not left the active sediment storage reservoir. Its passage through the system was more or less continuous, with some periods of short-term storage within the active reservoir. Until 1560 minutes the increase in output of dyed sand was predominantly due to increased export of the coarser (≥ 0.6 mm) fraction (Figure 6.1b and c). This rise was associated with the continued input of dyed material until 1545 minutes, and was restricted to the coarser material because the transport velocities of individual particles in mixed sediments attain a maximum towards the coarse end of the size distribution (Meland and Norrman, 1969). By 1590 minutes the output of dyed material <0.6mm had increased also due to material that had not left the active reservoir. The fall in the output of dyed sand after 1590 minutes was a consequence of exhaustion of this continuously active supply, and all dyed material reaching the downstream end of the tray after this time had either been incorporated into another storage reservoir or had been temporarily stored within the active reservoir (by hiding processes, for

example) during transit.

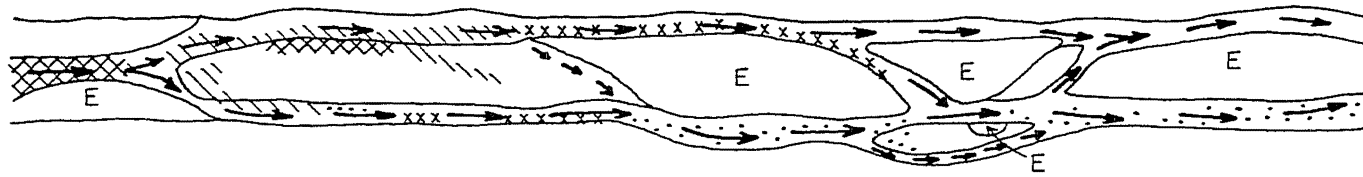
6.1.3 Redistribution of dyed sand within the tray

The initial redistribution of dyed sand was visually estimated with reference to a percentage cover chart (Gardiner and Dackombe, 1983; Figure 13.2). Figure 6.2 shows these distributions at 1520, 1580 and 1610 minutes. Figure 6.2a (1520 minutes) demonstrates the initial deposition of material in bedload transporting channels, at the head of a bar which was undergoing both lateral and vertical accretion (at 3m), and at other locations where there was bedload transport across bar surfaces. The density of cover by the dyed sand decreased downstream, and penetrated further down the left bank channel than the right bank one upstream of their confluence at 10m. This occurred even though water and sediment discharges were greater in the right bank channel at this time, which suggests that the dyed material was diluted by greater mixing with existing channel sediments in the right bank channel. The pattern 1 hour later at 1580 minutes (Figure 6.2b) was similar; the left bank channel had greater concentrations than the right bank one and the zone of maximum concentration of dyed sand at the surface had moved downstream. The previously high concentration upstream of 2.5m had been reduced by both the removal of material to different depositional locations downstream and burial of the dyed material by that introduced subsequently. The former process was reflected in the increase in concentration of dyed sand on the inter-channel bar surface between 3m and 5m. Of note is the zone of greater (10-50 % cover) concentration close to the left bank side of the main (right) channel between 10m and 12m. This material was largely derived from the left bank channel further upstream and retained its coherence downstream of the confluence at 10m. This indicates a lack of lateral mixing of bed sediment across the channel.

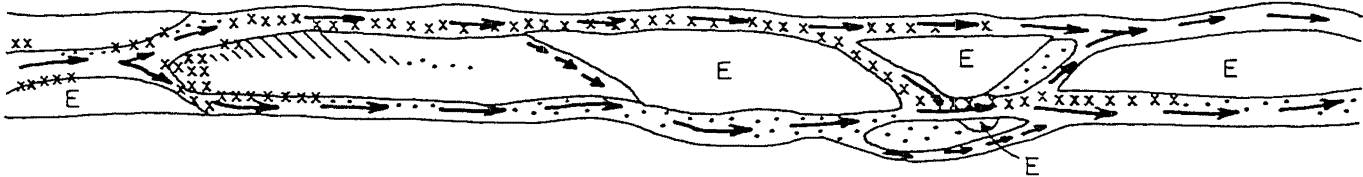
After a further 30 minutes (1610 minutes; Figure 6.2c) the downstream decline in surface concentration visible on the preceding two Figures had been dissipated. High concentrations (10-50 %; 50-75 %) of dyed sediment were by then restricted to depositional areas where there had been further deposition after the cessation of dyed sand input. These include parts of the bar surfaces in the region 2-5m and the left bank channel between 7m and 10.5m. The sediment transport rate in this channel was low due to falling water discharge as a response to degradation of the right bank channel in the 3-5m reach, leading to that channel capturing most of the flow. Other areas where some deposition was occurring also had limited quantities of dyed sediment visible. From 1610-1740 minutes most of these surface concentrations became gradually diluted. Exceptions to this were upper parts of the inter-channel bar at 2-4m (X on Figure 6.2c) which were emergent from the water by 1630 minutes, and the channel adjacent to the left bank between 9m and 11m (Y on Figure 6.2c) which had been abandoned by 1630 minutes.

The surficial distribution of dyed sand at 1690 minutes is given in Figure 6.3 along with the data collected from the samples taken every 2m along the tray, which yield a bulk concentration for up

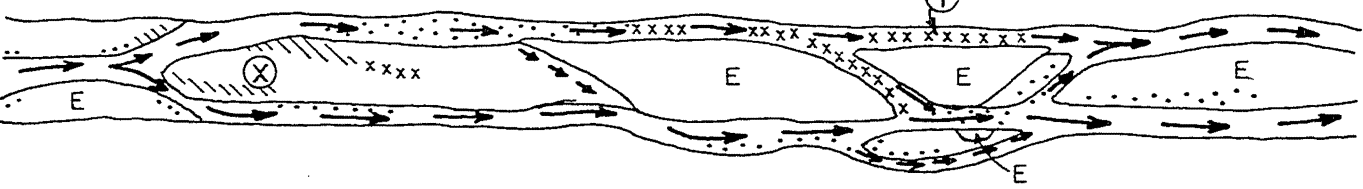
a) 1520 minutes



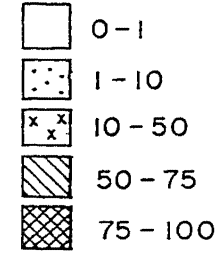
b) 1580 minutes



c) 1610 minutes



Percentage surface cover of dyed sand



→ Major channel

→ Minor channel

○ Submerged bar surface

⊖ E Emergent bar surface

Figure 6.2 Surficial distribution of dyed sand as visually estimated in Run 3.

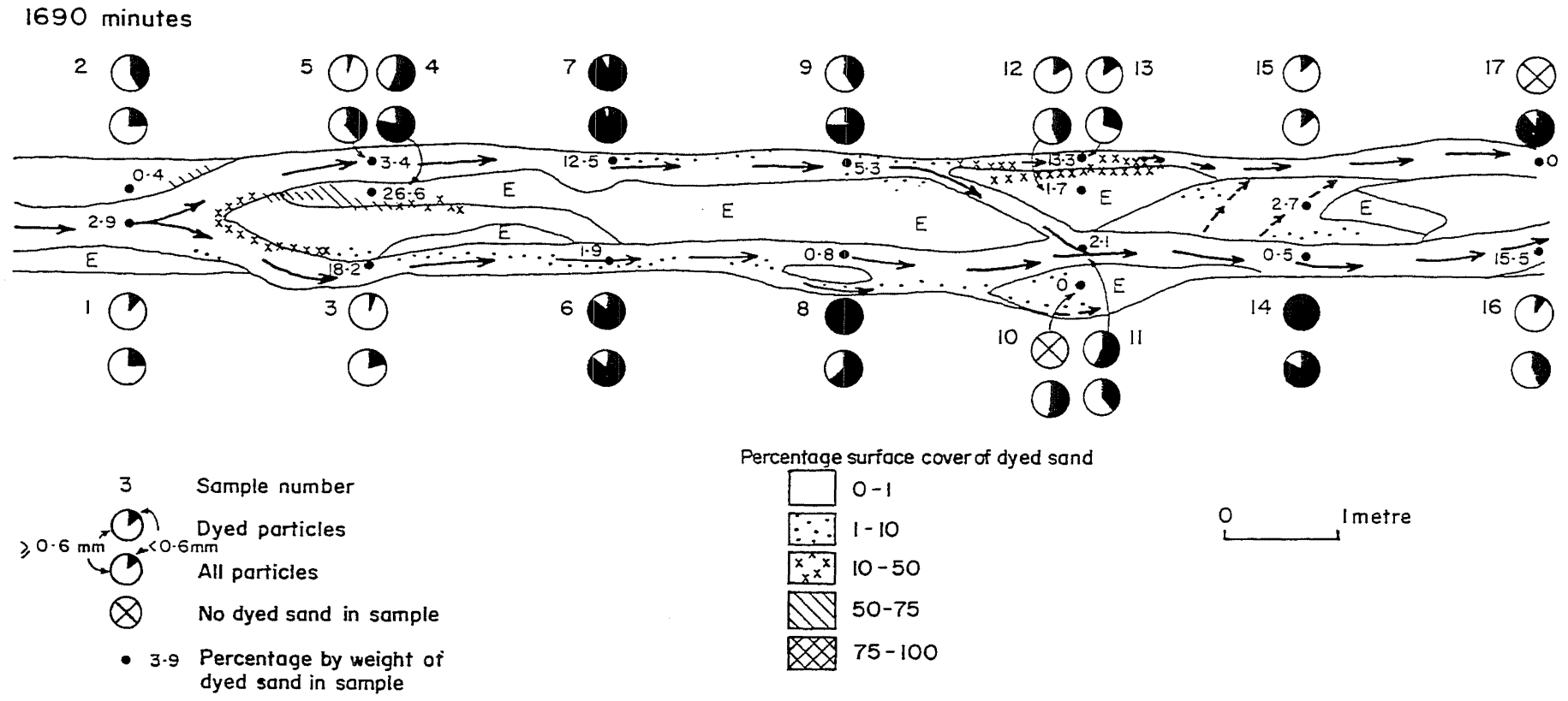


Figure 6.3 Distribution of dyed sand at Run 3, 1690 minutes, derived from visual estimation and sediment sampling at 2m intervals along the tray.

to 10mm depth (these data are detailed in Appendix 11 along with similar data from 1930-2890 minutes). There was considerable variability between samples in the concentrations and size distribution of dyed sand. The concentrations measured at any one location depend on the depositional history at that location, and variation in these evolutionary processes is responsible for the diversity in measured concentrations. For example, the concentration of 18.2 % in the right bank channel at the 4m cross-section (Sample 3; Figure 6.3) was dominated by material $\geq 0.6\text{mm}$ which was deposited soon after the onset of dyed sand input, subsequently buried, but re-exposed as a consequence of channel degradation and bank erosion at this section. 2m further downstream in the same channel the total concentration was 1.9 % (Sample 6), made up predominantly of material $<0.6\text{mm}$. Finer material dominated the bed material at this location and was derived from erosion of the channel left bank (i.e. the bank produced by the inter-channel bar). Locally high concentrations of dyed sand can sometimes be readily explained as resulting from deposition in stable areas (such as at sample 13; Figure 6.3). However, Sample 16 exhibited a high (15.5 %) concentration dominated by material $\geq 0.6\text{mm}$, and was located in a channel where there was considerable sediment transport. This high concentration presumably reflects the combined effect of erosion of depositional sites, sediment sorting processes, and variable transport velocities for different particle sizes.

After the next four hour period (1930 minutes) the same general patterns were visible in the concentration data (Appendix 11). While absolute values had altered, there were similar patterns of variation reflecting the localised nature of erosion and deposition processes. Changes in channel pattern and in the locations of erosion and deposition produced some alterations in the distribution of dyed sand between 1930 and 2940 minutes. Figures 6.4-6.6 illustrate the distributions at 2170, 2650 and 2890 minutes, respectively.

Comparison of Figures 6.3 and 6.4 reveals a tendency for the concentrations of dyed material at a given section to decline through time reflecting burial and dilution processes. Further, the major location of dyed sediment within the tray, the upper part of the inter-channel bar at 2-5m, became isolated from the two main channels by deposition at its head and on its sides. The dyed sand deposit was thus protected from erosion so limiting the supply of this material to the channels. The importance of this source of material is illustrated by the small bank attached bar at 3-4m (A in Figure 6.4) which had a concentration of 4.3 % entirely composed of particles $\geq 0.6\text{mm}$, derived from material that had previously been deposited in the upper bar area.

Between 2170 and 2650 minutes (Figures 6.4 and 6.5) channel pattern changed substantially upstream of 6m with the development of a new channel cutting through the long established bar surface (A on Figure 6.5), and bank erosion by the right bank channel (B on Figure 6.5). Both processes produced erosion of the area where much of the dyed sand had been initially deposited and so released a significant quantity of this material into the main channels. Dyed sand concentrations did not rise immediately, however; concentrations in samples 6-8 were 0 %,

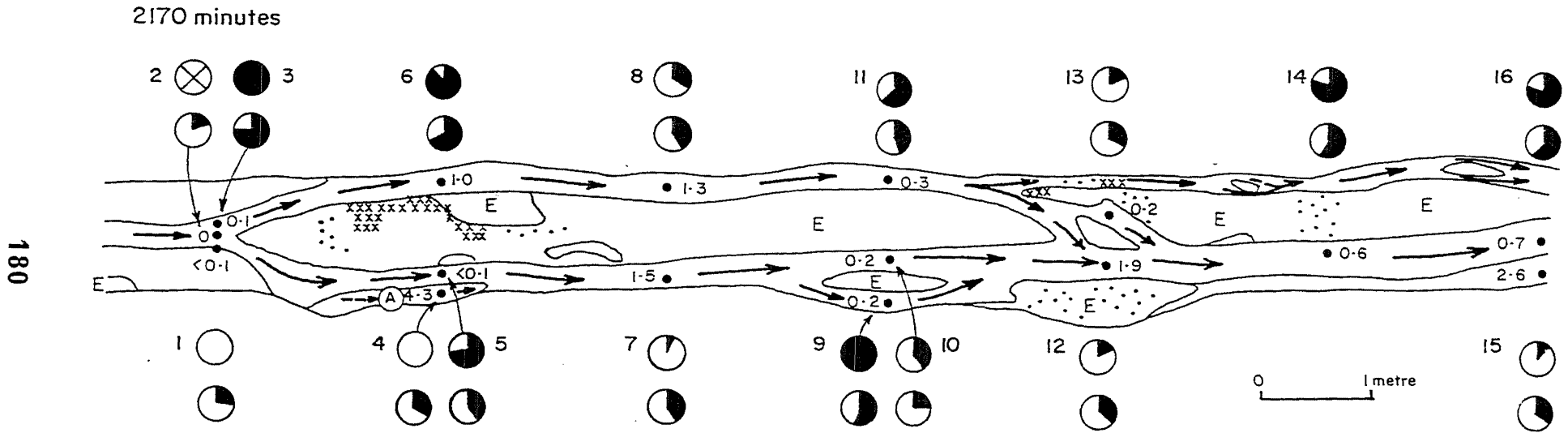


Figure 6.4 Distribution of dyed sand at Run 3, 2170 minutes, derived from visual estimation and sediment sampling at 2m intervals along the tray. For legend see Figure 6.3.

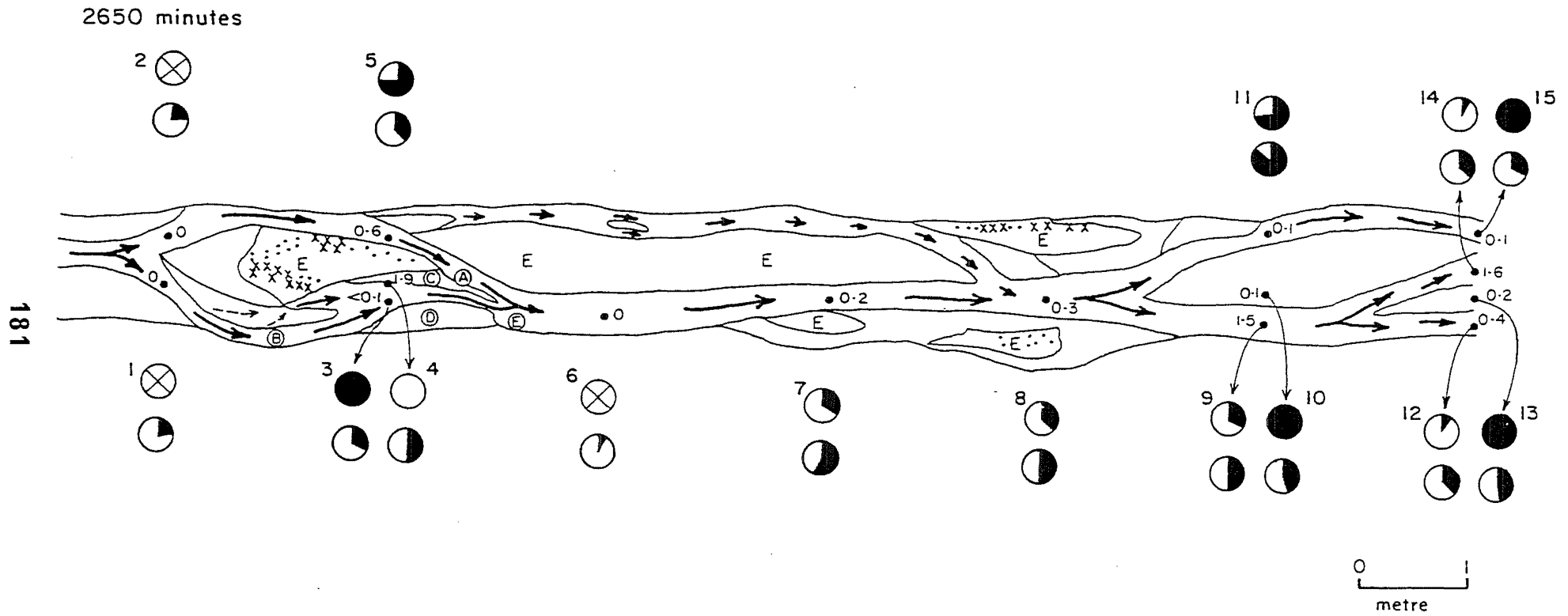


Figure 6.5 Distribution of dyed sand at Run 3, 2650 minutes, derived from visual estimation and sediment sampling at 2m intervals along the tray. For legend see Figure 6.3.

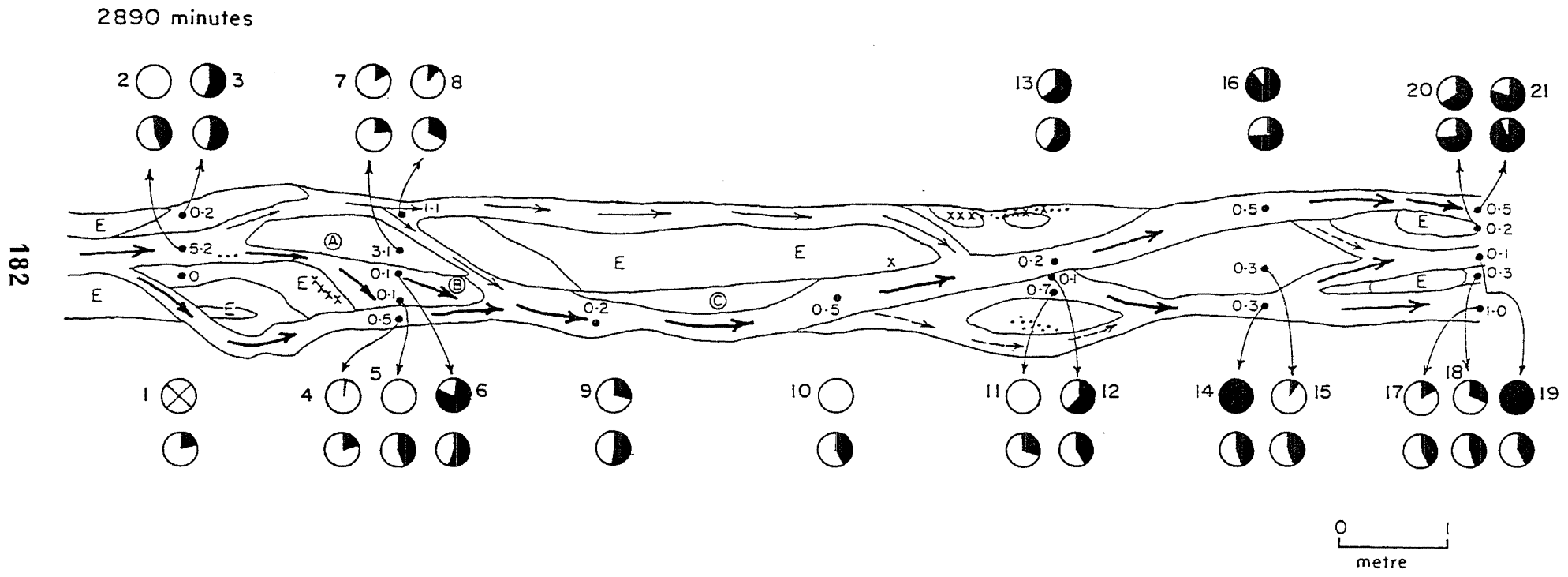


Figure 6.6 Distribution of dyed sand at Run 3, 2890 minutes, derived from visual estimation and sediment sampling at 2m intervals along the tray. For legend see Figure 6.3.

0.2 % and 0.3 % (Figure 6.5). Much of the eroded material was deposited in bars C and D (Figure 6.5) which were not sampled at 2650 minutes. Inspection of vertical photographs revealed that sample 6 was taken from an area of armoured channel. Between the sample site and the left bank of the channel was a lobe of finer (< 0.6mm) material derived from channel A, which may have contained much of the dyed sand released by development of that channel. It is possible that sample 6 failed to locate a high concentration of dyed sand in this finer material. This suggests a limited degree of cross-channel mixing of bed sediment which is consistent with observations at 1580 minutes (Figure 6.2b) discussed previously, and with the suggestion of Best (1987) that sediment from confluent channels is routed around the zone of confluence scour (F on Figure 6.5) and then remains toward that side of the channel from which it was introduced.

During the following four hour period, 2650-2890 minutes (Figures 6.5 and 6.6) channel and bar morphologies continued to change. There was degradation at the 2m cross-section (see Figure 5.2a) which exposed some of the dyed sand initially deposited in this area. This accounts for the higher concentration in sample 2 (5.2 %) than that in samples taken from the same location previously, and its composition entirely of material $\geq 0.6\text{mm}$ although material in this fraction accounted for just over half of the material in the bulk sample (Figure 6.6). Some dyed sand from this degradation could have been incorporated into surface B along with some eroded from surface A (Figure 6.6), but was considerably diluted. Surface A retained a relatively high concentration of material (3.1 %; Figure 6.6) even though it had been deposited post-2650 minutes. This indicates that some of the dyed sand previously located in the bars upstream of the 4m cross-section had only been moved short distances during the period of degradation and channel pattern modification. Much of the dyed material eroded from this reach was transferred to the main channels and was presumably relocated into both channel and bar deposits (such as bar C; Figure 6.6) by 2890 minutes. The low concentrations of dyed material recorded can be explained as a result of dilution of the dyed sand as it interacted with material previously within the tray and that added after the dyed sand input (by 2890 minutes, 24 times the volume of dyed sand had been input to the tray after the cessation of the dyed input). Dilution occurred as the dyed sand underwent vertical exchange with the host material, and there is evidence that this exchange is directly related to the transport distance of particles (Schick, Hassan and Lekach, 1987).

Conclusions reached by Meland and Norrman (1969) were used in Chapter 5 to suggest that sedimentary deposits can exhibit a wide range of particle size characteristics as a result of different size fractions having different thresholds for entrainment and transport velocities. Consequently a complex pattern of size sorting in both time and space would be expected. Figures 6.3-6.6 illustrate such a situation where there appears to be little consistency in either particle size sorting or the relationship between the sizes of dyed sand and the host material. The complexity of sediment redistribution processes is apparent from these data and it is difficult to derive any general principles to characterise them. Bar stability influences redistribution as illustrated by the

aggradation and subsequent erosion and degradation in the 1-4m reach. Not only is bar planform important but the depth to which degradation occurs influences sediment transfer. Where aggradation is ongoing, sediment can remain stored within the active and semi-active reservoirs throughout smaller degradational episodes imposed on the aggradational trend. The loci of deposition depend on the particular bar and channel processes occurring at any one time, and these have been shown previously (Chapter 5) to vary considerably as aggradation and degradation alternate. Redistribution of the dyed sand reflected these processes and included both the formation of new bar forms and lateral and vertical accretion onto pre-existing deposits. A similar pattern was described by Kondolf and Matthews (1986) for tracer material redistribution in a 50m wide gravel-bed river, and Butler (1977) illustrated how transport distances for individual particles are influenced by their initial position on a cross-section.

6.1.4 Implications of the dyed sand redistribution patterns

The output of dyed sand from the tray and redistribution within it suggest that description of sediment redistribution by single measures of dispersion, transport velocity or residence time is unlikely to be a reliable means of describing the range of behaviour that occurs. The shape of the cumulative output vs. time plot for the dyed sand (Figure 6.1a) indicates that the mean throughput time will considerably exceed the median. After 24 hours (at 2890 minutes) an appreciable volume of dyed sand had moved no more than 4m along the tray. It could have taken 10^3 - 10^4 minutes or longer before all of this material was evacuated. Any estimate of mean transit time based on the available data would be too low. A corollary of this is that the age distribution of material within a given storage reservoir will also be complex and should not be approximated by mean age. Adequate description of the transit or residence time functions would require a considerable quantity of data.

The redistribution patterns also illustrate the difficulties of using tracer studies in prototype rivers for the estimation of particle transport velocities and bedload discharges. Without knowledge of the reliability of sampling procedures it is impossible to accurately describe the dispersion patterns. This study confirms the conclusion of Dietrich *et al.* (1982) that poor recovery rates are a major constraint on the use of tracer materials, which they considered to be a severe problem limiting the quantitative use of tracer study data.

The patterns of tracer dispersion are dependent upon channel and bar processes which vary through time and between different types of stream system (e.g. aggrading vs. degrading), so implying that the nature of tracer study results is specific to the stream system and condition under investigation. This study was concerned with a braided system undergoing long-term aggradation, interspersed with shorter periods of degradation. Much of the dyed sand was deposited within the upper 4m of the tray and subsequently buried by material introduced to the system at a later time. Were aggradation not occurring in this reach it is likely that its transit time

through the tray would be less than in the present example.

The body of dyed sand did not maintain any form of coherence as it was redistributed within and through the tray, and underwent considerable interaction with the host bed material. Bed waves were identified within the sand tray during the time when the dyed sand was dispersing (section 5.1; Figure 5.2). These are therefore made up of material that was brought together by the sediment redistribution processes within the tray, rather than of sediment supplied at the upstream end migrating downstream as a coherent mass. The implication of this for exogenous bed waves for which such downstream migration has been suggested is that the wave form may migrate downstream, but the material comprising it will be subject to continual exchange with other sources of bed sediment.

The above discussion suggests that sediment transfer can be considered as a series of exchanges between different storage elements within a stream system. This is conveniently conceptualised using the sediment storage reservoirs defined in sub-section 3.1.4 as a basis. Bed waves have been identified in Chapters 4 and 5 on the basis of volumes of sediment stored in different reservoirs, suggesting that numerical modelling of bed waves will be possible if these volumes can be reliably predicted. This is the subject of the following section.

6.2 Stochastic modelling of sediment redistribution

The role of mathematical modelling in geomorphology has been recently reviewed by Anderson and Sambles (1988). They emphasised process modelling and highlighted recent progress in the development of efficient models of this type. Sediment routing models have also tended to be based on process considerations, whether they are concerned with routing through a catchment as a whole (Simons, Li, Ward and Shiao, 1982) or entirely within river channels (Pickup, 1988). Many models have attempted to describe the behaviour of large systems by combining detailed models of their component parts (Pickup, 1988) and their precision is limited by the level of understanding of each component as well as the nature of their interactions. Pickup (1988) has described the limitations of such models in detail, but remained generally optimistic about their potential for future development. An alternative approach which avoids some of these limitations is to use stochastic modelling. There are numerous forms of such models which can be grouped into two main categories; one type describes individual processes such as particle entrainment by probability functions, so circumventing some of the problems produced by inadequate understanding of processes; the second category considers variations in morphological variables, such as channel pattern or sediment storage volumes and treats their changes through time in a stochastic manner. This latter approach is applicable at greater spatial and temporal scales and lumps the outcomes of numerous processes together. Kelsey *et al.* (1987) have utilised this methodology for the description and prediction of sediment exchanges and yields, and concluded that the modelling procedure is not only of descriptive and predictive value, but

that is also able to account for processes that have not been comprehensively described by deterministic process modelling.

The approach developed by Kelsey *et al.* (1987) is used herein for the analysis of sediment storage changes through time within the tray and of sediment outputs from it. Because of the different physical environments being modelled the following sections contain several modifications to their original model.

6.2.1 Description of the model

A. Reservoir definition. The model is based on the identification of reservoirs defined as spaces occupied by volumes of sediment. Eriksson (1971) described reservoir theory noting that the aim of the modelling procedure is to define the characteristics of the reservoirs in terms of volumes and age distributions of material in storage. The reservoir definitions introduced in sub-section 3.1.4 (Figure 3.8) are based on those of Kelsey *et al.* (1987). Note that although the reservoir names are the same as in Kelsey *et al.*'s paper, they are defined differently. This reflects their application of the approach to channel and floodplain sediments, whereas here it is applied to different zones within what they classified as the active channel. The reservoirs are referred to subsequently both by their full names and in abbreviated form as follows: Active - A; Semi-active - S; Inactive - I; Never active - N. The absorbing state is referred to as B. The age distribution of material in a reservoir can be defined in several ways (Eriksson, 1971) including the frequency distribution of ages, transit times (time spent by a particle in the reservoir), or flushing times (time taken for a particle to reach an absorbing state).

The whole sand tray was regarded as one reach when considering potential transfers of material between reservoirs. The four types of reservoir represent four states into which sediment can be transferred. A fifth state is the absorbing state represented by the sediment output from the tray, and a sixth state is the input of material to the tray. Possible interactions between these states are shown in Figure 6.7. Note that material cannot be input to the never active state. The figure depicts transfers that could occur in the 4 hour interval between surveys. Over a shorter interval some of the indicated changes become impossible (e.g. to get to the inactive reservoir material from the never active must pass through at least the active one). The transfers indicated in the figure can occur as the result of either static or dynamic transfer processes (see sub-section 3.1.4 for discussion).

Since the entire sand tray is being considered as a single reach for present purposes there is no distance related component in Figure 6.7. It is possible for material to be in the same reservoir at the start and end of a measurement period but to have moved anything from 0m to 14m downstream, possibly having been exchanged with other reservoirs several times. The whole range of sediment transfer processes illustrated in section 6.1 is thus combined into a single set

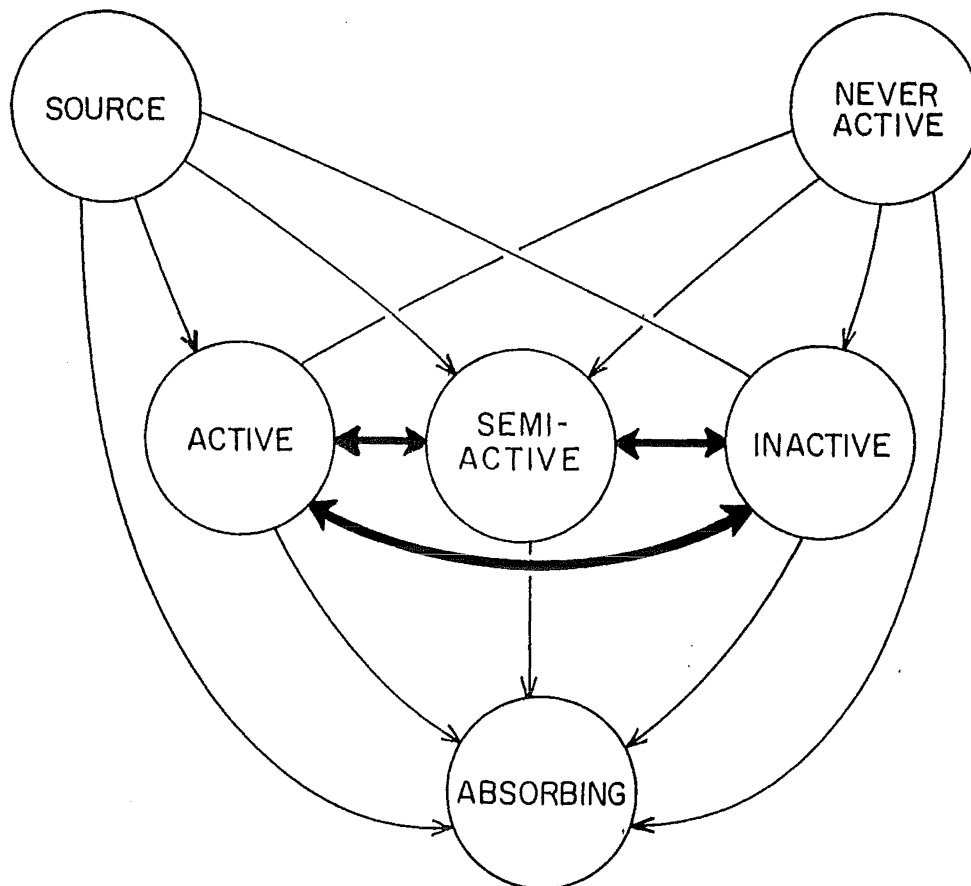


Figure 6.7 Possible transfers of sediment between the four storage reservoirs, the source, and the absorbing state. The time interval between sediment being in one state and another is 4 hours (the period between successive cross-section surveys in the tray).

of possible transfers which can be modelled stochastically.

The model is structured as follows. Sediment output from the tray includes Types A, B and C material. Type A and B inputs are derived from the sediment stored within the tray at the outset of the time period. In addition, static and dynamic transfers alter the distribution of material between reservoirs. These two processes are considered by the first component of the model. Type C material is that input at the head of the tray. Its redistribution forms the second component of the model. Summation of these two components provides the distribution of material between reservoirs and the absorbing state at the end of a time period.

The transfers between the six states in Figure 6.7 can be described in terms of their probabilities of occurrence. There being a finite number of states an appropriate descriptive form is a finite Markov chain. The critical element of the modelling procedure involves the assignment of probabilities to each transfer depicted in Figure 6.7. Particle movement in such a model is dependent only upon the reservoir that it is in at a given time, and is independent of its previous history or the length of time spent in the reservoir (Kelsey *et al.*,1987). In the subsequent analysis each time step is taken as 4 hours and the probabilities of a given transfer taking place are for one such interval.

B. Mathematical definition of transfer processes. In the following discussion, matrices are designated by upper case bold type, **A** and row and column vectors by lower case bold type, **v**. Individual elements of matrix **A** are designated a_{pq} etc. where p is the row reference and q the column reference of the element.

First consider the redistribution of sediment within the reach, ignoring input of material from upstream. The distribution of sediment between the five states (ignoring the source) at time $t=0$ can be described by the row vector **v**, where,

$$\mathbf{v} = (0 \quad v_a \quad v_s \quad v_j \quad v_n).$$

The 0 first element refers to the absorbing state which is initially assumed to contain no sediment. The probabilities of material initially in each of the four storage reservoirs being located in different reservoirs after a time interval of 1 unit can be defined by the matrix **Q**. **Q** is a 4 x 4 matrix, there being 4 reservoirs, and its leading diagonal contains the probabilities that sediment will start and end one time period in the same reservoir. The probabilities of sediment being transferred to the absorbing state from one of the four reservoirs are given by the column vector **r**. The transition matrix, **T**, which describes the exchanges between the four reservoirs and the absorbing state has the general form (Kelsey *et al.*,1987),

$$\mathbf{T} = \left(\begin{array}{c|c} \mathbf{I} & \mathbf{0} \\ \hline \mathbf{r} & \mathbf{Q} \end{array} \right) \quad (6,1),$$

where I is a 1×1 identity matrix and $\mathbf{0}$ is a null vector. The identity matrix represents the absorbing state i.e. all of the material in that state at time t will remain there at $t+1$. The volumes of sediment in each of the five states after a single time interval are given by the result $\mathbf{v}' = \mathbf{v} \cdot \mathbf{T}$, which can be expressed in full as;

$$\begin{pmatrix} a & v_a' & v_s' & v_i' & v_n' \end{pmatrix} = \begin{pmatrix} 0 & v_a & v_s & v_i & v_n \end{pmatrix} \begin{pmatrix} 1 & 0 & 0 & 0 & 0 \\ r_{ab} & q_{aa} & q_{as} & q_{ai} & q_{an} \\ r_{sb} & q_{sa} & q_{ss} & q_{si} & q_{sn} \\ r_{ib} & q_{ia} & q_{is} & q_{ii} & q_{in} \\ r_{nb} & q_{na} & q_{ns} & q_{ni} & q_{nn} \end{pmatrix} \quad (6,2),$$

where v_a' is the volume of sediment in the active reservoir at time $t+1$, and a is the volume stored in the absorbing state at this time. For example, $v_a' = (v_a q_{aa} + v_s q_{sa} + v_i q_{ia} + v_n q_{na})$. In the absence of any sediment input from upstream, equation (6,2) would describe the changes in storage volumes over the period t to $t+1$. Since transfer into the never active reservoir is impossible by definition, $q_{an} = q_{sn} = q_{in} = 0$.

Sediment enters the reach from upstream necessitating an additional component in the model. This component has three parts. Firstly there is a row vector, \mathbf{e} , which describes the proportion of the input sediment which passes directly through to the absorbing state by $t+1$. This proportion (the 'transfer constant') is designated k and the total volume of material input in one time unit is e , giving

$$\mathbf{e} = (e.k \quad e(1-k) \quad 0 \quad 0 \quad 0) \quad (6,3).$$

The sediment volume $e(1-k)$ which remains within the reach at $t+1$ is redistributed amongst the active, semi-active and inactive reservoirs. The volume that is deposited in each reservoir depends on the degree of interaction between the upstream sediment supply and the different reservoirs. This is described by the redistribution matrix, \mathbf{D} , where

$$\mathbf{D} = \begin{pmatrix} 1 & 0 & 0 & 0 & 0 \\ 0 & d_{ea} & d_{es} & d_{ei} & 0 \\ 0 & 0 & 0 & 0 & 0 \\ 0 & 0 & 0 & 0 & 0 \\ 0 & 0 & 0 & 0 & 0 \end{pmatrix} \quad (6,4),$$

in which d_{ea} is the proportion of the input material (extra) deposited in the active reservoir in a time period. The unit value in d_{11} is to allow for the transfer of throughput material to the absorbing state. However, this interaction depends on the distribution of sediment between reservoirs. This second aspect is allowed for by a volume matrix, \mathbf{W} , defined as

$$\mathbf{W} = \begin{pmatrix} 1 & 0 & 0 & 0 & 0 \\ 0 & w_{aa} & 0 & 0 & 0 \\ 0 & 0 & w_{ss} & 0 & 0 \\ 0 & 0 & 0 & w_{ii} & 0 \\ 0 & 0 & 0 & 0 & 0 \end{pmatrix} \quad (6,5),$$

in which $w_{aa} = 3 \times v_a / (v_a + v_s + v_i)$. This definition of w_{aa} results from the need to express volume stored in each reservoir as a fraction of the total volume in storage. Multiplying this ratio by 3 converts it to a ratio of volume to one-third of total volume i.e. it is comparing the actual volume distribution with one that has the same volume of material in the three reservoirs.

The resulting redistribution of input sediment is given by the product $\mathbf{e} \cdot \mathbf{D} \cdot \mathbf{W}$, which is a 5 x 1 row vector. Note that since input material cannot enter the never active reservoir, d_{en} and w_n have been set to 0 in equations (6,4) and (6,5).

Allowing for this redistribution, \mathbf{v}' is equal to the sum of the transition and redistribution components and is given by

$$\mathbf{v}' = \mathbf{v} \cdot \mathbf{T} + \mathbf{e} \cdot \mathbf{D} \cdot \mathbf{W} \quad (6,6).$$

Equation (6,6) is analogous to equation (5) of Kelsey *et al.* (1987). It can be used to predict volumes of sediment in different storage locations given an initial distribution of sediment between reservoirs, an input rate of sediment from upstream and the probabilities associated with the various exchanges between states. Determination of these probabilities is crucial and is described below.

A useful property of finite Markov chains is that in the fundamental matrix, \mathbf{N} , the summation of the pth row gives the mean length of time for material starting in the pth state to reach the absorbing state (Isaacson and Madsen, 1976; Kelsey *et al.*, 1987). \mathbf{N} is defined as

$$\mathbf{N} = (\mathbf{I} - \mathbf{Q})^{-1} \quad (6,7),$$

in which $(\mathbf{I} - \mathbf{Q})^{-1}$ indicates the inverse of the matrix $(\mathbf{I} - \mathbf{Q})$. The summation of the pth row of \mathbf{N} is defined as the 'flushing time' (Kelsey *et al.*, 1987), the variance of which can be computed from

$$\sigma^2 = \mathbf{N} (2\mathbf{f} - \mathbf{1}) \quad (6,8)$$

where \mathbf{f} is the vector of flushing times, f_p for state p, and σ^2 is the vector of variances, σ_p^2 (Isaacson and Madsen, 1976).

C. Estimation of model parameters The model can be calibrated using some of the data on dyed sand redistribution described in section 6.1. The calibration fixes the values of \mathbf{e} and \mathbf{D} to be used throughout the subsequent discussion. The method of calculation of \mathbf{T} is also described herein, and this component is varied subsequently.

The second component of v' , namely the product $e.D.W$, will be considered first. W is known from the cross-sectional survey data reported extensively in Chapter 5, and the volume of input sediment, e , is also known. The transfer constant, k , requires estimation. This can be achieved by using the results from the dyed sand tracing experiment reported in section 6.1. The proportion of dyed sand that had been output from the tray within 4 hours of the median time of introduction is used as the value of k . 18.05 % of the total dyed sand input had been exported by 1770 minutes (the closest time to 4 hours after the median). The value of k was thus set to 0.1805.

Estimation of d_{ea} , d_{es} , and d_{ej} also utilised the tracing results. At 1690 minutes in the middle of the time period from which k was estimated, 17 samples were taken from within the tray (Figure 6.3) and the dyed sand percentages in each measured. Each sample was associated with a storage reservoir and was assumed to be representative of an area of the tray given by the area of the bar or channel unit in which it was located. This enabled an estimate to be made of the volume of dyed sand stored in each reservoir. Table 6.1 presents these data.

Table 6.1 Areas of storage reservoirs and concentrations of dyed sand within them at 1690 minutes, Run 3. See Figure 6.3 for sample locations. Note that not all morphological units within the tray were sampled so the total of the reservoir areas is less than the total area of the channel.

Reservoir	Sample Number	Area of reservoir represented by sample (A) (m ²)	Percentage of dyed sand in sample (P)	Unit volume of dyed sand in sample (=P.A /100) (m ²)
Active	1	1.23	2.88	0.0354
	3	0.51	18.22	0.0929
	5	0.56	3.41	0.0191
	6	0.55	1.91	0.0105
	7	0.44	12.49	0.0550
	8	0.71	0.84	0.0060
	9	0.46	5.29	0.0243
	11	0.67	2.05	0.0137
	14	0.55	0.54	0.0030
	16	0.40	15.48	0.0619
	17	0.37	0.00	<u>0.0000</u>
			$\Sigma=$	0.3218
Semi-active	2	0.76	0.36	0.0027
	10	0.46	0.02	0.0001
	13	0.20	13.30	0.0266
	15	1.07	2.69	<u>0.0288</u>
			$\Sigma=$	0.0582
Inactive	4	0.43	26.59	0.1143
	12	0.65	1.73	<u>0.0112</u>
			$\Sigma=$	0.1256

From the information in Table 6.1 estimates of the probabilities of dyed sand being located in each reservoir were obtained and scaled by the volume contained in each reservoir at 1450 minutes i.e. just prior to the input of dyed material (Table 6.2). This procedure is not completely reliable for several reasons: too few samples were used, especially for the semi-active and inactive reservoirs; dispersion had only occurred for three hours at the time of sampling whereas the standard time interval in the model was 4 hours; and, areas occupied by each reservoir are used in Table 6.1 as a surrogate for the volumes stored in each. The distribution thus obtained should therefore be regarded as an estimate of the actual distribution. Visual inspection of the surficial distribution of dyed sand (Figure 6.3) suggests that the estimate should closely approximate the actual distribution.

Table 6.2 Conversion of volumes of dyed sand in different reservoirs to probabilities that input material will be located in each reservoir after one 4 hour time period.

Reservoir	Total unit volume of dyed sand in reservoir (m ²)	Proportion of dyed sand in reservoir	Proportion occupied by each reservoir by volume at 1450 minutes	Probabilities of dyed sand being in each reservoir at 1690 minutes, scaled by volume at 1450 minutes
Active	0.322	0.637	0.403	0.397
Semi-active	0.058	0.115	0.483	0.060
Inactive	0.126	0.248	0.115	0.543

The proportion of dyed sand in each reservoir at 1690 minutes (Table 6.2) can be used to estimate the redistribution of input material directly for the 1450-1690 minutes period. The method described subsequently was used for other time periods to which the data required to use this approach were not available. From Table 6.2, $d_{ea} = 0.397$, $d_{es} = 0.060$, and $d_{ei} = 0.543$. Calculation of the probabilities assumes that they scale linearly as volume changes. This is almost certainly not the case but is a necessary assumption in the absence of further data. Errors are introduced by this assumption such that the sum of predicted increments of sediment in the active, semi-active and inactive reservoirs ($\sum I_p$) can differ from the value of $e(1-k)$. When this occurs the predicted values are incremented by the proportion of this error that would be expected to be accounted for by each reservoir based on the d_{ep} probabilities and the volume distribution i.e. the volume in the j th reservoir has $([e(1-k) - \sum I_p] \times d_{ep} \times w_{pp} / \{\sum d_{ep} w_{pp}\})$ added. This correction needs to be applied so that there is no 'missing' or extra sediment introduced by the calculation.

Estimation of the transition matrix probabilities has been demonstrated by Kelsey *et al.* (1987) to be the critical control of model behaviour. The first step therein is to estimate the elements of the column vector, r , which gives the probabilities of material from each reservoir entering the

absorbing state between time t and $t+1$. The total mass of sediment output from the tray ($\sum G_b$) was measured for each time period, and converted to a volume. This is not directly comparable with the measured volumes within the tray because of the presence of voids in the latter case. The ratio between sediment volume and total volume including voids was measured for depths of sediment between 0.05m and 0.15m, giving a mean value of 1.66 ± 0.02 ($n=5$). Volumes of sediment input to and output from the tray were therefore multiplied by 1.66 to make them comparable with the surveyed volumes. Total sediment output is therefore equivalent to $1.66 \times \sum G_b / 2650$, and is denoted Q_{bt} (m^3) with G_b in kg. This material is derived from both throughput of sediment input at the head of the tray and erosion of that stored within it. The volume of throughput material is equal to $e.k$. Thus the volume derived from within the tray in a unit time period is $Q_{bt} - e.k$. The 'residence time' of sediment within a reservoir is defined as the volume of sediment in that reservoir divided by the average sediment transport rate for that reservoir, which is only known for the active reservoir. For this reservoir the residence time, RT_a , is defined as, $RT_a = v_a / (Q_{bt} - e.k)$. Since transport rates through the other reservoirs are not known, their residence times have to be estimated and this is a weakness in the model (Kelsey *et al.*, 1987). Following Kelsey *et al.* the residence times for the reservoirs were estimated by the following equations;

$$\begin{aligned} RT_a &= v_a / (Q_{bt} - e.k) \\ RT_s &= (v_a + v_s) / (Q_{bt} - e.k) \\ RT_j &= (v_a + v_s + v_j) / (Q_{bt} - e.k) \\ RT_n &= (v_a + v_s + v_j + v_n) / (Q_{bt} - e.k) \end{aligned} \quad (6,9).$$

Thus the residence times for all reservoirs are indices of their volumes. The results of this approximation technique were reasonable given the magnitude of throughput times for the input sediment (Figure 6.1a), and Kelsey *et al.* (1987) made a similar observation on the basis of their field data. For each reservoir $(1/RT) / \sum (1/RT)$ gives the proportion of the total output material that is derived from that reservoir, where $\sum (1/RT)$ is the sum for all four reservoirs. These proportions (ϕ_p) can then be scaled by the output volume and the volume of material in each reservoir at time t to give the probability of material from within each being exported by $t+1$. For the p th reservoir this probability, r_p , is defined as,

$$r_p = \phi_p \times (Q_{bt} - e.k) / v_p \quad (6,10).$$

The elements of matrix Q depend on the probabilities of exchange between reservoirs, which involve both static and dynamic processes. The method used to estimate these involved subdividing each surveyed channel cross-section into different reservoirs at times t and $t+1$. Using reservoir width as a basis, material stored in each reservoir at time t was allocated to the same or a different reservoir at $t+1$ (Figure 6.8), and the width of material involved in each transition recorded. The cumulative data from all 12 cross-sections was then used to derive a matrix of probabilities of destinations of material stored in each reservoir at time t . This is an estimate of Q and has row sums equal to 1. However the row sums in T are equal to 1 by definition, so the estimates of q_{pq} were re-scaled by multiplication by $(1 - r_p)$.

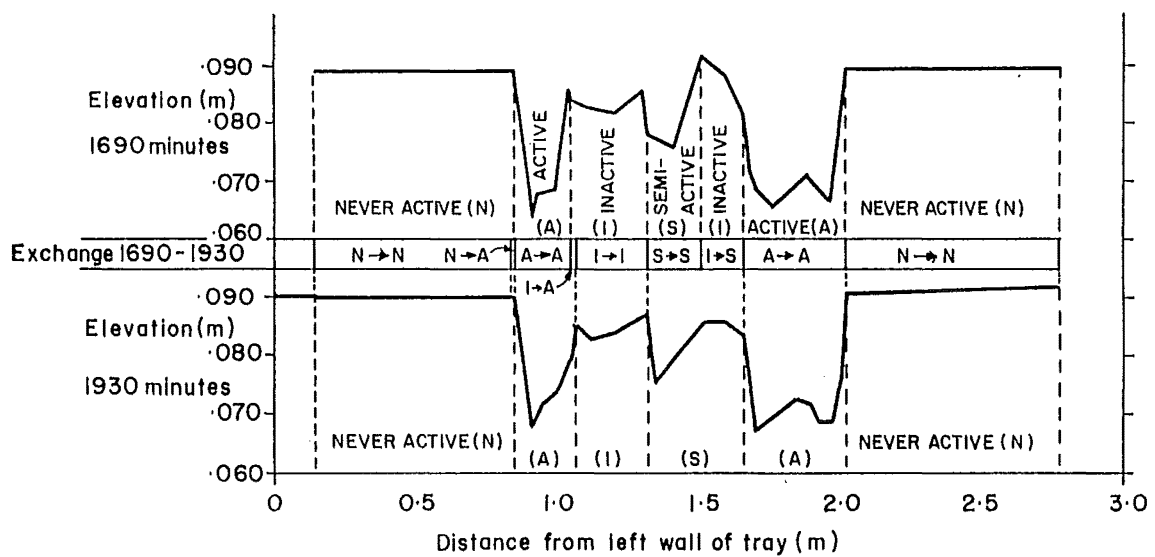


Figure 6.8 Definition of transfers of material between reservoirs at times t and $t+1$, illustrated by the 5m cross-section at 1690 and 1930 minutes (Run 3).

D. An example of the calculation procedure

At 1450 minutes $v = (0 \ 0.2568 \ 0.3090 \ 0.0726 \ 1.0104)$, with all units in m^3 (see Appendix 13 for reservoir volume data). The volumes were calculated from the 12 cross-sections surveyed at this time assuming that all sections except those at 2m and 13m represent a 1m length of the tray. The 2m data were taken to apply from 0.5-2.5m, and the 13m section was used for the reach from 12.5-14.2m. k is taken as 0.1805 and the sediment input between 1450 and 1690 minutes was 36 kg, which converts to $2.255 \times 10^{-2} m^3$ of sediment in the tray. This is the value of e and hence $e.k$ is $4.070 \times 10^{-3} m^3$. Thus $e = (4.070 \times 10^{-3} \ 1.848 \times 10^{-2} \ 0 \ 0 \ 0)$. Using the results of Table 6.2,

$e \cdot D \cdot W =$

$$(4.070 \times 10^{-3} \ 1.848 \times 10^{-2} \ 0 \ 0 \ 0) \begin{pmatrix} 1 & 0 & 0 & 0 & 0 \\ 0 & 0.397 & 0.060 & 0.543 & 0 \\ 0 & 0 & 0 & 0 & 0 \\ 0 & 0 & 0 & 0 & 0 \\ 0 & 0 & 0 & 0 & 0 \end{pmatrix} \begin{pmatrix} 1 & 0 & 0 & 0 & 0 \\ 0 & 1.2068 & 0 & 0 & 0 \\ 0 & 0 & 1.4521 & 0 & 0 \\ 0 & 0 & 0 & 0.3412 & 0 \\ 0 & 0 & 0 & 0 & 0 \end{pmatrix}$$

$$= (4.07 \times 10^{-3} \ 8.85 \times 10^{-3} \ 1.61 \times 10^{-3} \ 3.42 \times 10^{-3} \ 0).$$

However the sum of the 2nd-4th elements in this vector should equal 1.848×10^{-2} , but is actually 1.389×10^{-2} . These elements are thus incremented by 2.93×10^{-3} , 5.32×10^{-4} , and 1.13×10^{-3} respectively, to correct for this error, giving

$$e \cdot D \cdot W = (4.07 \times 10^{-3} \ 1.18 \times 10^{-2} \ 2.14 \times 10^{-3} \ 4.56 \times 10^{-3} \ 0).$$

Since this time period was that during which the data on redistribution probabilities were collected, the third column of Table 6.2 (proportion of dyed sand in each reservoir) serves as an alternative estimate of $D \cdot W$. Using these values gives,

$$e \cdot D \cdot W = (4.07 \times 10^{-3} \ 1.18 \times 10^{-2} \ 2.13 \times 10^{-3} \ 4.58 \times 10^{-3} \ 0),$$

which are within 1 % of those calculated previously, the differences being due to roundoff errors.

Total sediment output (Q_{bt}) during the period 1450 to 1690 minutes was 43.40 kg, equivalent to $2.719 \times 10^{-2} m^3$ of in-tray volume. With $e.k = 4.070 \times 10^{-3} m^3$, the output derived from within the tray during this period was $2.312 \times 10^{-2} m^3$. Given the row vector v above, residence times are calculated from equation (6,9) as ;

$$RT_a = 0.2568 t / 2.312 \times 10^{-2} = 11.11 t$$

$$RT_s = (0.2568 + 0.3090) t / 2.312 \times 10^{-2} = 24.48 t$$

$$RT_j = (0.2568 + 0.3090 + 0.0726) t / 2.312 \times 10^{-2} = 27.62 t$$

$$RT_n = (0.2568 + 0.3090 + 0.0726 + 1.0104) t / 2.312 \times 10^{-2} = 71.33 t,$$

where t is the time interval between measurements (= 4 hours). The proportions of output material derived from each reservoir and the probabilities of material being exported during a time

period (equation 6,10) are:

	ϕ_p	r_p
Active	0.4970	0.0448
Semi-active	0.2256	0.0169
Inactive	0.2000	0.0637
Never active	0.0774	0.00177

The probabilities of exchange between reservoirs were estimated from surveys of the 12 cross-sections at 1450 and 1690 minutes. These exchanges are documented in Table 6.3.

Table 6.3 Exchanges of sediment between reservoirs from 1450 to 1690 minutes, Run 3. Units are metres of channel which underwent each transfer. Bracketed figures express the transitions from each state at 1450 minutes as a proportion of all transitions from that state.

State at 1450 minutes	State at 1690 minutes			
	Active	Semi-active	Inactive	Never active
Active	3.99 (0.7112)	1.52 (0.2709)	0.10 (0.0178)	— (—)
Semi-active	1.24 (0.2070)	1.29 (0.2154)	3.46 (0.5776)	— (—)
Inactive	0.15 (0.0980)	0.14 (0.0915)	1.24 (0.8105)	— (—)
Never active	0.25 (0.0144)	0.04 (0.0023)	— (—)	17.11 (0.9833)

The row sums of T are equal to 1 so the bracketed numbers in Table 6.3 require scaling down by $(1 - r_p)$ to obtain the probability associated with each transition. This gives;

$$T = \begin{pmatrix} 1.0000 & 0 & 0 & 0 & 0 \\ 0.0448 & 0.6973 & 0.2588 & 0.0170 & 0 \\ 0.0169 & 0.2035 & 0.2118 & 0.5678 & 0 \\ 0.0637 & 0.0918 & 0.0857 & 0.7589 & 0 \\ 0.00177 & 0.0143 & 0.0023 & 0 & 0.9816 \end{pmatrix}$$

Calculating the result $v \cdot T + e \cdot D \cdot W$ is now a simple procedure which yields,

$$v.T + e.D.W = (0.0272 \ 0.2702 \ 0.1426 \ 0.2395 \ 0.9918).$$

The values measured at the end of this time period are compared with these predictions subsequently.

Flushing times can be estimated from equation (6,7). $(I - Q)$ is;

$$(I - Q) = \begin{pmatrix} 0.3207 & -0.2588 & -0.0170 & 0 \\ -0.2305 & 0.7882 & -0.5678 & 0 \\ -0.0918 & -0.0857 & 0.2411 & 0 \\ -0.0143 & -0.0023 & 0 & 0.0184 \end{pmatrix}$$

$N [(I - Q)^{-1}]$ is thus;

$$N = \begin{pmatrix} 8.891 & 4.016 & 10.08 & 0 \\ 6.773 & 4.765 & 11.70 & 0 \\ 5.793 & 3.223 & 12.15 & 0 \\ 7.757 & 3.717 & 9.299 & 54.35 \end{pmatrix}$$

The row sums of N are the flushing times and are given in Table 6.4 along with their standard deviations (equation (6,8)). These results are interpreted below.

Table 6.4 Flushing times computed from the transition matrix derived using Run 31450-1690 minutes data.

Reservoir	Flushing Time (time periods)	(hours)	Standard deviation (time periods)
Active	22.99	92.0	31.61
Semi-active	23.24	92.9	31.70
Inactive	21.16	84.6	30.15
Never active	75.12	300.5	94.93

6.2.2 Model testing and application

A. Model checking against the 1450-1690 minutes data. The model has been calibrated with data collected from the 1450-1690 minutes period. Table 6.5 summarises the comparison between observed sediment storage changes and the model predictions for this period. Given that this was the calibration period perfect agreement between measured and modelled sediment storage changes might be expected. There are several reasons why this is not the case, most significant among which are: the sand tracing results rely on a small sample of the total dyed sand

input and are therefore subject to sampling errors, which affect the estimates of k and the probabilities in \mathbf{D} ; the matrix \mathbf{Q} is based on areas within different reservoirs at the 12 cross-sections rather than on volumes throughout the entire tray, again producing a sampling problem. The model predictions for the semi-active and inactive reservoirs, both of which underwent substantial change during this time period, are within 4.1 % and 3.9 % of the measured changes, respectively. Where smaller volume changes occurred the magnitudes of absolute errors in the model were similar but equate to much larger percentage errors (144 % for the active reservoir and 31 % for the never active). The perfect prediction of the sediment output is a consequence of the parameter estimation procedure.

Table 6.5 Modelled and measured sediment output and sediment storage changes, 1450-1690 minutes, Run 3. All units are m^3 .

	Volumes measured at 1450 minutes	<u>Volume change, 1450-1690</u>		Difference between measured and modelled changes, 1450-1690
		Measured	Modelled	
Sediment output	—	0.0272	0.0272	0.0000
Active	0.2568	0.0055	0.0134	-0.0079
Reservoir				
Semi-active	0.3090	-0.1599	-0.1664	0.0065
Inactive	0.0726	0.1736	0.1669	0.0067
Never active	1.0104	-0.0269	-0.0186	-0.0083

B. Model performance when applied to other data. Sediment output and volume distribution data are available for 5 consecutive time periods each of 240 minutes duration after the calibration period. The model was tested against these data sets, assuming that the patterns of sediment redistribution (i.e. \mathbf{e} , \mathbf{D} and \mathbf{T}) during the 1450-1690 period were replicated in the later periods. Table 6.6 compares the modelled and measured outputs of sediment from the tray during these periods and uses the net change of volume of sediment stored within the tray as an indication of stream condition. The data show that the model severely over-predicts the sediment output from the tray for all periods except the calibration period. However, this is the only period during which there was net degradation and the data of Chapters 4 and 5 have suggested that sediment output rates are appreciably greater during degradational episodes than at other times. To test the influence exerted by stream condition over model performance, the measured and predicted changes in sediment storage patterns can be compared (Figure 6.9). For one period of stability and one of aggradation (1690-1930 and 2170-2410 minutes) the model predicts changes in sediment storage that are in the correct direction and of approximately correct orders of magnitude. During more rapid aggradation the directions of change in the active and never active

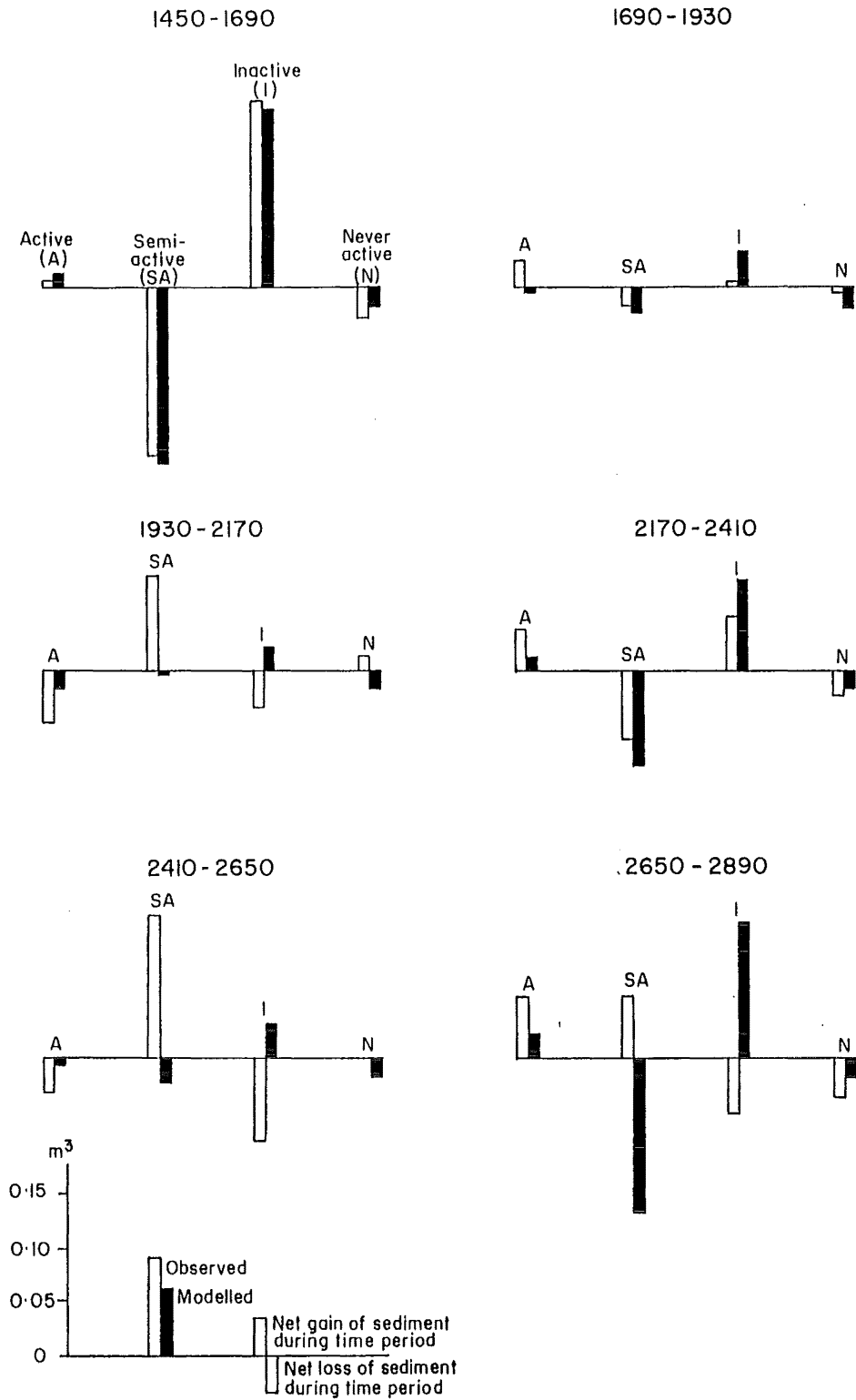


Figure 6.9 Comparison of modelled and observed sediment storages, 1450-2890 minutes (Run 3) based on the 1450-1690 transition matrix.

reservoirs are modelled (2410-2650 and 2650-2890 minutes), but for the other two reservoirs the modelled directions of storage change are without exception incorrect. This is consistent with the idea that during degradation the inactive reservoir gains material at the expense of the semi-active, with the reverse during aggradation (e.g. Figure 5.8). Thus a model developed during a degradational phase might be expected to predict incorrect directions of change during aggradation. The 1930-2170 minutes pattern was closer to that during other aggrading periods than during the stable one. This may reflect the diachronous behaviour of different reaches within the tray with net stability defined as output minus input failing to account for the spatial predominance of aggradation at that time. A similar but inverted argument applies to the 2170-2410 period.

Table 6.6 Modelled and measured outputs of sediment from the sand tray, 1450-2890 minutes, using the transition matrix derived from 1450-1690 minutes data.

Time period (minutes)	<u>Sediment output</u>		Measured-modelled sediment output (m ³)	Net volume change in tray (m ³)	Stream condition
	Measured (m ³)	Modelled (m ³)			
1450-1690	0.0272	0.0272	0.0000	-0.0046	Degrading
1690-1930	0.0235	0.0358	-0.0123	0.0009	Stable
1930-2170	0.0232	0.0370	-0.0138	-0.0006	Stable
2170-2410	0.0203	0.0343	-0.0140	0.0023	Aggrading
2410-2650	0.0118	0.0380	-0.0262	0.0108	Aggrading
2650-2890	0.0106	0.0337	-0.0231	0.0120	Aggrading

These results imply that a single transition matrix cannot account for both aggradational and degradational phases in a stream system. It is possible to estimate transition matrices for the stable and aggrading states, and their performance is now evaluated.

C. Model modifications to account for different channel conditions. Because sediment redistribution data are only available for 1450-1690 minutes, no new estimates can be made of **k** or **D** for the other time periods. These components are left constant and the sensitivity of the model to their variation is addressed subsequently in section E. Only the transition matrix can be re-evaluated, and this was done using the procedure outlined in sub-section 6.2.1C for all five remaining time periods (1690-1930, 1930-2170, 2170-2410, 2410-2650, and 2650-2890 minutes). The resulting transition matrices were as follows (Appendix 12 contains the sediment exchange data from which the **Q** matrices were derived):

$$1690-1930; \begin{pmatrix} 1.0000 & 0 & 0 & 0 & 0 \\ 0.0337 & 0.9118 & 0.0280 & 0.0265 & 0 \\ 0.0378 & 0.2279 & 0.4051 & 0.3292 & 0 \\ 0.0143 & 0.0844 & 0.1605 & 0.7408 & 0 \\ 0.0014 & 0.0086 & 0.0046 & 0 & 0.9854 \end{pmatrix} \begin{matrix} \text{Absorbing (Ab)} \\ \text{Active (A)} \\ \text{Semi-active (S)} \\ \text{Inactive (I)} \\ \text{Never active (N)} \end{matrix}$$

$$\begin{matrix} \text{Ab} & \text{A} & \text{S} & \text{I} & \text{N} \end{matrix}$$

$$1930-2170; \begin{pmatrix} 1.0000 & 0 & 0 & 0 & 0 \\ 0.0299 & 0.8228 & 0.1150 & 0.0333 & 0 \\ 0.0425 & 0.1023 & 0.7126 & 0.1425 & 0 \\ 0.0141 & 0.0294 & 0.2018 & 0.7547 & 0 \\ 0.0015 & 0.0128 & 0.0041 & 0 & 0.9817 \end{pmatrix} \begin{matrix} \text{Ab} \\ \text{A} \\ \text{S} \\ \text{I} \\ \text{N} \end{matrix}$$

$$\begin{matrix} \text{Ab} & \text{A} & \text{S} & \text{I} & \text{N} \end{matrix}$$

$$2170-2410; \begin{pmatrix} 1.0000 & 0 & 0 & 0 & 0 \\ 0.0337 & 0.8348 & 0.1055 & 0.0260 & 0 \\ 0.0189 & 0.0953 & 0.5639 & 0.3219 & 0 \\ 0.0129 & 0.0897 & 0.1127 & 0.7846 & 0 \\ 0.0012 & 0.0193 & 0.0023 & 0.0006 & 0.9767 \end{pmatrix} \begin{matrix} \text{Ab} \\ \text{A} \\ \text{S} \\ \text{I} \\ \text{N} \end{matrix}$$

$$\begin{matrix} \text{Ab} & \text{A} & \text{S} & \text{I} & \text{N} \end{matrix}$$

$$2410-2650; \begin{pmatrix} 1.0000 & 0 & 0 & 0 & 0 \\ 0.0127 & 0.6471 & 0.3341 & 0.0060 & 0 \\ 0.0143 & 0.3507 & 0.4865 & 0.1485 & 0 \\ 0.0051 & 0.0645 & 0.3001 & 0.6304 & 0 \\ 0.0006 & 0.0089 & 0.0059 & 0 & 0.9846 \end{pmatrix} \begin{matrix} \text{Ab} \\ \text{A} \\ \text{S} \\ \text{I} \\ \text{N} \end{matrix}$$

$$\begin{matrix} \text{Ab} & \text{A} & \text{S} & \text{I} & \text{N} \end{matrix}$$

$$2650-2890; \begin{pmatrix} 1.0000 & 0 & 0 & 0 & 0 \\ 0.0139 & 0.6976 & 0.2699 & 0.0187 & 0 \\ 0.0053 & 0.2670 & 0.6684 & 0.0587 & 0 \\ 0.0057 & 0.1721 & 0.2403 & 0.5817 & 0 \\ 0.0005 & 0.0370 & 0.0155 & 0 & 0.9470 \end{pmatrix} \begin{matrix} \text{Ab} \\ \text{A} \\ \text{S} \\ \text{I} \\ \text{N} \end{matrix}$$

$$\begin{matrix} \text{Ab} & \text{A} & \text{S} & \text{I} & \text{N} \end{matrix}$$

The two components of the transition matrices, \mathbf{r} and \mathbf{Q} , reflect the conditions at the start of each period and the sediment storage changes therein. The vector \mathbf{r} is dependent on the reservoir volumes at time t and the sediment output between t and $t+1$. The absolute values of the elements of \mathbf{r} are lower for aggrading than for stable and degrading cases, but which reservoirs have the greatest values of r_p depends on their volumes at time t . \mathbf{Q} depends on the

changes in storage between t and $t+1$, and reflects the predominant transfers associated with each channel condition. It is also sensitive to the distribution of sediment at time t ; although 1930-2170 and 2650-2890 minutes were associated with similar amounts of net aggradation (Table 6.6) their Q probabilities were different. In the former case there was less transfer out of the active reservoir (0.8228 as against 0.6976 for $A \rightarrow A$ exchanges) and inactive (0.7547 vs. 0.5817 for $I \rightarrow I$) reservoirs. In the latter case the active reservoir gained greater proportions of material from both the semi-active and inactive reservoirs than in the former.

The extent to which these differences between the transition matrices affect the performance of the model can be evaluated with reference to Table 6.7 (sediment output) and Figure 6.10 (sediment distribution between reservoirs).

Table 6.7 Modelled and measured outputs of sediment from the sand tray, 1450-2890 minutes, using transition matrices developed separately for each time period. For data from the 1450-1690 matrix see Table 6.6. All volumes are in m^3 .

a) Absolute values.

Time period (minutes)	Measured sediment output	Predicted outputs using transition matrices developed from the time periods indicated				
		1690-1930	1930-2170	2170-2410	2410-2650	2650-2890
1450-1690	0.0272	0.0269	0.0274	0.0207	0.0127	0.0102
1690-1930	0.0235	0.0234	0.0232	0.0200	0.0114	0.0105
1930-2170	0.0232	0.0238	0.0233	0.0207	0.0115	0.0108
2170-2410	0.0203	0.0250	0.0252	0.0203	0.0120	0.0104
2410-2650	0.0118	0.0245	0.0242	0.0209	0.0118	0.0108
2650-2890	0.0106	0.0273	0.0278	0.0213	0.0129	0.0106

b) Differences between measured and predicted values

Time period	Channel condition	Differences between measured and predicted values from the time periods indicated				
		1690-1930	1930-2170	2170-2410	2410-2650	2650-2890
1450-1690	Degrading	0.0003	-0.0002	0.0065	0.0145	0.0170
1690-1930	Stable	0.0001	0.0003	0.0035	0.0121	0.0130
1930-2170	Stable	-0.0006	-0.0001	0.0025	0.0117	0.0124
2170-2410	Aggrading	-0.0047	-0.0049	0.0000	0.0083	0.0099
2410-2650	Aggrading	-0.0127	-0.0124	-0.0091	0.0000	0.0010
2650-2890	Aggrading	-0.0167	-0.0172	-0.0107	-0.0023	0.0000
Mean discrepancy		0.0059	0.0059	0.0054	0.0082	0.0089

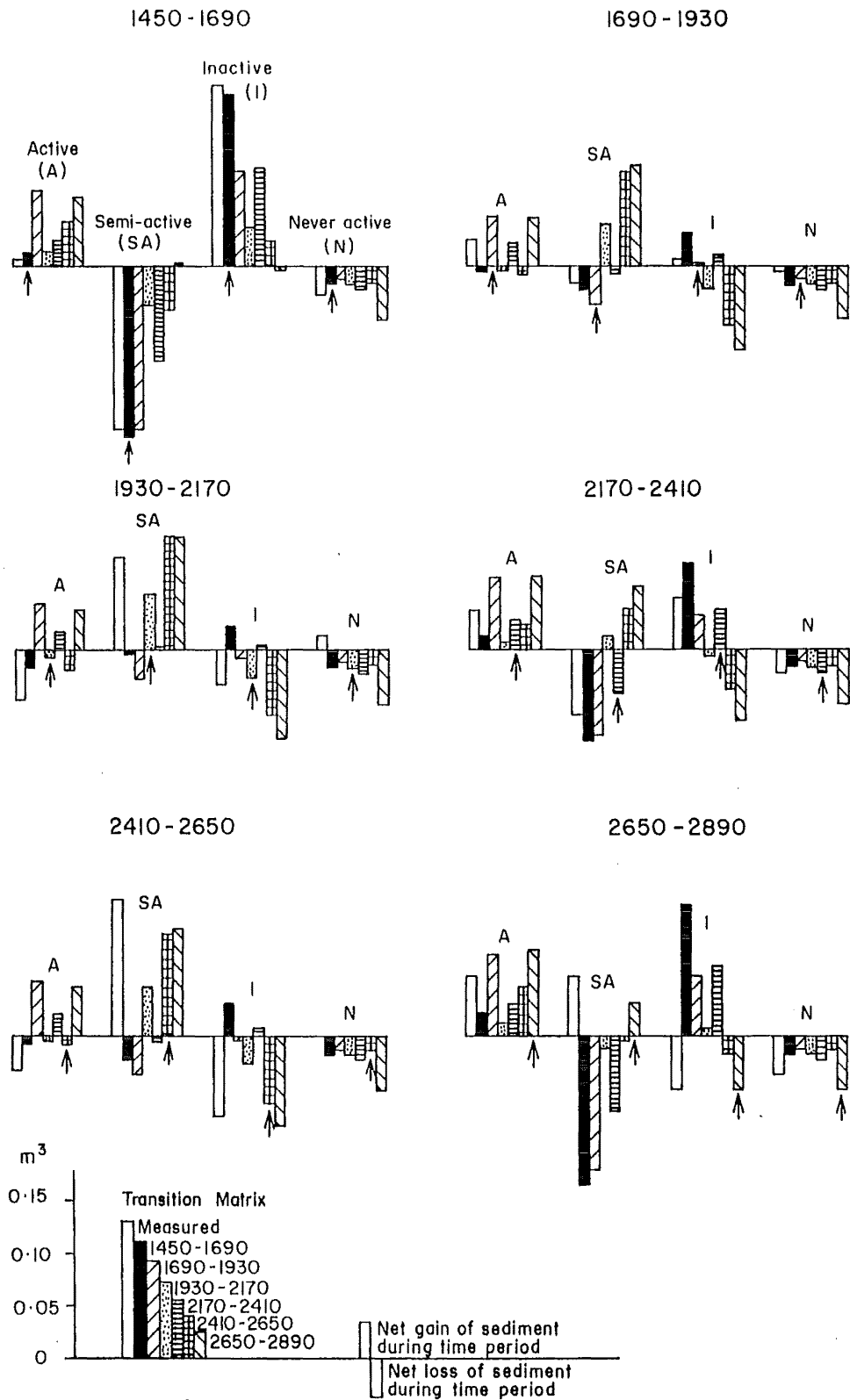


Figure 6.10 Comparison of modelled and observed sediment storages. The results of applying different transition matrices to a particular time period are shown. Arrows indicate the results of the transition matrix based on that particular time period.

Use of the transition matrices based on stable time periods (1690-1930 and 1930-2170) gave accurate predictions of net sediment output for both degrading and stable states (Table 6.7b). Reference to Table 6.6 suggests that these transition matrices perform better when applied to the degrading state than does the matrix from that state when applied to the stable condition. However their predictions worsen as the magnitude of net aggradation increases. The three aggradational phase derived matrices perform poorly when tested against the other channel conditions. Further, that from 2170-2410 when net aggradation was + 0.0023 m³ severely overpredicts the actual sediment output for 2410-2650 and 2650-2890 when net aggradation was about 5 times greater.

The estimation of reservoir volumes follows a similar pattern to net sediment output as regards relative model performance (Figure 6.10; these data are contained in Appendix 13). Note that the performance of transition matrices against the periods from which they were derived is imperfect due in part to the values of k and D being held constant. Although the models may predict net sediment output reliably this can conceal substantial errors in the predictions of storage volume changes in individual reservoirs. Thus, for the 1450-1690 time period the 1690-1930 matrix predicts sediment output to within 0.003 m³ and estimates net change in the semi-active volume precisely. However it overpredicts the increase in sediment stored in the active reservoir and correspondingly underpredicts that in the inactive. The two matrices based on stable time periods and the three on aggrading ones behave somewhat differently, reflecting the different exchanges between reservoirs that occurred in these periods. Net stability during 1690-1930 was associated with small net transfers from the semi-active to the active and inactive reservoirs. During 1930-2170 this situation was reversed and the magnitudes of the exchanges were greater, but the net result was the same. Similar contrasts exist for the aggradational phases. During 2410-2650 the semi-active reservoir gained material from both the active and the inactive, but during the subsequent 4 hour period (2650-2890) when the rate of aggradation increased, both the active and semi-active reservoirs gained material, with a substantial input derived from erosion of the never active reservoir. The period when the rate of aggradation was slower (2170-2410 minutes) shows yet another pattern, with the inactive reservoir gaining material from the semi-active. This pattern would usually be taken as indicative of degradation, and further illustrates that net sediment storage change (output minus input) fails to account for patterns of aggradation and degradation within the tray. An interesting example is provided by the matrices derived from 1930-2170 and 2410-2650 when the exchanges between reservoirs were similar, although the former period was one of stability and the latter one of aggradation. The matrices based on each period predict the directions of storage changes in each reservoir and are broadly correct in magnitude when applied to the other data set (Figure 6.10). This shows the importance of the types of sediment exchanges that occur on model performance.

To summarise these results it appears that transition matrices based on time periods when channel conditions were different can estimate net sediment output for other time periods when

similar changes in net sediment storage occurred. However the range of different channel states that can be associated with net stability, aggradation and degradation, and the spatial distribution of these conditions within a reach, precludes accurate prediction of changes in the sediment distribution between reservoirs except where those changes were similar in the data used for model parameter estimation.

D. Description of differences between transition matrices. The characteristics of each transition matrix can be described using the fundamental matrix, \mathbf{N} . It was stated in sub-section 6.2.1 that the row sums of \mathbf{N} are equal to flushing times, defined as the expected (i.e. mean) lengths of time for a particle from a given reservoir to be taken up by the absorbing state (i.e. exported from the tray) (Kelsey *et al.*, 1987). Table 6.4 presents the flushing times derived for the 1450-1690 period. Table 6.8 compares these with those from the matrices derived for each of the other 5 time periods. As the sediment output rate declined between the time periods 1450-1690 minutes and 2650-2890 minutes so the flushing times for the active, semi-active and inactive reservoirs increased (except for 1690-1930 and 1930-2170 minutes where both sediment output and flushing times were not significantly different). It is also notable that the flushing times for these three reservoirs and their standard deviations are approximately equal in all 6 cases. This implies that whichever reservoir a particle commences in, its most probable transit time to the absorbing state is about equal. Sediment transport rates through the active reservoir exceed those in the semi-active by several orders of magnitude, and there is zero transport in the inactive reservoir, by definition. The equality in flushing times suggests that interaction (both static and dynamic) between these three reservoirs is such that it balances out the differences in bedload transport rates (i.e. residence time) between them. This result appears independent of channel condition. Thus, although during aggradation the semi-active reservoir gains material from the inactive and its flushing time increases, its exchanges with the inactive reservoir ensure that this latter reservoir has a comparable flushing time. Similar arguments apply for the other reservoirs. Kelsey *et al.* (1987) also noted a broad equivalence in flushing times between different reservoirs and different reaches of channel. They noted that this result is a direct consequence of the probabilities contained in the transition matrix, and it is of interest that similar results are derived from their situation in Redwood Creek where there is limited interaction between reservoirs, and from that modelled herein where considerable interaction occurs (in the Redwood Creek case the probabilities on the leading diagonal of \mathbf{Q} were always greater than 0.9). Their results did not always suggest equality of flushing times and this result does not appear to be an artifact of the methods used to estimate the elements of \mathbf{Q} .

The increase in flushing times when aggradation occurred is a reflection of the reduction in sediment output from the tray at these times. It was shown in sub-section 6.1.2 that only 37 % of tracer material introduced to the tray during 1450-1690 had been exported by 2890 minutes i.e. in about 6 time periods. If the degradational trend during 1450-1690 minutes had continued, a flushing time of about 23 ± 32 time periods would be expected for this material. This is four times

as long as the time taken for 37 % to be exported. The actual time taken for flushing would have exceeded the estimate based on conditions at 1450-1690 minutes since periods of channel stability and aggradation by 2890 minutes were associated with considerably longer flushing times than occurred over the period 1450-1690.

Table 6.8 Mean flushing times and residence times for different estimates of Q based on observed exchanges of sediment between reservoirs in 6 time periods. Flushing time standard deviations in brackets. Units are time periods of 4 hours duration.

a) Flushing times

Reservoir	Transition matrix					
	1450-1690	1690-1930	1930-2170	2170-2410	2410-2650	2650-2890
Active	22.9 (31.6)	32.8 (46.4)	33.5 (47.1)	42.6 (61.3)	82.6 (116.7)	103.9 (147.1)
Semi-active	23.2 (31.7)	33.9 (47.4)	32.8 (46.6)	45.9 (63.8)	82.7 (116.8)	105.4 (148.2)
Inactive	21.2 (30.2)	35.5 (48.6)	35.1 (48.3)	46.4 (64.2)	84.3 (117.9)	105.6 (148.4)
Never active	75.1 (94.9)	98.5 (124.1)	85.4 (106.4)	84.0 (103.9)	144.4 (178.3)	122.2 (161.6)

b) Residence times

Reservoir	Transition matrix					
	1450-1690	1690-1930	1930-2170	2170-2410	2410-2650	2650-2890
Active	11.1	13.5	15.1	14.7	35.8	37.2
Semi-active	24.5	21.2	22.1	28.4	56.0	81.6
Inactive	27.6	33.9	35.4	41.9	90.9	110.8
Never active	71.3	84.5	86.9	103.0	213.5	259.1

Flushing times can also be compared with residence times (Table 6.8b). These are not equivalent as the flushing time measures the mean time taken for a particle to be output from the tray, whereas the residence time measures the mean length of time spent in a particular storage location. For the inactive reservoir, flushing and residence times are approximately equal, whereas for the two more frequently mobilised reservoirs the flushing times are longer than their residence times. Where flushing time exceeds residence time it suggests that between being in the active or semi-active reservoirs and entering the absorbing state, the average particle passes through a less active state. Thus the average particle from the active reservoir spends some time

in the semi-active and / or the inactive reservoir before being absorbed, and that from the semi-active reservoir spends some time in the inactive. As it cannot enter a less active state, the material from the inactive reservoir has a residence time equal to or slightly greater than its flushing time. This is also the case for the never active material which must pass through a more active reservoir before entering the absorbing state, so it inevitably has a shorter flushing time than residence time. The 1690-1930 time period matrix appears to violate this requirement, and this could be a result of the large flushing time standard deviation for the never active reservoir under this model.

A further explanation for the flushing time-residence time differences is due to the contrast between static and dynamic transfers of sediment. Residence times assume only dynamic transfer i.e. they are calculated in terms of net volumes of sediment stored within a reach. Flushing times are based on both static and dynamic transfers, and thus take account of static transfers occurring as a consequence of aggradation, degradation, and channel abandonment and re-occupation processes. The net effect of these processes is to cancel out differences in sediment mobility due to variations in sediment transport rates between the reservoirs. Whatever changes occur in a channel the equality of flushing times appears to be preserved.

The results of the analysis of flushing times can be summarised as follows: firstly, the three most active reservoirs have approximately equal flushing times and flushing time standard deviations; second, the flushing times increase as the rate of aggradation increases (i.e. as sediment output decreases in the present case where the input rate was constant); third, the relationship between residence times and flushing times is as would be expected i.e. residence times for the active and semi-active reservoirs are less than their flushing times, with the reverse situation for the inactive and never active ones.

E. Model sensitivity to input parameters. Sub-sections 6.2.2C and D have illustrated the sensitivity of model results to changes in the transition matrix. It is also important to obtain reliable estimates for the elements of r , which in are turn dependent upon residence time estimation. The procedure used for this last mentioned estimate is imprecise and makes the implicit assumption that the active reservoir empties before the others are evacuated (Kelsey *et al.*, 1987). This is unrealistic and ignores the actual processes of sediment exchange between reservoirs. It is extremely difficult to compute reliable estimates of residence time even for the active reservoir, since the mean time considerably exceeds the median due to extremely long residence times for some particles (Dietrich *et al.*, 1982). The consistency between computed residence and flushing times in the present study gives grounds for cautious optimism that the method of residence time estimation is reliable.

What form of variation might be expected in the transfer constant k is unclear. The value of 0.1805 was derived from a period of general degradation within the tray when a relatively high

proportion of sediment throughput could be expected. This may lie towards the upper end of the range of possible values. Throughput material accounted for between 18 % (1450-1690 data and transition matrix) and 39 % (2650-2890 data and matrix) of the output under different channel conditions. The model structure is such that variations in k affect the residence time determination and hence the elements of T in a way which causes measured and modelled sediment outputs to be equal when applied to the data from which the transition matrix was estimated. The effects of varying k on the distribution of sediment between reservoirs are noticeable but less important than other influences. The differences in predicted volumes between arbitrarily chosen values of k of 0.0 and 0.3 for the 1450-1690 data and transition matrix are, 0.0045 m^3 , 0.0011 m^3 , 0.0008 m^3 and 0.000 m^3 for reservoirs of decreasing mobility (note that the transition matrix was left unaltered, although varying k has a small effect on the estimates of r and the elements of Q). These variations are considerably less than most of the measured-modelled differences resulting from application of any of the 6 transition matrices to any of the data sets, and would have little effect on overall model performance (Figure 6.10).

Table 6.9 Sensitivity of the 1450-1690 minutes data and transition matrix to variations in redistribution probabilities. The estimates of these used in the model were; $d_{ea} = 0.3970$; $d_{es} = 0.0599$; $d_{ei} = 0.5430$, with appropriate scaling taking place to account for relative volumes of sediment stored in each reservoir.

d_{ea}	d_{es}	d_{ei}	Modelled volumes in reservoirs (m^3)			Differences between actual modelled values and values predicted when d_{ea} , d_{es} , and d_{ei} were varied (m^3)		
			Active	Semi-active	Inactive	Active	Semi-active	Inactive
0.4	0.0	0.6	0.2714	0.1405	0.2404	-0.0012	0.0021	-0.0009
0.4	0.6	0.0	0.2650	0.1523	0.2349	0.0052	-0.0097	0.0046
0.2	0.1	0.7	0.2656	0.1447	0.2420	0.0046	-0.0021	-0.0025
0.9	0.1	0.0	0.2747	0.1426	0.2349	-0.0045	-0.0000	0.0046
0.4	0.1	0.5	0.2696	0.1438	0.2389	0.0006	-0.0012	0.0006
0.1	0.4	0.5	0.2610	0.1528	0.2385	0.0092	-0.0102	0.0010

Actual values								
0.3970	0.0599	0.5430	0.2702	0.1426	0.2395			

Alteration of the redistribution probabilities contained in D would also affect model results. The maximum likely effects are tabulated in Table 6.9. These data show that the differences between the effects of extreme values of d_{ea} , d_{es} and d_{ei} and the actual modelled values are generally minor. Only in a few cases do the effects approach differences of 0.01 m^3 , and would generally

make little impact on the form of Figure 6.10.

This brief consideration of model sensitivity confirms the view of Kelsey *et al.* (1987) that it is the transition matrix, T , which dominates model performance. However this is for a comparison of the model performance when applied to channel conditions that are different from those during the parameter estimation period. Where the aim is to apply a model of this type to a situation in which channel behaviour is as it was for parameter estimation then the errors introduced by incorrect specification of k and D can be expected to become relatively more important.

E. Results of repeatedly running the storage model. As a further illustration of the changes in sediment storage predicted by the model, the transition matrix based on 1450-1690 data was run repeatedly using the distribution of sediment between reservoirs at 1450 minutes as the starting point. After 4 iterations (Figure 6.11) there were no significant changes in any of the storage volumes except the never active reservoir, or in sediment output rate. This continued until 50 iterations had been performed (the first 10 are shown in Figure 6.11). The reason for these patterns is that the model is specific to a degrading channel condition. However the total volume of sediment eroded during degradation is limited, and after 4 iterations this limit had been reached. The model then maintains sediment transport by continuous channel widening (i.e. reduction in the never active reservoir volume), which would not continue so regularly or for so long in practice, where the rate of decline of volume in the never active reservoir would reduce through time. The model appears to attain an equilibrium state rapidly. As degradation occurs so the transition and redistribution matrices would require modification as the probabilities of particular sediment exchanges were altered. This would cause model behaviour to be modified and the trends in storage volumes shown in Figure 6.11 would be reversed.

Use of this type of model to predict long term changes in sediment distribution requires that allowance is made for changes in the probabilities of sediment exchanges taking place, which occur as a direct consequence of the redistribution. Incorporation of such a feedback mechanism into the model would require more information on the redistribution of input sediment under different channel conditions, enabling better estimates of k and D to be made.

6.2.3 Uses and limitations of the modelling procedure

The finite Markov chain modelling approach utilised herein has proved to be of use in describing the exchanges of sediment between storage reservoirs. The requirement for alteration of model parameters when the channel state changes leads to problems in the present example since there is no data on sediment dispersion available for either stable or aggrading conditions. Development of an integrated dynamic model which contains built-in redefinition of the probabilities of inter-reservoir exchanges as channel condition changes is not possible with the data available. However the most important component of the model in terms of the sensitivity of

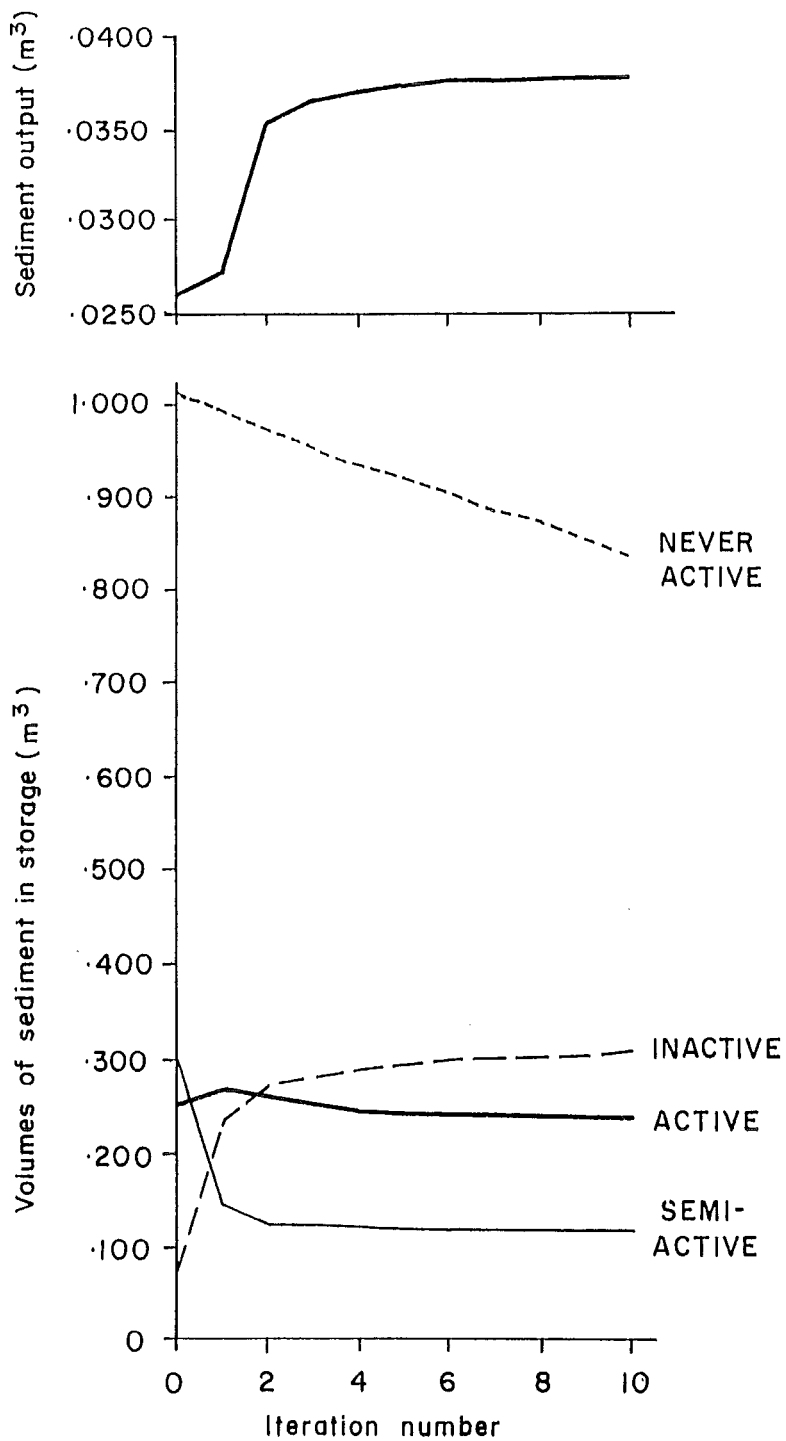


Figure 6.11 Results of running the model with the 1450-1690 minutes transition matrix 10 times. The data at $t=0$ was the distribution of sediment measured at 1450 minutes. Each iteration represents one 4 hour period.

the model predictions to its variation is the transition matrix, \mathbf{T} . This can be estimated from available data and the results discussed above suggest that variation in the elements of this matrix accounts for most of the variation in sediment exchanges between different channel states.

Obtaining a more reliable model would depend in part on improvement in the procedure for estimating the probabilities in \mathbf{T} . These are based on the estimated residence times for sediment in the different reservoirs, and on estimates of the probabilities of static and dynamic exchanges of sediment between reservoirs. The procedure for estimating residence times is inexact (Kelsey *et al.*, 1987) and information on transport rates of material through different reservoirs is required to improve these estimates. This could be obtained relatively easily in the laboratory by placing tracer materials within each reservoir and monitoring their dispersion. However, these would have to be placed throughout the full range of locations of different mobility within each reservoir (Dietrich *et al.*, 1982) and a considerable time could be required before sufficient material was recovered to enable reliable computation of mean residence times. In the present model, as in that of Kelsey *et al.* (1987), the procedure for estimation of residence times produced results which appear reasonable when compared with other information. Kelsey *et al.* estimated the elements of matrix \mathbf{Q} by a procedure based on residence times and the area of active erosion of each reservoir observed in field surveys and from aerial photographs. The data used herein enable a more precise determination of these probabilities than they were able to achieve, but combines static and dynamic transfers. Application of this model to a prototype river would require careful consideration of the definitions of the different reservoirs; in the laboratory these were easily defined based on the presence / absence of bedload transport and the depth of water cover. Such definitions could not be applied in a prototype situation. It would be useful to be able to differentiate static and dynamic transfers of material. This partition could be assessed in the laboratory using tracer material located within the different reservoirs but would be difficult to specify precisely.

The model developed above explicitly assesses the redistribution of material input to a reach from upstream. This component is useful in enabling the sources of output sediment to be evaluated, and it is notable that material coarser than the median size was exported from the sand tray more rapidly than finer material.

Application of this sort of model to field situations should be feasible, but there would be significant problems involved in specifying sediment throughput, redistribution and exchange, and the sediment tracing technique used in the laboratory would be extremely difficult to apply reliably. Further, the role of fluctuating discharge in the field would cause complications. The never active reservoir as defined herein is analogous to flood deposits in a prototype river, often taking the form of low terraces which become vegetated between periods of activity (e.g. the Kowai River example in Chapter 5). For a model concerned with the part of the river bed that is active at the 'dominant discharge' this serves as a component of the absorbing state and can be

modelled as such. However where longer temporal scales are considered this can be regarded as a reservoir with low but significant activity, as was done by Kelsey *et al.* (1987). Its interactions with both less active reservoirs and the more active ones are important in the prototype context. Rather than trying to build them into one model it may be useful to use two parallel models one of which focuses on the active - semi-active - inactive - never active - absorbing states as defined herein, while the other treats the first three together as 'regularly mobilised' and adds two or more less regularly mobilised subdivisions of the never active reservoir.

 ERRATA

In applying this model type to a prototype situation the long-term changes in channel condition which exist in the particular location under investigation would need to be taken into account. Kelsey *et al.* (1987) described a situation undergoing net aggradation although there were periods of both aggradation and degradation within this. Similarly, the transition matrices described herein apply to aggrading, stable or degrading states specifically. Application of the model to different rivers or to different reaches of the same river would require re-estimation of model parameters. Reliable application of the modelling scheme is thus dependent on the availability of a substantial amount of field data.

6.3 Discussion and conclusions

During the course of the present Chapter sediment tracing data have been used both qualitatively and quantitatively. The data on tracer output from the sand tray confirm the suggestion made by Kelsey *et al.* (1987) that the mean transit time for bed sediment particles far exceeds the median. The shape of the transit time frequency distribution is strongly positive skewed, and knowledge of this shape is important if transit times are to be reliably utilised. The transit time frequency distribution is analogous to the age distribution of sediment in a reservoir (Eriksson, 1971) and under certain circumstances this can be reliably evaluated (e.g. Nakamura (1986) used the development of even-aged forest stands to estimate this function). However, residence times cannot be readily calculated within the most active parts of a river bed. Even in the controlled and rapidly evolving stream system in the sand tray much of the tracer material remained stored within the channel at the end of the experiment. The most useful quantitative information derived from this experiment were the estimates of the transfer constant, k , and probabilities of sediment entering different reservoirs within a given time period, d_{ea} , d_{es} , and d_{ei} . None of these quantities rely on the full residence time frequency distribution. Because a large volume of tracer sand was used and the area where it could be deposited was only about 18 m², there was no need to attempt to recover all of the tracer material for these calculations. The sampling procedure adopted was adequate for present needs but it would be impossible to use an equivalent volume of tracer in a prototype river. In most cases the use of tracers for estimation of residence times and associated parameters will not be feasible, and indirect methods of obtaining such estimates have to be relied upon. Although the methodology of reservoir theory is well understood (e.g. Eriksson, 1971; Dietrich *et al.*, 1982) its applications are limited to situations where the data

required for its use are available. Nakamura (1986) and Nakamura *et al.* (1987) have obtained interesting results with this technique as noted above, and Dietrich *et al.* (1982) presented a similar example using the age distribution of cottonwood trees surveyed by Everitt (1968). The results of the present study confirm Dietrich *et al.*'s (1982) conclusion that approximate sediment budget estimates can be made using readily obtained information, but that the development of more accurate budgets requires further detailed long-term study.

It is possible to be somewhat more optimistic about the qualitative results of the tracing work. The observed patterns of sediment dispersion reflected the nature of channel activity at the time of introduction of the dyed sand. Dispersion was rapid with material becoming locally concentrated in depositional locations along the entire length of the tray. Mosley (1978) noted rapid dispersion and argued that bed waves would attenuate rapidly as a consequence. As was noted in Chapter 2, this conclusion ignores interaction between the tracer material and the rest of the bed sediment. Pickup *et al.* (1983) assumed that the shape of a bed wave is not constant as a result of dispersion, but this also is not a necessary conclusion. It is possible that dispersion leads to wave attenuation but the dispersion effect can also be countered by the deposition of material input from upstream or from localised bank erosion (e.g. Roberts and Church 1986). Localisation of deposition was clearly illustrated by the experiment conducted in Run 3 herein, and has also been noted from prototype situations (Kondolf and Matthews, 1986).

With equal dispersion from and concentration in a particular reach, a situation where a bed wave remains constant in terms of both size and position can be envisaged. Were migration to occur, a kinematic wave explanation could be used to explain how wave shape can be maintained during migration, even though particles derived from within the wave are dispersed. So long as the input of material from further upstream was equal to the output in both volume and relative location, wave form could be preserved. The kinematic wave hypothesis serves purely as an illustration of the fact that bed waves do not necessarily diminish in size as they migrate downstream. However, a kinematic wave is a poor approximation of how sediment transfer processes actually operate. Sediment sources and loci of deposition are spatially restricted and depend upon lateral and vertical alterations of channel form. The deposits formed at any one time can be viewed as unit bars which may coalesce to form complex features. Sediment sources are produced by local erosion of both channel and bar deposits. As a bed wave migrates downstream so sediment is eroded and re-deposited and the net effect of many such processes acting together could produce wave growth, stasis or decline as it moves downstream. The data used in developing the model of bed wave behaviour introduced in Chapter 5 suggested that whereas the aggradational phase tends to affect the entire width of the channel, degradation can be confined to a narrower part of the section. Thus the material which was deposited in the form of a bed wave at one location may remain in that location as other sediment is evacuated during degradation. This eroded material can then be responsible for the growth of a bed wave at a depositional location further downstream. In this way a waveform can be translated downstream but not all of the

sediment comprising it is necessarily relocated.

Such a process of wave translation need not occur in all circumstances. It is also possible for rapid attenuation to occur, and in the case of exogenous waves the material which produces the wave may remain as a relatively coherent mass. In the Kawerong River (Pickup *et al.*, 1983) this would appear likely as the sediment producing the waves had been periodically eroded from mining waste dumps, and this material caused the Kawerong to change from a narrow boulder-bed gully to a wide braided river occupying the whole of the valley width (Pickup, 1988). In other cases where there are large increases in sediment load, especially if it is of different calibre from the existing bed material, a similar degree of wave coherence may be expected. This would apply to many of the exogenous wave forms reviewed in Chapter 2. In the laboratory experiments reported here the wave form is independent of its constituent material. In the Kowai River this is also the case once the sediment reaches Porters Reach. Prior to this it is possible although unproven that the sediment periodically eroded from the Foggy River fan remains as a coherent unit until its initial deposition within this reach. Given the narrow channel between these two locations and the lack of sediment storage areas therein, this seems quite plausible.

A further sub-classification of exogenous bed waves is suggested by the preceding discussion. This separates those in which the wave is formed of material which undergoes minimal exchange with the underlying bed material from those where this exchange is significant. The former situation is most likely to arise where the wave is produced by relatively fine material supplied from an exogenous source. This is the case in the Kawerong River example, and also in the East Fork River where sand accumulations migrate over a gravel pavement (Meade, 1985). In the latter case the wave form migrates regularly downstream, associated with an annual flood season, and the same material remains within the wave as this occurs. Minimal exchange could also arise if a channel was to be overloaded with sediment during a high magnitude event. One response to this could involve migration of the wave through the river system with minimal interaction between this material and the host bed sediment. As such a wave migrates further downstream the degree of interaction may rise (as the wave becomes smaller relative to the magnitude of normal sediment inputs to the channel) and may be re-classified as a case where interaction occurs. Where there is appreciable sediment interaction, exogenous waves may behave similarly to endogenous ones, as was suggested in Chapter 5 on the basis of introduction of an exogenous bedload pulse to the sand tray. Where this interaction is minimal, wave behaviour may be distinctively different and involve the maintenance of coherence and downstream attenuation (e.g. Gilbert, 1917; Pickup *et al.*, 1983). This classification is returned to in Chapter 7.

The Markov chain modelling procedure was assessed in sub-section 6.2.3. It has proved beneficial as both a descriptive tool and a source of ideas about processes of sediment transfer through the stream system. The differences between the approach taken herein and many previous models of sediment transfer are that sediment storage changes are the object of the

model rather than being a consequence of flow parameters and sediment transport equations, and that sediment transfer was viewed stochastically rather than deterministically. Kelsey *et al.* (1987) have demonstrated the feasibility of such an approach which the present study has confirmed. Its ultimate utility lies in its ability to produce results that could not be reliably obtained by other means, and the equality of flushing times is an example of this. As such, further development of this approach seems justified and could be accomplished in many ways. These include addition of a component to account for variable transport distances for particles, different behaviour of different sized material, and feedback effects of modelled changes on the structure of the model.

The finite Markov chain modelling procedure further illustrated the differences between different parts of a bed wave cycle that were described in Chapter 5, in terms of both the probabilities of occurrence of different sediment exchanges and the rates of sediment transfer through the system. Flushing times increase as sediment is stored and output rates decline during aggradational phases, with the reverse occurring during degradation. The model results can be used to estimate the percentages of sediment output that are derived from different source types (Types A,B and C sediment supply). Noting that the value of the transfer constant is thought to be an overestimate for all except the 1450-1690 period, Table 6.10 gives these estimates for two values of k ; 0.1805 and 0.100.

The latter value is an estimate of k during aggradation, and there are no data to support a selection of 0.1 as opposed to 0.05 or 0.15, for example. In the table, Type C increases at the expense of Type B sediment as net aggradation rises. This may be exaggerated if k declines steadily as the magnitude of aggradation increases, but for 1450-1690 minutes it is reasonable to say that 15 % of the export material is Type C sediment and 85 % is Type B. For the conditions in the sand tray, Type A input is very small. For the periods of maximum aggradation with $k=0.1$, the percentages of Type C material are 19.5 % and 21.7 % i.e. allowing for a 'reasonable' variation in k , the data suggest that the time of maximum sediment output is associated with the maximum re-working of bed sediment. Bedload pulses do not simply represent increased efficiency of transfer of material from further upstream, but are at least partially produced by the erosion of earlier deposits. This is inevitable since there are periods when sediment output from the tray exceeds input to it, but the generally low throughput rates illustrate that the importance of Type B sediment supply is greater than would be estimated from consideration of sediment continuity alone. This is consistent with morphological evidence presented in Chapter 5. The 1450-1690 period is the only totally reliable one, and the sediment budget for the entire tray in this period can be expressed as in Figure 6.12. This shows a proportion of both Types A and C sediment passing through the tray in one time interval, and being augmented by Type B supply. The remaining Types A and C sediment contribute to net storage change along with the removal of Type B material. Further discussion of sediment input types and their role in bed wave generation is held over to Chapter 7.

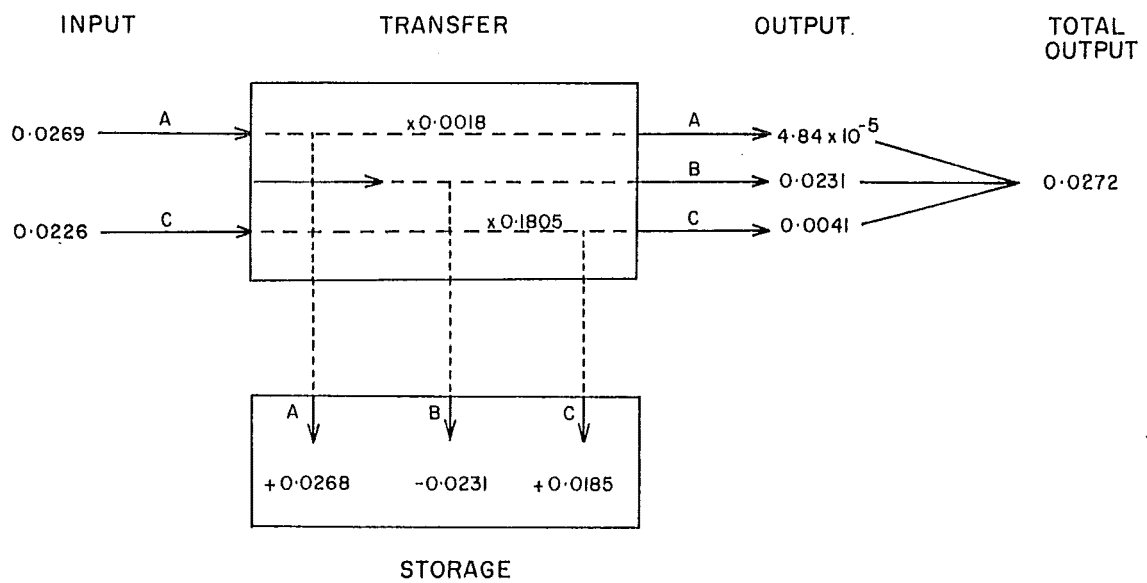


Figure 6.12 Sediment storage changes during the 1450-1690 minutes period for the whole sand tray. Types A, B and C input are defined in Chapter 2. Units are m^3 .

Table 6.10 Estimated sources of sediment output from the sand tray. The transition matrix used is that derived for the particular time period shown. Type C input is equal to $k \cdot e$. Type A is obtained by taking the measured reduction in never active sediment volume and multiplying by the probability of never active sediment being output from the tray in a single time period (r_n). Type B is obtained by subtracting Types A and C volumes from the measured output.

Time period (minutes)	Total output (m ³)	Sediment input volumes (m ³)			Proportions of input of each type		
		Type A	Type B	Type C	Type A	Type B	Type C
a) $k = 0.1805$							
1450-1690	0.0272	4.8×10^{-5}	0.0231	0.0041	0.001	0.849	0.151
1690-1930	0.0235	6.4×10^{-6}	0.0194	0.0041	0.001	0.825	0.174
1930-2170	0.0232	1.8×10^{-5}	0.0191	0.0041	0.001	0.823	0.177
2170-2410	0.0203	2.8×10^{-5}	0.0162	0.0041	0.001	0.797	0.202
2410-2650	0.0118	2.4×10^{-7}	0.0077	0.0041	0.000	0.653	0.347
2650-2890	0.0106	1.8×10^{-5}	0.0065	0.0041	0.002	0.609	0.387

b) $k = 0.1000$							
1450-1690	0.0272	4.8×10^{-5}	0.0249	0.0023	0.001	0.914	0.085
1690-1930	0.0235	6.4×10^{-6}	0.0212	0.0023	0.001	0.901	0.098
1930-2170	0.0232	1.8×10^{-5}	0.0209	0.0023	0.001	0.900	0.099
2170-2410	0.0203	2.8×10^{-5}	0.0180	0.0023	0.001	0.886	0.113
2410-2650	0.0118	2.4×10^{-7}	0.0095	0.0023	0.000	0.805	0.195
2650-2890	0.0106	1.8×10^{-5}	0.0083	0.0023	0.002	0.781	0.217

The main conclusions reached in this Chapter can be summarised as follows:

1. Diffusion of input sediment is rapid, and its rate and pattern depend upon the loci of sediment deposition under the particular channel condition at any one time.
2. Sediment dispersion does not necessarily imply attenuation of wave forms due to exchanges between wave sediments and the underlying bed material.
3. The sediment transfer process is amenable to stochastic modelling, but the form of the model varies with channel condition.
4. Sediments stored in the active, semi-active and inactive reservoirs have approximately equal flushing times, which implies equal mobility of material from these different reservoirs.
5. Changes in sediment output from a reach are related to changes in the proportions of Types B and C sediment which contribute to the output material.

7. DISCUSSION

The preceding chapters have examined bed waves and bedload pulses using data from a prototype river and a small scale laboratory model. Discussion of their main results has been presented in the individual chapters and the aim of this chapter is to synthesise these results. The discussion commences with a re-evaluation of the classification of bed waves introduced in Tables 2.1 and 2.2, before addressing the issues of sediment supply controls over bed wave form and their linkages with channel processes. The discussion then concentrates on the implications of bed waves for definitions of channel equilibrium. These areas of analysis are related to the four areas identified in Chapter 2 as requiring further research. Finally, the uses and limitations of small scale physical modelling are discussed in the light of the data presented herein.

7.1 Spatial and temporal scales of bed waves and bedload pulses

Gravel-bed river bedforms in general and bed waves in particular were placed into a spatial and temporal classification scheme in Tables 2.1 and 2.2. This was derived from Jackson's (1975) discussion of bedforms and its subsequent adaptation for gravel-bed conditions by Church and Jones (1982). Bedload pulses and bed waves were classified on the basis of their scales and hypothesised explanations for these features derived from the literature exhibit differences between scales. At the meso-scale explanations rely on the development of bed armouring (e.g. Gomez, 1983), kinematic waves (e.g. Reid *et al.*, 1985), or on small scale bedforms of different types. The latter group include particle clusters (e.g. Kuhnle and Southard, 1988), bedload sheets (e.g. Iseya and Ikeda, 1987), and low angle dunes (e.g. Gomez *et al.*, 1989). The recognition of the importance of bedforms in gravel-bed rivers has tended to be overlooked because of their generally small size and supposed unimportance as elements of flow resistance (Simons and Simons, 1987). The types of bedform that develop in such rivers should be regarded as distinct from sand bedforms and rather than seeking gravel-bed analogues for the well understood sand-bed features, an entirely separate classification may be appropriate. This would require further research since gravel bedforms have rarely been described in detail and little is known about the conditions under which they form (Naden and Brayshaw, 1987). Any classification would need to include more than flow regime, however, since sediment size sorting is a crucial element of both small scale bedforms such as particle clusters (e.g. Brayshaw, 1985) and larger (macro) scale ones such as unit bars (Bluck, 1982). Thus the 'governing factor' for mesoforms in Table 2.1 (after Jackson, 1975) which states that such forms are independent of the geomorphological regime may be an oversimplification since it is this regime which determines the type of sediment present in the river. Despite this observation, within a given river it is likely to be the fluid dynamic regime which controls bedform genesis. Thus at any one site the fluid dynamic regime will control bedform size and spacing, but between sites the geomorphological regime may override this control, if there is sufficient variation between the sites.

The experiments described in Chapter 3 revealed three scales of variation in sediment transport rate (Table 4.1). The smallest of these was related to mesoscale processes and the longer two scales were consequent upon macro- and mega-scale processes. Chapter 5 demonstrated how the largest of these scales can be accounted for in terms of processes of aggradation and degradation that affect reaches that are several channel widths in length. Although these different scales can be identified, there is no consistent relationship between macroforms and megaforms in the way that might be expected with regularly superposed bedforms such as those reported by Gomez *et al.* (1989). This is because the fluid dynamic regime at any one section was not constant for sufficiently lengthy time periods to enable the evolution of bedforms that were in equilibrium with it. In Gomez *et al.*'s ERC run, flume width, sediment feed rate and water discharge were constant. The predominant bedform type (alternate bars) was therefore a function of the imposed flow conditions. Had either sediment feed rate (i.e. geomorphological regime), flow rate or slope (i.e. fluid dynamic regime) been altered, then the bedform type and associated pattern of bedload pulses would also have changed. In the present study the fluid dynamic regime within individual channels was constantly varying as they adjusted to changes in water and sediment discharges consequent upon changes in channel form which occurred further upstream. The dynamic nature of channel form is a consequence of the geomorphological regime i.e. the imposed sediment load and discharge lead to high sediment transport rates and unstable channels. Both macro- and mega- forms were dependent upon this fundamental characteristic of the river system.

The difference between the governing factors at different scales is suggested as the cause of the relationships between dimensionless discharge and stream power, and bedload pulse period that were noted in Chapter 2 (Figures 2.2 and 2.3). At any one value of q^* or ω^* pulses of different period develop, each related to different governing factors and / or bedform types. Within each scale there is some evidence for a positive correlation between ω^* and pulse period. As ω^* rises so does the dimensionless bedload transport rate (Ashmore, 1985) which implies that pulse periods are longer with greater transport rates. This presumably reflects correlation between bedform size and stream power, but little is known about gravel bedform relationships with flow conditions so this cannot be confirmed.

There are comparatively few data at the macro- and mega-scales, so distinguishing between them is difficult. The longest two periods of bedload transport rate fluctuation described herein from Runs 1 and 3 plot along with macro- and mega-scale data from other studies (Figure 4.9). Both scales of fluctuation from Run 2 plot with the macro-scale data, possibly due to the short duration of this run. The positions of these data on Figure 4.9 are consistent with the processes associated with each scale in Chapters 4 and 5 i.e. the longest period fluctuations are due to degradational episodes associated with bed waves which affected reaches of several channel widths in length; the shorter fluctuations were due to spatially more restricted processes of bar erosion and channel development. The former group relate to bar assemblages whereas the

latter are associated with features at the scale of unit bars. This is consistent with Table 2.1 and indicates that these two scales of fluctuation are associated with differences in the scales at which processes operate rather than with different governing factors.

Table 2.2 identified differences between endogenous and exogenous wave forms. The models developed in Chapter 5 to describe bed waves in the sand tray and the Kowai R. are similar, both describing channel response to variations in Types B and C sediment supply. Type A supply was negligible in both cases. In the study of dispersion processes in Chapter 6 it was suggested that the degree of interaction between the input sediment and the existing bed material serves as a means of differentiating two types of exogenous wave. The response of the sand tray to an exogenous (Type C) sediment supply pulse, and the similarity between the Kowai R. behaviour as Type C supply varied and that in the sand tray imply that exogenous bed waves can behave in the same way as endogenous ones under certain conditions. Situations in which this similarity of behaviour may not apply are those where the input sediment is either of distinctly different calibre to the 'host' bed material, or its volume exceeds the normal rate of sediment input by a considerable amount. Examples of the first case were given in Chapter 6 as the Kawerong and East Fork Rivers (Pickup *et al.*, 1983; Meade, 1985). Macklin and Lewin (1989) presented an interesting example where the rate of sediment input was increased largely due to an influx of relatively fine material. In addition the presence of lead in the finer sediments prevented vegetative recolonisation and so influenced the patterns of aggradation and degradation that followed the acceleration of sediment supply. Overloading of a river with sediment was responsible for many of the exogenous bed waves listed in Table 2.4. In either of these situations the sediment comprising the initial wave form is likely to undergo dispersion but may retain a degree of coherence as it is transferred through the drainage system. These waves are thus routed through the channel without undergoing appreciable interaction with the pre-existent channel sediments. In terms of wave behaviour it is not whether the wave material was endogenously or exogenously derived that is important but the calibre and quantity of this material relative to the normal sediment inputs to which the river system is adjusted.

The similarity of behaviour between endogenous bed waves and some exogenous waves suggests that the classification of waves into 'endogenous' and 'exogenous' is inadequate. Table 7.1 presents a revised version of Table 2.2 in which endogenous and exogenous waves are again identified. As well as using wave type as a classificatory basis, Table 7.1 uses the source of the sediment in the wave. Endogenous wave types can be produced by material that is endogenously (Type B sediment supply) or exogenously (Types A and C) supplied. Exogenous types are produced only by exogenously supplied sediment. Endogenous waves are transferred through the river system by processes that are within the range of 'normal' behaviour of the system. They can thus be regarded as part of the equilibrium geomorphological regime of the system. The source of sediment, whether endogenous or exogenous, is less relevant in determining the wave type than the predominant processes of sediment redistribution.

Exogenous waves occur as the sediment input causes a change in the equilibrium form of the river system, either by overloading it with sediment or inducing a change in the calibre of bed material. Such wave forms tend to remain coherent as they migrate downstream but undergo attenuation. This is not within the range of equilibrium behaviour of the river system and may induce the establishment of a new equilibrium condition with return to the initial equilibrium state being dependent upon exceedence of another threshold condition.

This re-classification was anticipated in Figure 2.4 where the processes generating endogenous bed waves were placed into four groups. Exogenous waves were left separate. The re-classification here leaves Figure 2.4 as a valid representation of bedload pulse / bed wave generating processes, but waves of exogenous sediment can be produced by process types 1-4 as well as Type 5 (Figure 2.4). Type 5 processes refer to exogenous waves.

Table 7.1 Types and scales of bed waves and bedload pulses in prototype rivers: modified version.

Pulse / wave scale	Wavelength (m)	Relaxation time	Sediment sources	
			Endogenous waves	Exogenous waves
Mesoscale	$10^{-1} - 10^2$	$\cong t_e$	endogenous or redistribution of exogenous inputs	--
Macroscale	$10^1 - 10^3$	$\geq t_e$	endogenous or redistribution of exogenous inputs	--
Megascale	$> 10^3$	Regime time	endogenous or redistribution of exogenous inputs	Redistribution of exogenous inputs of different calibre and / or greater volume than is within the range of 'normal' inputs to which the river system is adjusted.

7.2 Sediment supply - transport capacity relationships in bed waves

Lisle (1987) has observed that for channels formed in sediment the origins of supply- and capacity-limited regimes are unclear. He also suggested that channel morphology and the distribution of different sediment size fractions adjust to the recent history of sediment inputs in ways that remain poorly understood. In the sand tray experiments, sediment transport rates during cycles of aggradation and degradation varied more than can be accounted for by a simple definition of transport capacity. At different times, apparently supply-limited and capacity-limited regimes were observed with the former occurring during aggradation and the latter during periods of degradation.

Figure 4.7 showed a general tendency for aggrading channels to have greater transport

capacities than degrading or stable ones. (Mean values for Run 1 and Run 3 data combined were: aggrading - $4.55 \times 10^3 \pm 2.43 \times 10^3 \text{ kg s}^{-1}$; degrading - $2.34 \times 10^3 \pm 5.40 \times 10^4 \text{ kg s}^{-1}$; stable - $2.91 \times 10^3 \pm 1.78 \times 10^3 \text{ kg s}^{-1}$). In the aggradational phase this increase was due to channel multiplicity and a larger area of active bed (stream power per unit bed area values were approximately equal for aggrading and stable channels). However, the actual bedload transport rates were appreciably different from the calculated capacities for both aggrading and degrading states. In Chapter 4 this was related to the non-equilibrium conditions of these channels using an argument based on sediment continuity. It is also relevant to note that sediment supply is variable both within and between channels. Davoren and Mosley (1986) and Carson and Griffiths (1987) have referred to the localisation of sediment sources and transport zones within braided river systems. Erosion of bar faces, which adds a gravitational component to entrainment, is envisaged as an important source of bedload material by Carson and Griffiths (1987). The development of coarse armour layers in thalweg zones inhibits vertical scour of the bed and reduces bedload transport rates. Carson and Griffiths (1987) raised the question of whether the multiplicity of bar tail-chute-bar head sediment transfer systems in braided rivers outweighs the greater stream power if all of the flow were to be concentrated into a single channel. This controls whether a single channel will transport more or less sediment than a braided one with equal discharge. In the present case the greatest bedload transport rates occurred during degradational phases when most of the flow was concentrated into a single channel. However, multiple channels that were in equilibrium could transport equivalent volumes of material under certain conditions (see Figure 4.7b: Run 3, 1440, 1680 and 1920 minutes, versus 2160 and 2400 minutes). Thus it is not always the case that flow concentrated into a single channel has a greater bedload transport rate at a given discharge than when it is divided between multiple channels. All of the major peaks in bedload output in Runs 1 and 3 were associated with such concentration and this supports the results of Davies and Lee (1988) which suggested that narrowing a braided river will always increase the total bedload transport rate. The pattern noted in the Run 3 data is thus interpreted as reflecting the operation of a supply reducing mechanism in degrading channels.

Assume that when the flow becomes concentrated the bedload transport rate rises as a consequence of increased stream power per unit bed area. This leads to the evacuation of previously deposited sediment associated with channel degradation and / or widening as the channel adjusts its geometry toward a new equilibrium state, the form of which is governed by the increased discharge within it. As the new equilibrium is approached the rate of degradation declines so reducing sediment supply associated with gravitational entrainment and the direct results of non-equilibrium transport (the approach of bed level to equilibrium may take an exponential form; this is an untested assumption but is a commonly observed trend as geomorphic systems respond to disequilibrating influences (Graf, 1977)). Because bed armouring is associated with the degradational phase the availability of sediment for transport declines more rapidly than would be the case if it were due to the approach of channel geometry toward an equilibrium shape alone. These two processes thus lead to lower transport rates.

During a degradational phase the bedload transport rate thus declines until an equilibrium morphology and transport are established. This equilibrium is constrained by the presence of the armour layer.

Figure 7.1 presents a model of these changes making the following assumptions: prior to time $t=0$ there exists a multiple channel system in equilibrium; after $t=0$ there is a single channel conveying the entire water discharge, which remains constant; the supply of sediment from upstream is constant and non-zero; the rate of degradation rises rapidly and then declines exponentially; equilibrium bedload transport capacity (estimated using the Bagnold (1980) equation) adjusts rapidly to the channel geometry changes and thereafter is unaltered except for the effects of armour layer development on the threshold of motion. The model presented in Figure 7.1 has the features that the total bedload transport rate once the channel form is in equilibrium is less than that predicted from equilibrium formulae due to the effects of armouring on sediment availability. This is built in to the Bagnold (1980) equation in the form of an entrainment threshold so the equation may predict actual transport rates reliably if this component is totally efficient.

A similar model is proposed for the aggradational phase in Figure 7.2. Analogous assumptions apply to those for Figure 7.1. Armouring does not develop during aggradation and the reason for the channels transporting less bedload than they would under equilibrium conditions is that their adjustment to equilibrium requires aggradation as outlined in Chapter 4.

The application of these two models will be complicated by variations in water discharge and sediment inputs from further upstream due to the same sorts of processes occurring in adjacent reaches. Their general form can be envisaged to apply to actual changes in channel geometry and sediment transport. Ashmore (1988) suggested that the inverse relationship between bedload discharge and braiding intensity, which he observed in braided stream models and which was replicated herein, implies that a total bedload- stream power relationship requires adjustment to account for channel pattern. The results described in Chapter 4 and discussed above imply that it may not be the channel pattern *per se* but the direction and magnitude of the departure of channel form from equilibrium conditions which influences actual bed material loads. In many cases this can be approximated by a channel pattern index, but the temporal lags between changes in equilibrium state and responses in terms of channel pattern may make this sort of relationship subject to considerable scatter. Given that channel planform can be readily measured in braided streams it would seem useful to pursue the approach suggested by Ashmore (1988), while remaining cognisant of the fact that this involves the use of a surrogate for channel equilibrium / non-equilibrium state.

The sediment supply- transport capacity relationships at different locations along a bed wave can be summarised as follows: at sections which are in equilibrium, sediment is entrained by bed

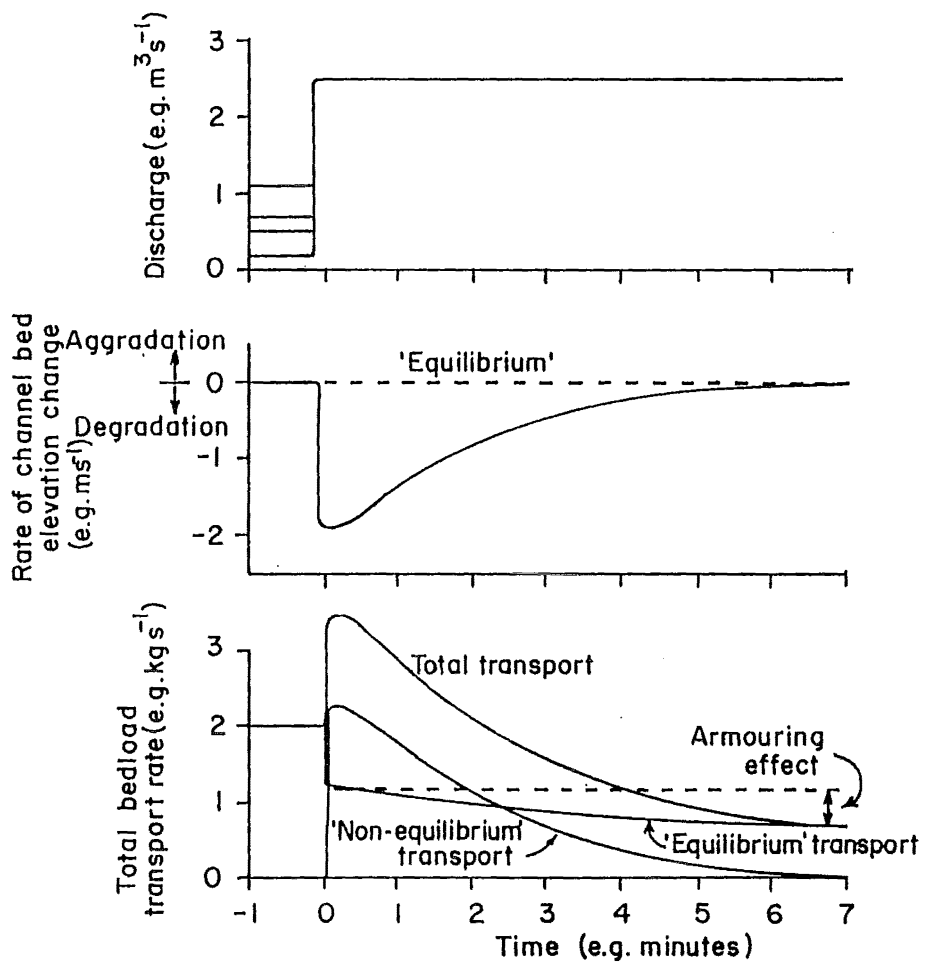


Figure 7.1 Hypothetical model of responses of channel bed elevation and bedload transport rates to concentration of flow into a single channel. The model assumes that total discharge and the sediment input rate are constant. All units are arbitrary and relative values are shown on the axes.

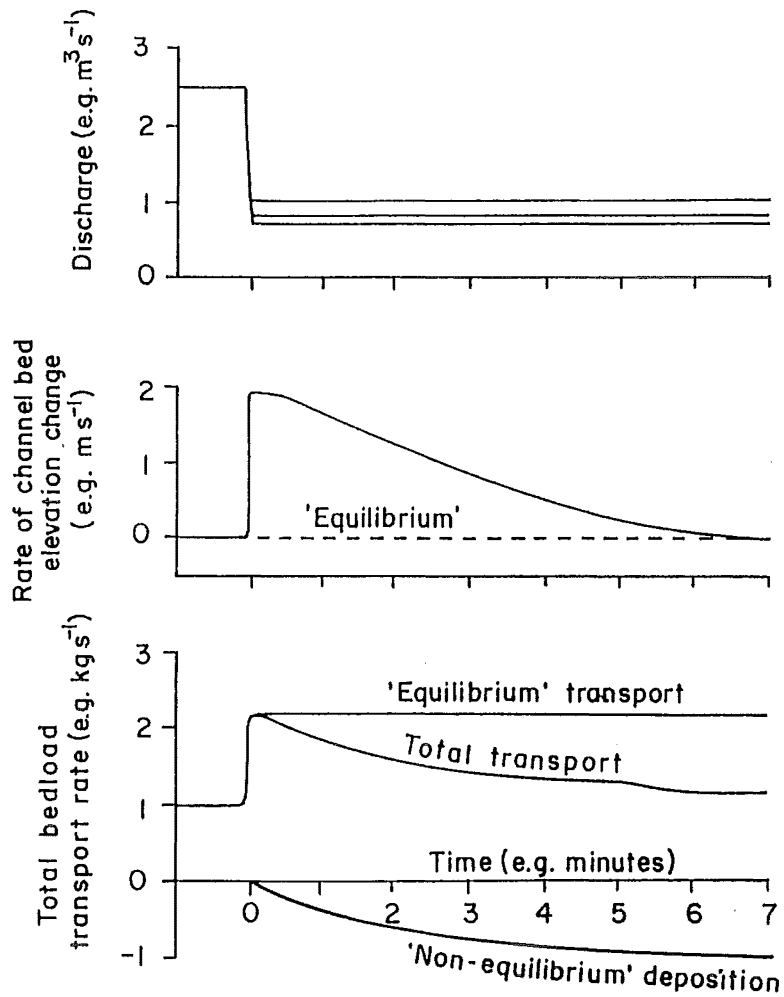


Figure 7.2 Hypothetical model of responses of channel bed elevation and bedload transport rates to an avulsion which divides the discharge between three channels. The model assumes that total discharge and the sediment input rate are constant.

scour and is transported at a rate approximately equal to the transporting capacity of the flow; at degrading sections, adjustments of channel cross-sectional geometry toward equilibrium result in both vertical and lateral extension of the channel and removal of the sediment thus eroded - this leads to actual bedload transport rates exceeding the theoretical equilibrium transporting capacity of the flow; aggrading sections are associated with rising channel bed levels and some of the sediment which enters a reach as bedload is deposited therein so leading to the actual bedload transport rate being below the equilibrium value. Thus, 'supply-limited' transport should only occur at the end of the degradational phase when armouring inhibits sediment availability, whereas 'capacity limited' transport should be prevalent during the equilibrium phase. The apparent supply limitation during aggradation and capacity limitation during degradation are due to channel non-equilibrium and not to sediment availability constraints. If these are widely occurring phenomena, Lisle's (1987) query as to the origin of supply- and capacity-limited regimes can be answered with reference to the occurrence of non-equilibrium conditions.

Non-equilibrium conditions within individual channels in a braided river are frequently encountered, thus it is not surprising that poor correlations have been found between measured and predicted bedload transport rates in such rivers where an assumption of channel equilibrium has been made. Using averaged parameters for a section leads to the results of applying conventional bedload equations being poor when compared with results obtained when sections are sub-divided into homogeneous parts and the results integrated across the section (Carson and Griffiths, 1987). Pickup and Higgins' (1983) and Ashmore's (1988) results showed that when mean parameters for several sections at different times are used (i.e. the integration is temporal as well as spatial) acceptable correspondence between measured and predicted transport rates can be obtained. Using one section involves sampling a set of channels each of which may be in equilibrium or non-equilibrium at the time of sampling. Measured and predicted rates would differ unless all were in equilibrium and the equations used were exact. Use of temporal integration may lead to aggradational and degradational phases cancelling out and the net result being equivalent to equilibrium conditions. This may enable bedload yields over long time intervals (e.g. annual) to be reliably estimated. In many situations net aggradation or degradation over time scales that are greater than the periods of interest prevent temporally integrated data from being equivalent to equilibrium conditions. Bedload equations thus require modification to allow for non-equilibrium effects if reliable estimates of actual transport rates are to be obtained. This may only apply to certain river types; more stable gravel rivers than those discussed herein may have channels in equilibrium condition for greater proportions of time and be more reliably analysed using an equilibrium assumption.

7.3 The use of channel pattern information for the identification of bed waves

7.3.1 Correlations between channel form and sediment transport rates

Numerous studies in which channel pattern data have been used to infer the existence of bed waves were reported in Chapter 2. The most valuable studies in this regard are those of Ashmore (1985, 1987) who correlated sediment transport rates at a section with channel pattern parameters over a 10m reach in a laboratory flume. In the present study, at-a-section sediment transport rates were correlated with channel geometries at the same section in Chapter 4 (see Table 4.4 for a summary). These relationships were then applied to reaches of variable length in Chapter 5 using a location-for-time substitution (Paine, 1985). This led directly to the model proposed in sub-section 5.2.3 (Figure 5.8) and was used as the basis for the classification of the Kowai River data in sub-section 5.4.3 (Figure 5.24). These results were fully discussed in Chapters 4 and 5. At this stage it is instructive to return to the sedimentary controls over channel pattern described in section 2.3.

Equation (2,6) suggested that higher / lower of bedload transport rate through a reach is related to higher / lower channel width, slope and meander wavelength, and lower / higher depth and sinuosity (Schumm, 1977a). For a single reach through which bedload transport rate varies the data which were summarised in Table 4.4 suggest the following equations;

$$Q_b^+ \Leftrightarrow b^-, h^+, \lambda^+, (S^+), \Sigma P^- \quad (7,1a)$$

$$Q_b^- \Leftrightarrow b^+, h^-, \lambda^-, (S^-), \Sigma P^+ \quad (7,1b),$$

in which ΣP (total sinuosity) is used in place of P (sinuosity) and \Leftrightarrow implies a relationship the causal direction of which is uncertain. Comparison with equation (2,6) reveals that the directions of change for width and depth are reversed in equation (7,1). This occurs because an increase in sediment transport rate in the sand tray was generally associated with the concentration of flow into one or two dominant channels, thus decreasing total channel width. The widths of individual channels were usually increased. The reverse situation applied during times of bedload transport rate decrease. For individual channels Schumm's (1977a) equations remain valid but they do not apply to the river system as a whole. The slope terms in equation (7,1) have been bracketed to indicate that slope variation was not consistent in its relationship with bedload transport rate. This reflects the predominant influences of width and depth changes on channel geometry with slope being a less important variable. However in combination with width and discharge, slope was shown to exert a weak though significant influence over the onset of degradation in Chapter 4, when degradation was related to stream power per unit bed area in the form of a gradational threshold.

7.3.2 Processes associated with aggradation and degradation

If it is accepted that bedload pulses are responses to channel non-equilibrium then an understanding of them depends upon identification of the processes which induce that non-equilibrium. In the discussion of Chapter 4 bedload pulses were related to channel non-equilibrium states and the hypothesis that stream power per unit bed area variations control changes in channel state was examined. The conclusion reached was that under conditions of constant discharge, aggradation will ultimately lead to an increase in slope which is sufficient to raise stream power per unit bed area to a threshold value for the onset of degradation. This threshold appears gradational because of discharge variations, sediment size sorting (i.e. armouring) effects, and the absence of data from close to the threshold condition. Such an explanation is similar to that of Hey (1979), and as noted in Chapter 2 the sedimentation zone long-profile suggested by Church and Jones (1982) closely resembles the predictions of Hey's (1979) dynamic process-response model of channel development. This explanation relies on the operation of a feedback mechanism; aggradation causes slope to reduce upstream and increase downstream, so inducing further aggradation in the upstream part of the reach (as a response to channel non-equilibrium and the reduction in sediment transporting capacity as slope is lessened) which further increases the slope in the downstream part of the aggrading reach. The feedback loop operates until the threshold for the onset of degradation in this downstream reach is exceeded after which degradation commences so promoting concentration of the flow into a reduced number of channels. This in turn initiates channel adjustment toward equilibrium which exacerbates degradation. A second feedback mechanism then operates in which the rate of channel shape adjustment toward equilibrium reduces as equilibrium is approached. These aggradational and degradational feedback mechanisms are illustrated in Figure 7.3 for the specific case of a channel in which discharge undergoes an instantaneous change and is thereafter constant.

The situation depicted in Figure 7.3 is in practice complicated by the changes in channel form that occur in association with aggradation and degradation. These were described in Chapter 5 and the most significant is the tendency for channel multiplication in aggrading reaches which may lead to accelerated aggradation as these channels evolve towards their own equilibrium conditions and as shallow over-bar flows affect greater areas so reducing in-channel discharge. Thus these changes in channel morphology, themselves responses to aggradation, may induce further aggradation. This additional aspect to the feedback mechanism described previously is a form of 'spatial feedback', which as Richards (1988) noted has been emphasised in several recent studies in fluvial geomorphology (e.g. Ashworth and Ferguson, 1986; Naden, 1987). The spatial component of the feedback mechanism is especially important in rivers which exhibit cross-channel variations in behaviour and it is thus critical in braided rivers.

The nature of the feedback mechanisms is complex and a simplified diagrammatic representation

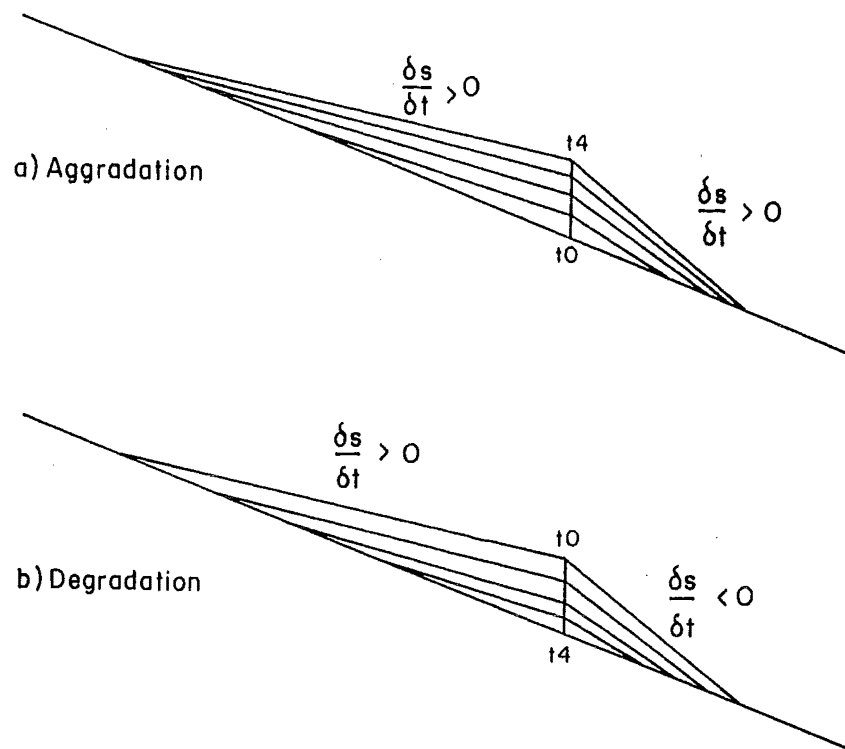


Figure 7.3 Two dimensional representation of aggradation and degradation as a bed wave passes through a reach. The rates of aggradation and degradation decrease from t_0 through t_4 . $\delta S / \delta t$ is the rate of change of bed slope.

of them is given in Figure 7.4. The figure does not attempt to illustrate all of the potential channel responses to changes in discharge or sediment load but to illustrate the general form of the spatial feedback loops that exist. Many of the loops illustrated in Figure 7.4 involve self-limiting mechanisms which lead to the declines in the rates of aggradation and degradation through time that have previously been noted. It was suggested in Chapter 5 that the spatial scales over which aggradational and degradational processes operate are themselves variable, such that spatial feedback mechanisms also affect a range of scales.

Ashworth and Ferguson (1986) have suggested that the normal processes of channel division and confluence in braided rivers are responsible for producing bed waves. This is a macro-scale explanation and other studies have also related waves at this scale to processes which produce the characteristic planform morphology of braided rivers (Kang, 1982; Southard *et al.*, 1984; Rundle, 1985b; Ashmore, 1987). Description of both laboratory and prototype situations in Chapter 5 suggested that megaforms are produced by the coalescence of numerous macroform features, and unit bars were recognised as being important in this. Thus the development of aggradational wedges as illustrated in Figure 7.3a relies upon processes which produce unit bars in particular, although smaller scale bedload sheets were also observed to be important constructional processes in some locations (especially in shallow over-bar flows).

Braiding has often been associated with general aggradation. The association of reaches of maximum channel pattern complexity with aggrading conditions in the sand tray appears to support this. Even under these conditions aggradation occurred predominantly within the channels which occupied less than half of the total bed width. The overall impression of the channel in this condition was one of constructional development in which the channels were actively involved. This contrasts with Carson and Griffiths' (1987) assertion, echoed by Rundle (1985b), that braided river patterns give the impression of a constructional surface dissected by channels. In the present case it was possible to observe the development of the channel bed during the 'flood' conditions rather than after flow recession and falling stage modification of the deposits. The constructional nature of the river bed during aggradation is of critical importance for channel pattern development. As aggradation proceeds and water levels rise, more flow becomes over-bar and the potential for avulsion into previously formed channels, the development of new proto-channels, or chute cut-offs across bars is increased. These processes produce the increased channel pattern complexity that has been suggested herein to be diagnostic of aggradation. Channel patterns observed at low flows should not be assumed to represent post-depositional dissection of deposits but as the remnants of zones of flow concentration during deposition which may have been subject to modification during flow recession. Even with this modification the general planform pattern (as indexed by the total sinuosity) will be preserved and the aggradational reaches remain as areas of relative complexity.

Reaches where degradation occurred in the sand tray experiments were characterised by prior

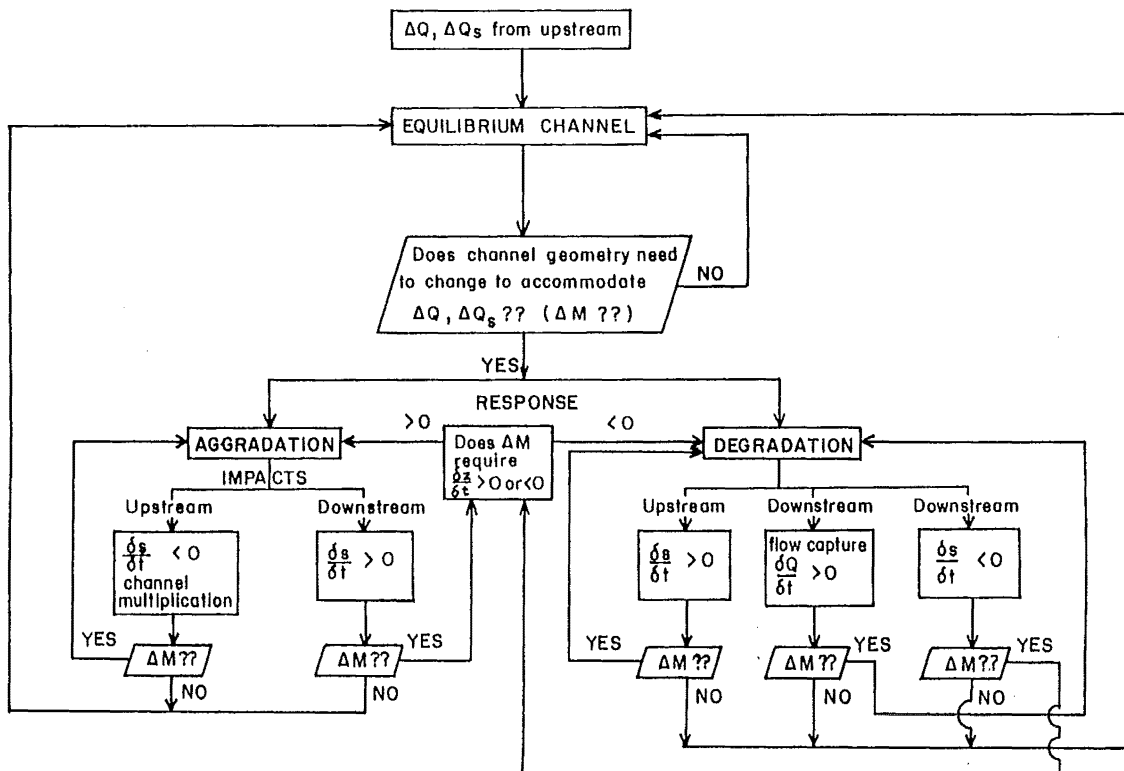


Figure 7.4 Schematic representation of the controls over aggradation and degradation defined in terms of channel adjustments toward equilibrium. Q = water discharge; Q_s = sediment discharge input from upstream; $\Delta M??$ = 'Is a change in channel morphology required to offset the effects of changes in water and sediment discharges (ΔQ and ΔQ_s) ; S = water surface slope; z = bed elevation.

deposits being left as low terraces adjacent to the main channel or channels. Even during 'flood' conditions these reaches had the form of dissected depositional surfaces. In this case falling stage modification could lead to an apparent increase in pattern complexity if, for example, medial bar deposition occurred in a channel which was taking all of the flow leading to bifurcation at low stage. Such deposition was often observed to be one of the first indications of the end of a degradational phase in the tray, and it would be impossible to differentiate these two origins of channel splitting at low flow.

The general form of processes of sediment redistribution involved deposition concentrating in unit bars and sediment sheets, which were producing lateral and vertical extension of pre-existent deposits. These are meso- and macro-scale forms and both depositional and erosional processes operate at these scales. The overall control over channel form is mega-scale however; this is the progressive build up of aggradational bar complexes which are periodically eroded. The megaforms themselves are responsible for the channel changes and the exceedence of threshold conditions which control the onset and end of aggradational phases. Responses to these controls occur at the macroscale (mesoscale responses are generally less significant in terms of their effects on megascale features) and it is a combination of macroscale features that produces both depositional bar complexes and erosional features at the megascale. This is consistent with Table 2.1 wherein both macro- and mega-forms are suggested to be controlled by the geomorphological regime of the system. In both model and prototype studies, megaforms are collections of macroforms but it is the behaviour of the latter which delineates the conditions under which processes operate at the former scale.

Both the macro- and mega-scale processes described herein in relation to bed waves and bedload pulses are subject to spatial and temporal lags. The various processes of channel adjustment occur at different rates; channel degradation and widening were usually more rapid processes than aggradation and narrowing in the sand tray (Hoey and Sutherland, forthcoming). Hence the aggradational phases usually lasted longer than the degradational ones. Ashmore (1987) also reported a lag between changes in the sediment supply rate and channel pattern response. These temporal lags are mirrored by spatial effects, such as the distance between the locations of maximum aggradation and the onset of degradation which was further downstream and subsequently propagated upstream.

Different variables respond in different ways to the history of flow and sediment inputs to a reach. Channel pattern complexity was increased as a direct consequence of aggradation and these processes were almost contemporaneous, whereas the decrease in the bed relief index which generally accompanied these two changes was in some cases delayed or did not occur at all, depending upon the cross-sectional shape at the onset of aggradation. Indices of pattern complexity are difficult to use in prototype rivers at low stages, but can be used to infer high stage processes when the forms produced therein are preserved during flood recession. Thus Davies

(1987) identified periodicity in pattern complexity of the Rakaia River, New Zealand, at low flow and this may be related to the locations of bed waves in that river. The width of the 'active' channel bed (i.e. width of the bare gravel surface) has been used to indicate sediment storage (e.g. Church and Jones, 1982; Beschta, 1983b; Macklin and Lewin, 1989). This indexes the volumes of sediment in storage at different sections since there is a close correlation between width and volume (Magilligan, 1985; Nakamura, 1986), but does not necessarily imply differences in bed elevation or slope. These may be determined from channel patterns in some cases, but whereas width and sediment storage are likely to be correlated, channel pattern and storage may be offset with the most complex patterns extending both upstream and downstream from the location of maximum storage.

7.3.3 An example of inference of sediment storage volumes from channel morphology: the Kowai River

Two reaches of the Kowai River were used in Chapter 5 to derive a model of channel form-sediment storage links, based in part on conclusions derived from the laboratory modelling work. Beschta (1983b) has previously used active channel widths in this river to infer sediment storage patterns.

Figure 7.5 presents data on channel morphology in 1987 which is compared with the 1980 active channel width data (Beschta, 1983b; personal communication, 1987). The presentation of data on Figure 7.5 differs from that used in representation of the model of channel change through time in Figure 5.24 due to the nature of the available data. Active channel width data are not available for the entire 22km channel length sufficiently often to enable reliable estimates of long-term mean widths to be derived. Instead of plotting the active channel width relative to long-term mean values for each section, the 1987 data are presented along with changes in active channel width since 1980. The three variables plotted in Figure 7.5 have all been smoothed using a 5-point running mean (the original data points were 0.1km apart) which in some cases distorts the correspondence between locations where the channel is confined and minimum widths.

The active channel width (ACW) data for this river are difficult to interpret directly due to variations in valley width in the upper 5km of the reach, and in the distance between confining fluvio-glacial terraces further downstream. Beschta (1983b) used aggregated data for separate reaches to infer that changes in the active channel width reflected sediment storage patterns more closely than the recent history of flood discharges. This interpretation was utilised in sub-section 5.4.1 to examine sediment storage changes in Porters and Bridge Reaches. When the data are differenced the sediment storage patterns become more apparent. The 1980-87 width changes exhibit an irregular periodicity with wavelengths in the range 2-5 km. Given that active channel

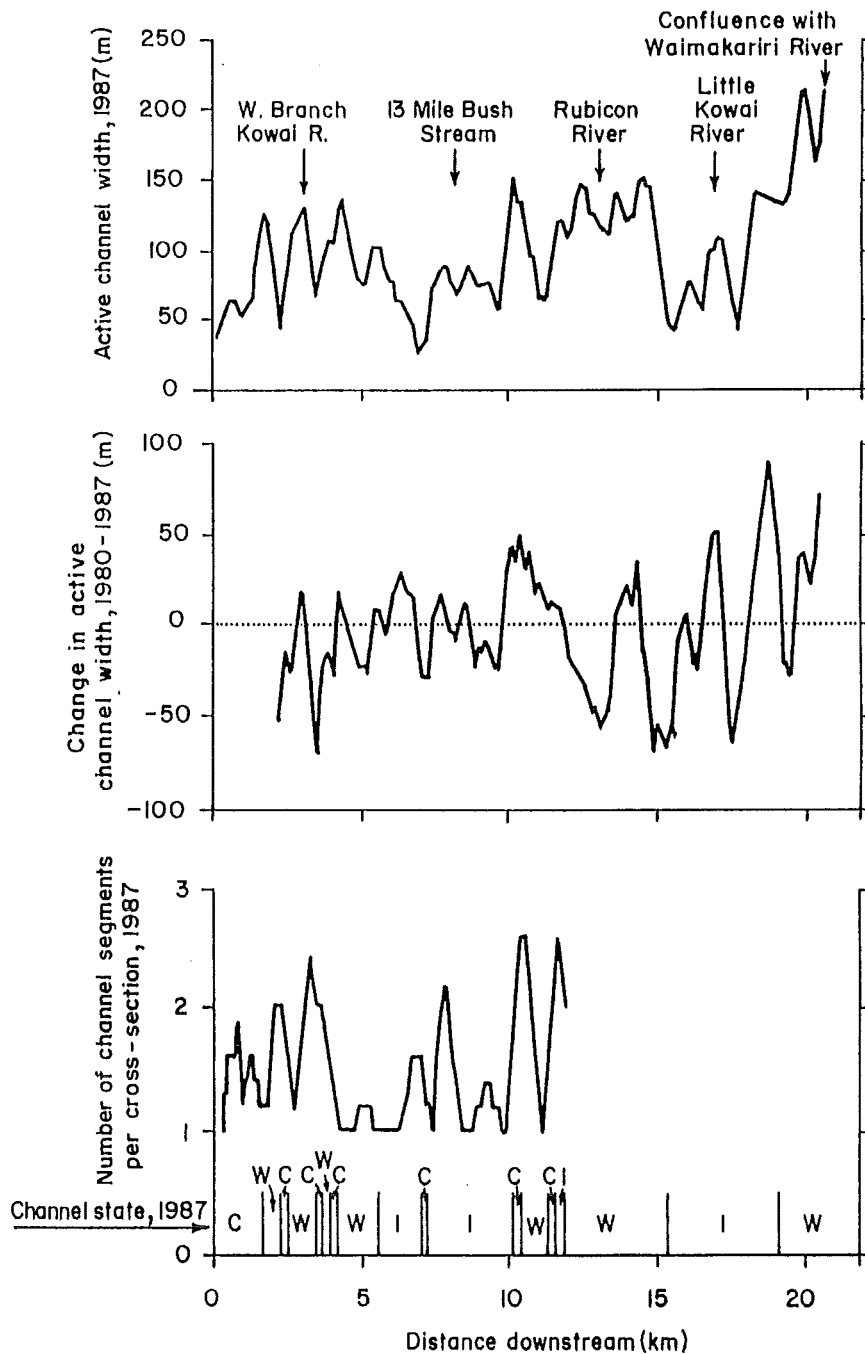


Figure 7.5 Active channel width, changes in the ACW 1980-1987, number of channels / cross-section, and channel condition for the Kowai River, 14.8.87. Based on aerial photographs. All data have been smoothed using a 5-point running mean. Data points were 0.1km apart. ↓ = location of tributary confluences. Channel conditions are: C = confined by bedrock gorges, fluvio-glacial terraces, or bridge structures; I = reaches with vegetated islands within the active channel bed; W = reaches where the channel is wandering and is unaffected by vegetated islands. 1980 active channel width data provided by R.L. Beschta (personal communication, 1988).

width is closely correlated with the volume of stored sediment these data suggest that irregularly spaced bed waves are present in the Kowai system. Periodicity in channel widths has previously been noted by Beschta (1983b) with the nature of the cycles being dependent upon larger scale processes, such as the general aggradation that occurred in some reaches after a major sediment input event. The present data support Beschta's interpretations and by using changes in channel width the patterns are more clearly shown.

A correlation also exists between the number of channel segments / section and the active channel width as was suggested in Figure 5.24. This correlation is imperfect as would be expected using channel pattern at a very low flow (about $2 \text{ m}^3 \text{ s}^{-1}$) to infer sediment transport processes occurring at much greater discharges. The aerial photographs show that the low flow channels wander across the active bed and often take on meandering forms. There are a few locations where the main low flow channel remains straight for 300-400m in the absence of obvious influences from banks or stable vegetated islands within the river bed. Similar patterns were observed in the sand tray experiments and indicate that these may represent the early stages of degradation, where the channel has cut into a prior sedimentary deposit and has remained in that form after the end of the flood event. Total sediment storage in the reaches affected will be reduced by degradation in this case. The associated transfer of material from the active and semi-active reservoirs into the inactive (using the terminology applied in Chapter 5) does not become immediately apparent since it relies upon vegetative colonisation of the 'inactive' material which takes 1-2 years to become apparent.

Use of the readily measured ACW for the purpose of identifying sediment storages is thus subject to some practical difficulties. In a river such as the Kowai which is often almost dry it is difficult to gain much useful information from the channel pattern at low stage and the ACW is the most reliable of the easily measured variables. In larger rivers, such as the Rakaia, the pattern of low flow channels may be a more sensitive indicator than the active channel width.

An interesting association on Figure 7.5 is that where vegetated islands occurred (and the river can thus be classified as Wandering Type II using Carson's (1984a) scheme; shown as I on Figure 7.5) the magnitude of channel width changes 1980-87 was lower than in reaches where the pattern was closer to Wandering Type I, in which morphology was dominated by dissected bars. Mean values are 34.6m (n=89) and 43.3m (n=93), respectively, which are significantly different at $\alpha=0.05$ (t-test). This illustrates the significance of vegetated islands in stabilising parts of the river bed and in limiting the volumes of sediment that can be stored in these reaches. They thus serve as confining elements, and it is suggested that these reaches function as transfer reaches under normal flow conditions. They are likely to change over longer time periods due to the effects of infrequent high magnitude floods removing the vegetative cover and mobilising the inactive sediment. Reaches with vegetated islands are thus areas of relatively low sediment storage of active bed sediment but can be important locations of material stored in the inactive reservoir.

This was illustrated for Porter's Reach in sub-section 5.4.1 (Figure 5.13) where between 1975 and 1987 a stable vegetated island was eroded, thus transferring sediment from the inactive reservoir into the active and semi-active ones.

This example is intended as an illustration of how the model presented in sub-section 5.4.3 can be utilised to infer sediment storage patterns from channel morphology. It has shown the importance of using comparative information from different times and has illustrated some of the problems caused by temporal lags between sediment storage changes and obvious morphological responses. It is suggested that use of as many types of data as are available is important if accurate conclusions are to be derived. Taken in isolation, the active channel width data for 1987 would yield unreliable estimates of relative sediment storage in different reaches along the river.

7.4 The implications of bed waves for the assessment of channel equilibrium

SEE ERRATA
In the discussion of Chapter 4, equilibrium was defined as a state in which at channel forming discharge the channel geometry is unchanging and it is not armoured. This is a restricted definition of equilibrium and is equivalent to a regime condition for constant water and sediment inputs. This equilibrium of form implies process equilibrium (Richards, 1982) and under such conditions equilibrium formulae for the prediction of channel geometry and sediment transport should be applicable. It is unrealistic to expect instantaneous balance of force and resistance (Richards, 1982) due to temporal lags between water discharge, sediment transport and channel form changes (Allen, 1983). Definition of equilibrium thus requires a degree of temporal integration and / or recognition of some variation about a static equilibrium state. Any definition of equilibrium is thus timescale dependent and two such scales are considered herein, based on Table 2.1. Firstly, equilibrium at the macroscale (greater than a nominal 'event time') is considered since this is the scale at which channel cross-sectional geometry adjusts to imposed flow and sediment discharges. Secondly, megascale equilibrium is considered, and this is applicable at 'regime' time which is defined with reference to the geomorphological regime of the drainage basin and which is therefore subject to the influence of climatic fluctuations. It should be noted that equilibrium need not apply to all elements of the system under consideration (Howard, 1988).

At the macroscale, a form of static equilibrium was defined in the sand tray experiments but was difficult to identify precisely, and the approach to equilibrium was frequently interrupted by changes in the water and sediment input rates. This resulted in infrequent occurrence of conditions to which equilibrium sediment transport and channel geometry relationships could be applied. Where equilibrium could be identified, the sediment transport rate was close to that predicted by an equilibrium formula (see Figure 4.7) but the success of channel geometry predictions was considerably poorer (Hoey and Sutherland, forthcoming) for reasons which may include imperfect model scaling as well as system non-equilibrium.

Considering only sediment transport, 6 out of the 16 (38 %) data points plotted on Figure 4.7 are from times when equilibrium conditions were identified. When all of the measured channel cross-sections are considered 110 / 244 (45 % ; Run 1) and 58 / 167 (35 % ; Run 3) of channels were considered to be in equilibrium (Table 4.8). If these data are representative, about 40 % of channels in a braided river in which total discharge is constant can be said to be in equilibrium at any one time. Moreover, bedload transport equations can only be expected to yield reliable results in about 40 % of cases. This could be peculiar to the constant discharge case. However, Ashmore (1985, 1988) obtained agreement within 15% between measured and predicted bedload transport rates using the Bagnold (1980) equation with spatially and temporally integrated mean parameters. Pickup and Higgins (1979) obtained mean errors of 16 % using the Meyer-Peter and Müller (1948) equation over a 13.5 month period in a braided river. This correspondence implies that equilibrium may be attained over a longer time interval than the macroscale definition used herein, although there was good evidence for the passage of bed waves through braided channels in Ashmore's experiments and the sediment input rate at the head of his experimental channel was variable. As Davies (1987) noted, an approach using mean parameter values is 'black-box' and ignores the processes of bedload transport. For practical purposes this may be all that is required, but the present study has demonstrated how considerable variation in channel conditions and the types of process that govern bedload transport rates can be masked by spatial and temporal aggregation. In prototype rivers the effects of variations in discharge and exogenous sediment supply may cause a weakening of the value of the 'black-box' approach.

Identification of equilibrium at the megascale has been noted to be problematic (e.g. Richards, 1982). In the sand tray experiments, after the onset of a braided channel condition, Runs 1 and 2 had a rough balance between total sediment input and output, whereas aggradation continued in Run 3 (Figure 3.12). Runs 1 and 2 could therefore be considered to be in a form of long-term (megascale) equilibrium. Run 3 may exhibit a dynamic equilibrium condition under which continued aggradation was related to the imposed water and sediment loads. Within these broad equilibria there were fluctuations of varying duration and magnitude, and identification of equilibrium depends on the timescale considered. Over a shorter (macroscale) time period, aggradation and degradation could be regarded as equilibrium responses, but if equality of sediment input and output is used to define equilibrium this ceases to be the case. Bed waves can be superposed upon trends of net aggradation or degradation, and are not indicative of the system being out of equilibrium. They do however illustrate that the form of equilibrium which is in existence is not static.

In prototype rivers the suggestion has been made that bed waves may represent river response to disequilibrium, the degree of which is gradually reduced through time as a new equilibrium state is approached (e.g. Church, 1983; Pickup *et al.*, 1983). This applies to situations where exogenous bed waves are induced in a river system by localised acceleration of sediment inputs

(e.g. Beschta, 1983a; Pickup *et al.*, 1983) or by climatic changes (e.g. Church, 1983). Responses in such situations may involve exceedence of threshold conditions and may be modelled using a concept such as complex response (Schumm, 1977a; Beschta, 1983a) or catastrophe theory (Graf, 1988). Endogenous bed waves, whether produced by exogenous or endogenous sediment supplies, can be regarded as equilibrium forms at the megascale. This does not necessarily imply that they can be understood by the application of static equilibrium concepts, however. Pickup and Higgins' (1979) and Ashmore's (1988) correlations between measured and predicted sediment transport may be rarely repeated. The negative / positive impacts of departures from equilibrium in a given variable may not cancel out, even if that variable exhibits long-term equilibrium.

Unlike the laboratory work considered both herein, prototype rivers are subject to fluctuating water discharges and sediment inputs. Although the range of fluctuations is determined by the geomorphological regime, there is considerable potential within this for extreme events to have significant impacts. For example, Kirkby (1987) illustrated that the sequence of events may be as important as magnitude-frequency distributions in determining process impacts. Further, recovery from a major event is a slower process than the disturbance due to the event (e.g. Werritty and Ferguson, 1980) and the time between events can affect the response to them (e.g. Newson, 1980; Richards, 1982). Exogenous bed waves are produced by low frequency events and it has been argued that such waves will attenuate and eventually disappear from the river system. However, their presence within the river may be sufficient to induce endogenous waves to develop, and these could persist after the disappearance of the exogenous waves. This is equivalent to the extreme event causing a change in the process domain of the river system which persists beyond the effects of the event, and thus represents the exceedence of a threshold condition. Insufficient is known about the environmental history of river systems and about the impacts of extreme events through time to evaluate this suggestion. Hey (1979,1987) modelled the evolution of a drainage basin under constant discharge conditions and demonstrated that sediment output follows a damped oscillatory curve, much as observed in experimental work reported by Schumm (1977a). It is thus possible to produce bed waves in the absence of changing environmental controls or extreme events. The suggestion can be made therefore that these features are part of the equilibrium channel development processes when viewed at the megascale. As the timescale increases, climatic variations add further complications to the system and may enhance or obscure bed waves.

The conclusion reached herein is that endogenous bed waves are inherent features of river systems. Extreme events, climatic changes and the normal queuing of flow and sediment supply processes can enhance or cause attenuation of these features. Under certain conditions they can also cause exceedence of threshold conditions and lead to the river system entering a different process domain in which bed waves may be more apparent than previously. These catastrophic changes can also be produced by exogenous bed waves (e.g. the Kawerong River;

Pickup *et al.*, 1983; Pickup, 1988), but the impacts of such events are usually contained within the existing process domain, subject to time and place specific sensitivity of the system to change (Brunsdon and Thornes, 1979).

7.5 The potential for small scale modelling in fluvial geomorphology

Advantages and limitations of small scale modelling were discussed in Chapter 3. Some of the issues raised therein are now re-assessed in the light of the experiments described in Chapters 3-6.

One of the advantages of this approach is that experimental conditions can be readily controlled. A wide range of conditions can be achieved in such models: in the present case slope, discharge, sediment input rate and initial channel geometry could each have been altered, and variable water and sediment inputs used. Selection of a particular set of conditions is an arbitrary procedure within limits set by the aims of the investigation. Herein the aim was to investigate sediment output rate fluctuations in a braided stream, so slope and water discharge were set to values at which braiding develops, and the sediment feed rate was kept constant for much of the time. The same initial channel slope and shape were used in all three experiments, with the sediment feed rate differing between Run 1 and the others. The experimental results in terms of sediment output rate magnitudes and the evolution of channel patterns were distinctly different for the three runs. Thus, not only is it problematical to select appropriate boundary conditions for the experiments, but there is a range of behaviour associated with any given set of such conditions. Ashmore (1985) reported a case where a braided channel incised and took on a single thread form for 30 hours of an experimental run. The single thread channel transported bedload at double the rate of the braided channel. Davies (1987: reply) has interpreted this as an illustration of there being more than one equilibrium geometry for a given set of imposed conditions, and that the single channel state was attained as a consequence of a large energy input which enabled a threshold to be exceeded. It is uncertain to what extent such behaviour may occur in prototype channels and in the absence of information about the mechanisms involved in the transition it is unclear whether this should be regarded as a form of catastrophic behaviour. If this were to be the case then the single channel state may be as stable and persistent as the more frequently encountered braided morphology.

This example illustrates the difficulties of defining model characteristics and of assessing the representativeness of results. Church's (1984) requirement for the provision of statements describing the probabilities of experimental outcomes is thus difficult to meet in such experiments. Given that the replicability issue could be circumvented by multiple repetition of experiments the selection of boundary conditions becomes critical. Richards (1988) has noted the lack of appropriate physical theory which could be used to increase the control exercised over experimental conditions. Generalising from model results thus becomes difficult and although

useful for generating hypotheses about the operation of prototype systems, attempts to use models to assess the behaviour of particular prototypes are constrained by the problems noted above.

Schumm *et al.* (1987) argued that transfer of model results to prototype situations is the only full justification for performing small scale experiments. There are difficulties in doing this because of recognised deficiencies in the modelling procedure and the lack of physical theories which can be used to tie the different scales together and help to circumvent the absence of scale relationships for certain parameters (Richards, 1988). Deficiencies in the modelling procedure include the influence of viscous forces at some locations in the model channels and the under-representation of the coarse and fine tails of the sediment size distribution compared to prototype river sediments. The absence of vegetation which exerts an important stabilising influence in prototype rivers is another important omission (Davies, 1987).

It was noted in Chapter 3 that a regime theory which has been successfully applied to a prototype situation, is inapplicable to the channels developed in the sand tray (Thompson, 1987; Hoey and Sutherland, forthcoming), implying that Froude scaling may be inadequate over the gravel to sand size range. There is a requirement for scaling to be carefully checked before quantitative use can be made of model results (Davies, 1987). Scaling is a difficult issue because few processes scale linearly; Church (1984) noted that the form of hydraulic geometry equations (e.g. Table 3.4) in which the exponents are different for width and depth produces more than one length scale for a model channel. Two forms of checking scaling laws have been proposed. Davies (1987) suggested comparing models at 1:10 and 1:100, and Hoey and Sutherland (forthcoming) propose using prototype rivers as scale models of each other for the purpose of establishing scaling laws. Development of physical theory that should be applicable at all scales (e.g. Thompson, 1987) will assist this procedure and help to answer the criticism raised by Richards (1988) that the absence of such theory makes relating model results to prototype conditions difficult.

The stochastic model of sediment transfers developed in Chapter 6 was based on a model that has been used with success with prototype data (Kelsey *et al.*, 1987). There are often considerable difficulties in obtaining prototype data for calibration of such models, many of which can be avoided in small scale physical models. A greater quantity of reliable data can be readily obtained in the laboratory than in the field. This is not in itself justification for developing numerical modelling procedures which apply to small scale models, because the value of their results is limited if they cannot be directly applied to prototypes. Justification for this approach lies in the use of data that would be impossible to collect from prototypes, at least under conditions of controllable boundary conditions which can be used to simplify the computational procedures, to predict long-term changes in sediment storage. As noted above the use of the small scale physical model is primarily to generate hypotheses which are amenable to testing in prototype

situations. The equality of flushing times for different storage reservoirs that was noted in Chapter 6 is an example of how the results of small scale modelling can yield insights into the possible behaviour of prototype river systems.

The sediment dispersion data collected in the model may be considerably more reliable than could be collected in prototypes given the problems associated with tracer work. Being easier to obtain there is potential for direct application of this type of data to attempts to model sediment transfers in prototype rivers. Were small scale model data to be used in this way considerable care would be needed in definition of the boundary conditions of the model, given the differences between sediment exchanges during degrading, stable and aggrading periods that were noted in Chapter 6.

Although the experiments described herein have not led to the development of conclusions that can be directly applied to prototype rivers they have suggested several associations and processes that could be tested in field investigation. Some of these were utilised in the model of sediment transport and channel morphology changes presented for the Kowai River (Figure 5.24) which used the results of the physical modelling work as a basis. Without the laboratory results a less detailed understanding of the processes operating in the Kowai would have emerged. The most important results are: details of the linkages between channel planform and cross-sectional morphologies and fluctuations in the sediment transport rate; the nature of bar construction and erosion processes associated with these fluctuations; patterns of sediment dispersion and interaction between different sediment storage reservoirs; the frequency with which equilibrium conditions are prevalent in braided rivers. All of these results are able to be tested in prototype rivers and / or with small scale experiments designed to isolate specific factors. Small scale modelling as a means of generating testable hypotheses continues to be widely used, but direct application to prototype situations is difficult. There is an urgent need for more work on scaling relationships and non-scale dependent theoretical developments to enable this gap to be bridged and the potential benefits of small-scale modelling to be realised.

8. CONCLUSIONS

The discussions contained in the preceding Chapters have developed numerous conclusions, the most important of which are listed below. They include two (1 and 2) general conclusions regarding bed waves and bedload pulses in gravel-bed rivers, five (3-7) which resulted from the studies of braided rivers contained herein and which may be applicable to other gravel-bed river types, and one (8) regarding the methodology of small-scale physical modelling. These conclusions are followed by a prognosis and some suggestions for subsequent research.

1. Bed waves and bedload pulses can be classified according to their spatial and temporal scales and their generating processes. A more formal classification than that proposed by Gomez *et al.* (1989) has been developed (Table 7.1). This uses spatial and temporal scale (meso-, macro-, and mega-scales), sediment source (endogenous or exogenous) and the form of the wave relative to the 'normal' forms which are endogenous to the river system. The scales and types of bed wave that can develop in a given river system are dependent upon the geomorphological regime of the system. This includes such factors as gradient, sediment type and supply rate, and hydrological regime.

2. Endogenous bed waves can be regarded as forms which are in equilibrium with the geomorphological regime of the system. At each spatial and temporal scale the waves / pulses that develop involve departures from static equilibrium. Viewed at larger scales these periods of non-equilibrium cancel out. At the megascale a temporal / spatial scale one or two orders of magnitude greater than the scale of the phenomenon might be an appropriate one at which to define a static equilibrium. The development of endogenous bed waves will not affect the characteristic forms and processes of river systems. Exogenous bed waves are by definition outside the range of normal behaviour of the system. As such features are re-worked and transferred downstream they can be modified so as to begin to function as endogenous waves. Under certain conditions of system sensitivity to change and scale of sediment inputs an exogenous wave can cause catastrophic change in the nature of the river system, which may be irreversible so long as 'normal' sediment supply and hydrological processes continue to operate (e.g. the Kawerong River: Pickup *et al.* (1983); Pickup, 1988).

3. At the macro- and mega-scales bed waves develop as a consequence of non-equilibrium processes which are transient relative to the long-term equilibrium of the system. A result of the non-equilibrium condition is that cycles of aggradation and degradation are induced, with periods of static equilibrium being able to develop whether the river is in either an aggraded or degraded condition. The presence of non-equilibrium conditions can give the impression that sediment transport is 'supply-limited' and 'capacity-limited' at different times. This has implications for the already problematical definition of these states (Richards, 1988) given that conditions of static channel equilibrium are rare (Andrews and Parker, 1987 - discussion by M. Church). Static

equilibrium channel geometry was estimated as existing in about 40 % of all channels in the sand tray experiments described herein. This has implications for the application of equilibrium formulae for sediment transport and channel geometry. In some cases the effects of periods of non-equilibrium may cancel out over long time periods and enable such formulae to be readily applied.

4. Larger scale bed waves are composed of aggregated waves of smaller scale. In general, macro-scale waves in combination give rise to mega-scale features. Within the mega-scale waves of different size may combine, especially if waves of different size are transferred downstream at different rates. Meso-scale bed waves and bedload pulses are observed in association with the larger scale features but are not causally related to them, being governed by hydraulic rather than geomorphological factors.

5. Within one river system the spatial and temporal scales of bed waves and bedload pulses vary within ranges determined by the geomorphological regime of the system. This variation is a direct consequence of the stochastic nature of sediment supply, water discharge and channel form-sediment transport links. Stochastic behaviour was found under conditions of constant supply rate in the small scale model reported herein. Analysis of bed waves thus requires the stochastic component in their development to be recognised. In the case of exogenous waves which develop due to overloading of a river with sediment this may not be necessary, and deterministic modelling has proved successful in such cases (Pickup *et al.*, 1983; Weir, 1983).

6. The different stages of a bed wave cycle can be related to channel planform and cross-sectional morphologies in qualitative terms (Table 4.4; Figures 5.8, 5.24). The magnitudes of these relationships are not unique, since the response of a reach to each change in water discharge or sediment supply is dependent upon the previous history of channel and bar evolution in that reach. This inheritance was clearly recognised in the sand tray experiments, despite the absence of a sequence of varying flows, and illustrates the importance of such a sequence, as well as the absolute magnitudes of flood events, in determining channel form. In prototype situations similar relationships can be applied, although the effects of longitudinal non-uniformity (tributary inputs, rock gorges, vegetative stabilisation of deposits) exert significant influences. These can be corrected for if information is available on the historical development of the reaches concerned.

During a bed wave cycle the partitioning of stored sediment into reservoirs of different mobility changes in a predictable way. This occurs due to relocation of sedimentary particles from one reservoir to another, and as a passive effect of changes in channel morphology leading to the isolation of particular sedimentary deposits. The Kowai R. data (sub-section 7.3.3; Figure 7.5) confirm the view of Carson and Griffiths (1987) that stabilisation of relatively inactive deposits by vegetation is an important control over sediment susceptibility to transfer processes in prototype

rivers.

7. Processes of sediment exchange between reservoirs and of sediment transfer downstream vary between the different stages of a bed wave cycle. They are also different in endogenous and exogenous types of wave. Successful modelling of sediment exchanges is dependent upon understanding the processes of sediment redistribution in these different stages. Although it may be possible to use long-term average behaviour to produce a successful descriptive model which ignores the existence of bed waves, their significance for channel evolution over macro- and mega-scales is such that it will often be necessary to take account of them. One result of applying a stochastic modelling procedure to some of the sand tray data was to suggest that all storage reservoirs within the active bed of a braided river have equal flushing times (the time taken for a particle to be exported from the tray). This suggests that sediment redistribution processes preserve a form of equilibrium which ensures equality of mobility for particles in different reservoirs over a sufficiently long time period. This may not be the case for systems undergoing long-term aggradation or degradation in which the patterns of sediment transfer could be significantly different. It is more likely to occur over shorter timescales in braided rivers where the channels migrate across the active bed relatively rapidly. Where channel migration is slower, identification of such equality could require use of much longer timescales.

Application of this sort of model to a prototype river would require considerable data on sediment exchange processes. Although difficult to obtain in the prototype situation, such data could be approximated using small scale models, and the accuracy of these estimates would not necessarily be poorer than could be obtained using a direct prototype study.

8. One of the ways that was identified in sub-section 3.1.1 in which small-scale physical modelling can be used, is to generate hypotheses which can then be tested in prototype conditions. While rigorous testing may not always be possible, whether or not the prototype behaviour is consistent with the small scale model should be discernible. This was achieved in the present study by the investigation of links between parameters which can readily be monitored in prototype situations (channel patterns) and others which cannot (sediment transport rates and sediment storage volumes). This enables estimation in the prototype of the relative values of the latter group of variables from information about the former.

This approach can be extended by the use of techniques such as stochastic modelling of sediment transfer which enable the behaviour of small scale models to be more fully understood. This can lead to hypotheses of possible mechanisms of operation of prototype systems that could not be deduced from studies of the prototypes alone. While it is presently difficult to make quantitative transfers between model and prototype scales the transfer of qualitative ideas as to process operation is feasible.

As understanding of the operation of prototype systems improves, such uses of small scale modelling may become less valuable, and it may decline in utility or be replaced by models designed to examine more specific hypotheses than is presently the case.

8.1 Prognosis

The preceding Chapters have raised many suggestions for further research. At present it seems justifiable to make two assertions: firstly, the existence of bed waves and bedload pulses at a variety of scales is widely recognised; secondly, the relatively frequent occurrence of non-equilibrium forms and processes in gravel-bed rivers is now accepted. These imply a need to modify existing techniques for the prediction of sediment transport and channel morphology. Achieving this may not be straightforward given the range of types and scales of bedload pulses and bed waves that can be developed. However, Naden (1987) has demonstrated how mesoscale bedload pulses can be simulated, and Pickup *et al.* (1983), Weir (1983) and Kelsey *et al.* (1987) have been able to model megascale bed waves. Their success gives cause for optimism that these non-equilibrium features will be able to be incorporated into sediment transport and channel form models. The stochastic model developed in Chapter 6 of the present study is also promising in this regard. While requiring refinement and further data if it is to be of practical value, the results obtained herein suggest that it is likely to be a profitable line of future enquiry.

The question of links between channel form and bedload transport rates has only been comprehensively addressed in small scale modelling work. The use of the conclusions of this study in prototype rivers will depend on them being tested in such rivers. The limited data available from the Kowai River gave encouraging results and contributed substantially to the understanding of some of the observations made in the sand tray. This was achieved by use of sedimentological observations from the Kowai to elucidate the processes involved in bed wave development, which were observed in the model. More such tests of these ideas are required. While readily measured variables such as indices of channel planform hold most attraction (Davies, 1987), their reliable use as predictors of sediment storage volumes awaits comprehensive information on the processes which link these two components. If understanding of these links can be extended it may prove possible to generate quantitative information about sediment storage directly from measurements of total sinuosity or similarly easily obtained indices of channel morphology.

The widespread existence of bed waves and bedload pulses has important implications for palaeohydrological reconstructions and the interpretation of sedimentary deposits. Meso-scale bedload pulses and the processes which produce them show that indices such as particle size alone are unreliable indicators of flow conditions, and palaeohydraulic reconstructions need to take account of these factors (Reid and Frostick, 1987). Depositional forms can be related to

bedload transport rate fluctuations (e.g. Ashmore, 1987) and to non-equilibrium processes. Sedimentary deposits thus reflect non-equilibrium conditions and it is likely that the deposits associated with bed waves will be preserved in the sedimentary record. Identification of periods of degradation should not be necessarily interpreted as implying environmental change. Richards (1988) cautioned that regional environment, catchment conditions and reach scale processes need disaggregating in such studies, and the existence of bed waves reinforces his conclusion that reconstruction of reach scale conditions does not readily generate catchment or regional scale environmental information.

Of the avenues for further research that have been identified, the most significant are the following;

1. Prediction of bedload transport rates remains an important concern in gravel-bed rivers, but too little is known about the precise mechanisms of bedload transport for this to be reliably achieved. More research on the spatial and temporal variability in transport rates, the effects of hiding processes, responses of transport rates to channel non-equilibrium, and how these relate to channel morphology in cross-section and planform, is required.
2. In many cases the volumes of sediment stored in a particular river reach is of great significance for river management. Further development of models to describe sediment storage, and changes through time therein, is required. In particular, the differences in storage patterns between different river types and reaches of the same river under different conditions (e.g. aggrading vs. degrading; confined vs. unconfined) could be profitably investigated. Stochastic modelling of sediment storage volumes could be a useful way to approach this issue.
3. The responses of river systems to inputs of sediment from hillslopes or tributaries have not been documented fully. Further work on the dispersion of input material, the effects of inputs on channel morphology, and on the role of such interactions in determining the patterns of sediment delivery is required. The endogenous and exogenous bed wave types identified in Table 7.1 require description in more detail and under different conditions to enable the role of bed waves in sediment delivery to be fully comprehended.
4. Much valuable information can still be gained by conducting small-scale modelling of gravel-bed rivers. However, this needs to be supported by prototype investigations, and by development of more precise scaling relationships which enable the modelling results to be related to prototype behaviour. Prototype validation of model results is required. While the qualitative representativeness of model studies is apparent, there is presently a need to assess precisely the degree to which quantitative predictions can be made. This is urgently required if the maximum use is to be made of small scale modelling technology.

REFERENCES

- Ackers, P. and F.G. Charlton 1970. Dimensional analysis of alluvial channels with special reference to meander length. *Journal of Hydraulic Research* 8 : 287-316
- Allen, J.R.L. 1983. River bedforms: progress and problems. in Collinson, J.D. and J. Lewin (eds): *Modern and Ancient Fluvial Systems*. International Association of Sedimentologists Special Publication 6. Oxford, Blackwell, 575pp: 19-33
- Anderson, M.G. and A. Calver 1981. Laboratory channel pattern variability. *Area* 13 : 277-84
- Anderson, M.G. and K.M. Sambles 1988. A review of the bases of geomorphological modelling. in Anderson, M.G. (ed): *Modelling Geomorphological Systems*. Chichester, Wiley, 458pp: 1-32
- Anderson, O.D. 1976. *Time Series Analysis and Forecasting: The Box-Jenkins Approach*. London, Butterworths, 182pp.
- Andrews, E.D. 1983. Entrainment of gravel from naturally sorted riverbed material. *Geological Society of America Bulletin* 94 : 1225-31
- Andrews, E.D. and G. Parker 1987. Formation of a coarse surface layer as the response to gravel mobility. in Thorne, C.R., J.C. Bathurst and R.D. Hey (eds): *op. cit.*: 269-325 (includes discussion)
- Anthony, D.J. and M.D. Harvey 1987. Response of bed topography to increased bed load, Fall River, Colorado. in Beschta, R.L., T. Blinn, G.E. Grant, F.J. Swanson and G.G. Ice (eds): *Erosion and Sedimentation in the Pacific Rim*. International Association of Hydrologic Sciences Publication 165, Wallingford, 510pp: 387-8
- Ashmore, P.E. 1982. Laboratory modelling of gravel braided stream morphology. *Earth Surface Processes and Landforms* 7 : 201-25
- Ashmore, P.E. 1985. *Process and Form in Gravel Braided Streams: laboratory modelling and field observations*. Unpublished PhD Thesis, University of Alberta, Edmonton, 414pp.
- Ashmore, P.E. 1987. Bed load transfer and channel morphology in braided streams. in Beschta, R.L., T. Blinn, G.E. Grant, F.J. Swanson and G.G. Ice (eds): *Erosion and Sedimentation in the Pacific Rim*. International Association of Hydrologic Sciences Publication 165, Wallingford, 510pp: 333-42
- Ashmore, P.E. 1988. Bed load transport in braided gravel-bed stream models. *Earth Surface Processes and Landforms* 13 : 677-95
- Ashworth, P.J. and R.I. Ferguson 1986. Interrelationships of channel processes, changes and sediments in a proglacial braided river. *Geografiska Annaler* 68A : 361-71
- Bagnold, R.A. 1977. Bed load transport by natural rivers. *Water Resources Research* 13: 303-12
- Bagnold, R.A. 1980. An empirical correlation of bedload transport rates in flumes and natural rivers. *Proceedings, Royal Society of London* 372A : 453-73
- Begin, Z.B. 1981. The relationship between flow-shear stress and stream pattern. *Journal of Hydrology* 52 : 307-19

- Begin, Z.B. and S.A. Schumm 1984. Gradational thresholds and landform singularity: significance for Quaternary studies. *Quaternary Research* 21 : 267-74
- Bennett, R.J. 1979. *Spatial Time Series: analysis - forecasting - control*. London, Pion, 674pp.
- Beschta, R.L. 1982. Moving averages and cyclic patterns (note). *Journal of Hydrology (New Zealand)* 21 : 148-51
- Beschta, R.L. 1983a. Channel changes following storm-induced hillslope erosion in the Upper Kowai Basin, Torlesse Range, New Zealand. *Journal of Hydrology (New Zealand)* 22 : 93-111
- Beschta, R.L. 1983b. Long-term changes in channel widths of the Kowai River, Torlesse Range, New Zealand. *Journal of Hydrology (New Zealand)* 22 : 112-22
- Best, J.L. 1987. Flow dynamics at river channel confluences: implications for sediment transport and bed morphology. in Ethridge, F.G., R.M. Flores and M.D. Harvey (eds): *Recent Developments in Fluvial Sedimentology*. Society of Economic Palaeontologists and Mineralogists Special Publication 39: 27-35
- Bettess, R. and W.R. White 1983. Meandering and braiding of alluvial channels. *Proceedings of the Institution of Civil Engineers Part 2*, 75 : 525-38
- Blakely, R.J., P. Ackroyd and M. Marden 1981. *High Country River Processes*. Tussock Grasslands and Mountain Lands Institute, Lincoln College, Special Publication 22, 94pp.
- Bluck, B.J. 1982. Texture of gravel bars in braided streams. in Hey, R.D., J.C. Bathurst and C.R. Thorne (eds): *op. cit.*: 339-55 (includes discussion)
- Bluck, B.J. 1987. Bed forms and clast size changes in gravel-bed rivers. in Richards, K.S. (ed): *River Channels: Environment and Process*, Institute of British Geographers Special Publication 18, Oxford, Blackwell, 391pp: 159-78
- Box, G.E.P and G.M. Jenkins 1971. *Time Series Analysis: forecasting and control*. San Francisco, Holden Day, 553pp.
- Bradley, J.B. 1984. Transition of a meandering river to a braided system due to high sediment concentration flows. in Elliott, C.M. (ed): *River Meandering*. Proceedings of the Conference Rivers '83, American Society of Civil Engineers: 89-100
- Bray, D.I. and K.S. Davar 1987. Resistance to flow in gravel-bed rivers. *Canadian Journal of Civil Engineering* 14 : 77-86
- Brayshaw, A.C. 1985. Bed microtopography and entrainment thresholds in gravel-bed rivers. *Geological Society of America Bulletin* 96 : 218-23
- Brayshaw, A.C., L.E. Frostick and I. Reid 1983. The hydrodynamics of particle clusters and sediment entrainment in coarse alluvial channels. *Sedimentology* 30 : 137-43
- Brierley, G.J. 1989. River planform facies models: the sedimentology of braided, wandering and meandering reaches of the Squamish River, British Columbia. *Sedimentary Geology* 61 : 17-35
- Brotherton, D.I. 1979. On the origin and characteristics of river channel patterns. *Journal of Hydrology* 44 : 211-30
- Brunsdon, D. 1973. The application of system theory to the study of mass movement. *Geologica Applicata e Idrogeologia* 8 : 185-208

- Brunsdon, D. and J.B. Thornes 1979. Landscape sensitivity and change. *Transactions, Institute of British Geographers NS 4* : 463-84
- Bruun, P. 1966. Model geology: prototype and laboratory streams. *Geological Society of America Bulletin 77* : 959-74
- Bruun, P. 1968. Model geology: prototype and laboratory streams: Reply *Geological Society of America, Bulletin 79* : 395-8
- Butler, P.R. 1977. Movement of cobbles in a gravel bed stream during a flood season. *Geological Society of America Bulletin 88* : 1072-4
- Carey, W.P. 1985. Variability in measured bedload-transport rates. *Water Resources Bulletin 21* : 39-48
- Carson, M.A. 1984a. Observations on the meandering-braided river transition, the Canterbury Plains, New Zealand. *New Zealand Geographer 40* : 12-17, 89-99
- Carson, M.A. 1984b. The meandering-braided river threshold: a reappraisal. *Journal of Hydrology 73* : 315-34
- Carson, M.A. 1986. Characteristics of high-energy "meandering" rivers: the Canterbury Plains, New Zealand. *Geological Society of America Bulletin 97* : 886-95
- Carson, M.A. and G.A. Griffiths 1987. Bedload transport in gravel channels. *Journal of Hydrology (New Zealand) 26* : 1-151
- Chatfield, C. 1980. *The Analysis of Time Series: an introduction (2nd edition)*. London, Chapman and Hall, 268pp.
- Chayes, F. 1970. On deciding whether trend surfaces of progressively higher order are meaningful. *Geological Society of America Bulletin 81* : 1273-8
- Chin, C.O. 1985. Stream bed armouring. *Report No. 403, Department of Civil Engineering, University of Auckland* : 253pp.
- Chorley, R.J. 1967. Models in geomorphology. in Chorley, R.J. and P. Haggett (eds): *Models in Geography*. London, Methuen, 816pp: 59-96
- Church, M. 1972. Baffin Island sandurs: a study of Arctic fluvial processes. *Bulletin of the Geological Survey of Canada 216* : 208pp.
- Church, M. 1983. Pattern of instability in a wandering gravel bed channel. in Collinson, J.D. and J. Lewin (eds): *Modern and Ancient Fluvial Systems*. International Association of Sedimentologists, Special Publication 6. Oxford, Blackwell, 575pp: 169-80
- Church, M. 1984. On experimental method in geomorphology. in Burt, T.P. and D.E. Walling (eds): *Catchment Experiments in Fluvial Geomorphology*. IGU Commission on Field Experiments in Geomorphology, Norwich, Geo Abstracts 593pp: 563-80
- Church, M. and D. Jones 1982. Channel bars in gravel-bed rivers. in Hey, R.D., J.C. Bathurst and C.R. Thorne (eds): *op. cit.*: 291-338 (includes discussion)
- Cox, N.J. 1983. On the estimation of spatial autocorrelation in geomorphology. *Earth Surface Processes and Landforms 8* : 89-93
- Custer, S.G., N. Bugosh, P.E. Ergenzinger and B.C. Anderson 1987. Electromagnetic detection of pebble transport in streams: a method for measurement of sediment-transport waves. in

- Ethridge, F.G., R.M. Flores and M.D. Harvey (eds): *Recent Developments in Fluvial Sedimentology*. Society of Economic Palaeontologists and Mineralogists Special Publication 39: 21-6
- Davies, T.R.H. 1987. Problems of bed load transport in braided gravel-bed rivers. in Thorne, C.R., J.C. Bathurst and R.D. Hey (eds): *op. cit.*: 793-828
- Davies, T.R.H. 1988. Modification of bedload transport capacity in braided rivers. *Journal of Hydrology (New Zealand)* 27: 69-72
- Davies, T.R.H. and A.L. Lee 1988. Physical hydraulic modelling of width reduction and bed level change in braided rivers. *Journal of Hydrology (New Zealand)* 27: 113-27
- Davies, T.R.H. and A.J. Sutherland 1983. Extremal hypotheses for river behaviour. *Water Resources Research* 19: 141-8
- Davoren, A. and M.P. Mosley 1986. Observations of bedload movement, bar development and sediment supply in the braided Ohau River. *Earth Surface Processes and Landforms* 11: 643-52
- Dietrich, W.E., T. Dunne, N.F. Humphrey and L.M. Reid 1982. Construction of sediment budgets for drainage basins. in Swanson, F.J., R.J. Janda, T. Dunne and D.N. Swanston (eds): *Sediment Budgets and Routing in Forested Drainage Basins*, USDA Forest Service, Pacific Northwest Forest and Range Experimental Station, General Technical Report PNW-141, 165pp: 5-23
- Ehrenberger, R. 1931. Direkte Geschiebemessungen an der Donau bei Wien und deren bisherige Ergebnisse (Direct bedload measurements on the Danube at Vienna and their results to date). *Die Wasserwirtschaft* 34: 1-9 (cited by Reid, I., L.E. Frostick and J.T. Layman 1985: *op. cit.*) *
- Einstein, H.A. 1937. Die Eichung des im Rhein verwendeten Geschiebefangers (The calibration of the bedload trap used in the Rhine). *Schweizerische Bauzeitung* 110: 29-32 (cited by Reid, I., L.E. Frostick and J.T. Layman 1985: *op. cit.*)
- Emmett, W.W. 1975. The channels and waters of the Upper Salmon River area, Idaho. *United States Geological Survey Professional Paper 870-A*: 116pp
- Engelund, F. and E. Hansen 1967. *A Monograph on Sediment Transport in Alluvial Streams*. Copenhagen, Teknisk Forlag, 62pp.
- Ergenzinger, P. 1987. Chaos and order: the channel geometry of gravel bed braided rivers. in Ahnert, F. (ed): *Geomorphological Models: theoretical and empirical aspects*. Catena Supplement 10, 210pp: 85-98
- Eriksson, E. 1971. Compartment models and reservoir theory. *Annual Review of Ecology and Systematics* 2: 67-84
- Ettema, R. 1984. Sampling armor-layer sediments. *Journal of Hydraulic Engineering* 110: 992-6
- Everitt, B.L. 1968. Use of the cottonwood in an investigation of recent history of a flood plain. *American Journal of Science* 266: 417-39
- Fahnestock, R.D. 1963. Morphology and hydrology of a glacial stream - White River, Mt. Rainier, Washington. *United States Geological Survey Professional Paper 422-A*: 67pp.

- Ferguson, R.I. 1972. Theoretical models of river channel pattern. *Unpublished PhD Thesis, University of Cambridge.*
- Ferguson, R.I. 1977. Meander migration: equilibrium and change. In Gregory, K.J. (ed): *River Channel Changes*. Chichester, Wiley, 448pp: 235-48
- Ferguson, R.I. 1981. Channel forms and channel changes. In Lewin, J. (ed): *British Rivers*. London, Allen and Unwin, 216pp: 90-125
- Ferguson, R.I. 1987. Hydraulic and sedimentary controls of channel pattern. In Richards, K.S. (ed): *River Channels: Environment and Process*. Institute of British Geographers Special Publication 18. Oxford, Blackwell, 391pp: 129-58
- Ferguson, R.I. and A. Werritty 1983. Bar development and channel changes in the gravelly River Feshie, Scotland. In Collinson, J.D. and J. Lewin (eds): *Modern and Ancient Fluvial Systems*. International Association of Sedimentologists Special Publication 6. Oxford, Blackwell, 575pp: 181-93
- Gardiner, V. and R. Dackombe 1983. *Geomorphological Field Manual*. London, Allen and Unwin, 254pp.
- Gibbs, C.J. and C.R. Neill 1973. Laboratory testing of model VUV bed-load sampler. *Report No. REH/73/2, Research Council of Alberta.*
- Gilbert, G.K. 1917. Hydraulic mining debris in the Sierra Nevada. *United States Geological Survey Professional Paper 105* : 154pp
- Gomez, B. 1983. Temporal variations in bedload transport rates: the effect of progressive bed armouring. *Earth Surface Processes and Landforms 8* : 41-54
- Gomez, B., R.L. Naff and D.W. Hubbell 1989. Temporal variations in bedload transport rates associated with the migration of bedforms. *Earth Surface Processes and Landforms 14* : 135-56
- Gorycki, M.A. 1973. Hydraulic drag: a meander initiating mechanism. *Geological Society of America Bulletin 84* : 175-86
- Graf, W.L. 1977. The rate law in fluvial geomorphology. *American Journal of Science 277* : 178-91
- Graf, W.L. 1988. Applications of catastrophe theory in fluvial geomorphology. In Anderson, M.G. (ed): *Modelling Geomorphological Systems*. Chichester, Wiley, 458pp: 33-47
- Gregory, D.I. and S.A. Schumm 1987. The effect of active tectonics on alluvial river morphology. In Richards, K.S. (ed): *River Channels: Environment and Process*. Institute of British Geographers Special Publication 18. Oxford, Blackwell, 391pp: 41-68
- Griffiths, G.A. 1979. Recent sedimentation history of the Waimakariri River, New Zealand. *Journal of Hydrology (New Zealand) 18* : 6-28
- Griffiths, G.A. 1980. Stochastic estimation of bed load yield in pool-and-riffle mountain streams. *Water Resources Research 16* : 931-7
- Griffiths, G.A. 1981. Flow resistance in coarse gravel bed rivers. *Journal of the Hydraulics Division, Proceedings of the American Society of Civil Engineers 107* : 899-918

- Guy, H.P., R.E. Rathbun and E.V. Richardson 1967. Recirculating and sand-feed type flume experiments. *Journal of the Hydraulics Division, Proceedings of the American Society of Civil Engineers* 93 (HY5) : 97-114
- Hassan, M.A., A.P. Schick and J.B. Laronne 1984. The recovery of flood-dispersed coarse sediment particles: a three-dimensional magnetic tracing method. in Schick, A.P. (ed): *Channel Processes- Water, Sediment, Catchment Controls*. Catena Supplement 5: 153-62
- Hayward, J.A. 1979. Mountain stream sediments. in Murray, D.L. and P. Ackroyd (eds): *Physical Hydrology: New Zealand experience*. Wellington, N.Z. Hydrological Society 229pp: 193-212
- Hayward, J.A. 1980. *Hydrology and stream sediment from Torlesse Stream catchment*. Tussock Grasslands and Mountain Lands Institute, Lincoln College, Special Publication 17, 236pp.
- Hayward, J.A. and A.J. Sutherland 1974. The Torlesse Stream vortex-tube sediment trap. *Journal of Hydrology (New Zealand)* 13 : 41-53
- Hein, F.J. 1974. *Gravel Transport and Stratification Origins, Kicking Horse River, British Columbia*. Unpublished M.Sc. Thesis, McMaster University, Hamilton, Ontario, 135pp.
- Hein, F.J. and R.G. Walker 1977. Bar evolution and development of stratification in the gravelly, braided, Kicking Horse River, British Columbia. *Canadian Journal of Earth Sciences* 14 : 562-70
- Hey, R.D. 1979. Dynamic process-response model of river channel development. *Earth Surface Processes* 4 : 59-72
- Hey, R.D. 1987. River dynamics, flow regime and sediment transport. in Thorne, C.R., J.C. Bathurst and R.D. Hey (eds): *op. cit.*: 17-40
- Hey, R.D., J.C. Bathurst and C.R. Thorne (eds) 1982. *Gravel-Bed Rivers: Fluvial processes, Engineering and Management*. Chichester, Wiley, 875pp.
- Hickin, E.J. 1969. A newly-identified process of point bar formation in natural streams. *American Journal of Science* 267 : 999-1010
- Hickin, E.J. 1972. Pseudomeanders and point dunes - a flume study. *American Journal of Science* 272: 762-99
- Hoey, T.B. in press, 1989. Reconstruction of the recent flow history of a braided gravel river. *Journal of Hydrology (New Zealand)* 28
- Hoey, T.B. and A.J. Sutherland Forthcoming 1989. Self formed channels in a laboratory sand tray. Paper to be presented to the XXIIIrd Congress, International Association for Hydraulic Research, Ottawa, Canada.
- Hong, L.B. and T.R.H. Davies 1979. A study of stream braiding: summary. *Geological Society of America Bulletin* 90 : 1094-5
- Hooke, R. LeB. 1968. Model geology: prototype and laboratory streams: Discussion. *Geological Society of America Bulletin* 79 : 391-3
- Howard, A.D. 1988. Equilibrium models in geomorphology. in Anderson, M.G. (ed): *Modelling Geomorphological Systems*. Chichester, Wiley, 458pp: 49-72
- Howard, A.D., M.E. Keetch and C.L. Vincent 1970. Topological and geometrical properties of braided streams. *Water Resources Research* 6 : 1674-88

- Hubbell, D.W. 1987. Bed load sampling and analysis. in Thorne, C.R., J.C. Bathurst and R.D. Hey (eds): *op. cit.*: 89-118 (includes discussion)
- Isaacson, D.L. and R.W. Madsen 1976. *Markov Chains: theory and applications*. New York, Wiley, 256pp.
- Iseya, F. and H. Ikeda 1987. Pulsations in bedload transport rates induced by a longitudinal sediment sorting: a flume study using sand and gravel mixtures. *Geografiska Annaler 69A* : 15-27
- Jackson, R.G. 1975. Hierarchical attributes and a unifying model of bed forms composed of cohesionless material and produced by shearing flow. *Geological Society of America Bulletin 86* : 1523-33
- Jackson, W.L. and R.L. Beschta 1982. A model of two-phase bedload transport in an Oregon Coast Range stream. *Earth Surface Processes and Landforms 7* : 517-27
- Jackson, W.L. and R.L. Beschta 1984. Influences of increased sand delivery on the morphology of sand and gravel channels. *Water Resources Bulletin 20* : 527-33
- Kang, S-D. 1982. *Sediment Transport in a Small Glacial Stream: Hilda Creek, Alberta*. Unpublished M.Sc. Thesis, University of Illinois at Chicago Circle, 267pp.
- Kellerhals, R. and D.I. Bray, 1971. Sampling procedures for coarse fluvial sediments. *Journal of the Hydraulics Division, Proceedings of the American Society of Civil Engineers 97* : 1165-80
- Kelsey, H.M., R. Lamberson and M-A. Madej 1987. Stochastic model for the long-term transport of stored sediment in a river channel. *Water Resources Research 23* : 1738-50
- Kirk, R.M., R.F. McLean, J.S. Burgess and M.B. Reay 1974. The production of fluorescent sand tracer. *Geologiska Föreningens i Stockholm Förhandlingar 96* : 208-11
- Kirkby, M.J. 1972. Alluvial and non-alluvial meanders. *Area 4* : 284-8
- Kirkby, M.J. 1980. The stream head as a significant geomorphic threshold. in Coates, D.R. and J.D. Vitek (eds): *Thresholds in Geomorphology*. London, Allen and Unwin, 498pp: 53-73
- Kirkby, M.J. 1987. The Hurst effect and its implications for extrapolating process rates. *Earth Surface Processes and Landforms 12* : 57-67
- Kirkby, M.J. and I. Statham 1975. Surface stone movement and scree formation. *Journal of Geology 83* : 349-62
- Klingeman, P.C. and W.W. Emmett 1982. Gravel bedload transport processes. in Hey, R.D., J.C. Bathurst and C.R. Thorne (eds): *op. cit.*: 141-79 (includes discussion)
- Komar, P.D. and Z. Li 1986. Pivoting analyses of the selective entrainment of sediments by shape and size with application to gravel threshold. *Sedimentology 33* : 425-36
- Kondolf, G.M. and W.V.G. Matthews 1986. Transport of tracer gravels on a coastal California River. *Journal of Hydrology 85* : 265-80
- Krigström, A. 1962. Geomorphological studies of sandur plains and their braided rivers in Iceland. *Geografiska Annaler 44* : 328-46
- Kuhnle, R.A. and J.B. Southard 1988. Bed load transport fluctuations in a gravel bed laboratory channel. *Water Resources Research 24* : 247-60

- Lane, E.W. 1957. A study of the shape of channels formed by natural streams flowing in erodible material. *U.S. Army Corps of Engineers, Missouri River Division, Sediment Series 9* : 106pp.
- Langbein, W.B. and L.B. Leopold 1968. River channel bars and dunes - theory of kinematic waves. *United States Geological Survey Professional Paper 422-L*.
- Laronne, J.B., M.J. Duncan and P.A. Rodley 1986. Bar dynamics in the North Ashburton River. in Smart, G.M. and S.M. Thompson (eds): *Ideas on the Control of Gravel Bed Rivers*. Publication No. 9, Hydrology Centre, Christchurch, 248pp: 230-41 (includes discussion)
- Lee, A.L. and T.R. Davies 1986. Dominant discharge of braided streams. in Smart, G.M. and S.M. Thompson (eds): *Ideas on the Control of Gravel Bed Rivers*. Publication No. 9, Hydrology Centre, Christchurch, 248pp: 220-9 (includes discussion)
- Lekach, J. and A.P. Schick 1983. Evidence for transport of bedload in waves: analysis of fluvial sediment samples in a small upland stream channel. *Catena 10* : 267-79
- Leopold, L.B. and M.G. Wolman 1957. River channel patterns: braided, meandering and straight. *United States Geological Survey Professional Paper 282-B* : 39-85
- Lewin, J., S.B. Bradley and M.G. Macklin 1983. Historical valley alluviation in mid-Wales. *Geological Journal 18* : 331-50
- Lisle, T.E. 1987. Overview: Channel morphology and sediment transport in steepland streams. in Beschta, R.L., T. Blinn, G.E. Grant, F.J. Swanson and G.G. Ice (eds): *Erosion and Sedimentation in the Pacific Rim*. *International Association of Hydrologic Sciences Publication 165*, Wallingford, 510pp: 287-297
- Macklin, M.G. and J. Lewin 1989. Sediment transfer and transformation of an alluvial valley floor: the River South Tyne, Northumbria, U.K. *Earth Surface Processes and Landforms 14* : 233-46
- Madej, M.A. 1982. Sediment transport and channel changes in an aggrading stream in the Puget Lowland, Washington. in Swanson, F.J., R.J. Janda, T. Dunne and D.N. Swanston (eds): *Sediment Budgets and Routing in Forested Drainage Basins*, USDA Forest Service, Pacific Northwest Forest and Range Experimental Station, General Technical Report PNW-141, 165pp: 97-108
- Magilligan, F.J. 1985. Historical floodplain sedimentation in the Galena River basin, Wisconsin and Illinois. *Annals of the Association of American Geographers 75* : 583-94
- Maizels, J.K. 1983a. Proglacial channel systems: change and thresholds for change over long, intermediate and short timescales. in Collinson, J.D. and J. Lewin (eds): *Modern and Ancient Fluvial Systems*. International Association of Sedimentologists, Special Publication 6. Oxford, Blackwell, 575pp: 251-66
- Maizels, J.K. 1983b. Palaeovelocity and palaeodischarge determination for coarse gravel deposits. in Gregory, K.J. (ed): *Background to Palaeohydrology*. Chichester, Wiley, 486pp: 101-39
- Meade, R.H. 1985. Wavelike movement of bedload sediment, East Fork River, Wyoming. *Environmental Geology and Water Science 7* : 215-25

- Meland, N. and J.O. Norrman 1969. Transport velocities of individual size fractions in heterogeneous bed load. *Geografiska Annaler* 51A : 127-44
- Melton, M.A. 1962. Methods for measuring the effect of environmental factors on channel properties. *Journal of Geophysical Research* 67 : 1485-90
- Meyer-Peter, E. and R. Müller 1948. Formulas for bed-load transport. *Proceedings of the International Association of Hydraulic Research, 3rd Annual Conference* : 39-64
- Miall, A.D. 1977. A review of the braided-river depositional environment. *Earth Science Reviews* 13 : 1-62
- Mosley, M.P. 1978. Bed material transport in the Tamaki River near Dannevirke, North Island, New Zealand. *New Zealand Journal of Science* 21 : 619-26
- Mosley, M.P. 1981. Semi-determinate hydraulic geometry of river channels, South Island, New Zealand. *Earth Surface Processes and Landforms* 6 : 127-37
- Mosley, M.P. 1982. A procedure for characterising river channels. *Water and Soil Miscellaneous Publication 32*, Wellington, National Water and Soil Conservation Organisation: 68pp.
- Mosley, M.P. 1987. The classification and characterisation of rivers. in Richards, K.S. (ed): *River Channels: Environment and Process*. Institute of British Geographers Special Publication 18. Oxford, Blackwell, 391pp: 295-320
- Mosley, M.P. 1988. Bedload transport and sediment yield in the Onyx River, Antarctica. *Earth Surface Processes and Landforms* 13 : 51-67
- Mosley, M.P. and G.L. Zimpfer 1978. Hardware models in geomorphology. *Progress in Physical Geography* 2 : 438-61
- Moss, A.J., P. Green and J. Hutka 1982. Small channels: their experimental formation, nature and significance. *Earth Surface Processes and Landforms* 7 : 401-15
- Mühlhofer, L. 1933. Untersuchungen über die Schwebstoff und die Geschiebeführung des Inn nächst Kirchbichl (Tirol) (Investigations into suspended load and bedload of the River Inn, near Kirchbichl, Tirol). *Die Wasserwirtschaft* 26 : 1-4, 17-21, 31-4, 48-51, 55-7, 70-4 (cited by Reid, I., L.E. Frostick and J.T. Layman 1985: *op. cit.*)
- Naden, P. 1987. Modelling gravel-bed topography from sediment transport. *Earth Surface Processes and Landforms* 12 : 353-67
- Naden, P. and A.C. Brayshaw 1987. Small- and medium- scale bedforms in gravel-bed rivers. in Richards, K.S. (ed): *River Channels: Environment and Process*. Institute of British Geographers Special Publication 18. Oxford, Blackwell, 391pp: 249-71
- Nakamura, F. 1986. Analysis of storage and transport processes based on age distribution of sediment. *Transactions, Japanese Geomorphological Union* 7-3 : 165-84
- Nakamura, F., T. Araya and S. Higashi 1987. Influence of river channel morphology and sediment production on residence time and transport distance. in Beschta, R.L., T. Blinn, G.E. Grant, F.J. Swanson and G.G. Ice (eds): *Erosion and Sedimentation in the Pacific Rim*. International Association of Hydrologic Sciences Publication 165, Wallingford, 510pp: 355-64
- Nanson, G.C. 1974. Bedload and suspended load transport in a small, steep, mountain stream. *American Journal of Science* 274 : 471-86

- Newson, M.D. 1980. The geomorphological effectiveness of floods- a contribution stimulated by two recent events in mid-Wales. *Earth Surface Processes* 5 : 1-16
- Neill, C.R. and V.J. Galay 1967. Systematic evaluation of river regime. *Journal of the Waterways and Harbors Division, Proceedings of the American Society of Civil Engineers* 93 (WW1) : 25-53
- Nordin, C.F. and J.H. Algert 1966. Spectral analysis of sand waves. *Journal of the Hydraulics Division, Proceedings of the American Society of Civil Engineers* 92 (HY5) : 95-114
- North Canterbury Catchment Board and Regional Water Board (NCCB) 1982. *The Water Resources of the Ashley Catchment*. Christchurch, New Zealand, 240pp.
- Ore, H.T. 1964. Some criteria for recognition of braided stream deposits. *Wyoming University Contributions to Geology* 3 : 1-14
- Osterkamp, W.R. 1978. Gradient, discharge, and particle-size relations of alluvial channels in Kansas, with observations on braiding. *American Journal of Science* 278 : 1253-68
- Paine, A.D.M. 1985. 'Ergodic' reasoning in geomorphology: time for a review of the term ? *Progress in Physical Geography* 9 : 1-15
- Parker, G. 1976. On the cause and characteristic scales of meandering and braiding in rivers. *Journal of Fluid Mechanics* 76 : 457-80
- Parker, G. 1982. Discussion of Bray, D.I. 1982. *Regime equations for gravel-bed rivers* in Hey, R.D., J.C. Bathurst and C.R. Thorne (eds): *op. cit.*: 542-51
- Parker, G. and A.W. Peterson 1980. Bar resistance of gravel-bed streams. *Journal of the Hydraulics Division, Proceedings of the American Society of Civil Engineers* 106 : 1559-75
- Parker, G. and P.C. Klingeman 1982. On why gravel bed streams are paved. *Water Resources Research* 18 : 1409-23
- Parker, G., P.C. Klingeman and D.G. McLean 1982. Bedload and size distribution in paved gravel-bed streams. *Journal of the Hydraulics Division, Proceedings of the American Society of Civil Engineers* 108 : 544-71
- Pearson, C.P. and S.M. Thompson 1986. Comments on basket sampling of bedload. in Smart, G.M. and S.M. Thompson (eds): *Ideas on the Control of Gravel Bed Rivers*. Publication No. 9, Hydrology Centre, Christchurch, 248pp: 242-6
- Pickup, G. 1977. Downstream variations in morphology, flow conditions and sediment transport in an eroding channel. *Zeitschrift für Geomorphologie NF19* : 443-59
- Pickup, G. 1988. Hydrology and sediment models. in Anderson, M.G. (ed): *Modelling Geomorphological Systems*. Chichester, Wiley, 458pp: 153-215
- Pickup, G. and R.J. Higgins 1979. Estimating sediment transport in a braided gravel channel- the Kawerong River, Bougainville, Papua New Guinea. *Journal of Hydrology* 40 : 283-97
- Pickup, G., R.J. Higgins and I. Grant 1983. Modelling sediment transport as a moving wave - the transfer and deposition of mining waste. *Journal of Hydrology* 60 : 281-301
- Pitlick, J.C. and C.R. Thorne 1987. Sediment supply, movement and storage in an unstable gravel-bed river. in Thorne, C.R., J.C. Bathurst and R.D. Hey (eds): *op. cit.*: 151-83 (includes discussion)

- Reid, I., A.C. Brayshaw and L.E. Frostick 1984. An electromagnetic device for automatic detection of bedload motion and its field applications. *Sedimentology* 31 : 269-76
- Reid, I. and L.E. Frostick 1984. Particle interaction and its effect on the thresholds of initial and final bedload motion in coarse alluvial channels. in Koster, E.H. and R.J. Steel (eds): *Sedimentology of Gravels and Conglomerates*. Canadian Society of Petroleum Geologists Memoir 10: 61-8
- Reid, I. and L.E. Frostick 1987. Toward a better understanding of bedload transport. in Ethridge, F.G., R.M. Flores and M.D. Harvey (eds): *Recent Developments in Fluvial Sedimentology*. Society of Economic Palaeontologists and Mineralogists Special Publication 39: 13-19
- Reid, I., L.E. Frostick and J.T. Layman 1985. The incidence and nature of bedload transport during flood flows in coarse-grained alluvial channels. *Earth Surface Processes and Landforms* 10 : 33-44
- Reid, I., J.T. Layman and L.E. Frostick 1980. The continuous measurement of bedload discharge. *Journal of Hydraulic Research* 18 : 243-9
- Richards, K.S. 1976. The morphology of riffle-pool sequences. *Earth Surface Processes* 1 : 71-88
- Richards, K.S. 1979. Stochastic processes in one-dimensional series: an introduction. *Concepts and Techniques in Modern Geography* 23. Norwich, Geo Abstracts, 57pp.
- Richards, K.S. 1982. *Rivers: form and process in alluvial channels*. London, Methuen, 358pp.
- Richards, K.S. 1988. Fluvial geomorphology. *Progress in Physical Geography* 12 : 435-56
- Richards, K.S. in preparation 1989. Sediment delivery and the drainage network.
- Roberts, R.G. and M. Church 1986. The sediment budget in severely disturbed watersheds, Queen Charlotte Ranges, British Columbia. *Canadian Journal of Forest Research* 16 : 1092-1106
- Robertson-Rintoul, M.S.E. and K.S. Richards in preparation 1989.
- Romashin, V.V. 1967. Some characteristics of the morphological process in a mountain stream. *GGI Trudy* 144 : 67-76 (cited by Church, M. and D. Jones 1982: *op. cit.*)
- Rundle, A. 1985a. The mechanism of braiding. *Zeitschrift für Geomorphologie Supplementband* 55 : 1-13
- Rundle, A. 1985b. Braid morphology and the formation of multiple channels, The Rakaia, New Zealand. *Zeitschrift für Geomorphologie Supplementband* 55 : 15-37
- Rust, B.R. 1975. Fabric and structure in glaciofluvial gravels. in Jopling, A.V. and B.C. McDonald (eds). *Glaciofluvial and Glaciolacustrine Sedimentation*. Society of Economic Palaeontologists and Mineralogists Special Publication 23, Tulsa, SEPM, 320pp: 238-48
- Samide, G.W. 1971. *Sediment Transport Measurements*. Unpublished M.Sc. Thesis, University of Alberta.
- Schick, A.P., M.A. Hassan and J. Lekach 1987. A vertical exchange model for coarse bedload movement: numerical considerations. in Ahnert, F. (ed): *Geomorphological Models-Theoretical and Empirical Aspects*. Catena Supplement 10: 73-83

- Schumm, S.A. 1960. The shape of alluvial channels in relation to sediment type. *United States Geological Survey Professional Paper 352-B* : 17-30
- Schumm, S.A. 1977a. *The Fluvial System*. New York, Wiley, 338pp.
- Schumm, S.A. 1977b. Report to Manawatu Catchment Board. in *South-eastern Ruahine investigation: consultants appraisal of erosion processes*. (cited by Blakely, R.J., P. Ackroyd and M. Marden 1981: *op. cit.*)
- Schumm, S.A. and H.R. Khan 1972. Experimental study of channel patterns. *Geological Society of America, Bulletin 83* : 1755-70
- Schumm, S.A., M. P. Mosley and W.E. Weaver 1987. *Experimental Fluvial Geomorphology*. New York, Wiley, 413pp.
- Simons, D.B., R-M Li, T.J. Ward and L.Y. Shiao 1982. Modelling of water and sediment yields from forested drainage basins. in Swanson, F.J., R.J. Janda, T. Dunne and D.N. Swanston (eds): *Sediment Budgets and Routing in Forested Drainage Basins*, USDA Forest Service, Pacific Northwest Forest and Range Experimental Station, General Technical Report PNW-141, 165pp: 24-38
- Simons, D.B. and R.K. Simons 1987. Differences between gravel- and sand-bed rivers. in Thorne, C.R., J.C. Bathurst and R.D. Hey (eds): *op. cit.*: 3-15 (includes discussion)
- Smith, N.D. 1970. The braided stream depositional environment: comparison of the Platte River with some Silurian clastic rocks, North-Central Appalachians. *Geological Society of America Bulletin 81* : 2993-3014
- Smith, N.D. 1974. Sedimentology and bar formation in the upper Kicking Horse River, a braided outwash stream. *Journal of Geology 82* : 205-23
- Smith, N.D. 1978. Some comments on terminology for bars in shallow rivers. in Miall, A.D. (ed): *Fluvial Sedimentology* Canadian Society of Petroleum Geologists, Memoir 5, Calgary, CSPG, 859pp: 85-9
- Smith, N.D. and J.B. Southard 1982. Field investigations of braiding and gravel transport in a small outwash stream. in *Abstracts, International Association of Sedimentologists, 11th International Congress on Sedimentology*, Hamilton, Ontario.
- Smith, N.D. and D.G. Smith 1984. William River: an outstanding example of channel widening and braiding caused by bed-load addition. *Geology 12* : 78-82
- Solov'yev, N. Ya. 1967. Improvement and test on an instrument for recording coarse sediment. *GGI Trudy 141* : 58-78 (reprinted in *Soviet Hydrology 1967*: 158-72)
- Soni, J.P. 1981. Laboratory study of aggradation in alluvial channels. *Journal of Hydrology 49* : 87-106
- Southard, J.B., L.A. Boguchwal and R.D. Romea 1980. Test of scale modelling of sediment transport in steady unidirectional flow. *Earth Surface Processes 5* : 17-23
- Southard, J.B., N.D. Smith and R.A. Kuhnle 1984. Chutes and lobes: newly identified elements of braiding in shallow gravelly streams. in Koster, E.H. and R.J. Steel (eds): *Sedimentology of Gravels and Conglomerates*. Canadian Society of Petroleum Geologists Memoir 10: 51-9

- Tacconi, P. and P. Billi 1987. Bed load transport measurement by the vortex-tube trap on Virginio Creek, Italy. in Thorne, C.R., J.C. Bathurst and R.D. Hey (eds): *op. cit.*: 583-616 (includes discussion)
- Tandon, S.K. and R. Kumar 1981. Gravel fabric in a sub-Himalayan braided stream. *Sedimentary Geology 28* : 133-52
- Thompson, S.M. 1985. Transport of gravel by flows up to 500 m³/s, Ohau River, Otago, New Zealand. *Journal of Hydraulic Research 23* : 285-303
- Thompson, S.M. 1987. Field measurements in a gravel-bed river which confirm the theory of White *et al.* in Thorne, C.R., J.C. Bathurst and R.D. Hey (eds): *op. cit.*: 493-509 (includes discussion)
- Thorne, C.R., J.C. Bathurst and R.D. Hey (eds) 1987. *Sediment Transport in Gravel-Bed Rivers*. Chichester, Wiley, 995pp.
- Thornes, J.B. 1976. Autogeometry of semi-arid channel systems. in *Rivers '76: Symposium on Inland Waterways for Navigation, Flood Control and Water Diversions*. American Society of Civil Engineers. Volume II: 1715-25
- Weir, G.J. 1983. One-dimensional bed wave movement in lowland rivers. *Water Resources Research 19* : 627-31
- Werritty, A. and R.I. Ferguson 1980. Pattern changes in a Scottish braided river over 1, 30 and 200 years. in Cullingford, R.A., D.A. Davidson and J. Lewin (eds): *Timescales in Geomorphology*, Chichester, Wiley: 53-68
- White, W.R. and T.J. Day 1982. Transport of graded gravel bed material. in Hey, R.D., J.C. Bathurst and C.R. Thorne (eds): *op. cit.*: 181-223 (includes discussion)
- White, W.R., R. Bettess and E. Paris 1982. Analytical approach to river regime. *Journal of the Hydraulics Division, Proceedings of the American Society of Civil Engineers 108* : 1179-93
- Whiting, P.J., W.E. Dietrich, L.B. Leopold, T.G. Drake and R.L. Shreve 1988. Bedload sheets in heterogeneous sediment. *Geology 16* : 105-8
- Whittaker, J.G. 1987. Sediment transport in step-pool streams. in Thorne, C.R., J.C. Bathurst and R.D. Hey (eds): *op. cit.*: 545-579 (includes discussion)
- Williams, P.F. and B.R. Rust 1969. The sedimentology of a braided river. *Journal of Sedimentary Petrology 39* : 649-79
- Wilson, D.D. 1985. Erosional and depositional trends in rivers of the Canterbury Plains, New Zealand. *Journal of Hydrology (New Zealand) 24* : 32-44
- Wolman, M.G. and L.M. Brush 1961. Factors controlling the size and shape of stream channels in coarse, non-cohesive sands. *United States Geological Survey Professional Paper 282-G* : 183-210
- Yalin, M.S. 1971a. *Theory of Hydraulic Models*. London, Macmillan. 266pp.
- Yalin, M.S. 1971b. On the formation of dunes and meanders. *Proceedings, International Association for Hydraulic Research, 14th Congress , 3* : 101-8
- Yang, C.T. 1972. Unit stream power and sediment transport. *Journal of the Hydraulics Division, Proceedings of the American Society of Civil Engineers 98* : 1805-26

APPENDICES

APPENDIX 1 Bedload pulse and bed wave data from published studies

Q = discharge (m^3s^{-1}); b = channel width (m); q = discharge / unit width ($m^2 s^{-1}$); d_{50} = median bed material size (mm); S = channel slope; q^* = dimensionless discharge (equation 2,1); ω^{**} = dimensionless stream power index (equation 2,2); T = pulse period (s); λ^* = dimensionless wavelength (wavelength / channel width); L = sample length (s), or length of aggregated data period where data collection was continuous (marked c); F = interval between start of samples (s).

Q	b	q	d_{50}	S	q^*	ω^{**}	T	λ	Event
MESOSCALE									
Hayward (1979) L= 300-1200; F = 480-1380									
0.425	3.0	0.14	25	0.067	8.9	0.60	9000 (1)	-	12-15/8/73
0.730	3.0	0.24	25	0.067	15.3	1.03	6410	-	29-31/8/73
0.700	3.0	0.23	25	0.067	14.7	0.98	6400	-	28/1/75
1.750	3.0	0.58	25	0.067	36.7	2.46	17760	-	30/4/75
0.475	3.0	0.16	25	0.067	10.0	0.67	4110	-	19/8/75
0.520	3.0	0.17	25	0.067	10.9	0.73	2880	-	11/2/76
0.360	3.0	0.12	25	0.067	7.6	0.51	3530	-	10/8/76
1.300	3.0	0.43	25	0.067	27.3	1.83	3135	-	7-8/9/76
Gomez (1983) L = 30; F = 1200									
1.83	10.25	0.18	2.3	0.03	403.4	12.10	5940 (1)	-	17/8/79
1.83	10.25	0.18	2.3	0.03	403.4	12.10	7350	-	19/8/79
Reid <i>et al.</i> (1985) L = 1700 c									
-	3.0	-	16	-	-	2.25 (4)	5400 (3)	-	10/12/78
-	3.0	-	16	-	-	0.08	7200	-	28/12/78
-	3.0	-	16	-	-	0.09	5400	-	25/1/79
-	3.0	-	16	-	-	0.25	6840	-	31/1/79
-	3.0	-	16	-	-	0.26	6480	-	13/3/79
-	3.0	-	16	-	-	0.17	5400	-	17/3/79
-	3.0	-	16	-	-	0.35	5400	-	26/5/79
-	3.0	-	16	-	-	0.16	5040	-	9/12/79
-	3.0	-	16	-	-	0.66	6120	-	13/12/79
-	3.0	-	16	-	-	0.28	5760	-	27/12/79
-	3.0	-	16	-	-	0.51	6480	-	12/3/80
Custer <i>et al.</i> (1987) L = c									
3.7	8.3	0.45	12	0.02	84.3	1.69	36-600 (3)	-	
Tacconi and Billi (1987) L = 300c									
7.3	12.0	0.61	13	0.008	102.0	0.82	1110 (1)	-	Flood 7
5.7	12.0	0.48	13	0.008	79.6	0.64	1250	-	Flood 8
Whiting <i>et al.</i> (1988) F = 150									
1.3	6.0	0.22	4.6	0.0016	172.6	0.28	600 (1)	0.08-0.46	1984
3.0	6.0	0.50	4.6	0.0015	398.3	0.60	280	0.08-0.46	1986
Gibbs and Neill (1973) L = 30; F = 180									
0.17	1.22	0.14	3.1	0.0035	200.7	0.70	560 (1)	-	-

Q	b	q	d ₅₀	S	q*	ω*	T	λ	Event
MESOSCALE (Continued)									
Iseya and Ikeda (1987) L = 10; F = 10									
0.0004	0.10	0.004	1.54	0.021	16.5	0.35	73 (1)	-	R8
0.0004	0.10	0.004	1.65	0.024	14.8	0.36	65	-	R7
0.0004	0.10	0.004	1.90	0.033	12.0	0.40	79	-	R6
0.0004	0.10	0.004	2.16	0.040	9.9	0.40	54	-	R5
0.0004	0.10	0.004	2.60	0.042	7.5	0.32	60	-	R4
Kuhnle and Southard (1988) l = 30; F = 30									
0.021	0.74	0.028	3.03	0.019	41.7	0.79	370 (2)	-	L1
0.021	0.74	0.028	3.03	0.019	41.7	0.79	360,690, 1490	-	L2
0.019	0.53	0.035	3.03	0.019	52.2	0.99	588,852 1570	-	H1
0.005	0.15	0.035	3.03	0.024	52.2	1.25	450,600	-	H2,1
0.005	0.15	0.035	3.03	0.024	52.2	1.25	600	-	H2,2
0.005	0.15	0.035	3.03	0.024	52.2	1.25	300	-	H2,3
0.010	0.15	0.067	3.03	0.015	99.8	1.50	360,400	-	H3
Gomez <i>et al.</i> (1989) L = 6,18; F = 6,18									
6.04	2.74	2.200	23.50	0.0032	151.9	0.49	28,120,600 6000	-	SAFHL
MACROSCALE									
Jackson and Beschta (1982) L = 5-60; F = 6000									
1.53	3.2	0.48	4	0.01	469.8	4.70	43200	-	
Gomez <i>et al.</i> (1989) L = 300c									
0.54	4.0	0.1355	3.97	0.0066	134.1	0.89	10080	6-10	ERC
MEGASCALE									
Beschta (1983b)									
120	130	0.92	20	0.021	81.1	1.70	-	10	1943 Kowai R.
120	158	0.76	20	0.021	66.7	1.40	-	11.4	1960 Kowai R.
120	125	0.96	20	0.021	84.4	1.77	-	14.4	1972 Kowai R.
Griffiths (1979)									
1725	900	1.92	34	0.0018- 0.0041	2400	4.33- 9.85	-	11	Waimakariri R.
Church and Jones (1982)									
850	3w	-	-	-	-	-	-	42	Similkameen R.
850	6.1w	-	-	-	-	-	-	37	Lillooet R.
525	157	3.34	-	-	-	-	-	36.5	Bella Coola R.
Ashmore (1985, 1988) L = 60; F = 900									
0.003	0.95	0.003	1.16	0.015	18.91	0.28	5850, 24000 (6)	-	Run 2
0.0015	0.64	0.002	1.16	0.010	14.03	0.14	8140,36000	-	Run 3
0.0015	0.73	0.002	1.16	0.015	12.34	0.19	6840,36000	-	Run 4
0.0015	0.68	0.002	1.16	0.015	13.21	0.20	7800, 31000	-	Run 6
0.0015	0.46	0.003	1.16	0.010	19.53	0.20	10 990, 33500	-	Run 7
0.0045	1.06	0.004	1.16	0.010	25.42	0.25	9900, 36000	-	Run 8
0.0045	1.05	0.004	1.16	0.015	25.66	0.39	6390, 31000	-	Run 9
0.00225	0.88	0.003	1.16	0.015	15.31	0.23	8250, 27000	-	Run 10
0.0012	0.57	0.002	1.16	0.015	12.61	0.19	15100, 46800	-	Run 11

Q	b	q	d ₅₀	S	q*	ω*	T	λ	Event
MEGASCALE (Continued)									
Davies(1987) and Carson (1984a)									
2291	1250	1.83	39	0.0036	2110	7.59	-	≅4	Rakaia R.
Meade (1985)									
20	18	1.11	1.5	0.0007	4750	3.33	-	25-30	East Fork R.

Notes:

1. Period (T) was determined directly from published plots of sediment transport rate over time, by dividing the duration of the series by the number of peaks in the transport rate.
2. Period (T) obtained from Fourier analysis by the authors.
3. Period (T) determined by authors.
4. The authors only provided data for the onset and cessation of bedload transport. This was used to estimate a relationship between the stream power per unit bed area, ω ($\text{kg m}^{-1}\text{s}^{-1}; =\rho_w qS$) and flow depth, h. This gave $\omega = -3.98 + 35.6 h$ ($r^2 = 0.90$) by linear regression analysis. This relationship was used to estimate peak values of ω from published flood stage-time graphs.
5. For all field data with measured bedload transport rates peak water discharge was used. For bed wave data, the mean annual flood was used for the Rakaia and Waimakariri, two-year flood for the Kowai, and bankfull discharge for the East Fork R. (1.5 year recurrence interval), Lillooet R. and Similkameen R. A flood below bankfull stage of indeterminate recurrence interval was used for the Bella Coola R.
6. Periods were derived directly from sediment transport rate series. To convert to scaled values these should be multiplied by $\lambda_L^{1/2}$ ($=4.47$).

APPENDIX 2 Dimensioned and dimensionless hydraulic geometry data from the experimental runs

b = channel width (m); \bar{h} = mean flow depth (m); \bar{u} = mean flow velocity (m s^{-1}); Q = discharge (m^3s^{-1}); * indicates a dimensionless version of the quantity; $b^*=b/d_{50}$; $h^*=h/d_{50}$;

$Q^*=Q / ((S_s-1)g d_{50}^5)^{0.5}$; S = water surface slope; Channel conditions are: S=stable, A=aggrading, D=degrading, Sc=scour hole, W=widening, * = particle Reynolds number below threshold value of 70 so data set not used in hydraulic geometry calculations. Where the discharge obtained from $Q=b\bar{h}\bar{u}$ exceeded the input discharge of $1.9 \times 10^{-3} \text{ m}^3 \text{ s}^{-1}$, the discharge has been set to $1.9 \times 10^{-3} \text{ m}^3 \text{ s}^{-1}$.

b	\bar{h}	\bar{u}	Q	b^*	h^*	Q^*	S	Ch condition
RUN 1								
0.17	0.007	0.25	2.80×10^{-4}	298	12.3	8920	0.019	S
0.28	0.004	0.21	2.40×10^{-4}	491	7.0	7650	0.012	S
0.18	0.007	0.28	3.50×10^{-4}	316	12.3	11200	0.008	S
0.21	0.003	0.31	2.00×10^{-4}	368	5.3	6220	0.011	S
0.11	0.018	0.28	5.54×10^{-4}	193	31.6	17700	0.013	S
0.34	0.007	0.28	6.66×10^{-4}	597	12.3	21200	0.018	S
0.60	0.015	0.34	1.90×10^{-3}	1050	26.3	60900	0.007	D/Sc
0.60	0.012	0.36	1.90×10^{-3}	1050	19.3	60900	0.006	A
0.36	0.015	0.28	1.51×10^{-3}	632	26.3	48000	0.022	D
0.67	0.011	0.31	1.90×10^{-3}	1180	19.3	60900	0.008	D
0.59	0.008	0.38	1.76×10^{-3}	1035	14.0	56100	0.008	A
0.33	0.016	0.38	1.90×10^{-3}	579	28.1	60900	0.016	S
0.73	0.011	0.35	1.90×10^{-3}	1281	19.3	60900	0.011	A
0.09	0.010	0.21	1.90×10^{-4}	157	17.5	6060	0.013	S
0.17	0.005	0.28	2.40×10^{-4}	298	8.8	7650	0.016	A
0.10	0.009	0.26	2.30×10^{-4}	175	15.8	7330	0.020	A
0.30	0.012	0.32	1.20×10^{-3}	526	21.1	38300	0.008	A
0.31	0.021	0.32	1.90×10^{-3}	544	36.8	60900	0.014	A
0.18	0.005	0.21	1.90×10^{-4}	316	8.8	6060	0.013	A
0.67	0.008	0.30	1.61×10^{-3}	1180	14.0	51300	0.010	D
0.38	0.014	0.38	1.90×10^{-3}	667	24.6	60900	0.012	D
0.22	0.012	0.42	1.11×10^{-3}	386	21.1	36000	0.015	D
0.15	0.014	0.25	5.30×10^{-4}	263	24.6	16900	0.016	S
0.13	0.024	0.4	1.25×10^{-3}	228	42.1	39900	0.011	D

RUN 3								
0.29	0.012	0.43	1.42×10^{-3}	509	21.1	45300	0.008	A
0.18	0.010	0.34	6.00×10^{-4}	316	17.5	19100	0.008	S
0.22	0.005	0.31	3.10×10^{-4}	386	8.8	9880	0.012	S
0.18	0.009	0.31	4.70×10^{-4}	316	15.8	15000	0.006	S
0.26	0.006	0.28	4.40×10^{-4}	456	10.5	14000	0.006	S
0.15	0.013	0.31	6.10×10^{-4}	263	22.8	19400	0.010	A
0.32	0.014	0.28	1.30×10^{-3}	561	24.6	41400	0.008	W
0.21	0.020	0.34	1.40×10^{-3}	368	35.1	44600	0.006	D/W
0.28	0.016	0.34	1.50×10^{-3}	491	28.1	47800	0.010	A
0.23	0.010	0.34	7.50×10^{-4}	404	17.5	23900	0.008	A
0.38	0.008	0.34	9.80×10^{-4}	667	14.0	31200	0.011	D/W
0.18	0.004	0.31	7.20×10^{-4}	316	7.0	23000	0.015	S
0.26	0.013	0.34	1.10×10^{-3}	456	22.8	35069	0.018	A

b	\bar{h}	\bar{u}	Q	b*	h*	Q*	S	Ch condition
RUN 3 (Continued)								
0.14	0.003	0.17	7.00×10^{-5}	246	5.3	2230	0.014	A*
0.32	0.013	0.28	1.20×10^{-3}	561	22.8	38300	0.007	I-Sc
0.17	0.001	0.14	2.00×10^{-5}	298	1.8	638	0.017	S*
0.36	0.011	0.30	1.20×10^{-3}	632	19.3	38300	0.007	A
0.16	0.002	0.26	7.00×10^{-5}	281	3.5	2230	0.006	S*
0.36	0.011	0.38	1.50×10^{-3}	632	19.3	47800	0.015	S
0.25	0.011	0.34	9.20×10^{-4}	439	19.3	29300	0.004	A
0.28	0.002	0.26	1.40×10^{-4}	491	3.5	4460	0.009	A*
0.23	0.015	0.38	1.30×10^{-3}	404	26.3	41400	0.009	S
0.16	0.009	0.26	3.60×10^{-4}	281	15.8	11500	0.010	A
0.13	0.004	0.19	1.00×10^{-4}	228	7.0	3190	0.003	A
0.17	0.002	0.21	7.00×10^{-5}	298	3.5	2230	0.005	A*
0.44	0.010	0.34	1.50×10^{-3}	772	17.5	47800	0.007	D/W
0.20	0.009	0.23	4.10×10^{-4}	351	15.8	13100	0.005	A
0.25	0.012	0.30	8.90×10^{-4}	439	21.1	28300	0.010	W
0.26	0.008	0.31	6.10×10^{-4}	456	14.0	19400	0.016	A
0.17	0.005	0.24	2.10×10^{-4}	298	8.8	6700	0.010	A
0.24	0.009	0.40	8.90×10^{-4}	421	15.8	28400	0.009	S
0.34	0.005	0.27	4.80×10^{-4}	597	8.8	15300	0.009	S
0.25	0.013	0.30	9.60×10^{-4}	439	22.8	30600	0.007	S

APPENDIX 3 Flow parameters for the sand tray experiments

Re = Reynolds number ($=\bar{u} h / \nu$); Rep = particle Reynolds number ($=u_* d_i / \nu$); Fr = Froude number ($=\bar{u}/(g h)^{0.5}$); d_A = maximum armour layer particle size ($= 1.99\text{mm}$). In Runs 2 and 3 the letter B after the reference indicates that the channel was transporting bed material of all particle sizes.

Ref.	Re	Rep (d_{50})	Rep (d_A)	Fr	h/d_{50}	h/d_A	Ref.	Re	Rep (d_{50})	Rep (d_A)	Fr	h/d_{50}	h/d_A
RUN 1													
1.1.1	1354	17.9	62.6	1.00	10.5	3.0	1.3.16	7144	16.8	58.6	0.85	35.1	10.1
1.1.2	987	13.0	45.4	0.96	8.8	2.5	1.3.17	3158	18.8	65.8	0.66	24.6	7.0
1.1.3	1842	12.6	43.8	1.08	12.3	3.5	1.4.1	975	13.4	46.7	0.96	8.8	2.5
1.1.4	3948	27.6	96.3	0.74	26.3	7.5	1.4.2	1235	18.6	65.0	0.72	12.3	3.5
1.1.5	3948	23.4	81.8	0.74	26.3	7.5	1.4.3	3138	23.9	83.5	0.73	22.8	6.5
1.1.6	5527	24.3	84.9	0.62	36.8	10.6	1.4.4	3639	27.7	96.8	0.76	24.6	7.0
1.1.7	1598	12.4	43.5	1.54	8.8	2.5	1.4.5	2210	15.2	53.0	1.30	12.3	3.5
1.1.8	7671	21.8	75.9	0.70	42.1	12.1	1.4.6	1578	13.4	46.7	1.54	8.8	2.5
1.1.9	8310	22.6	79.0	0.67	45.6	13.1	1.4.7	2897	21.5	75.0	0.76	21.1	6.0
1.1.10	4644	14.8	51.7	1.06	22.8	6.5	1.4.8	3899	22.2	77.6	0.74	26.3	7.5
1.1.11	2876	12.3	43.1	1.14	15.8	4.5	1.4.9	3472	15.5	54.3	1.04	19.3	5.5
1.1.12	3948	30.5	106.4	0.74	26.3	7.5	1.4.10	5181	19.9	69.4	0.74	31.6	9.0
1.1.13	677	11.3	39.3	1.42	5.3	1.5	1.4.11	1439	11.7	40.9	1.40	8.8	2.5
1.2.1	5358	18.4	78.7	0.98	26.3	7.5	1.4.12	1783	16.9	59.0	0.87	14.0	4.0
1.2.2	5358	18.4	78.7	0.98	26.3	7.5	1.4.13	3166	17.4	60.7	0.94	19.3	5.5
1.2.3	1128	10.6	45.4	1.10	8.8	2.5	1.4.14	2860	15.5	54.3	0.86	19.3	5.5
1.2.4	3516	14.7	63.0	1.04	19.3	5.5	1.4.15	3138	16.9	59.0	0.73	22.8	6.5
1.2.5	4475	16.6	71.1	0.92	24.6	7.0	1.4.16	2228	20.3	70.9	0.78	17.5	5.0
1.2.6	2557	13.4	57.5	1.01	14.0	4.0	1.5.1	2331	17.8	62.0	1.10	14.0	4.0
1.2.7	3835	15.4	65.8	0.99	21.1	6.0	1.5.2	5433	25.9	90.4	0.83	29.8	8.5
1.2.8	3685	15.4	65.8	0.76	24.6	7.0	1.5.3	1579	17.1	59.8	0.76	14.0	4.0
1.2.9	2106	12.6	53.8	1.01	14.0	4.0	1.5.4	3384	23.4	81.8	0.63	26.3	7.5
1.2.10	5358	20.6	88.0	0.98	26.3	7.5	1.5.5	6430	25.7	89.6	0.90	31.6	9.0
1.2.11	3422	17.1	73.3	0.79	22.8	6.5	1.5.6	3205	19.3	67.3	0.94	19.3	5.5
1.2.12	1053	8.2	35.2	1.43	7.0	2.0	1.5.7	7351	24.1	84.3	0.72	40.4	11.6
1.3.1	14552	40.3	140.6	0.72	63.2	18.1	1.5.8	5537	23.1	80.8	0.72	33.3	9.5
1.3.2	1711	13.3	46.5	1.00	12.3	3.5	1.6.1	7119	27.6	96.4	0.73	38.6	11.1
1.3.3	4155	18.2	63.4	0.95	22.8	6.5	1.6.2	9004	27.6	96.4	0.91	38.6	11.1
1.3.4	2106	14.2	49.7	1.01	14.0	4.0	1.6.3	7957	22.5	78.7	0.81	38.6	11.1
1.3.5	987	11.3	39.3	0.96	8.8	2.5	1.6.4	5178	19.2	67.1	0.86	28.1	8.0
1.3.6	5255	17.1	59.8	1.19	22.8	6.5	1.6.5	2360	15.2	53.1	1.10	14.0	4.0
1.3.7	2331	13.4	46.9	1.10	14.0	4.0	1.6.6	5016	22.2	77.3	0.76	29.8	8.5
1.3.8	4061	20.1	70.3	0.58	31.6	9.0	1.6.7	3198	24.6	86.0	0.66	24.6	7.0
1.3.9	4475	20.8	72.7	0.92	24.6	7.0	1.6.8	1627	19.7	68.9	0.64	15.8	4.5
1.3.10	1579	13.6	47.6	1.17	10.5	3.0	1.6.9	3560	20.3	70.9	1.04	19.3	5.5
1.3.11	3158	20.8	72.7	0.66	24.6	7.0	1.6.10	2931	18.7	65.3	0.86	19.3	5.5
1.3.12	4475	22.9	80.1	0.69	29.8	8.5	1.6.11	1371	15.0	52.4	1.00	10.5	3.0
1.3.13	3158	20.8	72.7	0.66	24.6	7.0	1.6.12	2199	22.5	78.0	0.65	19.3	5.5
1.3.14	5114	22.3	77.7	0.86	28.1	8.0	1.6.13	2199	19.5	68.2	0.65	19.3	5.5
1.3.15	3205	22.9	80.1	0.94	19.3	5.5	1.6.14	2284	23.4	81.8	0.78	17.5	5.0
RUN 2													
2.1.1B	3743	20.0	70.0	0.99	21.1	6.0	2.1.12B	5615	25.4	88.8	0.81	31.6	9.0
2.1.2B	5615	19.0	66.4	0.81	31.6	9.0	2.1.13B	6239	22.9	80.0	0.77	35.1	10.1
2.1.3B	6239	15.4	53.6	0.77	35.1	10.1	2.1.14	1541	16.2	56.5	0.76	14.0	4.0
2.1.4	2312	16.9	59.1	0.95	15.8	4.5	2.1.15B	6862	26.8	93.6	0.73	38.6	11.1

Ref.	Re	Rep (d_{50})	Rep (d_A)	Fr	h/d_{50}	h/d_A	Ref.	Re	Rep (d_{50})	Rep (d_A)	Fr	h/d_{50}	h/d_A
RUN 2 (continued)													
2.1.5B	3743	17.4	60.7	0.99	21.1	6.0	2.1.16B	5404	23.0	80.3	0.72	33.3	9.5
2.1.6B	3413	17.4	60.7	0.90	21.1	6.0	2.1.17B	3339	47.2	164.8	0.79	22.8	6.5
2.1.7	2789	20.1	70.1	0.48	28.1	8.0	2.1.18	2862	13.1	45.6	0.68	22.8	6.5
2.1.8B	1321	11.6	40.6	1.00	10.5	3.0	2.1.19B	3743	15.1	52.8	0.99	21.1	6.0
2.1.9B	4550	21.8	76.2	0.78	28.1	8.0	2.1.20B	3413	12.0	42.0	0.90	21.1	6.0
2.1.10B	4881	25.1	87.7	0.66	33.3	9.5	2.1.21	2569	14.2	49.5	0.90	17.5	5.0
2.1.11	3523	20.6	71.9	0.61	28.1	8.0	2.1.22B	3413	12.0	42.0	0.90	21.1	6.0

RUN 3

3.1.1B	13408	22.9	79.9	0.84	54.4	15.6	3.2.14	3099	14.8	51.7	0.73	22.8	6.5
3.1.2B	8893	22.3	77.7	0.91	38.6	11.1	3.2.15B	8014	31.2	108.8	0.80	40.4	11.6
3.1.3B	5659	22.6	79.0	1.15	24.6	7.0	3.2.16	2751	17.2	60.0	0.52	26.3	7.5
3.1.4B	3205	18.5	64.5	0.94	19.3	5.5	3.2.17B	3136	22.5	78.6	1.27	15.8	4.5
3.1.5B	7501	24.3	84.9	0.83	36.8	10.6	3.3.1B	5433	13.8	48.3	0.83	29.8	8.5
3.1.6B	2256	19.1	66.8	0.78	17.5	5.0	3.3.2B	1711	13.3	46.5	1.00	12.3	3.5
3.1.7B	5114	19.0	66.3	0.86	28.1	8.0	3.3.3B	10509	25.7	89.6	0.84	45.6	13.1
3.1.8	2623	17.4	60.9	1.04	15.8	4.5	3.3.4	5733	21.4	74.6	0.81	31.6	9.0
3.1.9B	3205	17.6	61.5	0.94	19.3	5.5	3.3.5	2440	16.8	58.6	0.84	17.5	5.0
3.1.10	1748	10.1	35.2	1.27	10.5	3.0	3.3.6	6994	32.9	114.8	0.64	42.1	12.1
3.1.11B	2623	12.3	43.1	1.04	15.8	4.5	3.3.7	3835	27.7	96.6	0.59	29.8	8.5
3.1.12	2106	11.6	40.6	1.01	14.0	4.0	3.3.8	1579	15.0	52.4	0.76	14.0	4.0
3.1.13B	4371	21.6	75.3	0.81	26.3	7.5	3.4.1	2265	10.5	36.6	0.53	22.8	6.5
3.1.14B	1748	11.6	40.6	1.27	10.5	3.0	3.4.2	1155	9.2	32.1	0.88	10.5	3.0
3.1.15	2895	15.7	55.0	0.86	19.3	5.5	3.4.3B	4053	16.0	55.9	0.95	22.8	6.5
3.1.16B	6712	25.5	89.1	0.75	36.8	10.6	3.4.4	2742	13.5	47.2	0.63	22.8	6.5
3.1.17B	1730	15.7	55.0	0.81	14.0	4.0	3.4.5B	1476	14.0	49.0	0.86	12.3	3.5
3.1.18	6994	24.7	86.1	0.64	42.1	12.1	3.4.6B	5520	19.9	69.3	1.15	24.6	7.0
3.1.19B	5753	17.4	60.9	0.81	31.6	9.0	3.4.7	3576	22.5	78.6	0.68	26.3	7.5
3.1.20B	7351	25.5	88.9	0.72	40.4	11.6	3.4.8	624	11.6	40.6	0.86	7.0	2.0
3.1.21B	2876	14.2	49.7	1.14	15.8	4.5	3.4.9	1394	21.8	75.9	0.67	14.0	4.0
3.1.22B	6073	25.3	88.5	0.79	33.3	9.5	3.4.10	1568	19.5	68.1	0.64	15.8	4.5
3.1.23	4475	18.8	65.8	0.92	24.6	7.0	3.4.11B	5520	18.8	65.8	1.15	24.6	7.0
3.2.1B	4264	25.2	87.9	0.81	26.3	7.5	3.4.12	5969	30.8	107.4	0.68	36.8	10.6
3.2.2B	5924	31.0	108.4	0.79	33.3	9.5	3.4.13	3127	17.6	61.5	0.74	19.3	5.5
3.2.3	1321	14.2	49.7	1.00	10.5	3.0	3.4.14B	6308	20.1	70.3	1.07	28.1	8.0
3.2.4	1027	11.6	40.6	1.43	7.0	2.0	3.4.15	6620	21.9	76.6	0.88	33.3	9.5
3.2.5B	8014	25.5	88.9	0.80	40.4	11.6	3.4.16	4988	20.1	70.3	0.86	28.1	8.0
3.2.6	779	14.0	49.0	0.77	8.8	2.5	3.4.17	2742	14.8	51.7	0.63	22.8	6.5
3.2.7	2604	15.4	53.7	0.71	21.1	6.0	3.4.18B	4365	17.8	62.0	0.92	24.6	7.0
3.2.8B	7170	19.7	68.8	0.72	40.4	11.6	3.4.19	4108	19.0	66.3	0.72	28.1	8.0
3.2.9	771	16.9	59.2	0.58	10.5	3.0	3.4.20B	4053	12.1	42.3	0.95	22.8	6.5
3.2.10	3301	17.2	60.0	0.63	26.3	7.5	3.4.21	1476	16.6	58.0	0.86	12.3	3.5
3.2.11B	8014	21.3	74.3	0.80	40.4	11.6	3.4.22B	1540	10.1	35.2	1.17	10.5	3.0
3.2.12B	3310	19.4	67.6	0.44	33.3	9.5	3.4.23	4264	18.4	64.2	0.81	26.3	7.5
3.2.13	3136	20.8	72.5	1.27	15.8	4.5							

APPENDIX 4 Sources of aerial photographs, Kowal River

Frame numbers are for frames covering Porters and Bridge Reaches. * indicates North Canterbury Catchment Board photos.

Date	Survey #	Frame #	Approximate scale
4.5.1943	251	05916	1:15 000
14.2.1960	1063	2761/35	1: 27 000
30.10.1965	-		1: 8 000
27.9.1966	1801	J/5, J/7	1: 8 600
13.2.1975	2799	B/2, B/3	1: 8 000
24.2.1976	2956 HB		1: 13 000
14.8.1987 *	-		1: 5 600

APPENDIX 5 Sediment output rates and particle sizes for the experimental runs

* indicates the sampling time immediately prior to flow shut downs. Volume change is equal to sediment input - output in a 15 minute time period.

Time (min)	Sediment input rate (g s ⁻¹)	Sediment output rate (g s ⁻¹)	Volume change (kg)	d ₅₀ (mm)	Time (min)	Sediment input rate (g s ⁻¹)	Sediment output rate (g s ⁻¹)	Volume change (kg)	d ₅₀ (mm)
RUN 1									
15	4.17	0.96	2.88		1515	2.78	4.74	-1.77	
30	4.17	0.72	3.10		1530	2.78	7.50	-4.25	
45	4.17	0.98	2.87		1545	2.78	10.31	-6.78	
60	4.17	1.09	2.77	0.75	1560	2.78	8.61	-5.25	0.91
75	4.17	1.29	2.59		1575	2.78	5.12	-2.11	
90	4.17	1.41	2.48		1590	2.78	3.96	-1.07	
105	4.17	1.35	2.54		1605	2.78	4.94	-1.94	
120	4.17	1.14	2.72	0.54	1620	2.78	4.24	-1.32	0.49
135	4.17	1.22	2.65		1635	2.78	3.98	-1.08	
150	4.17	1.17	2.69		1650	2.78	6.16	-3.05	
165	4.17	1.24	2.64		1665	2.78	7.60	-4.34	
180	4.17	1.42	2.48	0.54	1680*	2.78	4.47	-1.52	0.78
195	4.17	1.49	2.41		1695	2.78	5.93	-2.84	
210*	4.17	1.32	2.56		1710	2.78	4.04	-1.13	
225	4.17	1.17	2.70		1725	2.78	4.04	-1.13	
240	4.17	0.84	2.99	0.70	1740	2.78	5.47	-2.42	0.48
255	4.17	1.09	2.77		1755	2.78	4.45	-1.50	
270	1.39	1.55	-0.14		1770	2.78	3.42	-0.58	
285	1.39	1.55	-0.14		1785	2.78	2.93	-0.13	
300	1.39	2.38	-0.89	0.67	1800	2.78	3.19	-0.37	0.48
315	1.39	1.99	-0.54		1815	2.78	2.52	0.23	
330	1.39	1.92	-0.48		1830	2.78	2.38	0.36	
345	1.39	1.51	-0.11		1845	2.78	2.18	0.53	

Time (min)	Sediment input rate (g s ⁻¹)	Sediment output rate (g s ⁻¹)	Volume change (kg)	d ₅₀ (mm)	Time (min)	Sediment input rate (g s ⁻¹)	Sediment output rate (g s ⁻¹)	Volume change (kg)	d ₅₀ (mm)
RUN 1 (continued)									
360	1.39	2.01	-0.56	0.69	1860	2.78	1.99	0.71	0.54
375	1.39	2.31	-0.82		1875	2.78	2.04	0.67	
390	1.39	2.13	-0.67		1890	2.78	1.73	0.94	
405	1.39	3.08	-1.52		1905	2.78	1.73	0.94	
420*	2.08	2.35	-0.24	0.66	1920*	2.78	1.87	0.82	0.62
435	2.08	2.25	-0.15		1935	2.78	1.39	1.25	
450	2.08	1.32	0.69		1950	2.78	0.62	1.94	
465	2.08	3.25	-1.05		1965	2.78	1.26	1.36	
480	2.08	8.31	-5.60	0.58	1980	2.78	1.70	0.97	0.63
495	2.08	7.16	-4.57		1995	2.78	2.25	0.47	
510	2.08	3.20	-1.00		2010	2.78	2.09	0.61	
525	2.08	5.04	-2.66		2025	2.78	1.88	0.81	
540	2.08	6.57	-4.04	0.50	2040	2.78	1.46	1.18	0.55
555	2.08	7.47	-4.85		2055	2.78	1.09	1.51	
570	2.08	7.16	-4.57		2070	2.78	0.69	1.88	
585	2.08	6.58	-4.04		2085	2.78	0.63	1.93	
600	2.08	6.69	-4.14	0.54	2100	2.78	0.60	1.96	0.53
615	2.08	6.46	-3.94		2115	2.78	0.74	1.84	
630*	2.08	6.80	-4.25		2130	2.78	0.68	1.89	
645	2.08	7.08	-4.50		2145	2.78	0.68	1.89	
660	2.08	7.10	-4.52	0.69	2160	2.78	0.84	1.74	0.54
675	2.08	7.02	-4.45		2175*	2.78	1.24	1.38	
690	2.08	6.37	-3.85		2190	2.78	0.94	1.66	
705	2.08	6.40	-3.88		2205	2.78	0.87	1.71	
720	2.08	5.45	-3.03	0.46	2220	2.78	1.47	1.17	0.87
735	2.08	4.17	-1.88		2235	2.78	4.24	-1.32	
750	2.08	3.38	-1.17		2250	2.78	8.36	-5.02	
765	2.08	5.34	-2.93		2265	2.78	6.04	-2.94	
780	2.08	4.76	-2.41	0.53	2280	2.78	3.30	-0.47	0.91
795	2.08	4.55	-2.22		2295	2.78	2.38	0.36	
810	2.08	4.86	-2.50		2310	2.78	1.64	1.02	
825	2.08	4.05	-1.77		2325	2.78	1.27	1.36	
840*	4.17	3.45	0.65	0.57	2340	2.78	0.49	2.06	0.50
855	4.17	3.09	0.97		2355	2.78	0.54	2.01	
870	4.17	3.85	0.28		2370	2.78	0.51	2.04	
885	4.17	3.47	0.63		2385	2.78	0.84	1.74	
900	4.17	3.73	0.39	0.69	2400*	2.78	1.14	1.48	0.46
915	4.17	6.30	-1.92		2415	2.78	1.36	1.28	
930	4.17	8.39	-3.80		2430	2.78	0.87	1.72	
945	4.17	7.58	-3.07		2445	2.78	0.72	1.85	
960	4.17	6.56	-2.15	0.55	2460	2.78	1.13	1.48	0.61
975	2.78	4.81	-1.83		2475	2.78	2.23	0.49	0.72
990	2.78	3.74	-0.87		2490	2.78	3.78	-0.90	0.77
1005	2.78	3.16	-0.35		2505	2.78	4.31	-1.38	0.55
1020	2.78	2.65	0.11	0.53	2520*	2.78	8.49	-5.14	0.49
1035	2.78	2.04	0.67		2535	2.78	10.81	-7.23	1.03
1050	2.78	1.92	0.77		2550	2.78	7.59	-4.33	0.72
1065	2.78	3.07	-0.26		2565	2.78	7.34	-4.11	0.58
1080	2.78	3.58	-0.72	0.48	2580	2.78	6.35	-3.22	0.71
1095	0.00	2.18	-1.96		2595	2.78	5.34	-2.31	0.69
1110	0.00	2.76	-2.49		2610	2.78	4.76	-1.78	0.52
1125	0.00	2.04	-1.84		2625	2.78	4.13	-1.21	
1140	0.00	2.55	-2.29	0.55	2640*	2.78	3.46	-0.61	0.98
1155	2.78	2.15	0.56		2655	2.78	3.63	-0.77	

Time (min)	Sediment input rate (g s ⁻¹)	Sediment output rate (g s ⁻¹)	Volume change (kg)	d ₅₀ (mm)	Time (min)	Sediment input rate (g s ⁻¹)	Sediment output rate (g s ⁻¹)	Volume change (kg)	d ₅₀ (mm)
RUN 1 (continued)									
1170	2.78	1.59	1.07		2670	2.78	3.69	-0.83	
1185	2.78	1.06	1.55		2685	2.78	3.00	-0.20	
1200	2.78	0.83	1.75	0.55	2700	2.78	3.19	-0.37	0.82
1215*	2.78	2.25	0.47		2715	2.78	2.42	0.32	
1230	2.78	0.70	1.87		2730	2.78	3.16	-0.34	
1245	2.78	0.46	2.09		2745	2.78	1.57	1.09	
1260	2.78	0.31	2.22	0.61	2760*	2.78	2.33	0.40	0.63
1275	2.78	0.55	2.01		2775	2.78	4.06	-1.15	
1290	2.78	0.77	1.81		2790	2.78	1.38	1.26	
1305	2.78	1.05	1.56		2805	2.78	1.09	1.52	
1320	2.78	2.84	-0.05	0.68	2820	2.78	0.77	1.80	0.53
1335	2.78	1.28	1.35		2835	2.78	0.35	2.18	
1350	2.78	2.77	0.01		2850	2.78	0.29	2.23	
1365	2.78	3.24	-0.42		2865	2.78	0.26	2.26	
1380	2.78	3.02	-0.22	0.74	2880*	2.78	0.46	2.08	0.69
1395	2.78	2.73	0.04		2895	2.78	1.48	1.16	
1410	2.78	2.31	0.42		2910	2.78	5.47	-2.42	
1425	2.78	1.73	0.95		2925	2.78	4.41	-1.47	
1440*	2.78	1.16	1.46	0.50	2940	2.78	6.43	-3.28	0.90
1455	2.78	1.42	1.22		2955	2.78	4.93	-1.93	
1470	2.78	0.99	1.61		2970	2.78	3.57	-0.71	
1485	2.78	0.75	1.82		2985	2.78	1.55	1.11	
1500	2.78	1.62	1.04	0.59	3000	2.78	1.91	0.78	

RUN 2

15	2.50	0.31	1.97		885	2.50	1.83	0.60	
30	2.50	0.13	2.13		900	2.50	2.34	0.14	
45	2.50	0.26	2.02		915	2.50	2.75	-0.22	
60	2.50	0.41	1.88		930	2.50	2.62	-0.11	
75	2.50	0.45	1.84		945	2.50	2.52	-0.02	
90	2.50	0.45	1.85		960	2.50	2.48	0.02	
105	2.50	0.46	1.83		975	2.50	2.59	-0.08	
120	2.50	0.54	1.76		990	2.50	2.82	-0.29	
135	2.50	0.50	1.80		1005	2.50	2.82	-0.29	
150	2.50	0.42	1.87		1020	2.50	2.70	-0.18	
165	2.50	0.38	1.91		1035	2.50	2.21	0.26	
180	2.50	0.43	1.86		1050	2.50	2.88	-0.35	
195	2.50	0.56	1.75		1065	2.50	3.04	-0.48	
210	2.50	0.83	1.51		1080	2.50	2.44	0.05	
225	2.50	0.78	1.55		1095	2.50	2.11	0.35	
240	2.50	0.80	1.53		1110	2.50	1.94	0.51	
255	2.50	0.79	1.54		1125	2.50	2.10	0.36	
270	2.50	0.89	1.45		1140	2.50	2.24	0.24	
285	2.50	0.85	1.49		1155	2.50	1.77	0.66	
300	2.50	0.72	1.60		1170	2.50	2.05	0.40	
315	2.50	0.62	1.70		1185	2.50	1.91	0.53	
330	2.50	0.51	1.79		1200*	2.50	1.66	0.76	
345	2.50	0.45	1.84		1215	2.50	3.42	-0.83	
360	2.50	0.40	1.89		1230	2.50	2.03	0.42	
375	2.50	0.35	1.94		1245	2.50	1.95	0.49	
390	2.50	0.47	1.83		1260	2.50	1.94	0.51	
405	2.50	0.64	1.68		1275	2.50	1.94	0.51	
420*	2.50	0.69	1.63		1290	2.50	2.41	0.0	

Time (min)	Sediment input rate (g s ⁻¹)	Sediment output rate (g s ⁻¹)	Volume change (kg)	Time (min)	Sediment input rate (g s ⁻¹)	Sediment output rate (g s ⁻¹)	Volume change (kg)
---------------	--	---	--------------------------	---------------	--	---	--------------------------

RUN 2 (continued)

435	2.50	0.98	1.37	1305	2.50	2.37	0.11
450	2.50	0.61	1.70	1320	2.50	2.21	0.26
465	2.50	0.63	1.68	1335	2.50	2.30	0.18
480	2.50	0.63	1.68	1350	2.50	2.30	0.18
495	2.50	0.77	1.56	1365	2.50	2.33	0.15
510	2.50	1.13	1.23	1380	2.50	2.43	0.07
525	2.50	1.29	1.09	1395	2.50	2.49	0.01
540	2.50	1.49	0.91	1410	2.50	2.71	-0.19
555	2.50	1.70	0.72	1425	2.50	2.87	-0.33
570	2.50	1.58	0.83	1440*	2.50	2.50	0.00
585	2.50	1.52	0.88	1455	2.50	2.60	-0.09
600	2.50	1.14	1.22	1470	2.50	2.11	0.35
615	2.50	0.79	1.54	1485	2.50	2.28	0.20
630	2.50	1.02	1.33	1500	2.50	2.29	0.19
645	2.50	1.71	0.71	1515	2.50	2.76	-0.23
660	2.50	2.50	0.00	1530	2.50	2.64	-0.12
675	2.50	2.27	0.21	1545	2.50	2.66	-0.14
690	2.50	2.01	0.44	1560	2.50	2.46	0.04
705	2.50	1.69	0.73	1575	2.50	2.38	0.11
720	2.50	2.09	0.37	1590	2.50	2.28	0.19
735	2.50	3.92	-1.28	1605	2.50	2.19	0.28
750	2.50	2.67	-0.16	1620	2.50	1.98	0.47
765	2.50	2.26	0.21	1635	2.50	1.93	0.52
780	2.50	3.20	-0.63	1650	2.50	1.99	0.46
795	2.50	2.04	0.41	1665	2.50	2.05	0.40
810	2.50	1.95	0.50	1680*	2.50	1.99	0.46
825	2.50	1.32	1.06	1695	2.50	1.99	0.46
840*	2.50	1.55	0.85	1710	2.50	1.74	0.68
855	2.50	1.92	0.52	1725	2.50	2.15	0.32
870	2.50	1.76	0.66	1740	2.50	2.21	0.26

RUN 3

15	2.50	0.52	1.78	1485	2.50	2.79	-0.26
30	2.50	0.11	2.15	1500	2.50	2.77	-0.24
45	2.50	0.10	2.16	1515	2.50	2.57	-0.06
60	2.50	0.10	2.16	1530	2.50	2.40	0.09
75	2.50	0.10	2.16	1545	2.50	2.62	-0.10
90	2.50	0.11	2.15	1560	2.50	2.74	-0.21
105	2.50	0.10	2.16	1575	2.50	2.82	-0.29
120	2.50	0.18	2.09	1590	2.50	3.37	-0.79
135	2.50	0.32	1.96	1605	2.50	3.33	-0.75
150	2.50	0.35	1.93	1620	2.50	3.25	-0.67
165	2.50	0.35	1.94	1635	2.50	3.20	-0.63
180	2.50	0.29	1.99	1650	2.50	3.34	-0.76
195	2.50	0.28	2.00	1665	2.50	3.39	-0.80
210	2.50	0.24	2.04	1680*	2.50	3.36	-0.78
225	2.50	0.27	2.01	1695	2.50	3.13	-0.57
240	2.50	0.35	1.93	1710	2.50	3.00	-0.45
255	2.50	0.41	1.89	1725	2.50	3.00	-0.45
270	2.50	0.46	1.83	1740	2.50	2.99	-0.45
285	2.50	0.52	1.78	1755	2.50	2.81	-0.28
300	2.50	0.53	1.77	1770	2.50	2.73	-0.21
315	2.50	0.58	1.72	1785	2.50	2.55	-0.05

Time (min)	Sediment input rate (g s ⁻¹)	Sediment output rate (g s ⁻¹)	Volume change (kg)	Time (min)	Sediment input rate (g s ⁻¹)	Sediment output rate (g s ⁻¹)	Volume change (kg)
RUN 3 (continued)							
330	2.50	0.55	1.75	1800	2.50	2.52	-0.02
345	2.50	0.54	1.77	1815	2.50	2.37	0.12
360	2.50	0.53	1.77	1830	2.50	2.14	0.32
375	2.50	0.58	1.72	1845	2.50	2.07	0.39
390	2.50	0.64	1.67	1860	2.50	2.07	0.38
405	2.50	0.65	1.67	1875	2.50	2.45	0.04
420*	2.50	0.61	1.70	1890	2.50	2.60	-0.09
435	2.50	0.87	1.47	1905	2.50	2.65	-0.14
450	2.50	0.85	1.48	1920*	2.50	2.90	-0.36
465	2.50	0.96	1.39	1935	2.50	2.52	-0.02
480	2.50	0.84	1.49	1950	2.50	2.76	-0.23
495	2.50	0.61	1.70	1965	2.50	2.61	-0.10
510	2.50	0.51	1.79	1980	2.50	2.63	-0.11
525	2.50	0.50	1.80	1995	2.50	2.68	-0.17
540	2.50	0.40	1.89	2010	2.50	2.43	0.06
555	2.50	0.38	1.91	2025	2.50	2.45	0.05
570	2.50	0.39	1.90	2040	2.50	2.49	0.01
585	2.50	0.50	1.80	2055	2.50	2.55	-0.05
600	2.50	2.69	-0.17	2070	2.50	2.55	-0.05
615	2.50	1.94	0.51	2085	2.50	2.66	-0.15
630	2.50	3.69	-1.07	2100	2.50	2.81	-0.28
645	2.50	2.95	-0.40	2115	2.50	2.79	-0.27
660	2.50	2.03	0.42	2130	2.50	2.54	-0.04
675	2.50	1.37	1.02	2145	2.50	2.41	0.08
690	2.50	1.03	1.32	2160*	2.50	2.48	0.01
705	2.50	0.81	1.52	2175	2.50	2.25	0.22
720	2.50	0.64	1.67	2190	2.50	2.11	0.35
735	2.50	0.62	1.70	2205	2.50	2.18	0.29
750	2.50	0.62	1.69	2220	2.50	1.71	0.71
765	2.50	0.71	1.61	2235	2.50	1.88	0.56
780	2.50	0.49	1.81	2250	2.50	3.04	-0.49
795	2.50	0.43	1.86	2265	2.50	2.81	-0.28
810	2.50	0.52	1.78	2280	2.50	2.51	-0.01
825	2.50	1.12	1.24	2295	2.50	2.17	0.29
840	2.50	1.88	0.56	2310	2.50	2.26	0.21
855*	2.50	2.44	0.06	2325	2.50	2.71	-0.19
870	2.50	1.25	1.13	2340	2.50	2.87	-0.34
885	2.50	0.95	1.40	2355	2.50	1.79	0.64
900	2.50	0.70	1.62	2370	2.50	1.29	1.09
915	2.50	1.02	1.33	2385	2.50	2.47	0.03
930	2.50	2.12	0.35	2400*	2.50	2.29	0.19
945	2.50	1.96	0.48	2415	2.50	1.77	0.66
960	2.50	2.11	0.35	2430	2.50	1.24	1.13
975	2.50	2.07	0.39	2445	2.50	1.44	0.95
990	2.50	2.08	0.38	2460	2.50	1.24	1.14
1005	2.50	1.94	0.50	2475	2.50	1.02	1.33
1020	2.50	1.90	0.54	2490	2.50	0.97	1.38
1035	2.50	1.95	0.49	2505	2.50	1.41	0.98
1050	2.50	1.99	0.46	2520	2.50	1.58	0.82
1065	2.50	1.92	0.53	2535	2.50	1.57	0.84
1080	2.50	2.14	0.33	2550	2.50	1.38	1.01
1095	2.50	1.91	0.53	2565	2.50	1.19	1.18
1110	2.50	2.01	0.44	2580	2.50	1.17	1.20
1125	2.50	1.93	0.52	2595	2.50	1.17	1.20

Time (min)	Sediment input rate (g s ⁻¹)	Sediment output rate (g s ⁻¹)	Volume change (kg)	Time (min)	Sediment input rate (g s ⁻¹)	Sediment output rate (g s ⁻¹)	Volume change (kg)
RUN 3 (continued)							
1140	2.50	1.91	0.53	2610	2.50	1.17	1.19
1155	2.50	1.77	0.66	2625	2.50	1.30	1.08
1170	2.50	1.63	0.79	2640*	2.50	1.43	0.96
1185	2.50	1.23	1.14	2655	2.50	1.56	0.85
1200	2.50	0.95	1.40	2670	2.50	1.25	1.13
1215*	2.50	1.04	1.31	2685	2.50	1.27	1.10
1230	2.50	1.22	1.16	2700	2.50	1.24	1.14
1245	2.50	1.48	0.91	2715	2.50	1.08	1.28
1260	2.50	2.19	0.28	2730	2.50	1.32	1.06
1275	2.50	2.34	0.14	2745	2.50	1.19	1.18
1290	2.50	2.16	0.31	2760	2.50	0.73	1.60
1305	2.50	2.20	0.27	2775	2.50	0.63	1.68
1320	2.50	2.39	0.10	2790	2.50	0.78	1.55
1335	2.50	2.28	0.20	2805	2.50	0.90	1.44
1350	2.50	2.18	0.29	2820	2.50	0.89	1.45
1365	2.50	1.94	0.50	2835	2.50	0.88	1.46
1380	2.50	1.73	0.69	2850	2.50	1.16	1.20
1395	2.50	1.78	0.65	2865	2.50	1.64	0.77
1410	2.50	2.01	0.44	2880*	2.50	1.82	0.61
1425	2.50	1.95	0.49	2895	2.50	2.16	0.30
1440*	2.50	2.26	0.22	2910	2.50	1.60	0.81
1455	2.50	3.18	-0.61	2925	2.50	1.49	0.91
1470	2.50	3.13	-0.56				
RUN 3a							
2940	3.33	1.32	1.81	3375	2.50	0.95	1.39
2955	3.81	1.44	2.13	3390	2.50	0.94	1.41
2970	7.50	1.97	4.97	3405	2.50	1.27	1.11
2985	9.54	2.66	6.19	3420	2.50	1.21	1.16
3000	6.69	2.36	3.90	3435	2.50	1.33	1.05
3015	6.48	2.45	3.62	3450	2.50	1.27	1.10
3030	5.61	2.11	3.14	3465	2.50	1.16	1.20
3045	4.71	1.73	2.68	3480	2.50	1.01	1.34
3060	4.20	1.78	2.18	3495	2.50	1.06	1.30
3075	3.64	2.29	1.22	3510	2.50	1.03	1.32
3090	3.05	2.26	0.71	3525	2.50	0.96	1.38
3105	3.21	2.53	0.61	3540	2.50	0.98	1.37
3120*	3.26	2.09	1.05	3555	2.50	0.77	1.55
3135	2.65	1.76	0.79	3570	2.50	0.66	1.66
3150	2.81	1.65	1.04	3585	2.50	0.67	1.65
3165	2.13	1.48	0.59	3600*	2.50	0.68	1.63
3180	2.79	1.34	1.30	3615	2.50	1.31	1.07
3195	1.38	1.32	0.05	3630	2.50	0.99	1.36
3210	2.04	1.07	0.87	3645	2.50	0.95	1.39
3225	3.58	0.82	2.49	3660	2.50	0.99	1.36
3240	1.22	1.12	0.09	3675	2.50	0.72	1.60
3255	0.96	1.10	-0.12	3690	2.50	0.63	1.68
3270	0.68	1.00	-0.29	3705	2.50	0.63	1.68
3285	0.31	0.82	-0.46	3720	2.50	0.63	1.68
3300	0.26	0.69	-0.39	3735	2.50	0.67	1.65
3315	0.23	0.63	-0.36	3750	2.50	0.82	1.51
3330	0.41	0.67	-0.23	3765	2.50	0.88	1.46
3345	1.31	0.71	0.54	3780	2.50	0.83	1.50
3360*	2.50	0.70	1.62				

APPENDIX 6 Stream power per unit bed area and channel condition data, Runs 1 and 3

Stream power per unit bed area, $\omega = \rho q S$. Units are $\text{kg m}^{-1} \text{s}^{-1}$. In Run 3, BS indicates bed slope used to calculate ω , WS indicates that water surface slope was used.

RUN 1

Stable	Stable	Stable	Aggrading	Degrading	Scour	Indeterminate	
0.0651	0.0247	0.0090	0.0621	0.0205	0.0556	0.0633	0.0216
0.0567	0.0246	0.0073	0.0605	0.0202	0.0541	0.0616	0.0166
0.0491	0.0245	0.0071	0.0603	0.0201	0.0534	0.0573	0.0053
0.0475	0.0244	0.0070	0.0558	0.0200	0.0491	0.0461	
0.0449	0.0240	0.0070	0.0556	0.0200	0.0487	0.0436	
0.0446	0.0234	0.0070	0.0546	0.0196	0.0459	0.0427	
0.0434	0.0231	0.0070	0.0543	0.0191	0.0453	0.0425	
0.0393	0.0222	0.0068	0.0540	0.0184	0.0452	0.0419	
0.0388	0.0216	0.0067	0.0537	0.0183	0.0413	0.0316	
0.0378	0.0214	0.0067	0.0481	0.0180	0.0391	0.0116	
0.0372	0.0214	0.0046	0.0481	0.0171	0.0388		
0.0372	0.0214	0.0044	0.0480	0.0170	0.0337		
0.0368	0.0211	0.0039	0.0478	0.0168	0.0319		
0.0363	0.0210	0.0023	0.0478	0.0168	0.0309		
0.0357	0.0208		0.0464	0.0166	0.0305		
0.0354	0.0202		0.0457	0.0155	0.0304		
0.0354	0.0202		0.0448	0.0149	0.0296		
0.0353	0.0201		0.0424	0.0149	0.0279		
0.0350	0.0198		0.0393	0.0145	0.0268		
0.0349	0.0198		0.0388	0.0144	0.0260		
0.0345	0.0196		0.0386	0.0129	0.0256		
0.0339	0.0192		0.0382	0.0128	0.0247		
0.0337	0.0190		0.0375	0.0123	0.0245		
0.0334	0.0189		0.0373	0.0118	0.0226		
0.0325	0.0189		0.0364	0.0117	0.0223		
0.0321	0.0188		0.0354	0.0116	0.0213		
0.0306	0.0185		0.0334	0.0103	0.0207		
0.0304	0.0183		0.0306	0.0070	0.0184		
0.0297	0.0171		0.0296	0.0064	0.0169		
0.0296	0.0165		0.0293	0.0051	0.0167		
0.0291	0.0165		0.0291	0.0050	0.0166		
0.0289	0.0160		0.0290	0.0050	0.0159		
0.0287	0.0147		0.0290	0.0049	0.0155		
0.0286	0.0145		0.0286	0.0047	0.0142		
0.0280	0.0142		0.0282	0.0047	0.0123		
0.0270	0.0142		0.0273	0.0047	0.0094		
0.0268	0.0140		0.0265	0.0046	0.0068		
0.0266	0.0140		0.0264	0.0045			
0.0263	0.0136		0.0247	0.0023			
0.0262	0.0122		0.0246				
0.0262	0.0121		0.0246				
0.0259	0.0115		0.0246				
0.0253	0.0114		0.0241				
0.0253	0.0112		0.0230				
0.0252	0.0100		0.0223				
0.0251	0.0094		0.0220				
0.0251	0.0092		0.0219				
0.0248	0.0092		0.0218				

RUN 3

Stable BS	Stable WS	Aggrading		Aggrading		Degrading		Scour	
		BS	BS	WS	WS	BS	WS	BS	WS
0.0701	0.0494	0.0721	0.0218	0.0579	0.0235	0.0731	0.0661	0.0650	0.0323
0.0670	0.0459	0.0720	0.0217	0.0557	0.0225	0.0685	0.0555	0.0647	0.0219
0.0582	0.0450	0.0680	0.0190	0.0498	0.0223	0.0627	0.0488	0.0080	
0.0499	0.0428	0.0671	0.0189	0.0485	0.0218	0.0626	0.0417		
0.0495	0.0405	0.0484	0.0185	0.0433	0.0212	0.0590	0.0400		
0.0459	0.0395	0.0448	0.0183	0.0428	0.0210	0.0581	0.0373		
0.0454	0.0394	0.0428	0.0177	0.0409	0.0208	0.0571	0.0369		
0.0451	0.0381	0.0428	0.0175	0.0407	0.0207	0.0540	0.0338		
0.0449	0.0379	0.0411	0.0173	0.0405	0.0206	0.0508	0.0317		
0.0433	0.0374	0.0408	0.0162	0.0395	0.0204	0.0423	0.0296		
0.0414	0.0373	0.0390	0.0158	0.0388	0.0195	0.0411	0.0290		
0.0414	0.0366	0.0386	0.0149	0.0379	0.0195	0.0335	0.0283		
0.0413	0.0362	0.0385	0.0147	0.0375	0.0189	0.0334	0.0282		
0.0408	0.0357	0.0380	0.0145	0.0371	0.0184	0.0283	0.0281		
0.0396	0.0356	0.0371	0.0139	0.0371	0.0175	0.0264	0.0278		
0.0373	0.0349	0.0367	0.0139	0.0366	0.0162	0.0258	0.0265		
0.0352	0.0342	0.0366	0.0130	0.0362	0.0160	0.0234	0.0264		
0.0323	0.0341	0.0366	0.0129	0.0352	0.0159	0.0224	0.0263		
0.0314	0.0339	0.0363	0.0122	0.0350	0.0142	0.0207	0.0254		
0.0296	0.0334	0.0356	0.0106	0.0344	0.0126	0.0180	0.0249		
0.0296	0.0329	0.0353	0.0083	0.0326	0.0115	0.0177	0.0248		
0.0291	0.0329	0.0345	0.0079	0.0324	0.0092	0.0175	0.0236		
0.0286	0.0329	0.0335	0.0074	0.0323	0.0037	0.0169	0.0232		
0.0286	0.0327	0.0325	0.0068	0.0323		0.0165	0.0231		
0.0277	0.0323	0.0324	0.0053	0.0320		0.0139	0.0200		
0.0273	0.0323	0.0307	0.0050	0.0314		0.0114	0.0158		
0.0271	0.0313	0.0300	0.0031	0.0314		0.0092			
0.0265	0.0307	0.0296	0.0026	0.0314		0.0070			
0.0264	0.0305	0.0291	0.0023	0.0290					
0.0258	0.0296	0.0290	0.0020	0.0288					
0.0257	0.0295	0.0290		0.0278					
0.0254	0.0286	0.0287		0.0270					
0.0251	0.0286	0.0285		0.0266					
0.0248	0.0280	0.0283		0.0265					
0.0243	0.0278	0.0281		0.0264					
0.0231	0.0277	0.0278		0.0261					
0.0225	0.0274	0.0272		0.0260					
0.0217	0.0269	0.0270		0.0254					
0.0209	0.0266	0.0266		0.0248					
0.0208	0.0258	0.0260		0.0248					
0.0205	0.0256	0.0240		0.0244					
0.0198	0.0239	0.0239		0.0244					
0.0187	0.0234	0.0238		0.0242					
0.0164	0.0225	0.0237		0.0240					
0.0158	0.0217	0.0234		0.0240					
0.0150	0.0195	0.0232		0.0239					
0.0147	0.0193	0.0228		0.0239					
0.0145	0.0190	0.0226		0.0238					
0.0140	0.0184								
0.0132	0.0182								
0.0118	0.0096								
0.0114	0.0055		Stable						
0.0109	0.0038		BS (contd)						
0.0083			0.0073						
0.0074			0.0036						

Appendix 7 Cross-sectional morphology and sediment storage data, Runs 1 and 3

Times are in minutes after the start of the run. MBE= mean bed elevation (m relative to arbitrary datum); BRI=bed relief index; active, semi-active, inactive and never active refer to unit volumes stored in given storage reservoirs (m³/ m).

Section	Time	MBE	BRI	Active	Semi-active	Inactive	Never active
RUN 1							
XS2	1210	0.123	0.00488	0.011	0.053	0.020	0.052
	1450	0.123	0.00530	0.027	0.060	0	0.048
	1690	0.124	0.00600	0.012	0.077	0	0.048
	1930	0.123	0.00624	0.016	0.071	0	0.049
	2170	0.123	0.00584	0.011	0.006	0.071	0.049
	2410	0.123	0.00540	0.020	0.011	0.058	0.049
	2530	0.123	0.00474	0.021	0.004	0.065	0.047
	2650	0.125	0.00388	0.030	0.063	0	0.047
	2770	0.126	0.00497	0.023	0.073	0	0.047
	2890	0.126	0.00526	0.036	0.035	0.023	0.049
3010	0.126	0.00543	0.033	0.052	0.011	0.046	
XS3	1210	0.113	0.00517	0.029	0.043	0.020	0.037
	1450	0.109	0.00635	0.034	0.054	0	0.036
	1690	0.112	0.00350	0.022	0.070	0	0.036
	1930	0.114	0.00551	0.027	0.070	0	0.036
	2170	0.113	0.00680	0.030	0.017	0.048	0.036
	2410	0.113	0.00742	0.025	0.024	0.048	0.037
	2530	0.114	0.00668	0.026	0.035	0.037	0.036
	2650	0.114	0.00616	0.028	0.018	0.052	0.036
	2770	0.113	0.00626	0.029	0.030	0.038	0.037
	2890	0.115	0.00673	0.019	0.013	0.069	0.037
3010	0.114	0.00561	0.031	0.038	0.030	0.036	
XS4	1210	0.097	0.00476	0.027	0.027	0	0.081
	1450	0.095	0.00498	0.020	0.025	0.010	0.074
	1690	0.094	0.00299	0.030	0.022	0	0.076
	1930	0.098	0.00667	0.024	0.038	0	0.069
	2170	0.100	0.00344	0.015	0.062	0	0.056
	2410	0.099	0.00512	0.030	0.028	0.020	0.051
	2530	0.100	0.00473	0.032	0	0.049	0.049
	2650	0.099	0.00399	0.035	0.018	0.025	0.052
	2770	0.098	0.00496	0.033	0.018	0.025	0.051
	2890	0.099	0.00466	0.033	0	0.043	0.053
3010	0.100	0.00512	0.023	0.038	0.018	0.052	
XS5	1210	0.085	0.00719	0.022	0.021	0	0.087
	1450	0.082	0.00699	0.010	0.011	0.024	0.083
	1690	0.083	0.00662	0.008	0.034	0.004	0.082
	1930	0.083	0.00790	0.009	0.010	0.026	0.082
	2170	0.087	0.00477	0.011	0.047	0	0.077
	2410	0.089	0.00343	0.038	0.022	0	0.075
	2530	0.090	0.00325	0.021	0.040	0	0.075
	2650	0.089	0.00431	0.036	0.023	0	0.075
	2770	0.087	0.00561	0.016	0.043	0	0.074
	2890	0.092	0.00599	0.018	0.048	0	0.074
3010	0.090	0.00655	0.014	0.015	0.035	0.072	

Section	Time	MBE	BRI	Active	Semi-active	Inactive	Never active
RUN 1 (continued)							
XS6	1210	0.079	0.00719	0.015	0.037	0.010	0.082
	1450	0.079	0.00699	0.019	0.032	0.007	0.080
	1690	0.078	0.00662	0.015	0.037	0.007	0.079
	1930	0.076	0.00790	0.010	0.024	0.023	0.075
	2170	0.079	0.00477	0.024	0.030	0.007	0.077
	2410	0.082	0.00343	0.016	0.048	0	0.077
	2530	0.078	0.00325	0.027	0.008	0.026	0.074
	2650	0.076	0.00431	0.042	0.015	0.003	0.072
	2770	0.074	0.00561	0.026	0.029	0	0.076
	2890	0.077	0.00599	0.020	0.040	0	0.075
	3010	0.077	0.00655	0.028	0.032	0	0.074
XS7	1210	0.071	0.00843	0.008	0.035	0.010	0.110
	1450	0.071	0.00549	0.015	0.049	0.005	0.083
	1690	0.070	0.00584	0.026	0.046	0.004	0.072
	1930	0.070	0.00494	0.020	0.020	0.037	0.070
	2170	0.072	0.00423	0.021	0.021	0.039	0.073
	2410	0.073	0.00448	0.013	0.061	0.009	0.074
	2530	0.071	0.00636	0.029	0.034	0.018	0.069
	2650	0.071	0.00735	0.020	0.007	0.052	0.073
	2770	0.069	0.00776	0.015	0.009	0.054	0.069
	2890	0.071	0.00602	0.041	0	0.042	0.068
	3010	0.071	0.00647	0.039	0	0.043	0.067
XS8	1210	0.061	0.00377	0.046	0.022	0	0.081
	1450	0.062	0.00464	0.017	0.061	0	0.071
	1690	0.062	0.00494	0.040	0.055	0	0.049
	1930	0.059	0.00404	0.018	0.034	0.048	0.039
	2170	0.062	0.00410	0.040	0.028	0.041	0.033
	2410	0.062	0.00429	0.019	0.090	0	0.035
	2530	0.062	0.00465	0.038	0.046	0.025	0.034
	2650	0.061	0.00529	0.020	0.033	0.054	0.033
	2770	0.060	0.00493	0.018	0.023	0.064	0.033
	2890	0.062	0.00507	0.033	0	0.077	0.032
	3010	0.061	0.00462	0.034	0.019	0.056	0.021
XS9	1210	0.055	0.00545	0.010	0.058	0.020	0.055
	1450	0.054	0.00484	0.023	0.069	0	0.056
	1690	0.054	0.00548	0.039	0.044	0.018	0.045
	1930	0.051	0.00682	0.038	0.008	0.053	0.040
	2170	0.054	0.00403	0.017	0.075	0.018	0.036
	2410	0.053	0.00596	0.018	0.091	0	0.034
	2530	0.052	0.00522	0.039	0.050	0.018	0.033
	2650	0.050	0.00553	0.022	0.027	0.054	0.034
	2770	0.051	0.00481	0.028	0.024	0.052	0.035
	2890	0.052	0.00513	0.022	0.036	0.047	0.035
	3010	0.050	0.00466	0.028	0.052	0.023	0.035
XS10	1210	0.042	0.00414	0.015	0.046	0.020	0.074
	1450	0.042	0.00602	0.019	0.059	0	0.069
	1690	0.043	0.00563	0.028	0.052	0	0.071
	1930	0.041	0.00604	0.030	0.017	0.031	0.068
	2170	0.042	0.00586	0.024	0.055	0	0.070
	2410	0.042	0.00613	0.041	0.041	0.008	0.054
	2530	0.042	0.0049	0.035	0.055	0	0.055
	2650	0.041	0.00713	0.029	0.019	0.039	0.057

Section	Time	MBE	BRI	Active	Semi-active	Inactive	Never active
RUN 1 (continued)							
XS10	2770	0.043	0.00591	0.022	0.032	0.037	0.055
	2890	0.042	0.00628	0.033	0.055	0.002	0.056
	3010	0.043	0.00528	0.036	0	0.056	0.053
XS11	1210	0.030	0.00695	0.005	0.050	0	0.097
	1450	0.032	0.00712	0.023	0.048	0	0.080
	1690	0.035	0.00711	0.034	0	0.051	0.070
	1930	0.032	0.00335	0.024	0.032	0.022	0.070
	2170	0.032	0.00327	0.033	0.025	0.022	0.070
	2410	0.033	0.00544	0.023	0.045	0.012	0.071
	2530	0.032	0.00593	0.012	0.067	0	0.069
	2650	0.029	0.00715	0.019	0.008	0.047	0.069
	2770	0.030	0.00628	0.025	0.022	0.032	0.065
	2890	0.032	0.00425	0.040	0.043	0	0.066
	3010	0.031	0.00496	0.042	0	0.040	0.066
	XS12	1210	0.024	0.00636	0.016	0.056	0
1450		0.022	0.00570	0.022	0.037	0.013	0.081
1690		0.025	0.00391	0.034	0.015	0.057	0.045
1930		0.025	0.00395	0.025	0.034	0.046	0.045
2170		0.027	0.00492	0.019	0.066	0.024	0.046
2410		0.027	0.00375	0.020	0.088	0	0.045
2530		0.024	0.00524	0.013	0.091	0	0.044
2650		0.025	0.00505	0.021	0.019	0.065	0.046
2770		0.026	0.00492	0.021	0.048	0.038	0.044
2890		0.027	0.00572	0.048	0.061	0	0.045
3010		0.025	0.00588	0.048	0	0.057	0.045
XS13		1210	0.009	0.00393	0.029	0.026	0
	1450	0.010	0.00382	0.032	0.025	0	0.100
	1690	0.013	0.00316	0.027	0.032	0.022	0.070
	1930	0.012	0.00450	0.014	0.060	0.006	0.070
	2170	0.013	0.00405	0.025	0.051	0.007	0.067
	2410	0.017	0.00300	0.018	0.072	0	0.068
	2530	0.014	0.00582	0.024	0.052	0.008	0.069
	2650	0.011	0.00656	0.023	0.021	0.036	0.069
	2770	0.015	0.00551	0.038	0.014	0.035	0.068
	2890	0.015	0.00481	0.051	0.016	0.021	0.069
	3010	0.013	0.00742	0.028	0.011	0.045	0.065

RUN 3							
XS2	1210	0.110	0.00715	0.009	0.011	0.018	0.065
	1450	0.111	0.00590	0.009	0.030	0	0.072
	1690	0.111	0.00450	0.012	0.013	0.014	0.070
	1930	0.114	0.00374	0.016	0.026	0	0.068
	2170	0.116	0.00419	0.022	0.023	0	0.070
	2410	0.118	0.00459	0.027	0.021	0	0.069
	2650	0.121	0.00438	0.032	0.020	0	0.070
	2890	0.116	0.00714	0.009	0.027	0.013	0.071
	3130	0.118	0.00461	0.013	0.036	0	0.071
	3370	0.118	0.00611	0.023	0.003	0.025	0.071
	3610	0.117	0.00614	0.011	0.040	0	0.071
	3790	0.119	0.00402	0.012	0.039	0	0.072

Section	Time	MBE	BRI	Active	Semi-active	Inactive	Never active
RUN 3 (continued)							
XS3	1210	0.098	0.00683	0.011	0.014	0.010	0.072
	1450	0.101	0.00399	0.014	0.024	0	0.071
	1690	0.101	0.00461	0.020	0.004	0.017	0.067
	1930	0.103	0.00437	0.020	0.005	0.021	0.065
	2170	0.104	0.00317	0.022	0.029	0	0.060
	2410	0.103	0.00414	0.023	0.010	0.020	0.056
	2650	0.101	0.00607	0.013	0.015	0.024	0.055
	2890	0.102	0.00676	0.009	0.034	0.019	0.045
	3130	0.103	0.00698	0.009	0.033	0.021	0.044
	3370	0.105	0.00567	0.015	0.034	0.017	0.046
	3610	0.105	0.00439	0.009	0.057	0	0.047
3790	0.109	0.00451	0.036	0.037	0	0.048	
XS4	1210	0.088	0.00550	0.016	0.015	0.007	0.066
	1450	0.092	0.00410	0.013	0.029	0	0.068
	1690	0.090	0.00624	0.018	0.008	0.019	0.060
	1930	0.090	0.00676	0.020	0.012	0.013	0.061
	2170	0.091	0.00660	0.022	0.011	0.014	0.063
	2410	0.089	0.00531	0.029	0.018	0	0.060
	2650	0.087	0.00637	0.012	0.020	0.010	0.065
	2890	0.091	0.00447	0.025	0.024	0	0.060
	3130	0.095	0.00672	0.018	0.036	0	0.062
	3370	0.097	0.00521	0.029	0.017	0.011	0.063
	3610	0.099	0.00326	0.024	0.036	0	0.062
3790	0.099	0.00505	0.020	0.021	0.020	0.059	
XS5	1210	0.079	0.00511	0.017	0.017	0.013	0.070
	1450	0.082	0.00444	0.014	0.014	0	0.069
	1690	0.078	0.00774	0.015	0.015	0.017	0.067
	1930	0.078	0.00643	0.016	0.016	0.011	0.066
	2170	0.080	0.00598	0.019	0.019	0	0.070
	2410	0.080	0.00764	0.017	0.017	0.011	0.070
	2650	0.077	0.00822	0.021	0.021	0.012	0.069
	2890	0.080	0.00383	0.030	0.030	0.004	0.060
	3130	0.085	0.00403	0.019	0.019	0	0.058
	3370	0.087	0.00351	0.018	0.018	0	0.061
	3610	0.089	0.00554	0.026	0.026	0	0.058
3790	0.088	0.00481	0.021	0.021	0.027	0.060	
XS6	1210	0.072	0.00404	0.025	0.017	0	0.072
	1450	0.071	0.00785	0.014	0.025	0	0.076
	1690	0.071	0.00629	0.020	0	0.020	0.071
	1930	0.072	0.00602	0.021	0.015	0.007	0.071
	2170	0.071	0.00847	0.019	0.021	0	0.076
	2410	0.072	0.00768	0.024	0.006	0.016	0.068
	2650	0.071	0.00900	0.012	0.011	0.022	0.069
	2890	0.072	0.00686	0.018	0.011	0.022	0.062
	3130	0.074	0.00550	0.027	0.030	0	0.059
	3370	0.075	0.00449	0.025	0.035	0	0.058
	3610	0.077	0.00518	0.021	0.045	0	0.054
3790	0.081	0.00524	0.022	0	0.053	0.051	
XS7	1210	0.066	0.00612	0.024	0.019	0.009	0.079
	1450	0.065	0.00750	0.018	0.021	0.011	0.081
	1690	0.064	0.00625	0.024	0.002	0.025	0.078
	1930	0.066	0.00668	0.025	0	0.027	0.080
	2170	0.064	0.00847	0.019	0.006	0.024	0.081

Section	Time	MBE	BRI	Active	Semi-active	Inactive	Never active
RUN 3 (continued)							
XS7	2410	0.064	0.00892	0.021	0	0.027	0.081
	2650	0.063	0.00931	0.013	0.010	0.026	0.082
	2890	0.065	0.00592	0.024	0.012	0.026	0.068
	3130	0.066	0.00476	0.038	0.017	0.010	0.063
	3370	0.069	0.00415	0.031	0.037	0	0.066
	3610	0.070	0.00484	0.026	0.044	0	0.068
	3790	0.069	0.00519	0.021	0.022	0.026	0.067
XS8	1210	0.057	0.00554	0.018	0.042	0	0.070
	1450	0.056	0.00425	0.026	0.025	0.009	0.070
	1690	0.055	0.00545	0.021	0.013	0.025	0.069
	1930	0.055	0.00600	0.028	0.007	0.024	0.069
	2170	0.055	0.00717	0.019	0.008	0.031	0.069
	2410	0.055	0.00756	0.018	0.007	0.032	0.071
	2650	0.054	0.00786	0.009	0.018	0.031	0.068
	2890	0.056	0.00560	0.021	0.015	0.024	0.072
	3130	0.056	0.00518	0.032	0.009	0.019	0.071
	3370	0.058	0.00471	0.028	0.026	0.008	0.071
	3610	0.057	0.00511	0.040	0.011	0.011	0.070
	3790	0.057	0.00554	0.024	0.019	0.020	0.071
XS9	1210	0.047	0.00337	0.021	0.039	0	0.069
	1450	0.046	0.00336	0.021	0.021	0.018	0.072
	1690	0.045	0.00510	0.016	0.021	0.021	0.070
	1930	0.045	0.00594	0.015	0.018	0.024	0.072
	2170	0.045	0.00728	0.013	0.015	0.031	0.071
	2410	0.045	0.00687	0.016	0.020	0.022	0.072
	2650	0.045	0.00660	0.011	0.027	0.020	0.071
	2890	0.047	0.00515	0.019	0.026	0.015	0.072
	3130	0.049	0.00223	0.034	0.028	0	0.072
	3370	0.048	0.00488	0.030	0.032	0	0.072
	3610	0.048	0.00424	0.022	0.041	0	0.073
	3790	0.046	0.00369	0.035	0.014	0.011	0.070
XS10	1210	0.038	0.00451	0.022	0.047	0	0.064
	1450	0.038	0.00520	0.019	0.051	0	0.064
	1690	0.036	0.00677	0.013	0.013	0.040	0.066
	1930	0.035	0.00711	0.018	0.016	0.031	0.064
	2170	0.035	0.00831	0.008	0.018	0.039	0.065
	2410	0.036	0.00658	0.012	0.009	0.045	0.067
	2650	0.037	0.00561	0.014	0.026	0.028	0.067
	2890	0.041	0.00359	0.030	0.043	0	0.066
	3130	0.040	0.00372	0.023	0.049	0	0.064
	3370	0.039	0.00456	0.028	0.027	0.015	0.066
	3610	0.041	0.00487	0.032	0.041	0	0.069
	3790	0.037	0.00476	0.018	0.026	0.023	0.064
XS11	1210	0.024	0.00416	0.032	0.010	0.005	0.084
	1450	0.023	0.00495	0.022	0.024	0	0.083
	1690	0.023	0.00307	0.018	0.024	0.005	0.083
	1930	0.022	0.00554	0.021	0.007	0.019	0.083
	2170	0.022	0.00608	0.011	0.014	0.020	0.084
	2410	0.023	0.00489	0.013	0.010	0.023	0.082
	2650	0.027	0.00484	0.020	0.032	0	0.082
	2890	0.028	0.00520	0.023	0.030	0	0.085
	3370	0.025	0.00656	0.015	0.027	0.008	0.087

Section	Time	MBE	BRI	Active	Semi-active	Inactive	Never active
RUN 3 (continued)							
XS11	3610	0.026	0.00691	0.023	0.010	0.018	0.086
	3790	0.024	0.00644	0.021	0.011	0.016	0.085
XS12	1210	0.018	0.00746	0.025	0.002	0.024	0.085
	1450	0.016	0.00698	0.027	0	0.023	0.083
	1690	0.018	0.00648	0.018	0.012	0.023	0.084
	1930	0.017	0.00766	0.020	0	0.031	0.085
	2170	0.016	0.00682	0.018	0.005	0.027	0.087
	2410	0.018	0.00568	0.021	0.007	0.025	0.081
	2650	0.021	0.00508	0.026	0.032	0	0.081
	2890	0.021	0.00580	0.025	0.032	0	0.085
	3130	0.021	0.00569	0.027	0.019	0.011	0.085
	3370	0.020	0.00703	0.025	0	0.032	0.086
	3610	0.020	0.00747	0.026	0	0.031	0.083
	3790	0.018	0.00636	0.026	0	0.028	0.082
	XS13	1210	0.006	0.00520	0.025	0.012	0.021
1450		0.006	0.00481	0.033	0.005	0.021	0.073
1690		0.007	0.00416	0.035	0.016	0.009	0.073
1930		0.005	0.00456	0.032	0.004	0.021	0.071
2170		0.006	0.00426	0.020	0.015	0.023	0.073
2410		0.007	0.00337	0.025	0.016	0.019	0.075
2650		0.011	0.00308	0.030	0.035	0	0.074
2890		0.011	0.00209	0.040	0.025	0	0.076
3130		0.010	0.00451	0.037	0.027	0	0.074
3370		0.009	0.00489	0.039	0.025	0	0.075
3610		0.010	0.00455	0.042	0.002	0.020	0.075
3790		0.008	0.00424	0.029	0.033	0	0.075

APPENDIX 8 Volumes of stored sediment, Kowal River, 1975, 1979, 1987

1975 and 1979 survey data provided by Centre for Resource Management, Lincoln College.

* indicates where the survey may have included a gravel groyne.

Cross-section number	Distance downstream (m)	Volume of sediment stored in the active and semi-active reservoirs (m ³ /m)			Volume of sediment stored in active, semi-active and inactive reservoirs (m ³ /m)		
		1975	1979	1987	1975	1979	1987
		130	1270	221	208	191	221
131	1420	452	396	437	485	439	447
132	1580	385	313	463	442	484	493
133	1720	455	751	915	928	1070	1060
134	1870	227	631	763	1240	1140	1310
135	1930	239	824	534	842	971	974
136	2050	398	415	332	398	415	436
137	2180	584	206	384	584	458	553
138	2320	159	146	-	159	146	-
141	2650	560	585	564	999	912	971
142	2720	609	436	494	609	655	687
143	2780	480	481	479	480	481	479
144	2990	693	931*	559	693	1100*	665
145	3160	604	566	688	1046	929	1048
146	3280	524	508	592	524	508	592
147	3420	220	-	319	664	-	649
148	3600	105	116	114	105	116	114

APPENDIX 9 Particle size data, Kowal River

Surface refers to morphological surface identified on Figure 5.18. Distance down axis refers to the axis of surfaces G and M. $\sigma_g = (d_{84} / d_{16})^{0.5}$

Surface	Distance down axis (m)	d ₅₀ (mm)	d _{10x} (mm)	σ_g
G	19	56	172	2.3
G	54	19	70	2.6
G	71	24	111	2.7
G	179	25	135	10.3
G	195	10	64	2.8
G	264	11	71	3.3
G	313	11	133	5.3
G	320	14	93	4.5
G	324	15	75	2.7
G	393	24	95	3.0
M	86	25	112	3.4
M	161	20	68	2.0
M	161	15	118	9.1
M	240	10	94	2.9

Appendix 10 Output of dyed sand from experimental Run 3

Time is in minutes after the start of the run.

Time (mins)	Output sediment mass (kg)	Proportion of mass		% dyed sand in sample	Proportion of dyed sand		Cumulative % of input dyed sand that had been output		
		≥0.6mm	<0.6mm		≥0.6mm	<0.6mm	Total	≥0.6mm	<0.6mm
1515	2.31	0.59	0.41	1.4	0.61	0.39	1.5	1.8	1.1
1530	2.16	0.67	0.33	3.9	0.98	0.02	2.6	-	-
1545	2.36	0.44	0.56	5.4	0.84	0.16	3.6	-	-
1560	2.46	0.38	0.62	3.5	0.78	0.22	3.7	-	-
1590	5.58	0.25	0.75	8.3	0.62	0.38	8.9	13.1	4.9
1620	5.92	0.44	0.56	1.9	0.65	0.35	10.1	14.9	5.8
1650	5.89	0.59	0.41	1.9	0.84	0.16	11.4	17.0	6.1
1680	6.08	0.64	0.36	4.2	0.70	0.30	14.2	21.2	7.8
1710	5.51	0.60	0.40	0.9	0.61	0.39	14.8	21.9	8.2
1740	5.40	0.50	0.50	3.6	0.80	0.20	16.9	25.5	9.0
1770	4.99	0.58	0.42	2.0	0.54	0.46	18.1	26.7	10.0
1800	4.56	0.48	0.52	2.0	0.45	0.55	19.1	27.7	11.1
1830	4.06	0.45	0.55	1.9	0.47	0.53	19.9	28.5	12.0
1860	3.73	0.27	0.73	1.6	0.16	0.84	20.6	28.7	13.0
1890	4.55	0.48	0.52	1.8	0.77	0.23	21.5	30.2	13.5
1920	5.00	0.47	0.53	2.4	0.62	0.38	22.9	32.0	14.4
1950	4.75	0.48	0.52	1.4	0.63	0.37	23.6	32.9	14.9
1980	4.71	0.56	0.40	0.8	0.46	0.54	24.0	33.3	15.4
2010	4.60	0.70	0.30	0.7	0.66	0.34	24.3	33.8	15.6
2040	4.44	0.55	0.45	1.5	0.86	0.14	25.1	35.1	15.8
2070	4.56	0.55	0.45	2.2	0.85	0.15	26.2	37.0	16.1
2100	4.92	0.29	0.71	1.1	0.31	0.69	26.7	37.4	16.9
2130	4.80	0.63	0.37	1.5	0.88	0.12	27.5	38.8	17.1
2160	4.40	0.58	0.42	1.0	0.73	0.27	28.0	39.6	17.3
2190	3.93	0.61	0.39	0.8	0.54	0.46	28.4	40.0	17.7
2220	3.50	0.76	0.24	0.4	0.67	0.33	28.5	40.2	17.7
2250	4.43	0.37	0.63	0.7	0.41	0.59	28.9	40.5	18.4
2280	4.78	0.36	0.64	7.8	0.96	0.04	33.0	48.8	18.4
2310	3.99	0.49	0.51	1.8	0.80	0.20	33.8	50.1	18.8
2340	5.03	0.42	0.58	0.8	0.50	0.50	34.3	50.6	19.2
2370	2.78	0.56	0.44	0.5	0.81	0.19	34.4	50.8	19.2
2400	4.28	0.64	0.36	0.7	0.70	0.30	34.7	51.3	19.4
2430	2.71	0.66	0.34	0.5	0.90	0.10	34.9	51.6	19.5
2460	2.41	0.59	0.41	0.4	0.44	0.56	35.0	51.7	19.6
2490	1.80	0.79	0.21	0.3	0.92	0.08	35.0	51.8	19.6
2520	2.69	0.63	0.37	0.5	0.91	0.09	35.2	52.1	19.6
2550	2.66	0.89	0.11	0.4	0.91	0.09	35.3	52.3	19.6
2580	2.12	0.78	0.22	0.6	0.90	0.10	35.5	52.6	19.7
2610	2.11	0.51	0.49	0.2	0.21	0.79	35.5	52.6	19.7
2640	2.46	0.43	0.57	0.2	0.67	0.33	35.6	52.7	19.8
2670	2.53	0.87	0.13	0.6	0.97	0.03	35.7	53.0	19.8
2700	2.26	0.84	0.16	0.2	0.84	0.16	35.8	53.1	19.8
2730	2.16	0.59	0.41	0.2	0.68	0.32	35.8	53.2	19.8
2760	1.72	0.54	0.46	0.2	0.63	0.37	35.9	53.2	19.8
2790	1.27	0.57	0.43	0.3	0.81	0.19	35.9	53.3	19.8
2820	1.61	0.66	0.34	0.7	0.79	0.21	36.0	53.5	19.9
2850	1.84	0.34	0.66	0.2	0.47	0.53	36.1	53.5	19.9
2880	3.12	0.36	0.64	0.3	0.18	0.82	36.2	53.6	20.1
2910	3.39	0.74	0.26	0.1	0	1.00	36.2	53.6	20.2
2940	2.54	0.67	0.33	1.1	0.93	0.07	36.5	54.2	20.2

Appendix 11 Distributions of dyed sand within the model channel, Run 3

See Chapter 6 for explanations of sampling procedures, and the definition of the equivalent diameter index.

Time (min)	Sample #	% dyed sand	Proportion of dyed sand		Proportion of mass		Equivalent diameter index (mm)
			≥.6mm	<.6mm	≥.6mm	<.6mm	
1690	1	2.9	0.90	0.10	0.76	0.24	0.88
	2	0.4	0.56	0.44	0.76	0.24	0.88
	3	18.2	0.99	0.01	0.82	0.18	1.00
	4	26.6	0.48	0.52	0.22	0.78	0.39
	5	3.4	0.97	0.03	0.54	0.46	0.63
	6	1.9	0.10	0.90	0.14	0.86	0.33
	7	12.5	0.08	0.92	0.06	0.94	0.25
	8	0.8	0	1.00	0.40	0.60	0.52
	9	5.3	0.56	0.44	0.27	0.73	0.43
	10	0.0	0	1.00	0.49	0.51	0.59
	11	2.1	0.45	0.55	0.58	0.42	0.67
	12	1.7	0.85	0.15	0.57	0.43	0.66
	13	13.3	0.84	0.16	0.71	0.29	0.81
	14	0.5	0	1.00	0.18	0.82	0.36
	15	2.7	0.88	0.12	0.90	0.10	1.26
	16	15.5	0.91	0.09	0.52	0.48	0.62
	17	0	0	0	0.64	0.36	0.73
1930	1	2.9	0.93	0.07	0.77	0.23	0.90
	2	0.2	0.67	0.33	0.47	0.53	0.58
	3	1.3	0.99	0.01	0.74	0.26	0.85
	4	5.4	0.67	0.33	0.55	0.45	0.64
	5	0.2	0	1.00	0.48	0.52	0.59
	6	2.2	0.90	0.10	0.52	0.48	0.61
	7	2.9	0.51	0.49	0.38	0.62	0.51
	8	0.2	0.86	0.14	0.69	0.31	0.78
	9	0.6	0.64	0.36	0.70	0.30	0.80
	10	0.4	0.27	0.73	0.52	0.48	0.62
	11	0.7	0.27	0.73	0.26	0.74	0.42
	12	0.1	0.68	0.32	0.59	0.41	0.68
	13	1.0	0.01	0.99	0.15	0.85	0.33
	14	1.2	0.68	0.32	0.70	0.30	0.79
	15	1.1	0.97	0.03	0.63	0.37	0.71
	16	1.6	0.70	0.30	0.34	0.66	0.48
2170	1	0	1.00	0	0.72	0.28	0.82
	2	0	0	0	0.80	0.20	0.96
	3	0.1	0	1.00	0.25	0.75	0.42
	4	4.3	1.00	0	0.66	0.34	0.75
	5	0.0	0.28	0.72	0.60	0.40	0.69
	6	1.0	0.12	0.88	0.34	0.66	0.48
	7	1.1	0.97	0.03	0.58	0.42	0.67
	8	1.3	0.66	0.34	0.60	0.40	0.69
	9	0.2	0	1.00	0.45	0.55	0.56
	10	0.2	0.59	0.41	0.75	0.25	0.87
	11	0.3	0.36	0.64	0.53	0.47	0.63
	12	1.7	0.83	0.17	0.63	0.37	0.71
	13	0.2	0.81	0.19	0.66	0.34	0.75
	14	0.6	0.15	0.85	0.47	0.53	0.58
	15	2.6	0.94	0.06	0.66	0.34	0.75
	16	0.7	0.21	0.79	0.40	0.60	0.52

Time (min)	Sample #	% dyed sand	Proportion of dyed sand		Proportion of mass		Equivalent diameter index (mm)
			≥.6mm	<.6mm	≥.6mm	<.6mm	
2410	1	0.1	1.00	0	0.79	0.21	0.93
	2	0	0	0	0.81	0.19	0.96
	3	0.1	0.08	0.92	0.40	0.60	0.53
	4	1.1	0.99	0.01	0.77	0.23	0.90
	5	1.0	1.00	0	0.64	0.36	0.73
	6	5.1	0.18	0.82	0.32	0.68	0.46
	7	0.0	1.00	0	0.45	0.55	0.56
	8	0	0	0	0.59	0.41	0.68
	9	1.5	0.68	0.32	0.48	0.52	0.59
	10	0.5	0.27	0.73	0.19	0.81	0.37
	11	0	0	0	0.51	0.49	0.61
	12	0.1	0	1.00	0.57	0.43	0.66
	13	0.2	0.10	0.90	0.32	0.68	0.46
	14	0.6	0.29	0.71	0.50	0.50	0.60
	15	0.4	0.69	0.31	0.40	0.60	0.53
2650	1	0	0	0	0.77	0.23	0.90
	2	0	0	0	0.76	0.24	0.89
	3	0.0	0	1.00	0.68	0.32	0.77
	4	1.9	1.00	0	0.49	0.51	0.59
	5	0.6	0.26	0.74	0.62	0.38	0.71
	6	0	0	0	0.91	0.09	1.29
	7	0.2	0.68	0.32	0.44	0.56	0.55
	8	0.3	0.64	0.36	0.50	0.50	0.60
	9	1.5	0.67	0.33	0.49	0.51	0.59
	10	0.1	0	1.00	0.55	0.45	0.64
	11	0.1	0.28	0.72	0.13	0.87	0.31
	12	0.4	0.90	0.10	0.62	0.38	0.71
	13	0.2	0	1.00	0.52	0.48	0.62
	14	1.6	0.97	0.03	0.63	0.37	0.71
	15	0.1	0	1.00	0.68	0.32	0.78
2890	1	0	0	0	0.78	0.22	0.91
	2	5.2	1.00	0	0.55	0.45	0.65
	3	0.2	0.42	0.58	0.47	0.53	0.57
	4	0.5	0.98	0.02	0.79	0.21	0.94
	5	0.1	1.00	0	0.55	0.45	0.64
	6	0.1	0.19	0.81	0.45	0.55	0.56
	7	3.1	0.84	0.16	0.76	0.24	0.87
	8	1.1	0.88	0.12	0.69	0.31	0.78
	9	0.2	0.72	0.28	0.48	0.52	0.59
	10	0.5	1.00	0	0.58	0.42	0.67
	11	0.7	1.00	0	0.70	0.30	0.79
	12	0.1	0.39	0.61	0.57	0.43	0.66
	13	0.2	0.37	0.63	0.43	0.57	0.55
	14	0.3	0	1.00	0.54	0.46	0.63
	15	0.3	0.90	0.10	0.55	0.45	0.64
	16	0.5	0.09	0.91	0.26	0.74	0.43
	17	1.0	0.84	0.16	0.56	0.44	0.65
	18	0.3	0.69	0.31	0.52	0.48	0.62
	19	0.1	0	1.00	0.60	0.40	0.68
	20	0.2	0.36	0.64	0.26	0.74	0.42
	21	0.5	0.15	0.85	0.06	0.94	0.24

APPENDIX 12 Exchanges of sediment between storage reservoirs (by area), Run 3

See Table 6.3 for 1450-1690 minutes data. Units are metres of channel which underwent each transfer. Bracketed figures express the transitions from each state at the first time as a proportion of all transitions from that state.

State at 1690 minutes	State at 1930 minutes			
	Active	Semi-active	Inactive	Never Active
Active	5.86 (0.9436)	0.18 (0.0290)	0.17 (0.0274)	0.00 (0.0)
Semi-active	0.72 (0.2368)	1.28 (0.4211)	1.04 (0.3421)	0.00 (0.0)
Inactive	0.41 (0.0856)	0.78 (0.1628)	3.60 (0.7516)	0.00 (0.0)
Never Active	0.15 (0.0086)	0.08 (0.0046)	0.00 (0.0)	17.19 (0.9868)

State at 1930 minutes	State at 2170 minutes			
	Active	Semi-active	Inactive	Never Active
Active	5.94 (0.8474)	0.83 (0.1184)	0.24 (0.0342)	0.00 (0.0)
Semi-active	0.28 (0.1069)	1.95 (0.7443)	0.39 (0.1489)	0.00 (0.0)
Inactive	0.14 (0.0299)	0.96 (0.2047)	3.59 (0.7655)	0.00 (0.0)
Never Active	0.22 (0.0128)	0.07 (0.0041)	0.00 (0.0)	16.94 (0.9832)

State at 2170 minutes	State at 2410 minutes			
	Active	Semi-active	Inactive	Never Active
Active	5.46 (0.8639)	0.69 (0.1092)	0.17 (0.0269)	0.00 (0.0)
Semi-active	0.37 (0.0971)	2.19 (0.5748)	1.25 (0.3281)	0.00 (0.0)
Inactive	0.39 (0.0909)	0.49 (0.1142)	3.41 (0.7949)	0.00 (0.0)
Never Active	0.33 (0.0193)	0.04 (0.0023)	0.01 (0.0006)	16.73 (0.9778)

State at 2410 minutes	State at 2650 minutes			
	Active	Semi-active	Inactive	Never Active
Active	4.30 (0.6555)	2.22 (0.3384)	0.04 (0.0061)	0.00 (0.0)
Semi-active	1.11 (0.3558)	1.54 (0.4936)	0.47 (0.1506)	0.00 (0.0)
Inactive	0.32 (0.0648)	1.49 (0.3016)	3.13 (0.6336)	0.00 (0.0)
Never Active	0.15 (0.0089)	0.10 (0.0059)	0.00 (0.0)	16.60 (0.9852)

State at 2650 minutes	State at 2890 minutes			
	Active	Semi-active	Inactive	Never Active
Active	4.11 (0.7074)	1.59 (0.2737)	0.11 (0.0189)	0.00 (0.0)
Semi-active	1.41 (0.2686)	3.53 (0.6724)	0.31 (0.0590)	0.00 (0.0)
Inactive	0.63 (0.1731)	0.88 (0.2418)	2.13 (0.5852)	0.00 (0.0)
Never Active	0.62 (0.0370)	0.26 (0.0155)	0.00 (0.0)	15.88 (0.9475)

APPENDIX 13 Stochastically modelled sediment storage volumes, Run 3

Time period on which transition matrix was based	Time period (minutes)	Volumes in storage reservoirs (m ³)			
		Active	Semi-active	Inactive	Never active
Measured volumes	1450-1690	0.262	0.149	0.246	0.984
	1690-1930	0.287	0.134	0.252	0.979
	1930-2170	0.239	0.221	0.220	0.991
	2170-2410	0.276	0.157	0.270	0.967
	2410-2650	0.243	0.290	0.191	0.968
	2650-2890	0.299	0.346	0.141	0.932

1450-1690	1450-1690	0.270	0.143	0.240	0.992
	1690-1930	0.257	0.125	0.281	0.965
	1930-2170	0.271	0.129	0.277	0.961
	2170-2410	0.254	0.132	0.301	0.973
	2410-2650	0.270	0.132	0.303	0.950
	2650-2890	0.267	0.145	0.318	0.950

1690-1930	1450-1690	0.331	0.151	0.167	0.996
	1690-1930	0.310	0.113	0.248	0.969
	1930-2170	0.330	0.108	0.248	0.965
	2170-2410	0.303	0.137	0.252	0.977
	2410-2650	0.326	0.120	0.269	0.953
	2650-2890	0.320	0.161	0.252	0.954

Time period on which transition matrix was based	Time period (minutes)	Volumes in storage reservoirs (m ³)			
		Active	Semi-active	Inactive	Never active
1930-2170	1450-1690	0.270	0.271	0.112	0.992
	1690-1930	0.259	0.191	0.226	0.966
	1930-2170	0.278	0.184	0.229	0.961
	2170-2410	0.246	0.235	0.215	0.973
	2410-2650	0.271	0.202	0.245	0.950
	2650-2890	0.256	0.279	0.202	0.950
2170-2410	1450-1690	0.282	0.214	0.168	0.987
	1690-1930	0.282	0.142	0.259	0.961
	1930-2170	0.302	0.137	0.259	0.956
	2170-2410	0.267	0.178	0.260	0.968
	2410-2650	0.296	0.151	0.280	0.945
	2650-2890	0.274	0.214	0.259	0.945
2410-2650	1450-1690	0.262	0.149	0.246	0.984
	1690-1930	0.255	0.241	0.189	0.968
	1930-2170	0.266	0.243	0.190	0.964
	2170-2410	0.263	0.260	0.183	0.976
	2410-2650	0.267	0.256	0.205	0.953
	2650-2890	0.288	0.287	0.174	0.953
2650-2890	1450-1690	0.323	0.311	0.070	0.957
	1690-1930	0.309	0.246	0.167	0.931
	1930-2170	0.324	0.243	0.170	0.927
	2170-2410	0.308	0.282	0.155	0.939
	2410-2650	0.324	0.260	0.181	0.916
	2650-2890	0.299	0.346	0.141	0.932